A University of Sussex DPhil thesis

Available online via Sussex Research Online:

http://sro.sussex.ac.uk/

This thesis is protected by copyright which belongs to the author.

This thesis cannot be reproduced or quoted extensively from without first obtaining permission in writing from the Author

The content must not be changed in any way or sold commercially in any format or medium without the formal permission of the Author

When referring to this work, full bibliographic details including the author, title, awarding institution and date of the thesis must be given

Please visit Sussex Research Online for more information and further details

University of Sussex

Dysregulated Toll-Like Receptor Mechanisms: The Cause of Atherosclerosis?

Frederick Gamper

Doctor of Philosophy in Immunology

Supervised by Dr. Kathy Triantafilou
and Dr. Martha Triantafilou

Submitted September 2010

Declaration

I hereby declare that this thesis has not been and will not be, submitted in whole or in part to another University for the award of any other degree.

.....

FREDERICK GAMPER

Acknowledgements

Firstly I would like to thank my tutors and mentors, Dr. Kathy Triantafilou and Dr. Martha Triantafilou for their invaluable guidance and support throughout this project. I am forever in debt for their time and patience over the years. Thank you also to my colleagues for making the lab an enjoyable environment to work.

I would also like to thank Dr. D. Golenbock for supplying HEK transfectants and Professor C. Lingwood for supplying heat shock protein 70.

UNIVERSITY OF SUSSEX

Frederick Gamper
Doctor of Philosophy in Immunology

Dysregulated Toll-like Receptor Mechanisms: The Cause of Atherosclerosis?

Summary

It is estimated that in the European Union 2 million deaths each year (42% of total) are as a result of cardiovascular disease, of which atherosclerosis is a major underlying factor. In 2006 this was estimated to cost the European Union an astonishing €192 billion. Once considered a lipid storage disorder it is becoming apparent that atherosclerosis is in fact due to an inflammatory dysfunction, with a number of endogenous and exogenous activators coming to light. The process of atheroma formation is poorly understood. This study seeks to discover the underlying mechanisms of plaque development with the view to develop novel therapeutics for this disease.

Our results demonstrate a modulatory role of endogenous low density lipoprotein (LDL), "bad cholesterol", on bacterial infections. Using primary human umbilical vein endothelial cells (HUVECs) I have shown that "non-self" oxidised LDL can reduce cell surface expression of pattern recognition receptors (PRRs) of the innate immune system, causing modulation of the cellular response directed towards atherosclerosis-associated bacterial pathogen-associated molecular patterns (PAMPs). Triple label fluorescent confocal microscopy of HUVECs revealed altered trafficking and targeting of PRRs of the innate immune system when endogenous LDL were combined with a bacterial infection in comparison to infection alone, indicating a source of the inflammatory dysfunction observed in this disease. This study illustrates that oxidatively modified LDL has a profound effect on bacterial infection, dramatically altering cellular response which may begin to explain the root cause of atherosclerosis. Through experimentation with human embryonic kidney (HEK) transfectants and HUVEC PRR silencing this study uncovered lipid raft dependant Toll-like receptors (TLRs) as fundamental culprits of this multi-factorial disease, with emphasis on TLR2 and TLR4. Future therapy designed for atherosclerosis will unquestionably involve the manipulation of TLR signalling.

Abbreviations

ACE	Angiotensin-converting enzyme
AMD3100	AMD3100 octahydrochloride
AP2	Adipocyte fatty acid–binding protein
ApoB-100	Apolipoprotein B-100
APOE	Apolipoprotein E
APS	Ammonium persulfate
ASPA	Animals (Scientific Procedures) Act 1986
C.pneumoniae	*Chlamydia pneumoniae*
CAD	Coronary artery disease
CBA	Cytometric bead array
CCR	Chemokine receptor
CEA	Carotid endarterectomy
CpG	Cytosine-phosphate-guanosine
CRP	C-reactive protein
CXCR4	CXC chemokine receptor 4
Cy5	Cyanine 5
DAMP	Damage-associated molecular pattern
DD	Death domain
DMSO	Dimethyl sulfoxide
dsRNA	Double-stranded ribonucleic acid
E.coli	*Escherichia coli*
ECL	Enhanced chemiluminescence
ECM	Extracellular matrix
ECV304	Human endothelial vascular 304
FACS	Fluorescence activated cell sorter
FCS	Foetal calf serum
FITC	Fluorescein isothiocyanate
FSC	Forward scattered light
GFP	Green fluorescent protein
GPI	Glycosylphosphatidylinositol
GSH	Glutathione
GST	Glutathione sepharose
H.pylori	*Helicobacter pylori*
HDL	High density lipoprotein
HEK293	Human embryonic kidney 293
hIL-1R	Human interleukin-1 receptor
HRP	Horse radish peroxidase
HSP	Heat shock protein
hTLR	Human TLR
HUVEC	Human umbilical vein endothelial cell
i.p	Intraperitoneal
IDL	Intermediate density lipoprotein

IFN	Interferon
IKK	IκB-kinase
IL	Interleukin
IMAC	Immobilized metal ion affinity chromatography
IRAK	Interleukin-1 receptor-associated kinase
IRF	Interferon regulatory factor
IκB	Inhibitor of NF-κB
LBP	LPS-binding protein
LDL	Low density lipoprotein
LDLR	Low density lipoprotein receptor
LOX-1	Lectin-like oxidized LDL receptor-1
LPS	Lipopolysaccharide
LRR	Leucine-rich repeat
LSGS	Low serum growth supplement kit
LTA	Lipoteichoic acid
MCD	Methyl-beta-cyclodextrin
mCD14	Membrane bound CD14
MCP-1	Monocyte chemotactic protein-1
MDV	Marek's disease virus
MHC	Major histocompatibility complex
MI	Myocardial infarction
mmLDL	Minimally modified low density lipoprotein
MMP	Matrix metalloproteinase
MODS	Multiple organ dysfunction syndrome
MyD88	Myeloid differentiation primary response gene 88
NF-κB	Nuclear factor kappa-light-chain-enhancer of activated B-cells
NLR	NOD-like receptor
oxLDL	Oxidised low density lipoprotein
OxPAPC	Oxidized 1-palmitoyl-2-arachidonoyl-sn-glycero-3-phosphorylcholine
P.gingivalis	*Porphyromonas gingivalis*
PAMP	Pathogen-associated molecular pattern
PE	Phycoerythrin
PFA	Paraformaldehyde
PG	Peptidoglycan
PMT	Photomultiplier tube
Poly {I-C}	Polyinosinic-polycytidylic acid
POVPC	1-palmitoyl 2-(59-oxovaleroyl) phosphatidylcholine
PRR	Pattern recognition receptor
RLR	RIG-I-like receptor
RNAi	RNA interference
S.aureus	*Staphylococcus aureus*
S.pneumoniae	*Streptococcus pneumoniae*
sCD14	Soluble CD14
SDS-PAGE	Sodium dodecyl sulphate polyacrylamide gel electrophoresis

SEM	Scanning electron microscopy
SFM	Serum free medium
siRISC	siRNA-induced silencing complex
SMC	Smooth muscle cells
SR	Scavenger receptor
SSC	Side scattered light
ssRNA	Single-stranded RNA
TAB	TAK1-binding protein
TAD	Transcription activation domain
TAK1	Transforming-growth factor-β-activated kinase
TEMED	N,N,N',N'-tetra- methylethylenediamine
TF	Tissue factor
TIR	Toll/interleukin-1 receptor
TLR	Toll-like receptors
TNF	Tumour necrosis factor
TRAF6	Tumour-necrosis-factor receptor-associated factor 6
TRAM	TRIF related adapter molecule
TRIF	TIR domain-containing adapter inducing IFN-β
TRITC	Tetramethyl rhodamine iso-thiocyanate
VLDL	Very low density lipoprotein
Y.pestis	*Yersinia pestis*

Contents

Chapter 1:

Introduction

1.1: Atherosclerosis

It is estimated that in the European Union 2 million deaths each year (42% of total) are as a result of cardiovascular disease (2008 statistics)[1], of which atherosclerosis is a major underlying factor. In 2006 this was estimated to cost the European Union an astonishing €192 billion, this includes the cost of health care at €110 billion and €82 billion on lost productivity and informal patient care[1]. In the Western world atherosclerosis gives rise to the majority of cardiovascular disease, and more global deaths than any other pathology except infection. Atherosclerosis is a multi-factorial disease that is characterized by the formation of lesions (plaques) in medium and large arterial blood vessel walls which can restrict and eventually cut off blood flow to vital organs. Early stages of plaque formation are asymptomatic allowing them to grow insidiously unbeknown to an individual. Over time plaques mature and can become unstable, if these rupture they will inevitably cause thrombosis resulting in vascular occlusion leading to tissue damage such as myocardial infarction.

Increase in plaque size reduces essential oxygen supply to vital organs such as to the cardiac muscle. If the oxygen demand is not met the muscle can become ischemic when the requirement for oxygen is raised, for example during exercise. A 50% reduction in luminal diameter will produce a 70% reduction of the luminal cross-sectional area which is sufficient for symptoms of ischemic heart disease to be experienced[2].

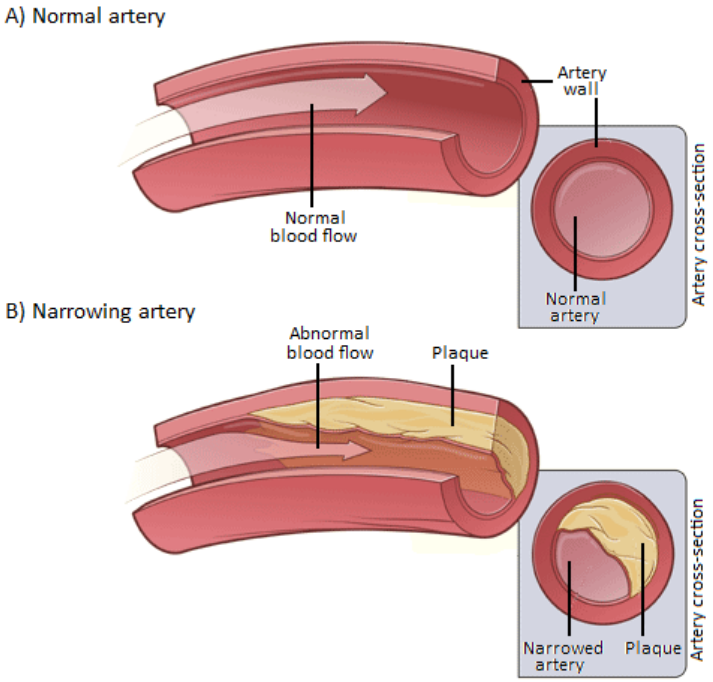

Figure 1.1: The normal (A) and atherosclerotic artery (B). The presence of plaque in the arterial wall effects blood flow (B). Increase in plaque size reduces oxygen supply to vital organs causing adverse conditions such as ischemic heart disease. Adapted from www.nhlbi.nih.gov/health/dci/Diseases/Atherosclerosis/Atherosclerosis_WhatIs.html (28/05/10).

Severe constricting chest pain, known as angina pectoris, is the most common symptom of ischemic heart disease and can be "stable" (experienced on exertion only) or "unstable" (experienced at rest) depending on the stage of plaque development. Plaque formation within coronary arteries can lead to myocardial infarction and sudden death if left untreated.

There are many components that are involved in the development of the atherosclerotic plaque from the early fatty streak to the more problematic mature lesion that is associated with increased risk of organ damage. These components include lipoproteins, crystalline cholesterol, cholesterol esters, phospholipids, extracellular matrix, collagen, foam cells, macrophages, mast cells, dendritic cells, T-cells and smooth muscle cells[3,4].

Due to the nature of plaque development the proportions of these factors alters over time giving rise to varied levels of severity ranging from asymptomatic (fatty streak) to life threatening (mature/complicated lesion).

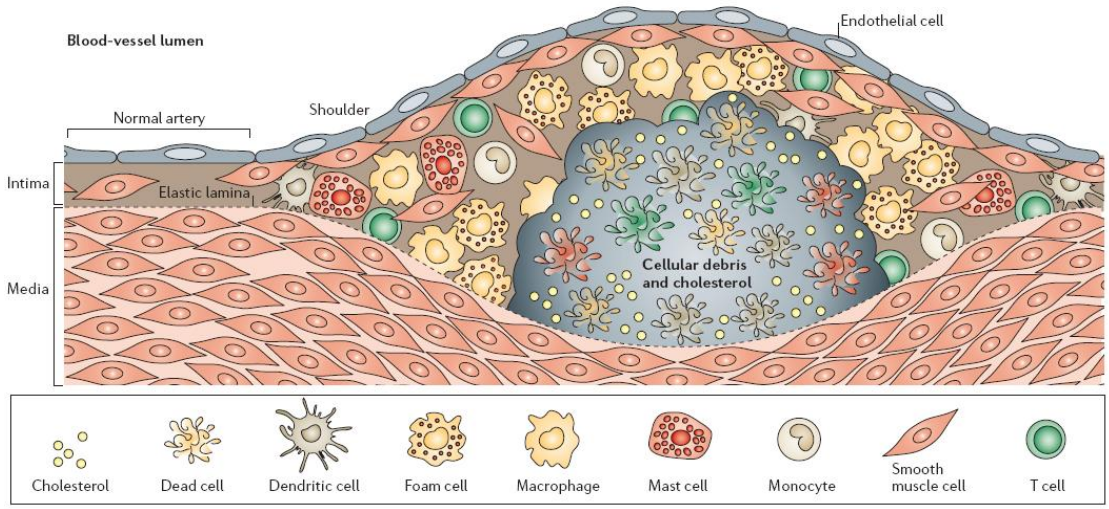

Figure 1.2: Composition of the mature atherosclerotic plaque. The atherosclerotic plaque has a core containing lipids (which include cholesterol esters and crystalline cholesterol) and debris from dead cells. Surrounding it, a fibrous cap containing smooth muscle cells, collagen fibres and extracellular matrix stabilize the plaque. Immune cells including macrophages, foam cells, T-cells and mast cells populate the plaque, and are frequently in an activated state. An intact endothelium covers the plaque unless rupture or erosion occurs. Göran K. Hansson and Peter Libby (2006)[4].

Once considered a lipid storage defect, atherosclerosis is now widely accepted to be due to a chronic inflammatory disease influenced by both genetic and environmental factors. However, hindered by the slow persistent nature of atherosclerosis exactly why and how this comes about remains unclear.

1.1.1: Activators of atherosclerosis

Recognised risk factors that can influence ones susceptibility to atherosclerosis include family history, smoking, hypertension, hypercholesterolemia, high plasma concentrations of low density lipoprotein (LDL), low plasma concentrations of high

density lipoprotein (HDL), lack of exercise, diabetes mellitus, obesity and autoimmune diseases such as rheumatoid arthritis and systemic lupus erythematosus[5-7]. The analysis of plaque composition revealed localised bacterial products and a significant upregulation of a number of components of the immune system, pulling inflammation into the limelight as a causative mechanism[8,9].

There have been a number of ligands associated with atherosclerosis. Recognised risk factors provide many endogenous activators (such as LDL and cholesterol), however a number of exogenous factors have more recently been associated with atherogenesis including those originating from bacterial and viral sources. It is proposed that these exogenous ligands cause inflammation in the arterial wall leading to, or initiating, plaque formation.

Surprisingly, infection has been implicated with atherosclerosis for more than 50 years. In 1960 Anitschkow *et al*.[10] identified macrophages and lymphocytes in the atherosclerotic plaque. This early identification of inflammation in atherosclerosis sparked little interest until sometime later. It was almost two decades after Anitschkow's discovery when Fabricant *et al*. (1978)[11] suggested a link between herpes virus and atherosclerosis. Fabricant *et al*. infected chickens with a poultry herpes virus named Marek's disease virus (MDV). It was shown that infection alone gave visible atherosclerotic lesions in large coronary arteries, aortas, and major aortic branches. In 1986 Jonasson *et al*.[9] published a paper demonstrating the presence of the immune cells macrophages and T-cells in the human atherosclerotic plaque which was still a novel concept, however this paper got a lot more interest that Anitschkow's in 1960. A number of studies have since confirmed a role for infection in the development of

atherosclerosis. For example, Lehr *et al*. (2001)[12] have demonstrated that repeated intravenous injection of *Escherichia coli* (*E.coli*) lipopolysaccharide (LPS) into hypercholesterolemic (atherosclerosis prone) rabbits accelerates the formation of atherosclerotic lesions. It is accepted now that elevated blood C-reactive protein (CRP), an acute phase protein that indicates inflammation, is indicative of increased risk of cardiovascular events[13,14]. Evidence for infection as a causative agent in plaque development is now overwhelming. In a large population study it was found that chronic infections such as those of the respiratory system, urinary tract and gums are linked with increased risk of atherosclerotic plaque development in the common carotid artery[15]. More specifically *Porphyromonas gingivalis* (*P.gingivalis*), *Helicobacter pylori* (*H.pylori*), *Chlamydia pneumoniae* (*C.pneumoniae*), herpes simplex virus (HSV), cytomegalovirus (CMV) and Epstein-Barr virus (EBV) have all been linked to atherosclerosis[16-25]. While the evidence for infectious inflammation is compelling, it has been shown that germ free mice can still develop atherosclerotic plaques[26]. This study could highlight the presence of non-infectious initiators of inflammation. Although infection may not be required for plaque formation, it is clear that it accelerates this process dramatically.

Consolidating a role for the immune system in atherogenesis are studies showing that immunization and vaccination against endogenous and exogenous factors respectively are associated with reduced disease state. Mice that were immunized with oxidised LDL were shown to have reduced atherosclerotic lesion development[27,28]. Also, mice that were immunized with peptides of apolipoprotein B-100, an important component of LDL, were observed to have reduced lesion area in comparison to controls[29]. In human

subjects a decreased probability of patients experiencing a second myocardial infarction (MI) was attributed to vaccination against influenza[7].

1.1.2: Atherosclerosis management

Although it is now widely accepted that atherosclerosis is an inflammatory disorder interestingly its treatment does not seem to address this. Patients at high risk of cardiovascular disease would be advised on life style changes, such as to stop smoking and increase exercise, and given "primary treatment". Primary treatment focuses only on the risk factors that are presented such as hypertension, raised serum lipids or hyperglycemia. For example, a GP will advise a patient on how and why they should reduce their serum cholesterol levels so they can reach an accepted target level set out in medical guidelines. (Optimal LDL cholesterol ≤100mg/dL {National Institutes of Health Publication No. 01-3670, May 2001}). Patients are closely monitored and the drug dose and selection is tailored for the individual.

Following an event such as a stroke or heart attack "secondary treatment" is commenced. The main difference from primary treatment being that all major risk factors are now treated, regardless of whether they are evident or not. For example, angiotensin-converting enzyme (ACE) inhibitors will be administered, regardless of blood pressure, as a protective measure and also statins (HMG-CoA reductase inhibitors) are administered regardless of blood cholesterol levels. Beta-blockers to reduce the prevalence of cardiac arrhythmias (a common cause of death following an event) and aspirin, which is not used in primary treatment due to its risk of gastrointestinal haemorrhage, used for its many properties such as blood thinning are also administered.

1.2: The immune system

Throughout life the human body is being constantly exposed to countless harmful pathogens that threaten health and survival. These organisms attempt to enter the body through epithelial surfaces such as the skin, respiratory tract, gastro-intestinal tract and genitourinary tract. The fast and efficient removal of these invading pathogens is performed by the immune system. This process is vital for existence in an environment full of potential hazards. The human immune system can be viewed as two delicately intertwined, yet functionally different, processes named the innate and adaptive immune systems.

1.2.1: Innate immune system

The innate immune system primarily involves anatomical barriers (skin), secreted antibacterial substances (such as lysozyme in tears/saliva), ciliary activity (such as cilia of the trachea which sweep mucus-caught foreign bodies out of the lungs), coughing and vomiting. The more complex role of the innate immune system involves germ-line encoded receptors that are able to recognise invading pathogens causing activation of inflammatory signalling cascades. Innate immunity is present from birth and does not improve in efficiency due to repeated exposure to a certain pathogen, as seen with adaptive immunity. The innate immune response is very fast where activation can be recorded within minutes; this reflects the rate at which a bacterium can colonise an environment. Bacteria that have a short proliferation rate have the potential of causing huge colony sizes in just one day, even from a single bacterium. Such infections could not be managed by the adaptive immune response for this requires at least four days for activation, by which time a bacterial colony for example could become well established with highly detrimental effects.

The innate immune system detects pathogens through molecular patterns that are expressed by, and unique for, infectious agents. These highly conserved motifs are named pathogen-associated molecular patterns (PAMPs) and are recognised as foreign to the body. PAMPs typically are molecular structures that are essential for survival and proliferation of a pathogen, thus their presence and recognition is inevitable. An example of some well established PAMPs are shown below.

PAMP	**Origin**
Lipopolysaccharide	Bacteria
Peptidoglycan	Bacteria
Lipoteichoic acid	Bacteria
CpG DNA	Virus
ssRNA	Virus

In conjunction with exogenous infectious agents it has been found that a number of non-infectious endogenous molecules are able to initiate an immune response causing sterile inflammation. Endogenous agents recognised by innate receptors include products of tissue stress released during necrotic cell death, oxidised LDL and products produced from extracellular matrix degradation. These ligands that are capable of mounting an immune response have been named damage-associated molecular patterns (DAMPs), for they are non-infectious and are often associated with injury.

PAMPs and DAMPs are detected through the germ-line encoded pattern recognition receptors (PRRs) which include Toll-like receptors[30] (TLRs), NOD-like receptors[31] (NLRs) and RIG-I-like receptors[32,33] (RLRs), the so called “trinity of innate sensors”. Binding of a PAMP or DAMP by a PRR causes the activation of intracellular signalling cascades that ultimately lead to the release of inflammatory cytokines that orchestrate pathogen removal, tissue repair and help induce an adaptive immune response.

1.2.2: Adaptive immune system

The adaptive immune response, in contrast to an innate immune response, is specific for a particular pathogen. This branch of the immune system mainly involves B-cells, T-cells and dendritic cells. This system works via generating a huge number of individual B-cell receptors and T-cell receptors through V-gene recombinations in the gene of the receptor that is expressed on the relevant cell. This system creates a vast arsenal of cells where one will inevitably have specificity for a PAMP expressed on an invading pathogen. When a B-cell detects an antigen the individual cell proliferates and generates plasma cells and memory cells. Plasma cells release antibodies relevant to the antigen recognised to orchestrate its clearance, whilst memory cells persist in the system ready for a second exposure to the same pathogen. From initial detection to a substantial immune response, via the generation and maturation of plasma and memory cells, it takes approximately four days. During secondary exposure the adaptive response is much faster, for memory cells to the particular antigen exist which expand immediately on pathogen recognition.

1.2.3: Immune system dysfunction

Although the immune system strives to protect the individual there are a number of cases where it does quite the opposite. Both Gram-positive and Gram-negative bacteria are able to cause the life threatening condition known as sepsis which is associated with systemic inflammation, circulatory failure and multiple organ dysfunction syndrome (MODS)[34,35]. Sepsis is the cause of the majority of deaths in surgical intensive care units[36]. A plethora of autoimmune diseases also have adverse effects. An autoimmune disease is where the immune system recognizes self antigens as foreign and thus attacks healthy tissue as it would if a PAMP was detected. Examples include; multiple

sclerosis, Graves' disease and Hashimoto's thyroiditis. The development of arterial atherosclerotic plaques in atherosclerosis is another example where the immune system does not function correctly.

1.3: Toll-like receptors

TLRs, one of the "trinity of innate sensors" (TLRs, NLRs and RLRs) are of great importance in pathogen recognition. There are ten known human TLRs which are type 1 transmembrane germ-line encoded protein receptors of the innate immune system. These receptors serve to recognise the vast array of molecular patterns expressed by invading pathogens and orchestrate their immediate removal.

The field of TLR research is relatively new and rapidly expanding. The emergence of the many roles of TLRs in a number of diseases and disorders has made them exciting therapeutic targets. The discovery of TLRs has enabled researchers to answer many questions in the area of infection and immunity, but in doing so has created many more.

1.3.1: A history of TLRs

In 1985 Dr. Nüesslein-Volhard screened *Drosophila melanogaster* for embryonic polarity genes[37]. She found one receptor that was clearly involved in the establishment of the dorsal-ventral axis of the developing embryo named Toll. Embryos that lacked Toll gene activity lost their dorsal-ventral distinction and appeared "toll", which loosely translated from German to English means "weird". When searching for proteins similar to *D.melanogaster* Toll, Gay *et al*.(1991)[38] found homology between the cytoplasmic domains of Toll and the human interleukin-1 receptor (hIL-1R). The reason for the 135 amino acid homology seen between a receptor involved in fly embryo development (Toll) and one involved in human inflammation (hIL-1R) was a mystery. Here Gay *et*

al. (1991)[38] also described the extracellular portion of Toll as containing leucine-rich repeats (LRRs). In 1996 Lemaitre *et al*.[39] found a direct role for Toll in *D.melanogaster* immunity to fungal infection. Lemaitre *et al*. infected Toll deficient adult flies with *Aspergillus fumigates* and observed 100% mortality within 3 days. Wild-type and un-infected Toll deficient adult flies had ~10% mortality, this study demonstrated the direct importance of Toll in protecting the fly against infection.

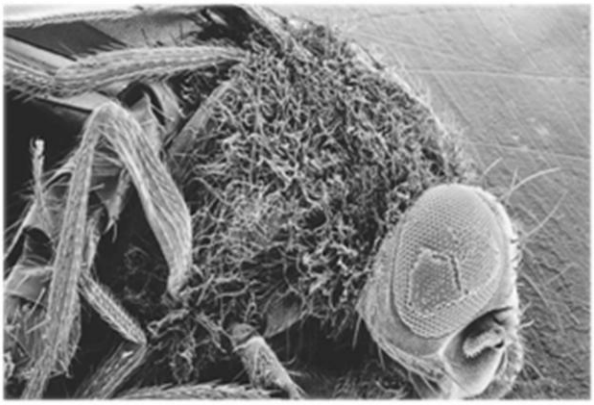

Figure 1.6: Scanning electron micrograph of germinating hyphae of *A.fumigates* on a dead *D.melanogaster* succumbed to the infection (200X magnification). Lemaitre *et al*. (1996)[39].

It was in 1997 when Medzhitov & Janeway discovered a human Toll homologue sharing homology with *D.melanogaster* Toll over the entire length of the protein chain[40]. The next year Rock *et al*. (1998)[41] described 5 human Tolls which were coined here as TLRs, and named them TLR1-5. In 1998 LPS of Gram-negative bacteria was discovered to be a ligand for TLR4 by Poltorak *et al*.[42]. It was found that mice with a missense mutation in TLR4 survived fatal LPS induced sepsis, linking TLRs and infection. TLR6 was discovered the following year by Takeuchi[43]. Human TLR7, TLR8 and TLR9 were described in 2000 by Chuang[44], who further discovered Human TLR10[45] the following year.

1.3.2: The TLR

TLRs are expressed on cells in areas that encounter invading organisms. These receptors are abundantly expressed by macrophages, neutrophils, dentritic cells and the epithelial cells lining the lung and gut. The activation of TLRs in multicellular organisms causes an inflammatory response via the activation of the transcription factors of the nuclear factor kappa-light-chain-enhancer of activated B-cells (NF-κB) and interferon regulatory factor (IRF) families which regulate the transcription of inflammatory mediators. This process orchestrates the immune response and helps induce an acquired immune response. The pattern of TLR activation is representative of the pathogen present. This signal is translated across the plasma membrane in such a way allowing appropriate action against the type of pathogen that has been identified.

1.3.2.1: TLR structure

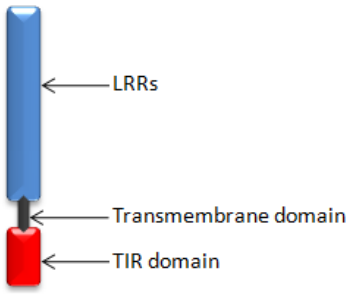

Figure 1.7: TLR family basic structure. The extracellular domain consists of 18-24 LRRs at the N-terminus. The cytoplasmic domain contains the Toll/interleukin-1 receptor homology domain (TIR) at the C-terminus. The LRRs form a right-handed super helix that creates the binding site for a PAMP or DAMP.

TLRs have between 18 and 24 multiple LRRs and a cysteine-rich domain (60 amino acids) which is proximal to the cell membrane in their extracellular domain at the N-terminus. The cytoplasmic domain contains a region of ~200 amino acids named the Toll/interleukin-1 receptor (TIR) homology domain, which is involved in signal transduction at the C-terminus[46]. The LRRs in the extracellular domain are around 20-

29 amino acids in size, with a conserved pattern of hydrophobic amino acids. The LRRs form a right-handed super helix that forms a horse shoe shaped surface of the extracellular domain, which is thought to create the binding site for PAMPs and DAMPs.

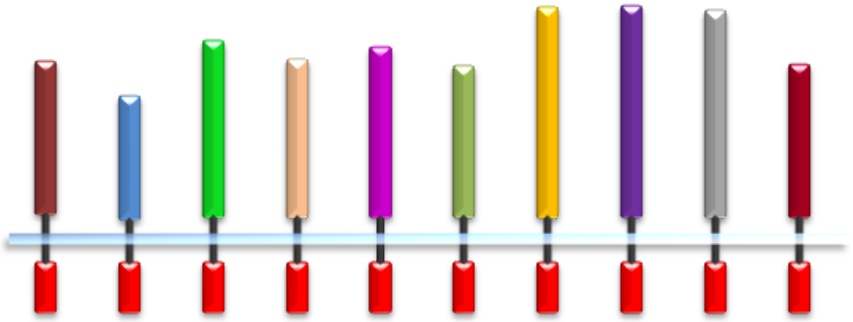

	TLR1	TLR2	TLR3	TLR4	TLR5	TLR6	TLR7	TLR8	TLR9	TLR10
Chromosomal location	4p14	4q22	4q35	9q22-33	5q33	4p14	Xp22	Xp22	3p21	4p14
No of amino acids	796	704	904	830	880	798	1040	1041	1022	811
Molecular weight (KDa)	84	84	97	90	91	91	121	120	116	95

Figure 1.8: TLR protein structure. All of the TLRs are Type 1 transmembrane proteins possessing a variable number (18-24) of N-terminal LRRs followed by a cysteine-rich domain, a transmembrane domain, and an intracellular TIR domain. The variation in amino acid number and molecular weight of the different TLRs is most significantly contributed by differences in the numbers of LRRs. Chromosomal locations for each of the TLRs are also given. Adapted from: R&D Systems Catalog (01/01/04).

1.3.2.2: TLR distribution

TLR homodimers and heterodimers recognise a large array of PAMPs and DAMPs. TLRs 1, 2, 4, 5, 6 and 11 are all present on the cell surface membrane with their LRR domain facing into the extracellular space. TLRs 3, 7, 8 and 9 are present in the endosomal membrane with their LRR domain facing into the endosomal compartment. TLR homo- and heterotypic associations are summarized below in Figure 1.9 with example ligands. For a comprehensive list of TLR ligands see Section 1.3.4.

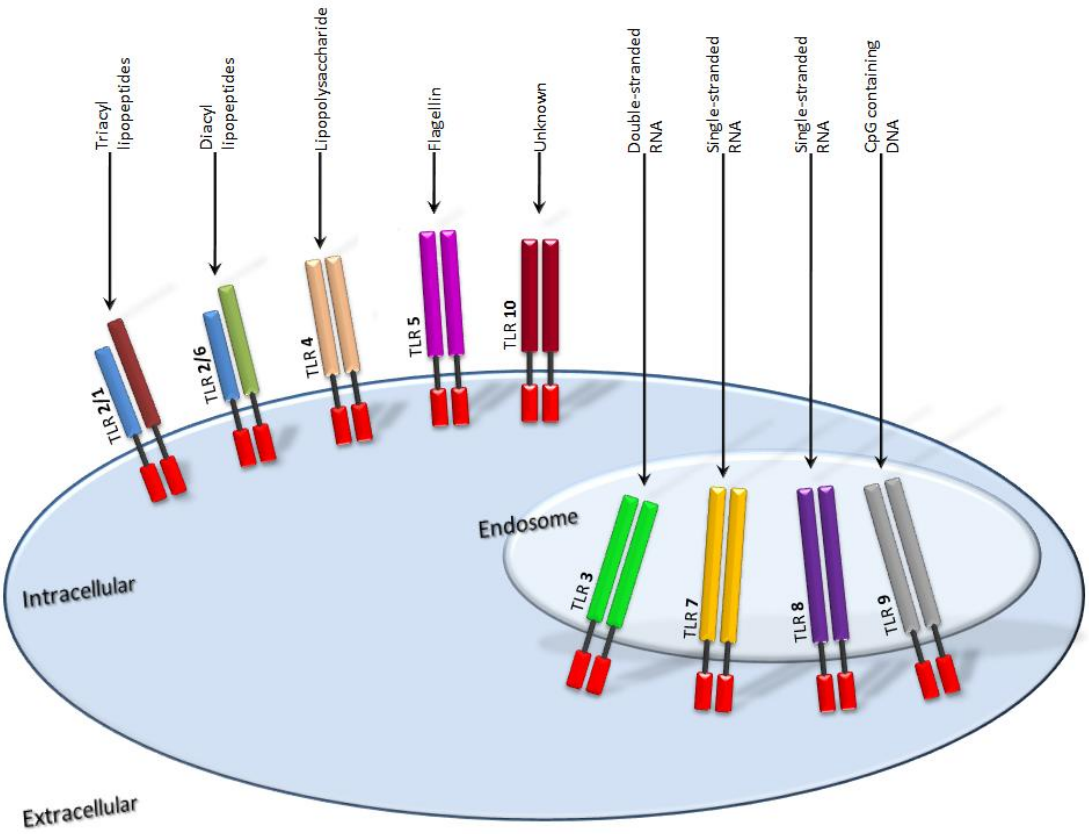

Figure 1.9: Summary of the TLRs and their ligands. Different TLRs recognise different PAMPs. Some form heterodimers to facilitate PAMP recognition. TLRs 1, 2, 4, 5, 6 and 11 are all present on the cell surface membrane. TLRs 3, 7, 8 and 9 are present in the endosomal membrane, with the intracellular domain in the cytosol, and extracellular domain in the endosome.

1.3.3: Individual TLRs

Since the discovery of the first human Toll homologue by Medzhitov & Janeway in 1997[40], and the subsequent discovery of the remaining members of the human TLR family[41,43-45], much research has gone into their structure, ligands and functional significance in a vast range of diseases and disorders. Information obtained from such research has proven fruitful with the creation of a number of successful TLR based therapeutics. For example, TLR targeted molecules have been used to combat basal cell carcinoma[47] and as an adjuvant in a Hepatitis B vaccine[48].

The evolutionary relationship, or family clustering, of TLRs seems to directly relate to their ligands and associations with one another. The cluster of TLRs 1, 2, 6 and 10, with the exception of TLR10 for which a ligand and use has yet to be uncovered, coincides with their heterotypic associations. TLRs 3, 7, 8 and 9 are closely related and so are their localisation and ligands.

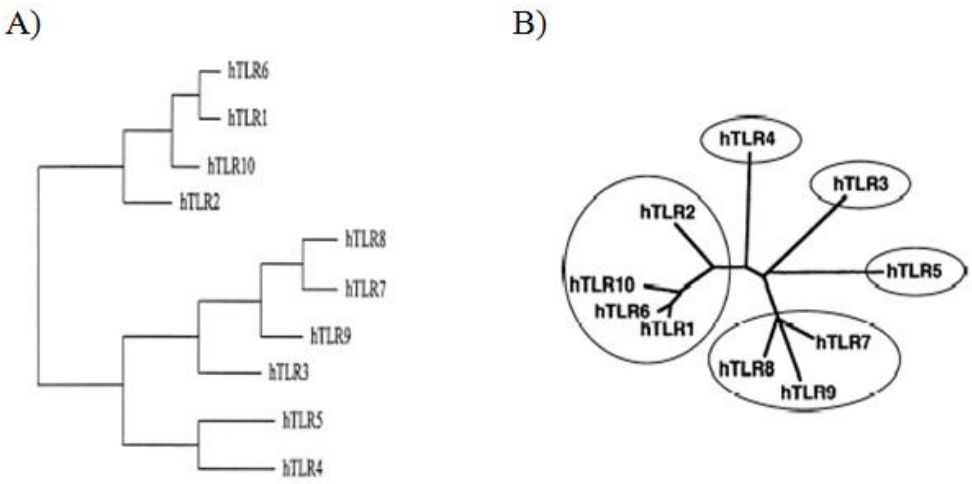

Figure 1.10: TLR relationships. A) Evolutionary relationships of TLRs represented by a phylogenetic tree derived from whole-sequence comparisons of all 10 TLRs. Chuang *et al*. (2001)[45]. B) Family clustering of TLRs. Takeda *et al*. (2003)[49].

The field of TLR research is relatively young with new mechanisms of action, ligands and interactions being continuously discovered and scrutinised. The TLRs have been extensively researched uncovering many potential therapeutic targets.

1.3.3.1: TLR2, TLR1 and TLR6

TLR2 is capable of forming heterodimers with TLR1 and TLR6. TLR2 has also been shown to interact with receptors that are not in the TLR family such as dectin-1, CD14 and CD36[50,51]. The ability of TLR2 to form heterodimers with other receptors allows it

to have a wide range of molecular components that it can recognize. TLRs 2, 1 and 6 are expressed on the cell surface.

TLR2, in conjunction with TLR1 or 6, recognizes a large number of different PAMPs and DAMPs, including lipoteichoic acid (LTA) from Gram-positive bacteria cell walls such as *Staphylococcus aureus* (*S.aureus*) and *Streptococcus pneumoniae* (*S.pneumoniae*)[52], peptidoglycan (PG) from *S.aureus*[53], lipopeptides and lipoproteins[54], host heat shock protein 70 (HSP70), lipoarabinomannan from mycobacteria, glycosylphosphatidylinositol anchors, phenol-soluble modulin, zymosan and glycolipids. Recently it has been shown that TLR2 can also bind the unconventional LPS found on the Gram-negative bacteria *P.gingivalis*[51], *H.pylori*[55] and *C.pneumoniae*[19], LPS is otherwise a well established TLR4 agonist.

Subtle changes in ligand have been shown to alter TLR2 heterodimers illustrating the sensitivity of the innate sensing of pathogens through TLR2. The TLR2/TLR1 heterodimer can recognise mycoplasma-derived diacyl lipopeptides but does not recognise triacyl lipopeptides[50]. In contrast the TLR2/TLR6 heterodimer can recognise triacyl lipopeptides but do not recognise diacyl lipopeptides[50].

In 2007 the crystal structure of the human TLR2/TLR1 heterodimer, bound to the tri-acylated lipopeptide Pam_3CSK_4, was uncovered in Korea by Jin *et al.*[56]. This discovery confirmed many hypotheses about signal transduction. Using the crystal structure Jin *et al*. propose that the formation of the heterodimer brings the intracellular TIR domains in close proximity therefore promoting dimerization and activation of these domains allowing initiation of the intracellular signalling cascade.

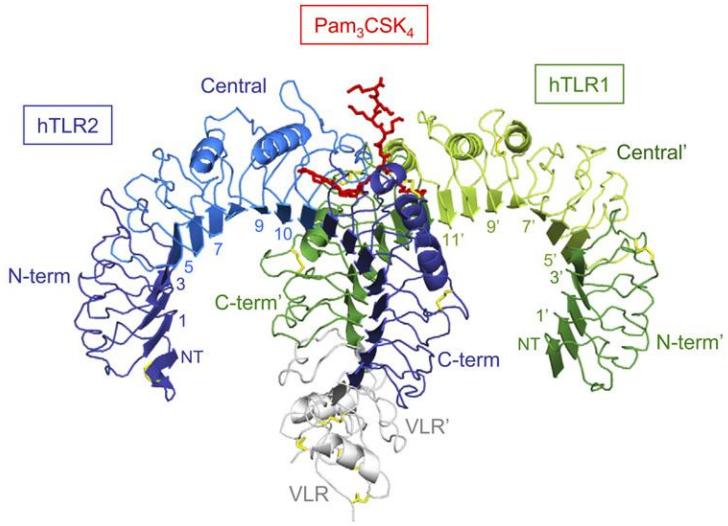

Figure 1.11: The structure of the human TLR2 (blue)/TLR1 (green) heterodimer ectodomains associated with the tri-acylated lipopeptide Pam_3CSK_4 (red). TLRs have amino-terminus (N-term) LRRs for ligand binding and a carboxy-terminus (C-term) intracellular TIR homology domain for signal transduction. pdb-2Z7X.. Jin *et al.* (2007)[56].

1.3.3.2: TLR3

TLR3 is located in the endosomal membrane with the LRR domain inside the endosome and TIR domain in the cytosol (Figure 1.9). This endosomal receptor is involved in the recognition of double-stranded ribonucleic acid (dsRNA). Alexopoulou *et al.* (2001)[57] demonstrated that mice deficient in TLR3 had a lowered ability to respond to dsRNA. Recently it has been found that TLR3 can also recognise viral single-stranded RNA (ssRNA) produced during the replication of dsRNA viruses[58]. A synthetic analogue of dsRNA named polyinosinic-polycytidylic acid (poly {I-C}) is recognised by TLR3 and is widely used in TLR research, this molecule is also being analysed for its potential as a therapeutic agent[59].

In 2008 Liu *et al.*[60] determined the crystal structure of the extracellular domains of a mouse TLR3 dimer bound with dsRNA, to a 3.4Å resolution (Figure 1.12). Both the C-

and N-terminal of each TLR3 in the dimer interact with dsRNA bringing the C-terminals together possibly causing the intracellular TIR domains to become in close proximity initialising signalling.

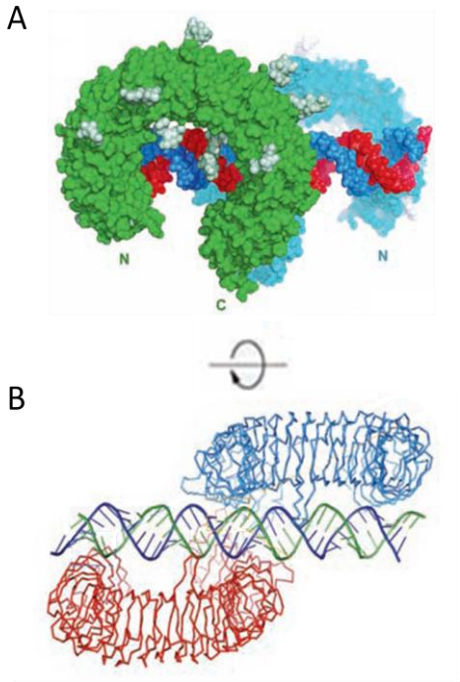

Figure 1.12: The binding of the ectodomains of the mouse TLR3 homodimer associated with double stranded RNA (dsRNA). A) Side view: TLR3 homodimer in green and cyan, dsRNA in blue and red. B) Top view: TLR3 homodimer in red and cyan, dsRNA in blue and green. pdb-3CIG. Adapted from Liu *et al*. (2008)[60].

1.3.3.3: TLR4

TLR4 is well researched and documented in the recognition of LPS[42,61], a component of the Gram-negative bacteria cell wall (Section 1.3.3.1.2). LPS recognition via TLR4 involves LPS-binding protein (LBP)[62], CD14[63] and MD-2[64]. LBP binds LPS and transfers it to CD14, CD14 then facilitates the transfer of LPS to the TLR4 signalling complex[65]. In response to LPS, TLR4 has been shown to associate in receptor clusters with proteins such as MD2, HSP70, CD11b/CD18 and CXCR4[66-69]. TLR4 is also

involved in the recognition of ligands such as the envelope protein of mouse mammary tumour virus[70] and glycoinositolphospholipids from *Trypanosoma*. It has long been thought that TLR4 does not associate with other TLRs. However, Stewart *et al*. (2010)[71] have recently proposed a TLR4/TLR6 heterodimer, which involves the scavenger receptor CD36[72], in response to oxLDL[73].

Due to the strength of LPS as an immune-activator only very small concentrations (pg/ml) are required for a response via TLR4, for this reason LPS contamination is not unknown. It is suspected that TLR4 is responsible for detecting endogenous ligands such as fibrinogen and HSP60 (Table 1.1). However, data concerning TLR4 activation via endogenous ligands has to be carefully analyzed. Endogenous ligands are required in high concentrations to activate a response via TLR4, the concentrating and expression of proteins in bacteria greatly increases risk of LPS contamination. It has been shown that studies observing the activation of TLR4 by endogenous ligands, such as HSP60 and HSP70, could be inaccurate due to LPS contamination, even in commercial preperations[74].

In 2007 Kim *et al*.[75] published the crystal structure of mouse TLR4 ectodomain as a heterodimer with MD-2, in a 1:1 ratio, bound to Eritoran in the journal Cell. In this paper a model of LPS induced TLR4-MD-2/TLR4-MD-2 homodimerization is proposed which induces intracellular signalling. Eritoran is a lipid A (the immunogenic component of LPS, see section 1.3.3.1.2) derivative which acts as a TLR4 antagonist.

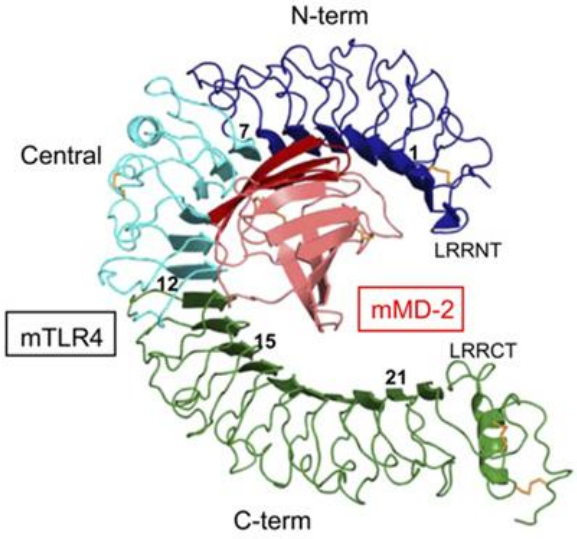

Figure 1.13: The structure of mouse TLR4 ectodomain bound to MD-2 in a 1:1 ratio. The amino-terminus (N-term), central, and carboxy-terminus (C-term) domains of TLR4 are coloured in blue, cyan, and green, respectively. MD-2 is shown in pink and red, and the LRRs modules of TLR4 are numbered. C-term is proximal to the membrane. pdb-2Z64. Kim *et al*. (2007)[75].

1.3.3.4: TLR5

TLR5 is responsible for the recognition of flagellin, a protein component of the flagella present on motile bacteria[76]. TLR5 is expressed on the basolateral side of intestinal epithelial cells, intestinal endothelial cells of the sub-epithelial compartment and on lung epithelial cells[76,77].

1.3.3.5: TLR7 and TLR8

TLR7 and TLR8 are very similar in structure and are located in the endosomal membrane with the LRR domain inside the endosome and TIR domain in the cytosol (Figure 1.9). These receptors are both responsible for the detection of viral (uridine-rich) single stranded RNA[78,79] (ssRNA). More specifically it is proposed that human TLR7 (hTLR7) and hTLR8 are involved in sequence specific recognition of ssRNA where uridine location rather that quantity is recognized[80]. It is also proposed that

hTLR7 is the main sensor of ssRNA with hTLR8 having a regulatory role on this detection[80].

TLR7 and TLR8 recognise the small synthetic immune modulating agents imidazoquinolines[81,82]. An imidazoquinoline named Imiquimod, which is marketed by 3M Pharma, has been highly successful in the treatment of papilloma-induced genital warts and basal cell carcinoma[47].

1.3.3.6: TLR9

TLR9 recognizes foreign deoxyribonucleic acid (DNA), this receptor is located in the endosomal membrane with the LRR domain inside the endosome and TIR domain in the cytosol (Figure 1.9). Studies of TLR9 knock-out mice have shown that TLR9 is responsible for the recognition of cytosine-phosphate-guanosine (CpG) DNA motifs that are found in the DNA of bacteria and DNA viruses, but not in humans[83]. The CpG motif consists of unmethylated dinucleotide CpG flanked by two 5` purine residues and two 3` pyrimidines. It is proposed that due to the high methylation of DNA in vertebrates TLR9 is not activated by "self" DNA. However in 2006 it was published in Nature Immunology by Medzhitov *et al.*[84] that the localisation of TLR9, rather than CpG motif specificity, allowed discrimination between "self" and "non-self" nucleic acids. It was proposed that host DNA does not come into contact with TLR9 for it is expressed in endosomal compartments. Fusion of TLR9 extracellular domain with TLR4 transmembrane and cytosolic domain caused expression of TLR9 (extracellular domain) on the cell surface which could be activated by endogenous "self" DNA[84]. This demonstrates that TLR9 can in fact bind "self" DNA but is physically kept away from it, through evolution, for this very reason.

Hemozoin, a hydrophobic haeme polymer which is derived from the digestion of haemoglobin by malaria parasites, is also capable of cellular activation through TLR9. Macrophages and dentritic cells are activated by hemozoin through TLR9 causing inflammatory cytokine and chemokine release[85].

1.3.3.7: TLR10

TLR10 is expressed in humans but not in mice. The ligand for, and cascade activated by, TLR10 is unknown.

1.3.3.8: TLR11

TLR11 is expressed in mice but not in humans. TLR11 is the most recently identified TLR. TLR11 is involved in the resistance to infection by uropathogenic bacteria in mice[86]. The ligand for this receptor has not yet been identified, nor has a human homologue. It is theorised that TLR11 in humans was unnecessary due to environmental factors and thus lost through evolution.

1.3.4: TLR ligands

TLRs homodimerize and heterodimerize to recognize a vast array of PAMPS and DAMPs (Table 1.1).

Receptor	Ligand	Origin of ligand
TLR1	Triacyl lipopeptides	Bacteria and mycobacteria
	Soluble factors	*Neisseria meningitidis*
TLR2	Lipoprotein/lipopeptides	Various pathogens
	Peptidoglycan	Gram-positive bacteria
	Lipoteichoic acid	Gram-positive bacteria
	Lipoarabinomannan	Mycobacteria
	Phenol-soluble modulin	*Staphylococcus epidermidis*
	Glycoinositolphospholipids	*Trypanosoma cruzi*
	Glycolipids	*Treponema maltophilum*
	Porins	*Neisseria*
	Atypical lipopolysaccharide	*Leptospira interrogans*
	Atypical lipopolysaccharide	*Porphyromonas gingivalis*
	Zymosan	Fungi
	Heat-shock protein 70*	Host
TLR3	Double-stranded RNA	Viruses
TLR4	Lipopolysaccharide	Gram-negative bacteria
	Taxol	Plants
	Fusion protein	Respiratory syncytial virus
	Envelope protein	Mouse mammary-tumour virus
	Heat-shock protein 60*	*Chlamydia pneumoniae*
	Heat-shock protein 70*	Host
	Type III repeat extra domain A of fibronectin*	Host
	Oligosaccharides of hyaluronic acid*	Host
	Polysaccharide fragments of heparan sulphate*	Host
	Fibrinogen*	Host
TLR5	Flagellin	Bacteria
TLR6	Diacyl lipopeptides	*Mycoplasma*
	Lipoteichoic acid	Gram-positive bacteria
	Zymosan	Fungi
TLR7	Imidazoquinoline	Synthetic compounds
	Loxoribine	Synthetic compounds
	Bropirimine	Synthetic compounds
	Single-stranded RNA	Viruses
TLR8	Imidazoquinoline	Synthetic compounds
	Single-stranded RNA	Viruses
TLR9	CpG-containing DNA	Bacteria and viruses
TLR10	N.D.	N.D.
TLR11	N.D.	Uropathogenic bacteria

Table 1.1: The TLRs, their ligands and ligand source. *Ligand preparations could have been contaminated with LPS. Adapted from Akira and Takeda (2004)[87].

1.3.4.1: Bacterial PAMPs

Bacteria are unicellular prokaryote microorganisms consisting of many members of various shapes and sizes. However, all bacteria display PAMPs that can be recognised by TLRs.

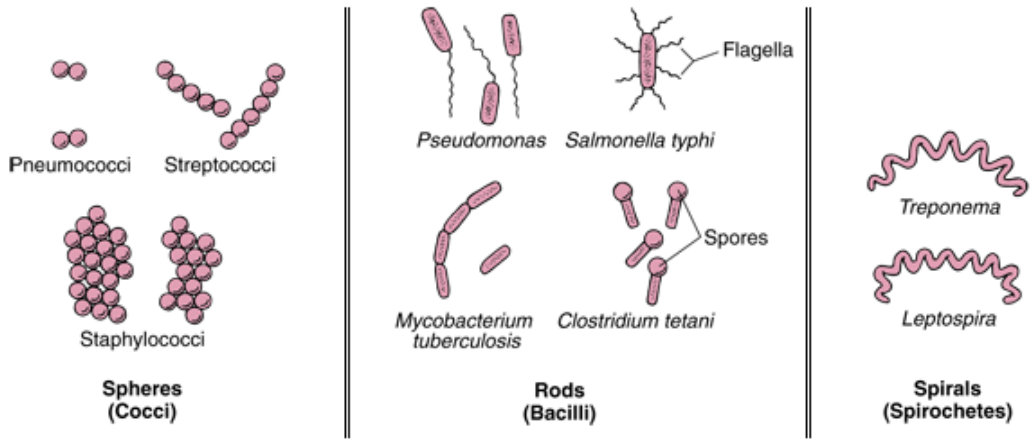

Figure 1.14: Schematic diagram of bacterial shapes and names (not to scale). Adapted from: www.merck.com/mmhe/sec17/ch190/ch190a.html?qt=bacterial%20shapes&alt=sh (19/06/10).

Bacteria can be split into two main groups; Gram-positive and Gram-negative. This separation is due to the composition of their cells walls as determined by the Gram stain test[88]. Gram-positive bacteria cells have a characteristic thick cellular wall due to a large amount (50-90%) of PG (Figure 1.15) in comparison to the 5-10% found in Gram-negative bacteria cell walls (Figure 1.17). Gram-positive bacteria are so called due to a positive result from the Gram's staining method. The large amount of PG in the Gram-positive bacteria cell wall retains the stain giving rise to a positive (purple) result. Gram-negative bacteria cell walls contain less PG and as a result are less capable of retaining the stain giving a negative (pink) result.

Gram-positive and Gram-negative bacteria can differ considerably. These can cause different types of infections, and different types of antibiotics are effective against them. Thus it is very important to determine which type of bacteria has caused an infection in a patient. The prototypic PAMPs found on Gram-positive and Gram-negative bacteria are LTA and LPS respectively.

1.3.4.1.1: Lipoteichoic acid

LTA is an immunostimulatory PAMP found on Gram-positive bacteria cell walls. The cell wall is also made up of LTA, PG, polysaccharides, teichoic acid and other proteins. These serve the purpose of membrane transport regulation, cell shape and expansion of the bacterium. The components of Gram-positive bacteria that have been shown to cause an inflammatory response are PG and LTA[52].

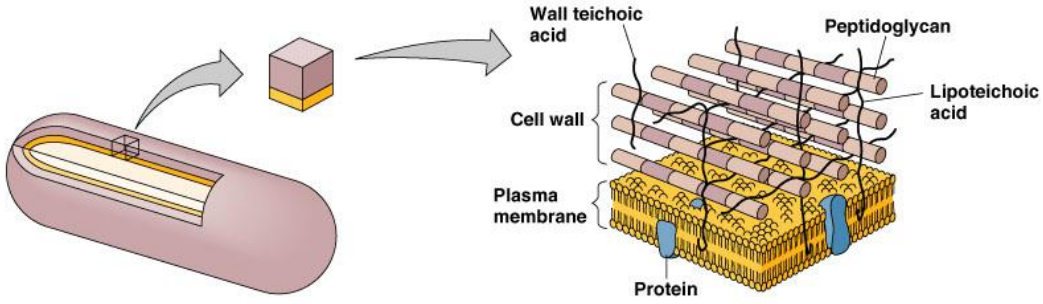

Figure 1.15: The Gram-positive bacteria cell wall. The cell wall is made up of LTA, PG, teichoic acid, polysaccharides and other proteins. These serve the purpose of membrane transport regulation, cell shape and expansion of the bacterium. Both LTA and PG are recognised by the innate immune system and are immunostimulatory. www.classes.midlandstech.edu/carterp/Courses/bio225/chap04/ss 4.htm (04/04/10).

LTA is an amphiphillic molecule that is hydrophobically anchored to the membrane of the cell-surface of Gram-positive bacteria[52]. There are a number of different LTAs found on different bacteria; however these are all structurally related macroamphiphiles. LTA toxin is released by Gram-positive bacteria, mainly due to bacteriolysis (the breakdown of bacteria cells) and cell growth/expansion.

All LTAs share a common structure; they have a diacylglycerol-containing glycolipid anchor and a covalently coupled polymeric backbone. The polymeric backbone consists of repeating units and is the cause of the variance of LTA found in different strains of Gram-positive bacteria. The polymeric backbone of LTA observed on the prototypic

Gram-positive bacteria *S.aureus* consists of repeated units of D-alanine (75-80%) and alpha-D-N-acetylglucosamine (≤10%) linked to a central linear 1,3-linked polyglycerophosphate chain of 25 glycerophosphates[89,90]. The polymeric backbone is covalently linked to a diacylglycerol-containing glycolipid anchor[91].

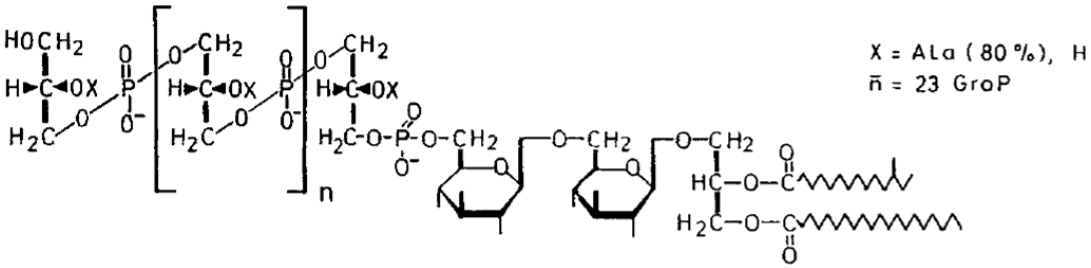

Figure 1.16: LTA from *S.aureus*. The polymeric backbone (D-alanine shown here as Ala {75-80%} and alpha-D-N-acetylglucosamine {≤10%} linked to a central linear 1,3-linked polyglycerophosphate chain of 25 glycerophosphates) is covalently linked to a diacylglycerol-containing glycolipid anchor. Fischer (1994)[90].

1.3.4.1.2: Lipopolysaccharide

LPS is an immunostimulatory PAMP found on Gram-negative bacteria cell walls. Gram-negative bacteria cell walls contain LPS, PG, lipoproteins, phospholipids and other proteins. LPS is highly immunogenic even at pg/ml concentrations.

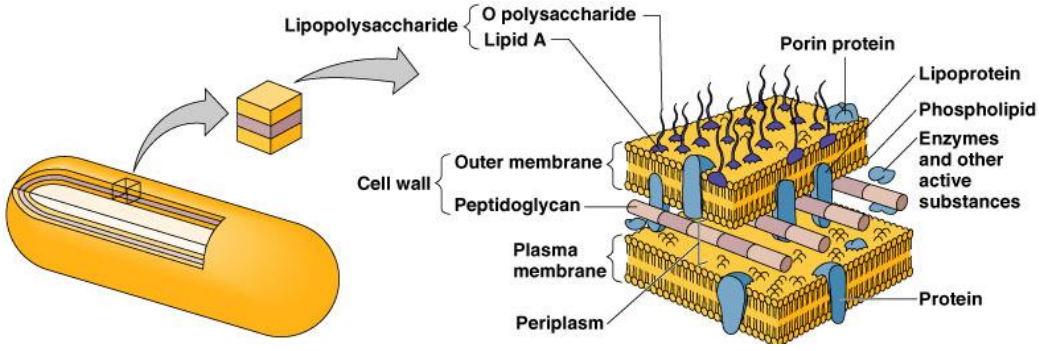

Figure 1.17: The Gram-negative bacteria cell wall. The cell wall is made up of LPS, PG, lipoproteins and other proteins. These serve the purpose of membrane transport regulation, cell shape and expansion of the bacterium. Both LPS and PG are recognised by the innate immune system and are immunostimulatory. www.classes.midlandstech.edu/carterp/Courses/bio225/chap04/ss4.htm (04/04/10).

LPS molecules consist of a lipid component covalently attached to a polysaccharide. The lipid component is named lipid A (endotoxin), it is hydrophobic and thus membrane bound anchoring the LPS molecule to the membrane. Lipid A is relatively conserved in comparison to the highly variable O-specific chain (O-antigen) of the attached polysaccharide (Figure 1.18). Interestingly the membrane bound lipid A has been shown to be the immunogenic component of the LPS molecule, not the projecting polysaccharide[92]. The hydrophilic polysaccharide unit is composed of a core and O-specific chain. The core contains an oligosaccharide and can contain phosphates, amino acids and sugars such as 2-keto-3-deoxyoctulosonic acid (Figure 1.18). The O-specific chain is highly variable giving rise to different Gram-negative bacterial strains. For example, more than 160 different O-specific chain structures have been identified in various *E.coli* strains alone[93].

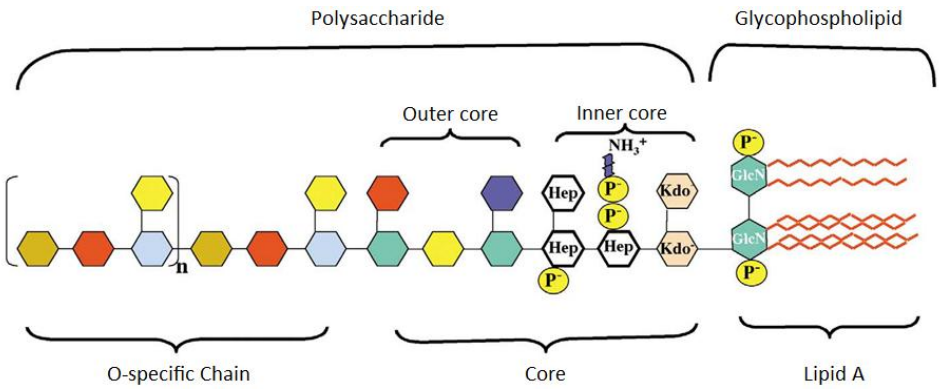

Figure 1.18: Schematic diagram of Gram-negative LPS. Abbreviations: Glucosamine (GlcN), 2-keto-3-deoxyoctulosonic acid (Kdo), L-glycero-D-*manno*-heptose (Hep), phosphate (P), ethanolamine (EtN) and zig-zag lines represent fatty acids. Adapted from Caroff *et al.* (2002)[94].

1.3.4.2: Host DAMPs

There are a number of non-infectious endogenous molecules capable of initiating an immune response. These molecules are often associated with injury and cause sterile inflammation in much the same manner as PAMPs. The non-infectious nature of these

molecules, but similarities to PAMPs, has led them to be named DAMPs. DAMPs recognised by receptors of the innate immune system include products of tissue stress released during necrotic cell death, oxidised LDL and products produced from extracellular matrix degradation. The DAMP of interest in this study of the molecular cause of atherosclerosis is LDL and its oxidised derivatives.

1.3.4.2.1: Low density lipoprotein

Lipoproteins allow the transport of water insoluble cholesterol and triglycerides within the blood. These have a non-polar core with a coating of amphiphillic molecules that allow the transport of water insoluble components. There are five main groups of lipoproteins named chylomicrons, very low density lipoprotein (VLDL), intermediate density lipoprotein (IDL), LDL and high density lipoprotein (HDL).

LDLs are the main carriers of cholesterol through the blood system. LDL particles are known as “bad cholesterol” for they are responsible for the deposition of cholesterol in arterial walls, which can lead to atherosclerosis. HDL on the other hand is known as “good cholesterol” for these transport cholesterol from the plasma to the liver for its catabolism and clearance, reducing the chance of plaque formation. For this reason elevated LDL serum levels and low HDL levels are two risk factors associated with atherosclerosis, and are routine checks for inquiring clinicians.

LDLs are structured particles with an average diameter of 20nm and a weight within 1.019-1.063g/ml[95]. The LDL core consists of approximately 5% triglyceride, 40% cholesteryl ester and 10% unesterifed cholesterol. The surface layer of LDL consists of approximately 20% phospholipid molecules and a single copy of apolipoprotein B-100

(apoB-100)[95,96]. Like all apolipoproteins, apoB-100 is an amphipathic molecule in that it has both hydrophobic and hydrophilic regions. A single copy of apoB-100 encircles the LDL particle, this protein is responsible for binding the LDL receptor that is expressed on cells that require cholesterol[97].

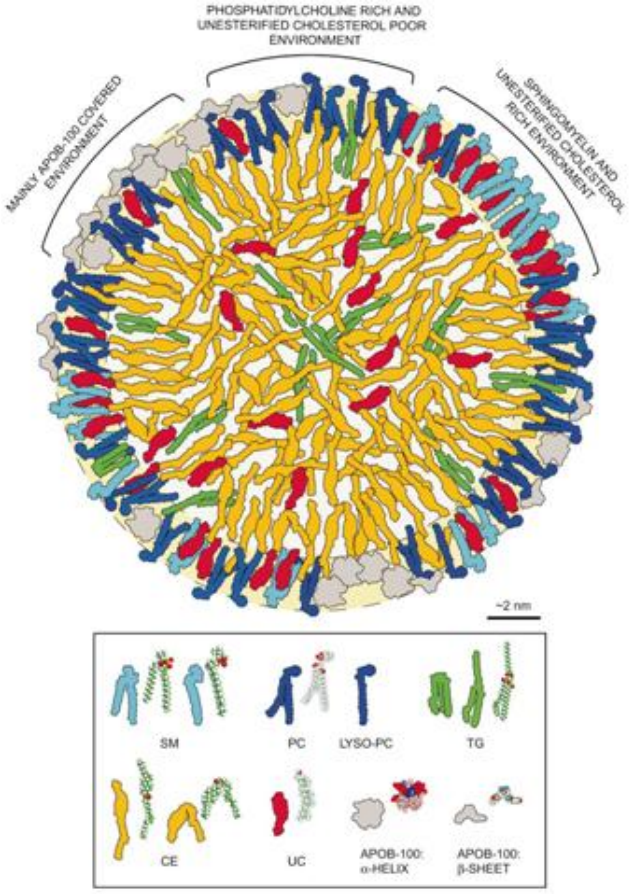

Figure 1.19: Schematic model of LDL at body temperature. LDL has an average diameter of 20 nm, with composition of 20% protein, 20% phospholipids, 40% cholesteryl ester (CE), 10% unesterifed cholesterol (UC), and 5% triglyceride (TG) on average. Sphingomyelin (SM), phosphatidylcholine (PC), lysophosphatidylcholine (LYSO-PC). LDL particles have a single copy of apoB-100. The molecular components of the particle are drawn in both the correct percentages and size ratios. Hevonoja *et al*. (2001)[96].

Under physiological conditions LDL can undergo oxidative modification[98] forming minimally modified LDL (mmLDL) and/or oxidised LDL (oxLDL). oxLDL has been shown to be immunogenic being associated with atherosclerosis and more specifically foam cell (lipid laden macrophage) formation; a major component of the atherosclerotic

plaque (Figure 1.2)[99]. It has been shown that human monocyte-derived macrophages respond to oxidised LDL but not to native LDL, causing upregulation of TLR4[100]. CD36 scavenger receptors (SRs) expressed on macrophages bind modified lipids and are involved in their endocytic internalization which, if dysregulated, can result in foam cell formation as seen in the atherosclerotic plaque[73,101,102]. However, some studies have suggested a protective role for oxLDL where it can reduce ligand activation of TLRs 2 and 4[103,104].

Another receptor for oxLDL is named lectin-like oxidized LDL receptor-1 (LOX-1) which is expressed primarily on endothelial cells. LOX-1 expression is upregulated by a number of factors such as oxLDL itself[105]. This endothelial receptor is involved in the binding, internalization and degradation of oxLDL[106].

Due to the size and composition of LDL its oxidised counterpart can contain large numbers of modified structures, termed "oxidation specific" epitopes[107]. When oxidised, these structures can turn from endogenous "self antigens" to "non-self" rendering them immunogenic. Since these ligands are capable of mounting an immune response yet, unlike a PAMP, they are non-infectious they are classed as DAMPs. As well as a major source of cholesterol, LDL is also a major source of extracellular phospholids which can become modified. Phospholipids, which make up 20% of LDL, can become oxidised forming molecules such as oxidized 1-palmitoyl-2-arachidonoyl-*sn*-glycero-3-phosphorylcholine (OxPAPC) and 1-palmitoyl 2-(59-oxovaleroyl) phosphatidylcholine (POVPC)[99]. It is these that are thought to cause the DAMP qualities of LDL. It has been shown that protein (such as apoB-100) as well as lipid

components of oxidised LDL are also recognised by macrophages[108], it has been demonstrated that these interactions act primarily through CD36[109] (Section 1.3.5.2).

1.3.5: TLR extracellular adapter molecules

Although TLRs are the principle detectors of PAMPs, they require adapter molecules for their effective activation. The efficacy of TLR activation is greatly enhanced by the presence of these adapter molecules. Receptor clusters can be vast, for example TLR4, CD14, CD36, CD11b/CD18, CD55, CD16a, CD32, CD64, Fcy RIIIa and CD81 have all been shown to cluster in response to both LPS and LTA[110].

Two well documented adapter molecules are CD14 and CD36 SR. CD14 is involved in the detection of Gram-negative[63] and Gram-positive[111] bacteria, CD36 is involved in the recognition of an array of diverse ligands.

1.3.5.1: CD14

CD14 is an adapter molecule for both TLR2 and TLR4 signalling that can be either membrane bound (mCD14) or in a soluble form (sCD14). mCD14 is a glycosylphosphatidylinositol (GPI)-anchored protein and thus, unlike the TLRs, does not have an intracellular domain from which it can signal. The sCD14 form lacks a GPI-anchor but is otherwise identical to mCD14.

mCD14 has a molecular weight of 52-55kDa, soluble CD14 which lacks the GPI-anchor has a lower molecular weight of 48-50kDa[112]. Kim *et al*. (2005)[113] have determined the crystal structure of mouse CD14 to a 2.5Å resolution. It was shown that the CD14 monomer contains 13 β strands. 11 of these β strands (β 3-13) overlap with conserved

LRRs drawing close similarities with the TLR family. CD14 exists as a dimer in solution and also in the crystallographic asymmetric unit (Figure 1.20).

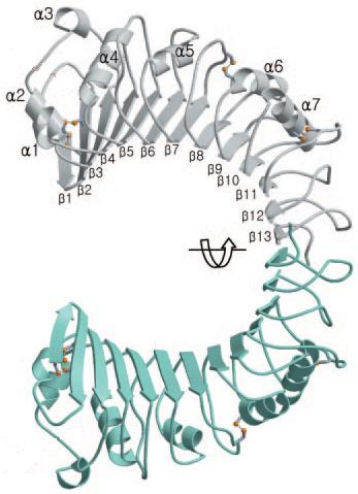

Figure 1.20: Overall structure of mouse CD14 dimer. Two monomers of CD14 in the crystal are coloured in grey and cyan. Disulfide bridges are shown in orange. pdb-1WWL. Adapted from Kim *et al*. (2005)[113].

CD14 has been shown to bind LPS[63] which is supported by work on CD14-deficient mice that have been shown to be highly resistant to LPS-induced septic shock[114]. Through reducing CD14 expression less LPS is detected avoiding an excessive immune response conferring survival in the mice. In addition to LPS from Gram-negative bacteria, CD14 has been shown to be involved in the detection of Gram-positive group B streptococci[111]. The CD14 receptor has also been shown to bind modified LDL[115].

The recognition of LPS through TLR4 is thought to involve the binding of LPS by LBP which transfers the LPS to CD14[62], CD14 then facilitates the transfer of LPS to the TLR4 signalling complex[65].

1.3.5.2: CD36

CD36 is a class B SR that has a great array of ligands which include oxLDL, long-chain fatty acids, retinal photoreceptor outer segments, *Plasmodium falciparum* malaria-parasitized erythrocytes, sickle erythrocytes, anionic phospholipids, apoptotic cells, collagen I and collagen IV[72]. This receptor has been implicated in a number of diseases such as Alzheimer's and atherosclerosis[102,116,117].

SRs were first discovered around 30 years ago. These are cell surface proteins that have the ability to recognize an astonishingly large number of diverse ligands. Three main families of SRs exist, grouped as A (SR-AI and SR-AII), B (SR-BI and CD36) and C (dSR-CI)[118]. Among many other processes SRs have been implicated in "self" and "non-self" discrimination, and thus seen key in the immune response. This is reinforced by their expression on many immunologically relevant cells and their involvement in receptor clusters formed in response to a number of pathogens[51]. Although TLRs and SRs both recognise endogenous and exogenous ligands they serve different functions. Ligation of TLRs leads to transmembrane signalling which can lead to the activation of transcription factors and subsequent secretion of pro-inflammatory cytokines, but ligation of SRs causes endocytosis and lysosomal degradation[118,119].

CD36 has a predicted consistency of 471 amino acids with a total weight of 53kDa[120]. There are 27 hydrophobic amino acids in the carboxy-terminus corresponding to the transmembrane domain of CD36, the majority of the receptor occurs extracellularly with only a 9-13 amino acid cytoplasmic tail[72,121]. It has also been suggested that the amino-terminus of the protein is anchored in the membrane. The primary amino acid sequence of CD36 has shown hydrophobic regions in the amino-terminus, like in the carboxy-terminus, that corresponds to an intracellular domain[120]. It was demonstrated

however, that a CD36 mutant truncated at the carboxy-terminus was no longer anchored to the membrane. This suggests that the amino-terminus does not reside inside the cell membrane[122].

1.3.6: TLR signalling

Formation of the TLR/ligand complex causes homodimerization and/or heterodimerization of TLRs resulting in a conformational change of the receptors. This causes activation of the intracellular TIR domains causing production of intracellular signalling cascades that result in the activation of transcription factors. The transcription factors are then translocated to the nucleus and cause the upregulation of genes involved in the inflammatory and antiviral response; depending on the TLR pathway activated.

TLR signalling can be divided into myeloid differentiation primary response gene 88 (MyD88)-dependant and MyD88-independant. MyD88 is an intracellular TLR signalling adapter protein which is required for TLRs 1, 2, 5, 6, 7, 8 and 9 signalling but not for TLR3 signalling. TLR4 can signal in a MyD88-dependant and independent manner resulting in an “early” and “late” response respectively. TLR signalling requires a number of intracellular adapter proteins to accurately transduce the signal such as MyD88, MyD88-adapter-like (MAL), TIR domain-containing adapter inducing IFN-β (TRIF) and TRIF related adapter molecule (TRAM). These all contain, and interact through, Toll–interleukin 1 receptor (IL-1R) homology domains (TIR domain) as do the intracellular domains of all the TLRs (Figure 1.7). Activation of TLR pathways ultimately leads to the activation of transcription factors of the NF-κB and IRF families. These transcription factors regulate the expression of genes involved in the inflammatory and viral response.

1.3.6.1: TLR2 MyD88-dependant NF-κB cascade

NF-κB proteins consist of a family of homodimeric or heterodimeric transcription factors of the NF-κB/Rel family. Five members of the NF-κB/Rel family have been identified in mammals which are named p65 (RelA), p50 (NF-κB-1), p52 (NF-κB-2), c-Rel, and RelB[123]. NF-κB proteins contain transcription activation domains (TADs) which are responsible for the transcriptional activation of certain inflammatory mediators. For example, p65 contains a 120 amino acid carboxy-terminal domain that contains at least two potent TADs that are crucial for gene activation[124]. NF-κB proteins are held in an inactive form in the cytoplasm by members of the inhibitor of NF-κB (IκB) family. To allow the activation of NF-κB it has to be relieved of this association. NF-κB is released from this complex by the degradation of IκB caused by activation of the intracellular TLR signalling cascade. All TLR pathways activate NF-κB excluding TLR3.

TLR2 heterodimerizes with TLR1 or TLR6 (Section 1.3.4.1). Activation of these receptor clusters causes the activation of the transcription factor NF-κB. When a TLR/ligand complex is formed the TLRs undergo a conformational change causing the intracellular TIR domains of the TLRs to associate with the adapter proteins MAL and MyD88. MyD88 and MAL also have TIR domains and so associate with the cytosolic region of the TLRs via a TIR/TIR interaction. MyD88 recruits interleukin-1 receptor-associated kinase 4 (IRAK-4) through a death domain (DD)-DD association, this then associates with IRAK-1 and IRAK-2 causing IRAK-1 phosphorylation and activation[125]. IRAK-1 autophosphorlyates and allows tumour-necrosis-factor receptor-associated factor 6 (TRAF6) to bind. IRAK-1 bound TRAF6 dissociates from the complex and then associates with TAK1-binding protein 1 (TAB1), TAK1-binding

protein 2 (TAB2) and then transforming-growth factor-β-activated kinase (TAK1). This complex leads to TAK1 activation which phosphorylates the IκB-kinase (IKK) complex that is made up of IKK-α, IKK-β and IKK-γ. IκB is phosphorylated by the active IKK complex which leads to IκB polyubiquitylation that labels the NF-κB inhibitor for proteasomal degradation. NF-κB is relieved from this inhibitory complex and then translocates to the nucleus where it upregulates inflammatory genes.

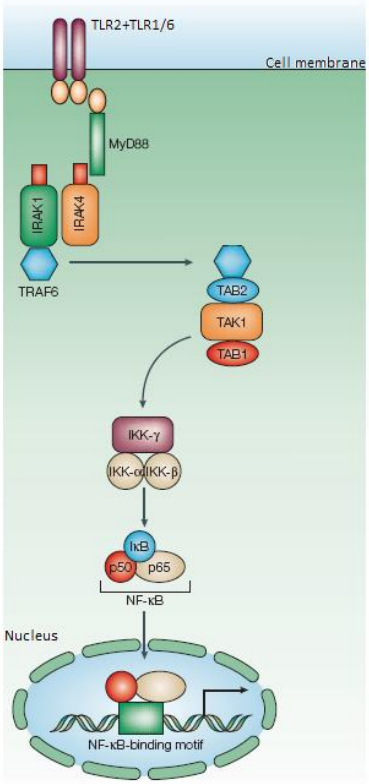

Figure 1.21: MyD88 dependant TLR2+TLR1/6 mediated NF-κB activation. TLR2 heterodimer activation causes association of MAL (not shown) and MyD88. MyD88 recruits interleukin-1 receptor-associated kinase 4 (IRAK-4). IRAK-4 associates with IRAK-1 and IRAK-2 causing IRAK-1 activation. TRAF6 binds activated IRAK-1. IRAK-1/TRAF6 dissociates from the complex and associate with TAK1-binding protein 1 (TAB1), TAK1-binding protein 2 (TAB2) and transforming-growth factor-β-activated kinase (TAK1). TAK1 is activated and phosphorylates the IKK (IκB-kinase) complex (IKK-α, IKK-β and IKK-γ). Inhibitor of nuclear factor-κB (IκB) is phosphorylated by the active IKK complex which leads to IκB polyubiquitylation that labels IκB for proteasomal degradation. NF-κB translocates to the nucleus and upregulates inflammatory genes. Adapted from Akira and Takeda (2004)[87].

1.3.6.2: Lipid rafts

Over the last couple of decades evidence has accumulated for the organisation of the plasma membrane into lipid-based microdomains or lipid rafts. Lipid rafts are envisaged as islands of highly ordered saturated lipids and cholesterol that are laterally mobile in the plane of a more fluid disordered bilayer of largely unsaturated lipids[126,127]. Crucial receptors and adapter proteins for both innate and acquired immunity oligomerize in lipid rafts bringing together intracellular signalling domains causing the activation of intracellular signalling cascades. The hallmark of the lipid raft hypothesis is the spontaneous partitioning of lipids and proteins in discrete membrane domains, a behaviour based on their physico-chemical characteristics. Also these microdomains and their associated protein machinery can be recovered as detergent-resistant entities using biochemical flotation experiments. Microdomains appear as small dynamic structures that can aggregate into larger platforms in response to various stimuli[128].

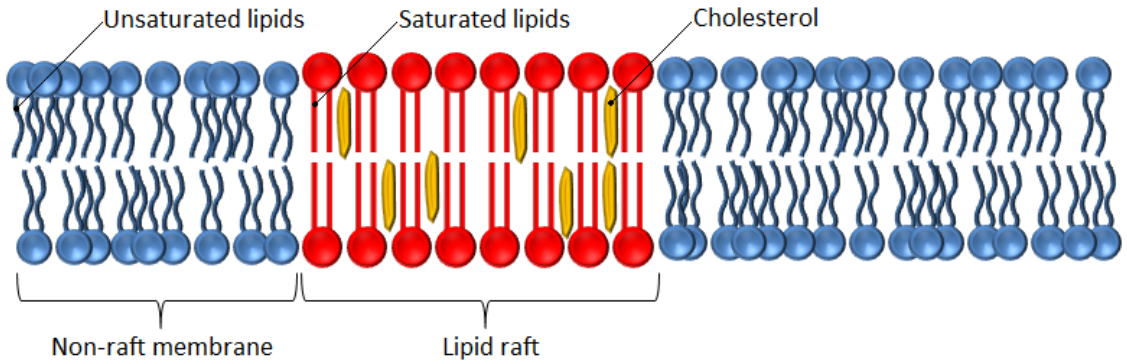

Figure 1.22: Schematic diagram of a lipid raft within a cell membrane. Lipid rafts are envisaged as islands of highly ordered saturated lipids and cholesterol that are laterally mobile in the plane of a more fluid disordered bilayer of largely unsaturated lipids. Adapted from: www.a-s.clayton.edu/emintzer/ (04/09/10).

Lipid rafts are thought to provide a means to explain the spatial segregation of certain signalling pathways emanating from the cell surface. They seem to provide the necessary microenvironment in order for certain specialised signalling events to take

place. Recent studies have shown the importance of lipid raft formation in the acquired immune response. Major histocompatibility complex (MHC)-restricted T-cell activation seems to be facilitated by lipid raft formation[129]. Furthermore, it has recently been found that mediators of the innate immune response also concentrate in lipid rafts in order to facilitate signal transduction thus suggesting that both the acquired and innate immune system utilise membrane partitioning as means of activation against invading pathogens[130,131]. It has been shown by a number of studies that the innate immune response to different ligands is triggered by combinational clustering of receptors[132,133]. Crucial receptors for both innate and acquired immunity seem to oligomerize in non-random membrane structures, bringing together their signalling machinery. The accumulation of receptors within these "floating islands", and thus oligomerization of intracellular receptor signalling domains, brings together all the adapter molecules that are necessary for signalling from the cell surface to within the cell.

1.3.7: TLR based therapeutics

The emerging role of TLRs in a wide range of diseases (including infectious, malignant, autoimmune and allergic diseases) has made them of great interest as potential therapeutic targets. TLR targeted molecules have proven successful in animal models as adjuvants (agents that activate innate immunity to induce and direct an adaptive immune response to another agent) in vaccines[134,135]. There are now many TLR targeted molecules in clinical development for humans as vaccines, vaccine adjuvants and those targeting allergic diseases, infectious diseases and even cancer[59,136].

A couple of TLR adjuvant based vaccine success stories include the hepatitis B vaccines Fendrix (GlaxoSmithKline {approved in the EU}) and Supervax[48] (Dynavax

Technologies {approved in Argentina}) which contain TLR4 adjuvants. However, the most successful TLR based therapeutic in use today is the small TLR7 agonist Imiquimod (Aldara {Imiquimod 5% cream}) produced by 3M Pharma. Aldara has been approved for the treatment of papilloma-induced genital warts and basal cell carcinoma[47].

A drug named Eritoran, a TLR4 ligand, is in phase III clinical trials. It is a lipid A derivative which acts as a TLR4 antagonist that is being used to combat severe sepsis[137]. Severe sepsis can lead to septic shock and subsequently in the majority of cases death. The estimated mortality rate for sepsis in the United States of America is 28.6%, or 215,000 deaths nationally each year[138]. If this drug emerges as successful and is approved it would become invaluable to millions of people worldwide.

TLR targeted drugs have undoubtedly already benefited tens of thousands of people demonstrating the potential of TLR based therapeutics. Many pharmaceutical companies are exploring TLR targeted molecules for their potential in treating various conditions, with a large number already in clinical trials. The prospect of drugs such as Eritoran and the success of Imiquimod demonstrate the importance and fruitfulness of TLR research. The TLR directed molecules in use and those being rigorously tested today demonstrate the tip of the iceberg in TLR directed therapeutics; for our knowledge of TLR signalling and thus the unravelling of drug targets is ever advancing.

This study explores two molecules for their potential in the prevention/treatment of atherosclerosis. These are HSP70 and AMD3100 octahydrochloride (AMD3100).

1.3.7.1: Heat shock protein 70

HSPs are a family of highly conserved proteins found in cells that have traditionally been described as intracellular chaperones. Their main functions have been found to be concerned with allowing the cell to carry on with normal tasks by assisting in processes such as protein folding, degradation, translocation across the membrane and disassembly of oligomers[139,140]. Infection along with many other cellular stresses or damage causes the production of HSPs. HSPs have been shown to be conserved across many species which highlights their importance in survival. Recently the roles of HSPs as endogenous modulators of the innate immune response have been explored. HSP70 has been shown to be involved in a number of processes such as the recognition of bacterial LPS[68] and the dampening of the immune system[141,142]; an cardioprotective role has also been suggested[143-145].

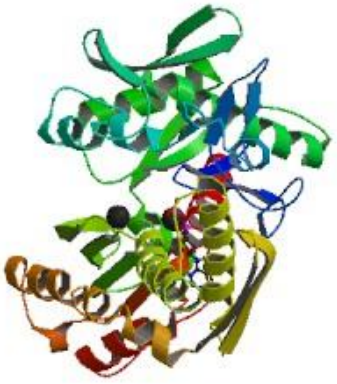

Figure 1.23: Human HSP70. HSPs are a family of highly conserved proteins involved in protein folding, degradation, translocation across the membrane and disassembly of oligomers. pdb-3IUC. Wisniewska *et al*. (2010)[146].

Studies have demonstrated that transgenic mice over expressing HSP70 have an increased resistance to ischemic heart injury[143,144]**.** This work is supported by patient studies demonstrating a positive correlation between elevated HSP70 levels and low coronary artery disease (CAD) risk[145]**.** The use of exogenous HSP70 has been shown to inhibit LPS-induced inflammatory responses in monocytes demonstrating its potential

as a therapeutic agent for many disorders[141]**.** The anti-inflammatory mechanism of HSP70 is thought to involve the sequestration of intracellular adapters of TLR signalling such as TRAF6[142]. Previous work conducted in the lab of Dr. K. Triantafilou has demonstrated the ability of HSP70 to reduce the protein expression of TLRs 2, 4, 6, 7, 8 and 9 diminishing cellular immune capabilities to TLR agonists[141].

1.3.7.2: AMD3100 octahydrochloride

AMD3100 (Chemical Name: 1,1'-[1,4 phenylenebis(methylene)] bis-1,4,8,11-tetraazacyclotetradecane octahydrochloride {referred to as AMD3100 from here on}**)** is a highly specific CXC chemokine receptor 4 (CXCR4) antagonist[147] that was previously, but unfortunately unsuccessfully, explored for its potential in HIV treatment[148]. CXCR4 is a chemokine receptor that belongs to the seven transmembrane-domain G-protein-coupled receptor family and has been shown to be involved in the "LPS-sensing apparatus"[69]. The antagonistic effect of AMD3100 on CXCR4 has previously been implicated in the reduction of inflammation[149,150].

Molecular Formula: $C_{28}H_{62}N_8Cl_8$
Molecular Weight: 794.5 (anhydrous)

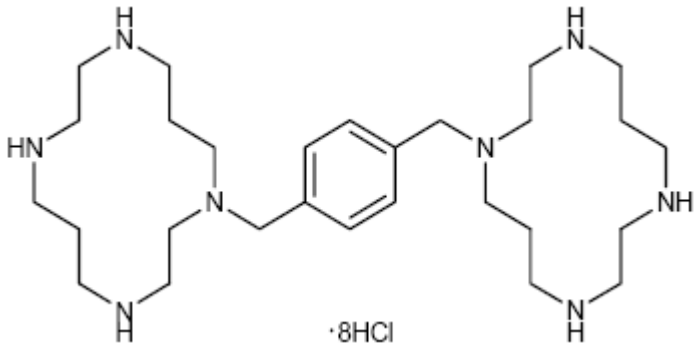

Figure 1.24: The molecular structure of AMD3100 octahydrochloride (Chemical Name: 1,1'-[1,4 phenylenebis(methylene)] bis-1,4,8,11-tetraazacyclotetradecane octahydrochloride). Sigma product information sheet: kaa 5/03

The expression of CXCR4 has been shown to increase after exposure to bacterial products[151]**.** In response to LPS, CXCR4 co-clusters with TLR4 and other receptors forming the "LPS-sensing apparatus". The formation of this cluster was found to be responsible for triggering LPS-induced responses[69]**.** Triantafilou *et al*. (2008)[69] have shown that CXCR4 co-clusters with the LPS receptors TLR4, CD55, HSP70, HSP90 and CD11b/CD18 on human monocytes and human endothelial cells following LPS stimulation. AMD3100 was found to inhibit these CXCR4 heterotypic associations with LPS receptors, such as TLR4, suggesting that AMD3100 inhibits the formation of the "LPS-sensing apparatus" reducing cellular response to LPS (Dr. K. Triantafilou from the University of Sussex {unpublished data}).

The specificity of AMD3100 to CXCR4, and thus the disruption of receptor associations required for cellular signalling in response to a pathogen, makes it a very interesting molecule. AMD3100 has the effect of attenuating TLR4 signalling. TLR4 has been implicated in many adverse conditions including sepsis[42] and atherosclerosis[152]. The modification/reduction of TLR4 signalling could prove very beneficial for the reduction and/or prevention of plaque formation and sepsis.

1.3.7.3: Immunoregulatory roles of lipids

Lipids have also been shown to have an immunoregulatory role. Lipid binding to LTA from Gram-positive bacteria (Section 1.3.3.1.1) and LPS from Gram-negative bacteria (Section 1.3.3.1.2) has been demonstrated in the lab of Dr. K. Triantafilou (University of Sussex. Mouratis *et al*. {submitted}). Inhibition of LPS signalling by OxPAPC has been shown to occur up-stream of MyD88, via the competitive binding of the adapter molecules CD14, MD2 and LBP[103,153]. OxPAPC is able to prevent LPS-activation of

p38 mitogen-activated protein (MAP) kinase, but has no effect on tumor-necrosis factor-α (TNF-α) induced activation of MAP kinase, thus prevents TLR4 activation but has no effect on TNFα receptor activation. Interleukin-1 receptor (IL-1R) signaling was also shown to be unaffected by OxPAPC. These findings illustrate specificity of lipid modulation to the TLR signaling cascade[103]. This "lipid immunoregulation" has been shown to be restricted to TLRs 2 and 4[153].

It has been found that a lipid emulsion (GR270773) can in fact mop up LPS and LTA with the effect of reducing the inflammatory response *in vitro* and *in vivo*[154,155]. However, phase II clinical trials (LIPOS study)[156] performed by GlaxoSmithKline for the therapeutic effects of GR270773 in the prevention of sepsis proved fruitless. Reasons for failure of efficacy of this therapy have yet to be published.

It is becoming apparent that lipids in the blood from exogenous and endogenous sources play an immunomodulatory role in the immune response. The role of lipid immunomodulation in atherosclerosis, once considered a lipid storage disorder, is of great interest in this study.

1.4: The innate immune response in atherosclerosis

In vivo studies on transgenic mice have produced strong evidence for the involvement of innate immunity in atherosclerosis. Many of these studies use an atherosclerotic mouse model as a basis to their model and then apply genetic manipulations on these, such as mutations in a TLR gene. Atherosclerotic models include C57BL/6 mice that lack either a functional apolipoprotein E (*ApoE*$^{-/-}$)[157] gene or a functional LDL receptor (*Ldlr*$^{-/-}$)[158] gene. C57BL/6 mice were used for they were found to be most susceptible to atherosclerosis. Apolipoprotein E (apoE) is an apolipoprotein found on chylomicron and IDL particles, similar to apoB-100 found on LDL (Section 1.3.3.2), which is essential

for the transport and metabolism of lipids. Decrease in functional apoE increases plasma cholesterol resulting in spontaneous development of atherosclerotic lesions. The LDL receptor removes cholesterol-rich LDL from the plasma. These receptors are particularly abundant on liver cells, which are responsible for removing excess cholesterol. A deficiency in these receptors increases plasma LDL and thus cholesterol levels which results in spontaneous development of atherosclerotic plaques.

Bjorkbacka *et al*. (2004)[159] found a significant reduction in early atherosclerosis (reduced lesion cross sectional area) in *ApoE*$^{-/-}$ mice that were also MyD88-deficient (*ApoE*$^{-/-}$*MyD88*$^{-/-}$) in comparison to *ApoE*$^{-/-}$ mice expressing wild-type MyD88. This work is supported by Michelsen *et al*. (2004)[152]. Bjorkbacka and Michelsen demonstrate the importance of MyD88 in the progression of atherosclerosis, which indirectly highlights the involvement of the germ-line encoded sensors of the innate immune system, the TLRs.

Studies on TLR deficient mice confirmed their significance in the development of atherosclerosis. Genetic deficiency of TLR4 (Section 1.3.4.3) in the atherosclerosis prone *ApoE*$^{-/-}$ mouse resulted in reduced total lesion area, reduced macrophage infiltration and reduced monocyte chemotactic protein-1 (MCP-1) serum concentrations in comparison to control wild-type TLR4 *ApoE*$^{-/-}$ mice[152]. This work not only points out that TLR4 is involved in plaque formation but indicates that cytokines produced from TLR activation may play a role in the disease such as causing monocyte infiltration into the arterial intima.

Similar results were obtained for TLR2 (Section 1.3.4.1). Reduced cytokine levels and lesion size were observed with *ApoE*$^{+/-}$*Tlr2*$^{-/-}$ mice in comparison to *ApoE*$^{+/-}$*Tlr2*$^{+/+}$ mice

fed on a high fat diet. The same result was found when these mice were subject to *P.gingivalis*[160], a Gram-negative TLR2 agonist associated with atherosclerosis. The role of an endogenous TLR2 ligand in the progression of atherosclerosis was highlighted by Mullick *et al*. (2005)[161] who showed that atherosclerosis prone $Ldlr^{-/-}$ mice that do not express TLR2 ($Ldlr^{-/-}Tlr2^{-/-}$) have reduced lesion size in comparison to $Ldlr^{-/-}$ mice expressing TLR2, even in the absence of any exogenous agonist. This data suggests the possibility of the presence of an endogenously sourced TLR2 agonist, which could also be involved in the progression of disease.

An immunological role for the cause of atherosclerosis in humans has been found. There exists two human polymorphisms in TLR4 which impair TLR4 signaling. These are TLR4 Asp299Gly and TLR4 Thr399Ile[162]. The TLR4 polymorphism Asp299Gly causes the innate immune system of an individual to be hypo-responsive to Gram-negative bacteria, but seems to display protection from atherosclerosis[163]. This human immune dysfunction resulted in lower levels of inflammatory markers and reduced intima-media thickness in comparison to wild-type individuals. However, contrasting data exists which suggest no association between the Thr399Ile or Asp299Gly polymorphisms with myocardial infarction or intima-media thickness respectively in large patient samples[164,165]. The discovery that CD14 may be involved in atherosclerosis in humans does support a role for TLR4 in this process. It has been shown that a C(-260)→T nucleotide change in CD14 in humans may be a risk factor for myocardial infarction[166]. The CD14 polymorphism results in an increased density of CD14 on monocytes, which makes individuals hyper-responsive to LPS.

These findings directly implement the innate immune system in this multi-factorial disease, with specific emphasis on TLRs 2 and 4.

1.4.1: TLRs in atherosclerosis

The innate immune system and more specifically TLRs seem to be central to the process of plaque formation in the vascular disease atherosclerosis. The majority of factors associated with atherosclerosis are known TLR ligands. It seems that the inflammatory response is activated through the innate immune system and maintained by these factors, via a process yet to be defined, that can cause the slow development of atheromatous plaques and the subsequent risk of myocardial or cerebral infarction. Studies of mouse and human genetic variations have confirmed a role for TLR signalling in atherosclerosis. The emerging pivotal function of TLRs in atherosclerosis has led to much research into their functional significance and interactions in order to unravel their responsibility in one of the largest contributors of mortality in the Western world.

1.4.1.1: TLRs in plaque initiation

Vascular endothelial cells line the lumen of arteries and are subject to challenge from circulating endogenous and exogenous ligands. These cells express an array of TLRs and SRs. Vascular endothelial cells are considered to be responsible for the initial steps in atherogenesis, the starting point of plaque formation. Augmented TLR expression has been observed in the atherosclerotic plaque in comparison to normal artery[8,167]. In particular the significant upregulation of TLRs 1, 2 and 4 on endothelial cells and macrophages has been shown[8]. Activation of these TLR-expressing cells in the plaque has been displayed by positive stain for active NF-κB, a transcription factor downstream of TLR signalling (Section 1.3.6), confirming their activation and thus indicating their involvement in atheroma formation[8].

The locality of atheroma development has been attributed to differential expression of these TLRs on endothelial cells throughout the vascular system. Pryshchep *et al*. (2008)[168] illustrated heterogeneous TLR expression in the subclavian, mesenteric, iliac, and temporal arteries. Differential expression of TLRs would result in varied sensitivity to a ligand throughout the vascular network, where one area could be more susceptible than another. This has been used to explain why plaques may preferentially form in the carotid artery. However, it has also been described that plaques may preferentially form at sites of disturbed blood flow. It is suggested that disturbed blood flow experienced in the artery creates shear stresses that adversely affects the biology of the arterial wall. Such stresses are suggested to increase susceptibility to fatty streak formation, and thus initiation of plaque development. The increased susceptibility to fatty streak formation has been attributed to increased TLR2 expression as a result of the disturbed flow[169].

1.4.1.2: TLRs in foam cell formation

Further TLR responsibility in atherogenesis is their role in foam cell (lipid laden macrophage) formation. Foam cells are a major component of the plaque core (Figure 1.2). Miller *et al*. (2009)[170] have demonstrated attenuated mmLDL uptake in macrophages of mice that were TLR4 deficient, demonstrating its role in oxidized lipoprotein phagocytosis. The expression of TLR4 on human monocyte-derived macrophages has been shown to be upregulated by oxidized LDL, but not native LDL[100]. This demonstrates that native LDL must be seen as "self" whilst LDL that has been oxidized is seen as "non-self". Macrophage activation via TLR pathways has been shown to cause altered gene expression in the macrophage resulting in increased lipid uptake thus foam cell formation. Adipocyte fatty acid–binding protein (aP2) is an intracellular transport protein strongly associated with lipid accumulation in

macrophages where increased aP2 mRNA expression results in increased cholesterol and triglyceride levels in the macrophage[171]. It has been described how both *E.coli* LPS and zymosan challenge were able to significantly increase aP2 by factors of ~56 and ~1500 respectively, greatly increasing lipid accumulation[171]. Zymosan which is far more effective at increasing aP2 expression is a TLR2 ligand, simulating macrophage response to LTA and the atherosclerosis-associated unconventional LPS from *P.gingivalis*[51], *H.pylori*[55] or *C.pneumoniae*[19,172].

1.4.1.2.1: CD36 in foam cell formation

CD36 SRs expressed on macrophages bind modified lipids and microbial diacylglycerides[73,101,173]. CD36 is involved in their internalization resulting in foam cell formation[102], it has been suggested that TLR4 is involved in this recognition[174]. CD36 has been shown to associate with TLR2[173]. Receptor clusters that form in response to atherosclerosis-associated *P.gingivalis* and *H.pylori* LPS consist of TLR2/TLR1/CD36[51]. This has the potential of directly linking lipoprotein uptake and bacterial infection where a receptor cluster can associate with both factors. Potential for interplay between these ligands is high and could shed light on the mechanism of foam cell and plaque formation.

1.4.1.3: TLRs in plaque stability

The integrity of the plaque cap is much under the control of macrophage/foam cell derived extracellular matrix (ECM) degrading enzymes of the matrix metalloproteinase (MMP) family[175]. The fibrous cap of the atherosclerotic plaque consists of smooth muscle cells (SMCs) and ECM (Figure 1.2). The ECM is under constant degradation and remodelling. Degradation of the ECM by MMPs, which are released by a large

number of localised lipid laden macrophages, is thought partly responsible for cap rupture linking TLRs and plaque stability. MMPs have been shown to be upregulated in human plaque[176,177]. Foam cells present in the plaque, of which TLRs are most part responsible for, are the main source of MMPs. Monaco *et al*. (2009)[178] have reported that blocking TLR2 significantly reduces MMP-1, -2, -3 and -9 production in human atheroma cell cultures, TLR4 blockade gave a reduction only in MMP-3 production. This work directly illustrates the involvement of TLRs in ECM degradation.

Other than TLRs bacteria themselves can lead to plaque instability. Bacterial biofilms, colonies adhered to themselves and a surface, secrete matrix-degrading enzymes in order to break down their higher structure to release individual cells and allow dispersal for the creation of new colonies[179]. Such colonies present in plaque could lead to ECM degradation and plaque rupture.

1.4.1.4: TLRs in thrombosis

TLRs have also been implicated in the initiation of the coagulation protease cascade. Tissue factor (TF), a protein responsible for the first stages of coagulation, has been found to be over expressed in the atherosclerotic plaque. Macrophages have been shown to produce TF on activation via *E.coli* LPS[180] and *P.gingivalis*[181] through TLR4 and TLR2 respectively. It is proposed that on cap rupture, plaque derived TF comes in contact with clotting factors in the blood causing thrombus formation. The subsequent dislodging of thrombus can cause blockage of a vital blood vessel leading to vascular occlusion.

It has also been suggested that fibrinogen, a glycoprotein involved in the blood coagulation cascade, could stimulate macrophages through TLR4 causing release of

cytokines and chemokines[182,183]. Fibrinogen is an acute phase protein upregulated at sites of infection. This could show a vicious feedback loop where the coagulation cascade, leading to thrombosis, exacerbates atherosclerosis.

1.4.2: Inflammatory mediators in atherosclerosis

Inflammatory mediators have been directly associated with atherosclerosis. TLR activation initiates intracellular signalling cascades, which result in the activation of transcription factors, that are then translocated to the nucleus and cause the upregulation of inflammatory mediators such as cytokines and chemokines (Section 1.3.6). Both cytokines and chemokines are involved in all steps of atherosclerosis including plaque initiation, foam cell formation, plaque stability and thrombosis highlighting their importance in this disease.

Inflammatory cytokines released on cell stimulation give rise to effects such as inflammation, apoptosis, inhibition of viral replication, T-cell differentiation, leukocyte recruitment, increased permeability and oedema[184]. Both pro- and anti-inflammatory cytokines have been shown to be upregulated in the peripheral blood taken from patients with atherosclerosis. Profumo *et al*. (2008)[185] demonstrated significantly higher expression of the pro-inflammatory cytokines tumour necrosis factor (TNF)-α, interferon (IFN)-γ, interleukin (IL)-1β, IL-6 and the anti-inflammatory cytokines IL-4 and IL-10. However, contrasting data exists which suggests a link between reduced anti-inflammatory cytokine interleukin-10 (IL-10) serum levels with increased intima thickness[186]. IFN-α, an anti-viral cytokine produced by leukocytes, has been shown to be capable of up-regulating TLR4 expression increasing cellular sensitivity to TLR4 atherosclerosis-associated ligands exacerbating plaque development and instability[187].

Chemokines are chemotactic cytokines, when released these direct migration of leukocytes into inflamed tissue via interaction with chemokine receptors present on the leukocyte cell surface[188]. These small signalling proteins have also been implicated in inducing cell proliferation, enzyme secretion, reactive oxygen species and foam cell formation[189,190]. Chemokines, such as MCP-1 and IL-8, direct leukocytes to the site of inflammation (plaque). Monocytes express chemokine receptor-2 (CCR-2) which binds MCP-1[188]. The release of MCP-1 at a site in the arterial vascular wall results in monocyte infiltration into that area, through the vascular endothelial wall, from the blood stream. Levels of the chemokine IL-8 have been associated with increased risk of future coronary artery disease and plaque instability[191,192]. It has been shown how elevated peripheral blood IL-8 values can indicate requirement for carotid endarterectomy (Section 1.1.3.1) regardless of other risk factors that may show a patient at low risk[185].

It has been demonstrated that the pattern or balance of inflammatory mediators could possibly be used as a fingerprint to diagnose and predict clinical outcome of disease allowing tailored patient treatment. This could be far more beneficial for the patient, not to mention saving time and money.

1.5: Aims of this project

This project is set out to investigate the participation of PRRs in atherosclerosis in view of treating, if not preventing, this disorder. Of particular interest is the functional significance of TLR associations in response to endogenous and exogenous ligands that have been implicated in atherogenesis and the alterations that may be caused to these associations when ligands are present at the same time. Ligands of interest in this project include LPS and LTA from atherosclerosis-associated bacterial products as well as modified endogenous lipoproteins such as oxLDL. This study will look at the trafficking and intracellular targeting of these PRR-ligand complexes and investigate the contribution of this to innate inflammatory signalling. In addition to this, the role of lipid rafts in signalling will be investigated. Ultimately, the *in vivo* inhibition of the atherosclerosis-associated inflammatory response will be explored, through manipulation of PRR signalling found to be involved in this disease.

Chapter 2:

Materials and Methods

2.1: Antibodies

Primary Antibodies	Species	Company
TLR1	Mouse	Hycult Biotechnology
TLR2	Goat	Santa Cruz Biotechnology, Inc
TLR4	Goat	Santa Cruz Biotechnology, Inc
TLR6	Goat	Santa Cruz Biotechnology, Inc
CD14	Mouse	Donated by Dr. K. Triantafilou
CD36	Rabbit	Santa Cruz Biotechnology, Inc
Golgi	Mouse	BD Biosciences Pharmingen
Endosome	Mouse	BD Biosciences Pharmingen
IKappaB-alpha (C-term)	Mouse	Cell Signalling technology
Phosho-IKappaB-alpha (Ser32)	Rabbit	Cell Signalling technology

Secondary Antibodies	Label	Company
Rabbit anti mouse	FITC	Dako cytomation
Rabbit anti goat	FITC	Dako cytomation
Swine anti rabbit	FITC	Dako cytomation
Donkey anti goat	Alexa555	Invitrogen. Molecular probes
Rabbit anti mouse	Cy3	Amersham Biosciences
Donkey anti rabbit	Cy5	Jackson ImmunoResearch Laboratories
Rabbit anti goat	Cy5	Jackson ImmunoResearch Laboratories
CD14 (26ic). DIRECT	PE	Donated by Dr. K. Triantafilou
Lipid raft. DIRECT	FITC	List Biological Laboratories
Rabbit anti mouse	TRITC	Dako cytomation
Swine anti rabbit	TRITC	Dako cytomation
Rabbit anti goat	HRP	Dako cytomation
Swine anti rabbit	HRP	Dako cytomation

Table 2.1: Primary and secondary antibodies used in this study. Secondary antibodies were labelled with either a fluorescent fluorochrome (Fluorescein isothiocyanate {FITC}, Alexa555, Cyanine 3 {Cy3}, Cyanine 5 {Cy5} and Tetramethyl rhodamine isothiocyanate {TRITC}) or horse radish peroxidase (HRP) for enhanced chemiluminescence (ECL).

2.2: Cell lines

2.2.1: Tissue Culture

To ensure sterile conditions during tissue culture a Microflow Advanced Biosafety Class II laminar flow hood was used. Plasticware, glassware and solutions were autoclaved (180°C) for tissue culture. Hood and equipment was sterilized with 1% aqueous Virkon (Antec International). Cells were incubated at 37°C with a 5% CO_2 humidified atmosphere.

2.2.2: Human endothelial vascular cells

Human endothelial cardiovascular 304 (ECV304) cells were cultured in 25cm^2 surface flasks (Nunc) in Medium 199 + GlutaMAX (GIBCO) supplemented with 10% foetal calf serum (FCS {Biosera}).

ECV304 cells were obtained from the European Collection of Animal Cell Cultures (ECACC). The ECV304 cell line is a spontaneously transformed cell line derived from an umbilical cord from a new born Japanese female.

ECV sub-confluent cultures (70-80%) were split with the use of the proteolytic enzyme trypsin (Sigma). Cells were frozen in freezing medium consisting of 10% (v/v) dimethyl sulfoxide (DMSO) in FCS.

2.2.3: Primary human umbilical vein endothelial cells

Primary human umbilical vein endothelial cells (HUVECs) were cultured in 24 well plates, with a surface area of 1.9cm^2 per well, (Nunc) in Medium 200 containing the Low Serum Growth Supplement Kit (Cascade Biologics). LSGS Kit contained: Foetal

bovine serum, 10ml. EGF, 1ml. bFGF (1.5µg/ml)/Heparin (5mg/ml)/BSA (100µg/ml), 1ml. Gentamicin/Amphotericin B, 1ml. Hydrocortisone (1mg/ml), 0.5ml.

HUVECs were obtained from the European Collection of Animal Cell Cultures (ECACC). These cells were obtained from normal human umbilical vein. Once in culture HUVECs can be propagated up to 16 times.

HUVECs were passaged by re-suspending the semi-adherent cells using a pipette, no more than 16 times. Cells were frozen in freezing medium consisting of 70% Medium 200+LSGS/20% FCS/10% (v/v) DMSO.

2.2.4: Human embryonic kidney 293 transfectants

TLR2/Green Fluorescent Protein (GFP)/human embryonic kidney 293 (HEK293) and TLR4/MD-2/GFP/HEK293 cells were cultured in 25cm^2 surface flasks (Nunc) in Dulbecco's Modified Eagle's Medium (DMEM) 4600/1000mg/L glucose medium (GIBCO) supplemented with 10% FCS (Biosera) with G418 (Sigma) selection antibiotic (500g/µml). HUVECs were seeded in 24 well plates (Nunc) with DMEM/FCS/G418 growth medium when assayed. TLR2/GFP/HEK293 and TLR4/MD-2/GFP/HEK293 cell lines were kindly provided by Dr. D. Golenbock from the University of Massachusetts Medical School, United States.

TLR2/GFP/HEK293 and TRL4/MD-2/GFP/HEK293 cells were passaged by re-suspending the semi-adherent cells using a pipette. Cells were frozen in freezing medium consisting of 70% DMEM 4600/1000mg/L glucose/G418/20% FCS (Biosera)/10% (v/v) dimethyl sulfoxide (DMSO).

2.2.5: Cryogenic preservation

Cryogenic preservation (<-100°C) was used to create and maintain reserve cell line stocks. Cell lines were placed in a -80°C freezer for 24h and then into liquid nitrogen for long-term storage. This step down in temperature allows cells to adjust to the liquid nitrogen.

Cells were washed and then re-suspended in 10ml of their growth media by; pipetting for semi-adhesive cells, or with the use of the proteolytic enzyme trypsin (Sigma) for adhesive cells. Cells were placed in a 15ml tube (Nunc) and spun at 145g RT for 5 minutes. The supernatant was aspirated off and the pellet re-suspended in 1500µl of their specific freezing medium (Table 2.2). Cells in freezing medium were quickly placed in cryotubes (Nunc) and then into the -80°C freezer for 24 hours. After 24 hours the cryotubes were then removed from the -80°C freezer and placed into liquid nitrogen (-196°C).

Cell line	Freezing medium
ECV	10% (v/v) dimethyl sulfoxide (DMSO) in FCS
HUVEC	70% Medium 200+LSGS/20% FCS/10% (v/v) DMSO
TLR2/GFP/HEK293	70% DMEM G418/20% FCS/10% (v/v) DMSO
TRL4/MD-2/GFP/HEK293	70% DMEM G418/20% FCS/10% (v/v) DMSO

Table 2.2: Freezing medium for cell lines. Cryogenic preservation in liquid nitrogen (<-100°C) was used to create and maintain reserve cell lines.

2.3: Cell counting

A haemacytometer is a cell counting device that allows one to obtain an approximation of the cell concentration (cells/ml) of a cell suspension. This allows consistence when seeding cells especially when growth surface area may be changed to suit the experiment.

It is, as stated, an approximation and works on the basis of there being an exact known volume in the chamber of the hemacytometer (Figure 2.1). A quartz cover slip sits precisely 0.1mm above the chamber floor, each grid (counting area highlighted) is 1mm by 1mm, thus the volume above each single grid is $0.1mm^3$ (0.1µl). By observing the chamber under the microscope and counting the number of cells in a suspension in the counting area, one can calculate cell concentration.

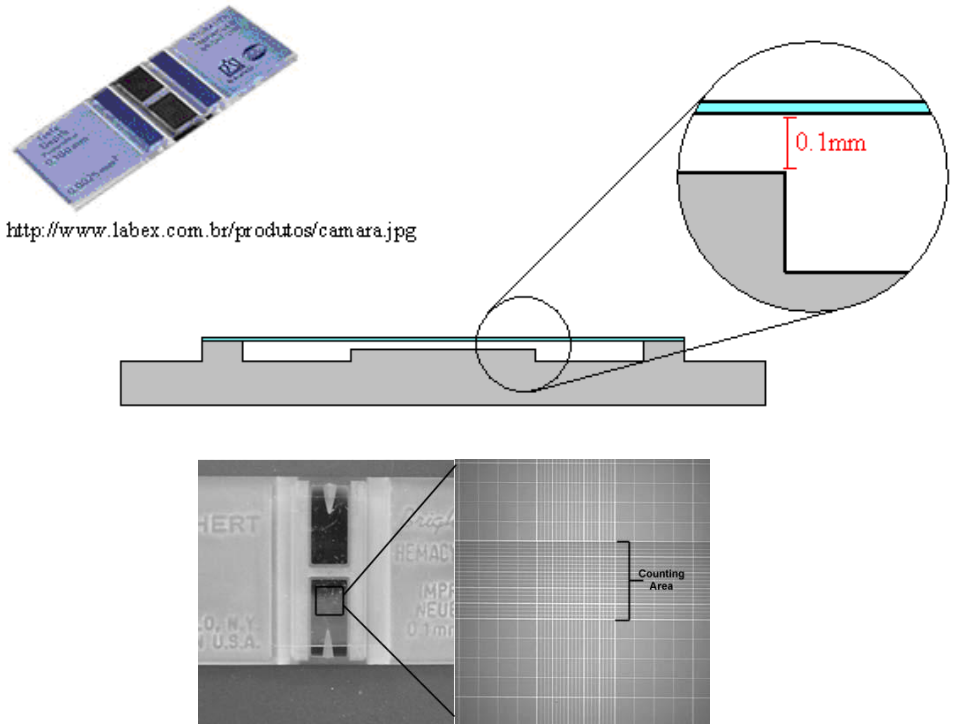

Figure 2.1: Hemacytometer: used to count cells in suspension. It works on the basis of there being an exact known volume in the chambers of the hemacytometer. A quartz cover slip sits exactly 0.1mm above the chamber floor, each grid (counting area highlighted) is 1mm by 1mm, thus the volume above each single grid is $0.1mm^3$ (0.1µl). Number of cells per "counting area" = number of cells per $0.1mm^3$. Adapted from: www.vivo.colostate.edu/hbooks/pathphys/reprod/ semeneval/ hemacytometer.html (30/12/09).

The number of cells in each grid in the counting area should be recorded and placed in the following calculation:

$$\frac{\text{Total Number of Cells}}{\text{Total number of grids used}} \quad x \quad 10^4 \quad = \quad \text{cells/ml}$$

2.3.1: Hemacytometer protocol

Cells were confluent when concentration was determined. Adherent cells were placed in suspension by the use of the proteolytic enzyme trypsin, semi-adherent cells were re-suspended by agitation with a pipette.

Cells were thoroughly re-suspended using a sterile Pasteur pipette, in order to ensure single-cell suspensions. A cover slip was placed on the Specialized Neubauer hemacytometer. Using a Pasteur pipette the cell suspension was loaded on the edge of the cover slip, ensuring that both chambers of the Neubauer hemacytometer were flooded. The slide was observed and the cells counted under a light microscope. Cells from the central and all corner grids were used. This data was entered into the calculation in Section 2.3.

2.4: Viability test

Trypan blue is a diazo dye that can be used to distinguish between live and dead cells. In this study the trypan blue viability test was used to determine cell toxicity of certain procedures.

Trypan viability test

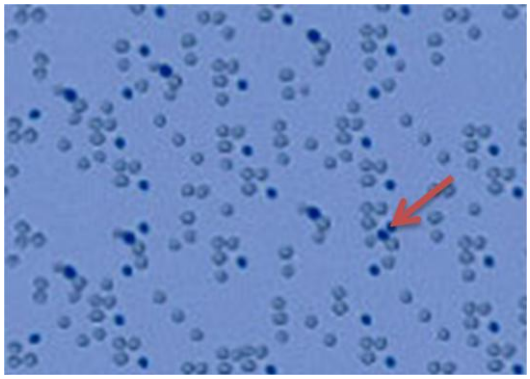

Figure 2.2: Trypan blue viability test. Live cells with intact membranes do not allow dye to pass into the cell. Dead cells (arrow) have disrupted membranes and thus allow the dye to enter and stain the cell dark blue. www.yamato-net.co.jp/english/products/bio/da_sell .htm (30/12/09).

The trypan blue viability test, also known as the dye exclusion test, works on the basis that live cells have intact membranes that are highly selective in their uptake and thus will not allow the dye to enter the cell. Dead cells whose membranes have been compromised allow the dye to enter the cell through the damaged membrane, and thus become stained blue.

Subsequent cell counting using a hemacytometer (Section 2.3) allows cell viability (%) to be calculated.

2.4.1: Trypan blue viability test procedure

Cells were washed with sterile X1 PBS. Enough trypan blue (Sigma) to cover the cells was then added and left for 10 minutes. The cells were then washed with sterile X1 PBS. Cells were analyzed using a Specialized Neubauer hemacytometer (Section 2.3).

2.5: Cell stimulations

All stimulations were carried out in hybridoma Serum Free Medium (SFM {GIBCO}) and incubated at 37°C in a 5% CO_2 humidified atmosphere. The use of SFM eliminates any effects that medium proteins may have on the experiment. Ligand concentrations were kept constant throughout this study (Table 2.3).

Ligand	Concentration
E.coli LPS	100ng/ml
S.aureus LTA	10µg/ml
P.gingivalis LPS	10µg/ml
C.pneumoniae LPS	10µg/ml
LDL	50µg/ml
mmLDL	50µg/ml
oxLDL	50µg/ml

Table 2.3: Ligand concentrations used in this study. All concentrations were kept constant throughout.

2.5.1: 25cm^2 Flask stimulation

ECV304s were stimulated in flasks with a surface area of 25cm^2 (Nunc). Sterile conditions were practiced throughout this procedure. The growth medium was aspirated off and the cells were washed with 3ml SFM (GIBCO). 2ml SFM was then added to the flask. The cells were then stimulated.

2.5.2: 24 well plate stimulation

Primary HUVECs and HEK cells were stimulated in 24-well plates with a surface area of 1.9cm^2 per well (Nunc). Sterile conditions were practiced throughout. The growth medium was aspirated off and the cells were washed with 1ml SFM (GIBCO). 500µl SFM was then added to each well. The cells were then stimulated.

2.5.3: Lab-Tek™ slide stimulation

For confocal microscopy, primary HUVECs were stimulated on 8 well glass slides (Lab-Tek™ Chamber Slide™ System). Each well surface area was 0.8cm^2. The growth medium was aspirated off and the cells were washed with 500µl SFM (GIBCO). 200µl SFM was then added to each well. The cells were then stimulated.

2.6: Preparation of low density lipoprotein derivatives

In order to simulate high cholesterol levels, human LDL (hLDL {3,500 kDa}) obtained from Sigma was used. The LDL was prepared from fresh human plasma. The protocol for the production of the LDL derivatives was obtained from Miller *et al*. (2003)[115] who consistently demonstrated the pro-atherogenic affects of their synthesised LDL derivatives.

In sterile conditions 1µl 1mM $CuSO_4$ was added to 1ml of 1mg/ml hLDL (Sigma) in an eppendorf tube. This was then placed in an incubator shaker at 37˚C at 130RPM for: 1 hour to produce mmLDL and 12 hours to produce oxLDL.

2.7: Immunofluorescence

Immunofluorescence is the labelling and visualisation of specific molecules with fluorescent monoclonal antibodies. Immunofluorescent labelling can be utilised to find the relative abundance and localisation of a chosen antigen. Fluorochromes that emit light of a set wavelength when excitated, are conjugated to antibodies. The binding of the fluorescent antibody to a specific antigen of interest, and thus subsequent emission of light at a certain wave length, allows it to be imaged and/or quantified by a number of techniques. The development of fluorescent labelling as a research tool has proven invaluable.

Fluorescence is emitted from fluorochromes that become excited when exposed to a laser beam of the correct wavelength. Electrons in the fluorochrome move into a higher energy state when a photon from the laser is absorbed. The atoms are said to change from their "ground state" to an "excited state". After an infinite amount of time the electrons jump back to their original position and a photon of a lower wavelength is emitted. Here the atom moves back to its "ground state". The emitted light is detected and can be use to shed light on the abundance and/or localisation of a chosen antigen.

There are a number of different fluorochromes available which utilise different excitation and emission wavelengths. Such specificity of antibodies coupled with the availability of different fluorochrome conjugates allows multiple labelling of molecules and/or structures in a single sample at any one time. Multiple labelling of cells with more than one type of fluorochrome can be used to uncover their colocalisation and trafficking. This study used fluorochrome labels whose emissions are in the visible light spectrum (Table 2.4).

Fluorochrome	Excitation λ	Emission λ
Alexa 555	555nm	565nm
Cyanine 3	550nm	570nm
Cyanine 5	650nm	667nm
Fluorescein isothiocyanate	495nm	519nm
Phycoerythrin	488nm	575nm
Tetramethylrhodamine isothiocyanate	547nm	572nm

Table 2.4: Excitation and emission of fluorochromes used in this study.

Two techniques were used in this study in order to label a specific antigen. These were direct and indirect immunofluorescence.

2.7.1: Direct immunofluorescence

Direct immunofluorescence involves the direct binding of a fluorochrome conjugated primary antibody/ligand to the antigen of interest (Figure 2.3). This is a simple procedure requiring one specific type of directly labelled antibody/ligand. Direct immunofluorescence allows one to examine ligand binding properties as well as label a specific antigen.

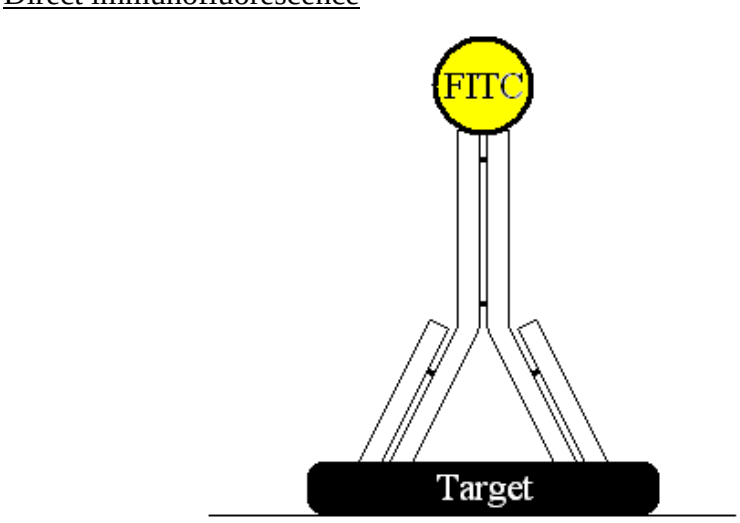

Figure 2.3: Direct immunofluorescence. Direct binding of a fluorochrome (example shown is fluorescein isothiocyanate {FITC}) conjugated monoclonal antibody/ligand to a target antigen. On excitation the fluorochrome emits fluorescence that can be detected and quantified.

When using direct immunofluorescence to label a protein in low abundance a weak signal may be achieved. To overcome this indirect immunofluorescence labelling can be used.

2.7.2: Indirect immunofluorescence

Indirect immunofluorescence is slightly more complex than direct immunofluorescence in that it requires two compatible antibodies in order to label a target protein. This procedure involves the initial binding of a primary antibody to a chosen target. A secondary fluorochrome conjugated antibody, specific to the primary antibody used, is then added to the sample (Figure 2.4). This will bind the primary and therefore label the antigen. The primary and secondary antibody binding is species-specific. If a mouse CD36 primary antibody was used for example, an anti-mouse fluorochrome conjugated secondary antibody will have to be used with this, such as a goat anti-mouse antibody.

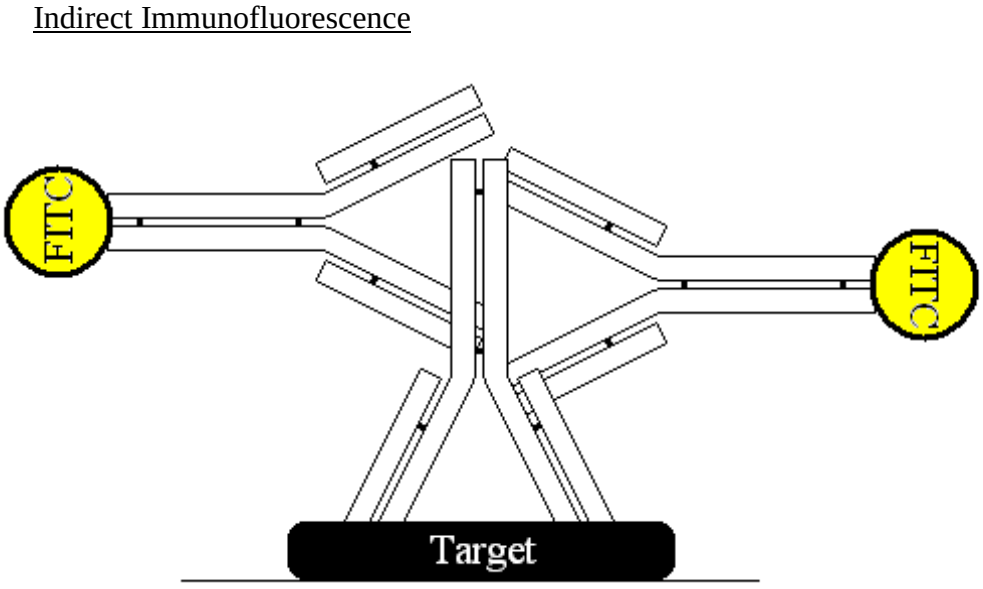

Figure 2.4: Indirect immunofluorescence: Indirect immunofluorescence involves the binding of a primary antibody to a chosen receptor, then the further binding of a fluorochrome (example used is fluorescein isothiocyanate {FITC}) conjugated secondary antibody to the primary antibody. The antibody binding is species-specific. On excitation the labelled fluorochrome emits fluorescence that can be detected and quantified.

Indirect immunofluorescence has the advantage of being more sensitive than direct immunofluorescence. This is because more than one secondary antibody can bind to any one primary antibody, thus giving a stronger signal.

2.8: Fluorescence activated cell sorter

The flow cytometer, also known as a Fluorescence Activated Cell Sorter (FACS), is able to quantify and distinguish between molecules according to their fluorescence and physiological structure. In this study fluorescently labelled cells and cytokines were analysed using a Becton Dickinson Fluorescent Activated Cell Sorter (FACSCalibur™) with CellQuest software also supplied by Becton Dickinson (Figure 2.5).

Flow cytometer

Figure 2.5: Becton Dickinson fluorescent activated cell sorter (FACSCalibur™). The flow cytometer can quantify and distinguish between molecules according to their fluorescence and physiological structure. www.cochin.inserm.fr/la_recherche/plates-formestechnologiques/cytometrie_en_flux/equipement-et-methodologie/analyse/images /FACSCalibur. jpg (05/01/10).

Fluorescently labelled cells that pass through the FACS are each individually exposed to a laser with a single wavelength of light. Fluorescein isothiocyanate (FITC) conjugated antibodies were used in this study to label specific receptors (Section 2.8.2.1). The resulting emitted light from the sample passes through a number of different detectors and analysed via the software. Cytokines can be labelled in much the

same way using a Cytometric BeadArray (CBA {BD Biosciences}) kit allowing the determination of their concentration in a sample (Section 2.8.2.2).

2.8.1: FACS System

FACS analysis can be divided into three main stages being fluidics, optics and signal processing.

2.8.1.1: FACS fluidics

FACS analysis requires the cells to be individually analyzed. When the cytometer is set to "acquire", the cells run through the chamber at very high speed in single file. This is achieved by the fluidics system of the FACS machine, via a process known as hydrodynamic focusing (Figure 2.6). Hydrodynamic focusing is achieved by injecting the sample from an inner core injector into sheath fluid (saline solution) in an outer core, surrounding the injector, which is flowing at a much higher velocity in the same direction.

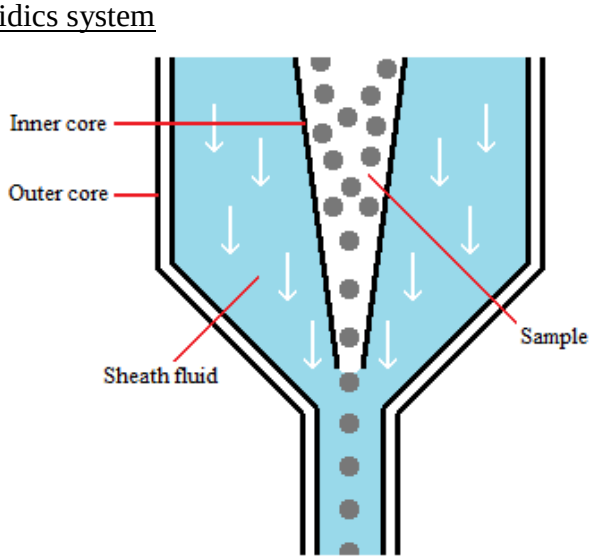

Figure 2.6: Hydrodynamic focusing of a sample by the fluidics system of the Fluorescence Activated Cell Sorter (FACS). The sample is injected from the inner core into sheath fluid (saline solution) from the outer core, which is flowing at a much higher velocity in the same direction. This causes the sample to exit in single file for analysis.

Hydrodynamic focusing results in the cells entering the flow cell in single file to be exposed to the optics system individually.

2.8.1.2: FACS optics

As the cells pass through the flow chamber one after the other they are subject to a laser that has a programmed wavelength. The light emitted from the sample will either be in the form of forward scattered light (FSC), side scattered light (SSC) or fluorescence from an activated fluorochrome label (Figure 2.7). FSC and SSC uncover the cells morphology whilst fluorochrome emission is used to quantify a labelled antigen.

FACS optics system

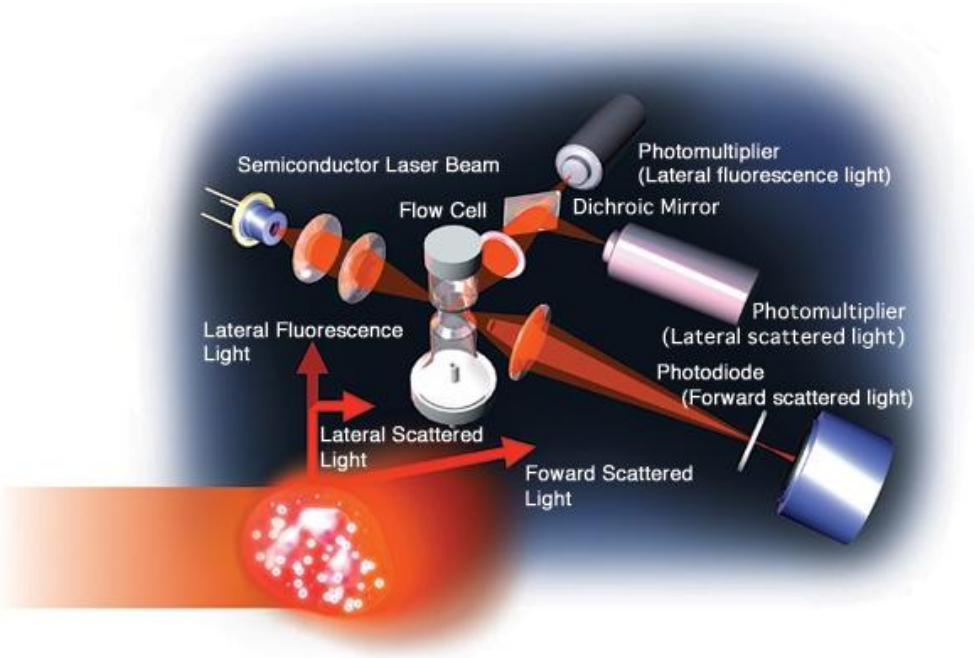

Figure 2.7: Arrangement of filters and detectors in the fluorescence activated cell sorter (FACS) optics system. Fluorescent detection and side scatter (SSC) is achieved at 90˚ to the path of the excitation laser beam. Forward scatter (FSC) is detected at 20˚ off the excitation laser beam. www.nci.cu.edu.eg/images/flow.jpg (05/01/10).

Fluorescence is emitted from fluorochromes that become excited when exposed to a laser beam of the correct wavelength (Table 2.4). Florescence is detected at 90˚ to the path of the excitation laser beam. The emitted light from a large population of cells,

which would have a wavelength specific to the fluorochrome used, is quantified. This information can be used to measure the mean quantity of a specific antigen a cell posses in a sample.

Scattered light that is given off when cells are subjected to the laser beam allows the FACS instrument to distinguish between cells with varied physiological structures. There are two types of scattered light that are detected; these are SSC and FSC. SSC highlights granules present in the cells and is collected by detectors at 90˚ to the path of the excitation laser beam. FSC is relative to cell size and can distinguish between live cells and debris. FSC is detected at 20˚ off the excitation laser beam. The result of the combination of these two factors is varied between, and can thus distinguish between, different cell-types, live/dead cells and different bead sizes in the CBA assay.

2.8.1.3: FACS signal processing

Signal processing was performed using CellQuest software. This software has complete control over the FACS allowing parameters to be refined for each experiment. Photons sensed by the photomultiplier tube (PMT) detectors are transformed to voltage and then relayed to the software. The combined information from the detectors is quantified, saved and displayed on the computer.

2.8.2: FACS application

Fluorescently labelled cells and cytokines were analysed using a Becton Dickinson Fluorescent Activated Cell Sorter (FACSCalibur™) with CellQuest software (Becton Dickinson). This was used to detect cellular PRR expression and released cytokine concentrations.

2.8.2.1: Pattern recognition receptor expression detection

Indirect immunofluorescence and flow cytometry were utilised in order to elucidate expression of TLR1, TLR2, TLR4, TLR6, CD36 and CD14 on ECV, HUVEC and HEK cell lines.

To perform the direct immunofluorescence assay, cell samples in 1.5ml eppendorf tubes were washed (centrifuged at 135g RT for 2 minutes, re-suspended in 500µl PBS/0.02% BSA {Bovine Serum Albumin [Sigma]}/0.02% NaN_3 and then centrifuged once again at 135g RT for 2 minutes) two times. The cells were then fixed by adding 300µl of 4% Paraformaldehyde (PFA {Sigma}) and left to incubate at room temperature for 10 minutes. Cells were then washed two times. The samples were then re-suspended in 200µl PBS/0.02% BSA/0.02% NaN_3. To this, 2µl of fluorochrome conjugated primary antibody was added. Cells were then incubated at room temperature for 4 hours and left over night at 4˚C. After incubation the cells were washed two times. The pellet was then re-suspended in 500µl PBS/0.02% BSA/0.02% NaN_3, and the samples were analysed using a Becton Dickinson Fluorescent Activated Cell Sorter (FACS Calibur™) with CellQuest software (Becton Dickinson).

2.8.2.2: Cytokine analysis

To quantify the inflammatory response of the various cell types used in this study the levels of released cytokines were measured. Cytokines are the messengers that co-ordinate the antibacterial and antiviral response and thus give a direct representation of cellular immune output.

In this study the Human Inflammation BD™ Cytometric Bead Array (CBA {BD Biosciences}) kit was used to measure cytokine concentrations. The Human

Inflammation CBA kit is capable of detecting six cytokines that play important roles in the human inflammatory response. These are interleukin-8 (IL-8), IL-1β, IL-6, IL-10, IL-12p70 and Tumor Necrosis Factor (TNF). CBA analysis allows the fast and highly sensitive quantification of an array of cytokines in any one sample.

In order to bind cytokines in a sample the beads are coated with capture antibodies specific for a particular cytokine. In the Human Inflammation BD™ CBA kit there are six bead populations with different morphologies, each specific for one of six cytokines. Once the beads have bound to the cytokines, a phycoerythrin (PE)-conjugated detection antibody mix is added; this is a mixture of PE-conjugated antibodies specific for each cytokine bead (Figure 2.8).

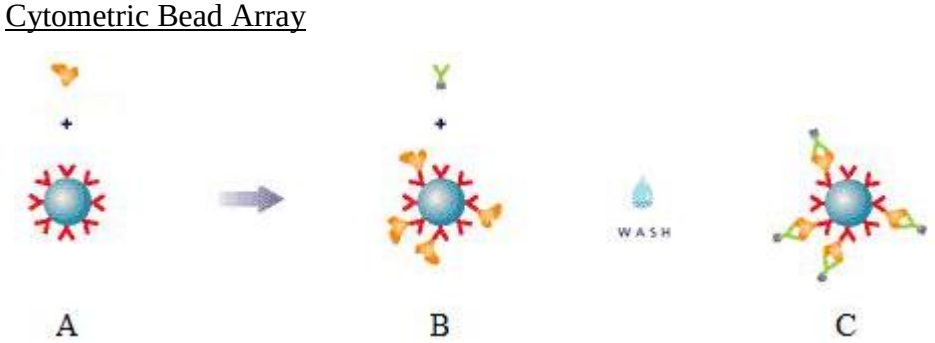

Figure 2.8: BD™ Cytometric bead array (CBA) system. A) CBA beads (blue) bind cytokines (yellow) in sample. B) Phycoerythrin (PE)-conjugated detection antibody (green) is added. Solution is incubated for 3 hours and then the excess washed off. C) Cytokine can be seen sandwiched between bead and the PE detection antibody. Adapted from: www.bd.com/scripts/resource .aspx?IDX=449 (15/01/10).

The Becton Dickinson Fluorescent Activated Cell Sorter (FACSCalibur™) was used in conjunction with CellQuest software (Becton Dickinson) in order to run the samples. Beads are distinguished by their morphology through detection of SSC and FSC (Section 2.8.1.2). CBA analysis software was used to process the raw data to cytokine concentration (pg/ml) using a previously calibrated standard curve.

2.8.2.2.1: CBA protocol

To analyze the inflammatory response of any given sample the medium was tested using the Human Inflammation BD™ Cytometric Bead Array (CBA {BD Biosciences}) kit.

For each sample, 25µl of bead mixture containing equal volumes of IL-8, IL-1β, IL-6, IL-10, IL-12p70 and TNF beads was added to a Falcon flow tube. To this, 25µl of sample were added and the mixture vortexed briefly. 25µl of phycoerythrin (PE)-conjugated detection antibody mixture was then added and vortexed briefly. The samples were left out of light to incubate at room temperature for 3 hours, gently shaking every 30 minutes. 1ml wash buffer (X1 PBS) was then added to each sample which was then centrifuged at 145g RT for 5 minutes. The supernatant was poured off leaving the pellet undisturbed. 300µl of wash buffer (BD Biosciences) was added to each tube and then vortexed very briefly. The samples were assayed using the Becton Dickinson Fluorescent Activated Cell Sorter (FACSCalibur™) used in conjunction with CellQuest software (Becton Dickinson). The cytokine concentration (pg/ml) was determined by data processing using CBA Analysis Software (Becton Dickinson).

2.9: Confocal Microscopy

Confocal microscopy was developed in 1955 by Marvin Minsky of Harvard University. This imaging technique proved to be far better than light or standard fluorescence microscopy. Confocal microscopes are able to produce images with a very high spatial and temporal resolution.

Confocal microscope

Figure 2.9: Confocal microscopes are able to filter out background light producing images with a resolution far greater than images obtained from conventional fluorescent microscopes. www.einstein.yu.edu/aif/instructions/aobs/index.htm (17/01/10).

Conventional microscopes function by exposing the whole sample to light, and then recording the light emitted. The image produced from such a technique includes in focus and out of focus light emitted from the whole depth of the specimen, from above and below the focal plane. This produces a blurred image where focused light is overlapped with the unfocused light. Confocal microscopy avoids this noise by excluding light from the sample that is not specifically in the focal plane, increasing the definition of the image.

The confocal microscope uses two lenses to focus light from the focal point through a pinhole aperture to where the light is detected. The pinhole diameter can be manipulated to cut out any light outside of the focal plane; as shown by the light blue light path in Figure 2.10. Mirrors are used to scan the laser light source across specimen in this manner in order to build up a total image.

Principle of the confocal microscope

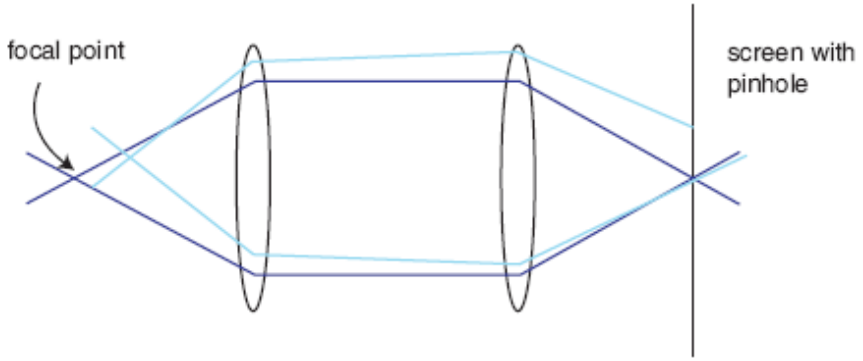

Figure 2.10: Lens layout of a confocal microscope. Confocal microscopy uses two lenses to focus light from the focal point of one lens to a pin hole where the light is detected. This method eliminates out of focus light producing a high resolution image. www.physics.emory.edu/~weeks/confocal (17/01/10).

Due to the accuracy of the confocal microscope and its ability to cut out unfocused light it is capable of three dimensional imaging. Multiple images taken along the Z axis of the microscope, through the depth of a sample, can be stacked together (Z-stack) to create a revealing three dimensional representation.

Another great advantage of the confocal microscope is that it makes it possible to perform live cell imaging at a very high resolution. Live cell imaging is not possible in other high resolution microscopy techniques, such as scanning electron microscopy (SEM), due to the complications of specimen preparation.

The laser beam passes through the microscope to the sample via a dichroic mirror and two motorised rotating mirrors. The motorised mirrors scan the laser beam over the sample. The light emitted is focused by two lenses, back in the direction of the original laser path, through a pinhole aperture and onto a photomultiplier tube (PMT) detector (Figure 2.11). The image points (voxels) collected from scanning the sample are processed by computer software into a two dimensional image.

Light path in a confocal microscope

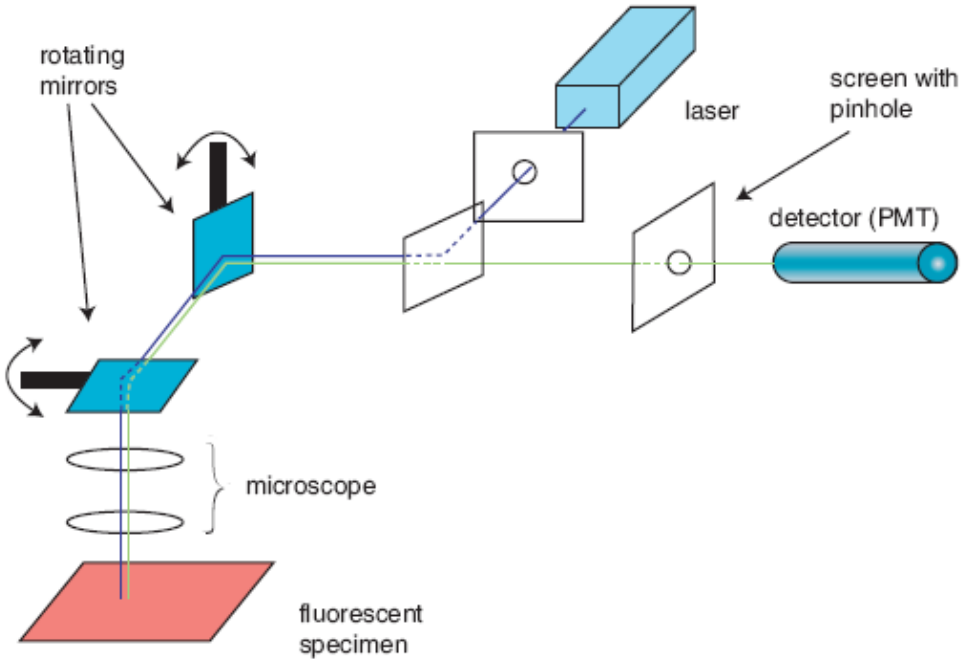

Figure 2.11: Light path in a confocal microscope. Two motorised rotating mirrors are used to scan the laser beam over the sample. Emitted light passes back in the direction of the laser through a pinhole, ridding of any more undesired light, and onto a photomultiplier tube detector. www.physics.emory.edu/~weeks/confocal (17/01/10).

The selective mechanisms used by confocal microscopy, in order to produce the high quality images that it is capable of, results in a relatively weak signal. The weak signal is overcome by the use of lasers and PMT detectors. The laser produces exceptionally bright, low-divergent, light that can be focused and collected with minimal light loss. PMT detectors amplify the weakened signal.

The imaging of biological samples with confocal microscopy usually involves the binding of fluorochromes to the specimen via direct or indirect immunofluorescence (Section 2.7). Fluorescence is emitted from fluorochromes that become excited when exposed to a laser beam of the correct wavelength (Section 2.7). The confocal microscope is capable of imaging different emission wavelengths from a single sample.

This allows multiple labelling of molecules and/or structures in a sample at any one time. Multiple labelling of cells with more than one type of fluorochrome can be used to uncover the location, abundance, colocalisation and trafficking of target proteins.

The Confocal microscope utilized in this study was a Zeiss LSM 510 META using a 1.4 NA 63x Zeiss objective, used in conjunction with Zeiss LSM 2.5 analysis software. Cells were cultured on 8 well glass slides (Lab-Tek™ Chamber Slide™ System) which were labelled via direct and/or indirect immunofluorescence.

Lab-Tek™ Chamber Slide™ System

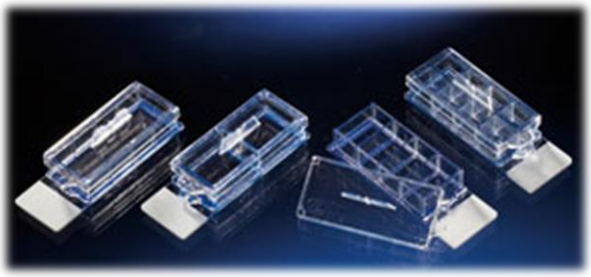

Figure 2.12: The Lab-Tek™ Chamber Slide™ System was utilised in this study for the confocal imaging of primary HUVECs. Cells are cultured, stimulated and labelled directly on the slide. www.nuncbrand.com/page .aspx?ID=234 (18/01/10).

2.9.1: Seeding HUVECs in Lab-Tek™ slides

HUVECs were cultured in 24 well plates (Nunc) in Medium 200 (Cascade Biologics) containing a Low Serum Growth Supplement Kit (LSGS {Cascade Biologics}). When the cells became confluent the wells were split (50/50) into fresh 24 well plates and left to grow for 48 hours.

To increase adherence of the HUVEC cell line to the 8 well slide surface (Lab-Tek™ Chamber Slide™ System) the slides were treated with collagen (type-I from rat tail {Sigma}). 250µl of sterile 10% collagen (1ml collagen in 9ml X1 PBS) was added to

each well. The slide was then incubated at 37˚C for 120 minutes. The collagen formed a thin film on the bottom of the slide and the PBS was carefully aspirated off.

After the two day incubation in 24 well plates the medium was removed from the HUVECs and replaced with 1ml fresh Medium 200 + LSGS. The cells were re-suspended thoroughly. 500µl of Medium 200 + LSGS was added into each collagen treated well of an 8 well glass slide (0.8cm^2 each well). 25µl of cell suspension was added to each well. The cell suspensions were homogenized and left to incubate at 37˚C with 5% CO_2 in a humidified atmosphere for two days.

The cells had grown in such a way that they were mature, spread out and flat. Ideal for confocal microscopy. HUVECs were stimulated directly on the slide (Section 2.5.3).

2.9.2: Labelling HUVECs on Lab-Tek™ slides

Both direct and indirect immunofluorescence (Section 2.7) techniques were used to label primary HUVECs on 8 well glass slides (Lab-Tek™ Chamber Slide™ System).

Medium was gently removed with a pipettor and the cells were gently washed two times with 500µl PBS/0.02% BSA/0.02% NaN_3. 300µl of 4% PFA (Sigma) was then added to each well and incubated for 10 minutes at room temperature. The wells were gently washed two times with 500µl PBS/0.02% BSA/0.02% NaN_3. 100µl of X1 PBS/0.02% BSA/0.02% NaN_3 (cell surface labelling) or X1 PBS/BSA 0.02% /SAPONIN (intracellular labelling) were then added to each well. 5µl of hybridoma or 2µl of commercial primary antibodies were added (Table 2.1). The slides were incubated for 4 hours at room temperature and left at 4˚C for 18 hours. The following day the wells

were washed three times with 500µl X1 PBS/0.02% BSA/0.02% NaN_3. 100µl of X1 PBS/0.02% BSA/0.02% NaN_3 (cell surface labelling) or X1 PBS/BSA 0.02% /SAPONIN (intracellular labelling) were then added to each well. 2µl of the relevant secondary antibody (indirect immunofluorescence) or 6µl of direct labelling antibodies (direct immunofluorescence) was added. Slides were incubated at room temperature for 45 minutes. Slides were then washed, antifade treated and sealed.

2.9.2.1: Antifade treatment

The wells of the Lab-Tek™ slides were then removed and the cells treated with SlowFadeR Light Antifade Kit (Molecular Probes, Invitrogen). One drop of Equilibration buffer (Molecular Probes, Invitrogen) was placed in each well and left at room temperature for 2 minutes and then gently poured off, this step was repeated one more time. The gasket of the Lab-Tek™ slide was then removed and one drop of anti-fade reagent in glycerol (Molecular Probes, Invitrogen) was placed on each well. Cover slips were gently placed on the slide, any excess reagent gently removed, and were sealed using nail polish.

Slides were viewed using a Zeiss LSM 510 META confocal microscope with a 1.4 NA 63x Zeiss objective, used in conjunction with Ziess LSM 2.5 analysis software (Section 2.9). The colocalisation of images was quantified using Costes' method through the analysis software ImageJ (Version 1.43) with the JACoP plugin (Section 2.9.3)

2.9.3: Quantification of colocalisation in confocal images

Colocalisation of molecules and/or structures in a cell can be determined by their multiple labelling and then detection to see to what extent these labels overlap.

Molecules and/or structures in a cell can be labelled with varied fluorochrome conjugated antibodies (Table 2.1) that emit light of different wavelengths (Section 2.7). Fluorescent microscopy allows the separate collection of these different wavelengths emitted from an image which can then be overlaid and analysed for colocalisation. Multiple labelling of cells with various fluorochrome conjugated antibodies for antigens of interest allows researchers great insight into the biological processes of the cell.

Confocal microscopy (Section 2.9) is commonly used for colocalisation studies due to its very high spatial and temporal resolution. These microscopes can be used to excitate specific fluorophores and subsequently gate a specific wavelength range of emitted light resulting in an image constructed of just, for example, the "green" labelled antigens. This image will show the location of the antigen bound by the "green" fluorochrome conjugated antibody. Merging this image with those obtained for other fluorochrome labelled antigens (red in the example) can allow one to speculate their colocalisation (shown as yellow).

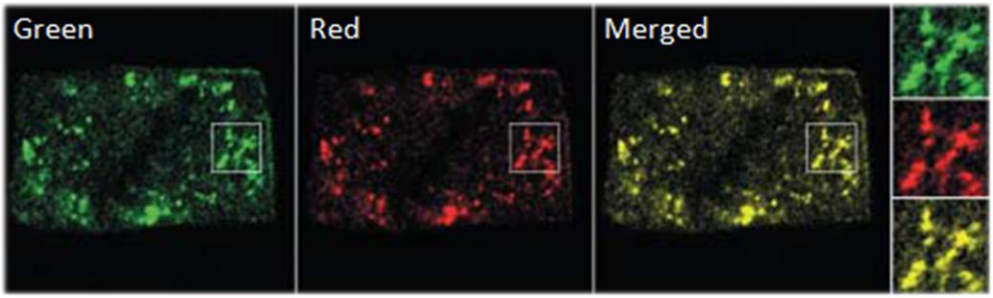

Figure 2.13: Complete colocalisation of "Green" and "Red" labelled antigens. Since "Green" and "Red" images are of equal intensity their colocalisation shown as yellow in the "Merged" image is clear. Golgi staining of fixed maize root cells. Boutté *et al.* (2006)[193].

Qualitative analysis of these images is however rather ambiguous and is not sufficient to conclude colocalisation. (After all, the human eye has its own limitations.) For example,

in an ideal world both labels ("green" and "red") would emit light of equal intensities as in Figure 2.13. This is, however, often not the case. If complete colocalisation exists but the "red" fluorophore is more intense than the "green", perhaps just due to the nature of the fluorophore (some are better than others), the "merged" image would not show a 50/50 mix of these two, and thus will not display yellow where colocalisation exists. This scenario is illustrated in Figure 2.14.

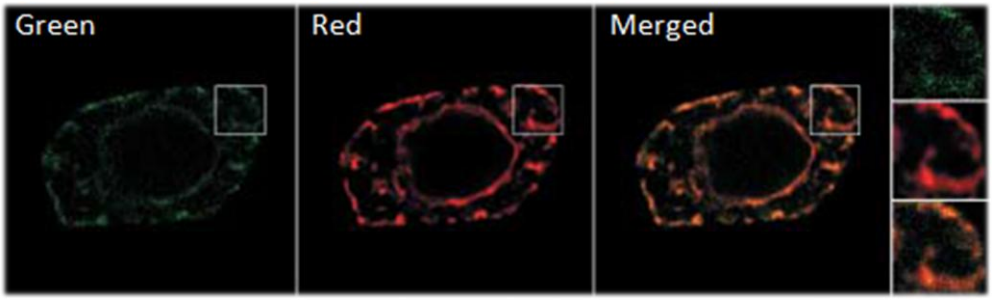

Figure 2.14: Complete colocalisation of "Green" and "Red" labelled antigens. Since the "Red" image is more intense than the "Green" image their colocalisation in the "Merged" image is less clear for the red has overpowered the green. Endoplasmic reticulum staining. Kluge *et al*. (2004)[194].

Colocalisation however, is independent of intensity. This should not be a factor influencing the analysis of colocalisation of two images. A number of other factors make the qualitative analysis of colocalisation unreliable and invalid. Pixels of overlaid images may be in close proximity and appear to the human eye as overlapping when they are not. Also when an image has a lot of background, due to non-specific binding for example, the qualitative analysis of such images can be invalid and thus inconclusive. Statistical software has been developed that can quantify colocalisation. By considering pixels individually in separately gated images, such programs can accurately quantify the amount of colocalisation between two fluorescent labels.

In this study the analysis software ImageJ (Version 1.43) with the JACoP plugin (Figure 2.15) was used[195]. This software allows the analysis of the colocalisation of two images using a number of standard analysis methods simultaneously. This study used the Costes' randomization method, which utilises the Pearson's correlation coefficient, to quantify colocalisation of fluorochrome labelled antigens in HUVECs.

ImageJ (Version 1.43) with JACoP plugin

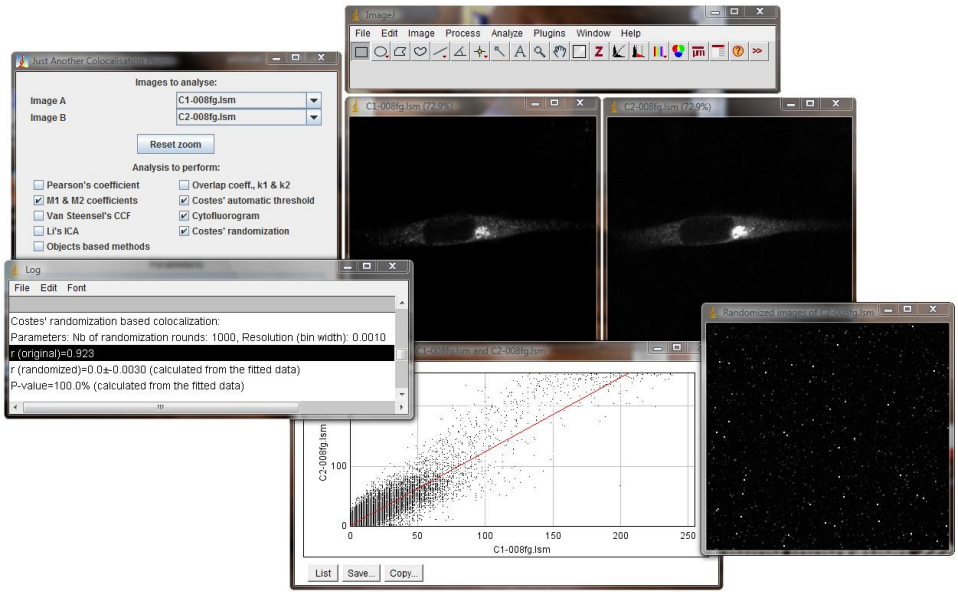

Figure 2.15: The interface of ImageJ (Version 1.43) software with the JACoP plugin. This software analyses two images for colocalisation using a number of standard colocalisation analysis methods simultaneously, such as the Pearson's correlation coefficient (Rr) and Costes' method[195].

The Pearson's correlation coefficient (Rr) is a method that measures the covariance between the intensities of corresponding pixels in each gated image. The images are both analysed as grey for consistency. This statistical analysis is independent of background. Pearson's correlation coefficient is also independent of pixel intensities for thresholds are automatically created for each gated image. The maximum intensity of an

image is used to set the image threshold. Results obtained from this analysis range from -1 (total negative correlation) to 1 (total positive correlation).

The Costes' method evaluates the statistical significance of the Pearson's correlation coefficient obtained. This method compares the Rr observed from the original two images (r{original} or r{obs}) with an average Rr obtained from comparing scrambled (randomized) images of the two original images (r{randomized}) which have been created by shuffling pixel blocks[196]. An image that has undergone Costes' randomization can be seen in the bottom right of Figure 2.15. r{randomized} is an average of a comparison of 1000 pairs of scrambled original images, it is representative of events occurring due to chance. The r{obs} and r{randomized} are then compared to obtain a p-value. Results obtained from this analysis range from 0 (total negative correlation) to 1 (total positive correlation).

2.9.4: Förster Resonance Energy Transfer

The Förster (or Fluorescence) resonance energy transfer (FRET) technique allows the quantification of the association between fluorescently labelled molecules ≤10nm apart. FRET microscopy works by capturing the interaction between labelled molecules when they are in close proximity, and then using this to calculate their distance relative to one another. Since FRET only occurs if the fluorochromes are ≤10nm apart, its detection has the effect of extending the resolution of fluorescence microscopy to the molecular level. This uncovers cellular localisations which were previously undetectable.

FRET utilises the non-radiative energy transfer between two specifically selected different fluorophores that have been used to label two molecules of interest. These

molecules could be present in a number of forms such as in solution or in/on single living or fixed cells. Energy transfer occurs from an excited donor fluorophore to an appropriate acceptor fluorophore[197]. This transfer of energy from one fluorophore to another can only occur when these are ≤10nm apart.

The rate of energy transfer is inversely proportional to the sixth power of the distance between the donor and acceptor[198,199]. The efficiency of energy transfer (E) is defined with respect to r and R_0, the characteristic Förster distance by:

$$E= 1/[\ 1 + (r/\ R_0)^6]$$

Kenworthy *et al.* (1998)[198].

R_0 is the Förster distance of the donor/acceptor pair. This is a constant that represents the distance at which the energy transfer efficiency between the fluorophores is 50%. The Förster distance varies between different donor/acceptor pairs.

Due to the nature of FRET the fluorophores have to be carefully selected to achieve an appropriate donor and acceptor fluorophore pair, referred to as a donor/acceptor pair. The emission wavelength from the donor has to be of the wavelength that excites the acceptor, the wavelength the acceptor absorbs, and therefore these have to overlap (Figure 2.16).

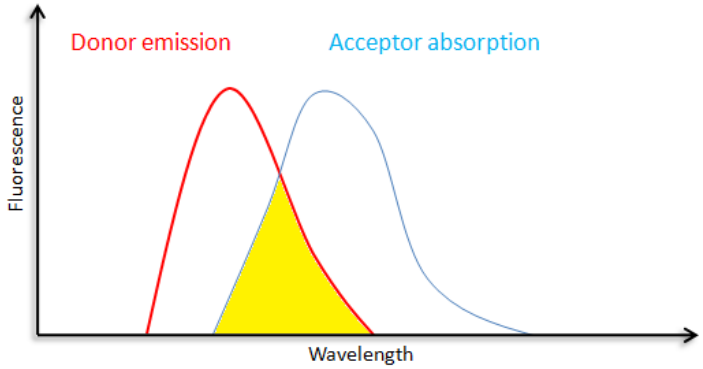

Figure 2.16: Schematic diagram showing the overlapping (yellow) of donor emission (red) and acceptor absorption (blue) spectra indicating an appropriate fluorophore pair for FRET. The emission wavelength from the donor has to be of the wavelength that excites the acceptor, the wavelength the acceptor absorbs, and therefore these have to overlap. FRET will only occur when donor and acceptor fluorophores are ≤10nm apart.

The donor fluorophore is excited by a laser which causes emission of light. If the acceptor fluorophore is ≥10nm apart from the donor this energy will be released as light unaffected by the acceptor. However, if the acceptor is ≤10nm in distance from the donor then two scenarios occur. Assuming a donor/acceptor pair, the emission wavelength of the excited donor fluorophore is sufficient to excitate the acceptor fluorophore, when these are ≤10nm apart, causing emission of light from the acceptor. The emitted light of the acceptor will be of a set known wavelength band and can be collected and quantified. Another result of FRET is a reduction in donor fluorophore emission on excitation. If donor and acceptor are ≤10nm apart, a portion of the energy emitted from the excited donor fluorophore will be absorbed by the acceptor fluorophore. This will also have the effect of reducing the light emission and excited state lifetime of the donor fluorophore for the energy has gone into acceptor excitation. The change in donor emission can be used to quantify FRET.

In this study, FRET was quantified using a method as previously described[198,199]. FRET was calculated by measuring the change in donor (Cy3) emission following acceptor (Cy5) bleaching. By bleaching the acceptor you are in effect removing the fluorophore.

If the acceptor is bleached (removed) then FRET will no longer occur between the pair and thus donor emission will no longer be sequestered. If the donor/acceptor pair are ≤10nm apart then donor emission will increase after bleaching of the acceptor. The association between the donor/acceptor pair was calculated using:

$$E(\%) \times 100 = 10{,}000 \times [(\text{Cy3 post-bleach} - \text{Cy3 pre-bleach})/\text{Cy3 postbleach}]$$

Scaling factor of 10,000 was used in order to expand E to the scale of the 12-bit images.

2.9.4.1: FRET Protocol

HUVECs were seeded on 8 well glass slides (Lab-Tek™ Chamber Slide™ System {Section 2.9.1}). Donor acceptor pair used was Cy3 and Cy5 (Table 2.1). Cells labelled only with the 26ic-Cy5 probe were used in order to determine the minimum time required to bleach Cy5. Cy5 was bleached by continuous excitation with an arc lamp using a Cy5 filter set for 5 minutes. Under these conditions, Cy3 was not bleached. The cells were rinsed twice in PBS/0.02% BSA/0.02% NaN_3, prior to fixation with 4% PFA for 15 minutes. HUVECs were labelled with 100µl of a mixture of donor conjugated antibody (Cy3) and acceptor conjugated antibody (Cy5). Cells were imaged on a Carl Zeiss LSM510 confocal microscope (with an Axiovert 200 fluorescent microscope) using a 1.4 NA 63x Zeiss objective used in conjunction with Zeiss LSM 2.5 analysis software. Cy3 and Cy5 were detected using the appropriate filter sets. Using typical exposure times for image acquisition (less than 5 seconds), no fluorescence was observed from a Cy3-labelled specimen using the Cy5 filters, nor was Cy5 fluorescence detected using the Cy3 filter sets. Zeiss LSM 2.5 analysis software processed the FRET images using:

$$E(\%) \times 100 = 10{,}000 \times [(\text{Cy3 postbleach} - \text{Cy3 pre-bleach})/\text{Cy3 postbleach}]$$

2.10: Sodium dodecyl sulphate polyacrylamide gel electrophoresis

Sodium dodecyl sulphate polyacrylamide gel electrophoresis (SDS-PAGE) is used for the separation of proteins according to length which is relative to weight. This method can be used for many things such as to determine protein abundance, identify a protein, determine protein size, find the number of proteins present and find the purity of a sample.

The proteins in a sample will have a number of differences including length, shape, weight and charge. For SDS-PAGE to work correctly the proteins must be put on a level playing field. SDS is an anionic detergent that disrupts the hydrogen bonds and Van der Waal's interactions in proteins, and also breaks down cell membranes. This destroys the secondary, tertiary and quaternary structures of the protein causing them to become linear. The resulting negative charge of any protein is relative to their size, for the number of anionic SDS molecules that bind is proportional to the number of amino acids in the polypeptide. This acts to calibrate the assay so that you are mostly looking at protein size.

The separation of the proteins occurs in the polyacrylamide gel, which is made up of many acrylamide monomers that create a sieve like matrix through which the proteins have to pass. The negative charge of the proteins are utilised to pull them through the gel by application of voltage. The cross-linked matrix makes it difficult for molecules to move through the polyacrylamide gel, the smaller proteins have an advantage due to their size and thus will move furthest through the gel toward the positive terminal (Figure 2.17B).

SDS-PAGE apparatus

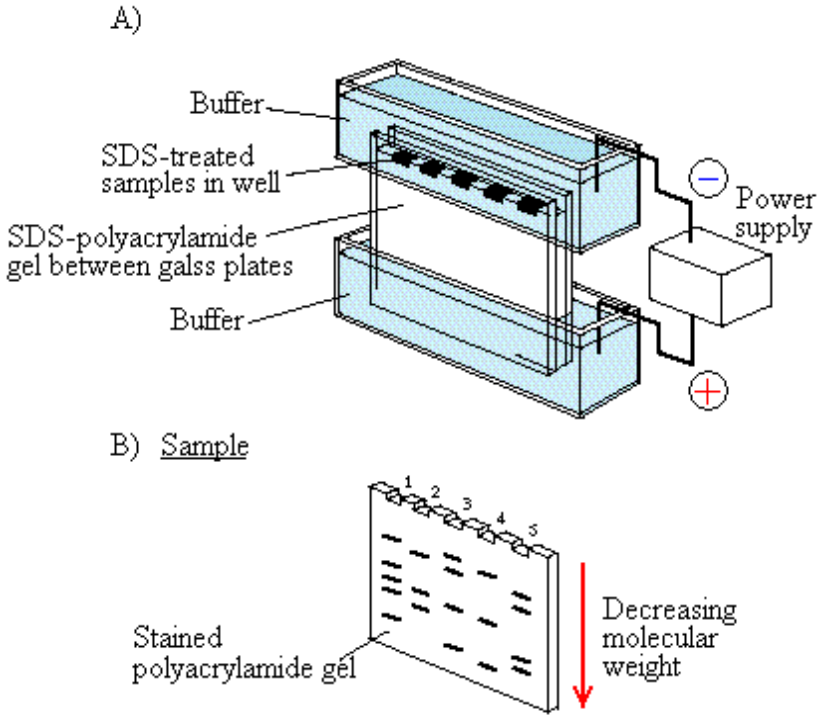

Figure 2.17: Sodium dodecyl sulphate polyacrylamide gel electrophoresis (SDS-PAGE) apparatus. SDS-PAGE is a technique for separating proteins in relation to size which is relative to weight. The application of voltage pulls negatively charged denatured proteins through a cross-linked polyacrylamide gel matrix. Smaller proteins have an advantage due to their size and move furthest through the gel matrix toward the positive terminal. Larger proteins do not migrate as far as smaller proteins, over a set time. Adapted from: www.library.csi.cuny.edu/~davis/Bio_327/lectures/protein_nucleicAnal/protein_nucleicAnal.html (22/03/06).

Pore size within the matrix can be manipulated by varying the concentration of Acrylamide/Bis in a gel mixture. This allows the selection of a gel that will suit your sample. For example, a mixture of small proteins would best suit a higher Acrylamide/Bis % gel (smaller pore size) so that they separate effectively and do not run off the gel easily. In this study a 10% gel was used. The gel is made up in liquid form and can be easily poured into appropriate casts to set. The polymerisation of the gel is caused by ammonium persulfate (APS) and N,N,N',N'-tetra-methylethylenediamine (TEMED). Once these chemicals are added the gel forms cross links creating the sieve like matrix required.

For SDS-PAGE analysis in this study the Mini-PROTEAN 3 apparatus (BioRad) was utilised (Figure 2.18).

Mini-PROTEAN 3 apparatus (BioRad)

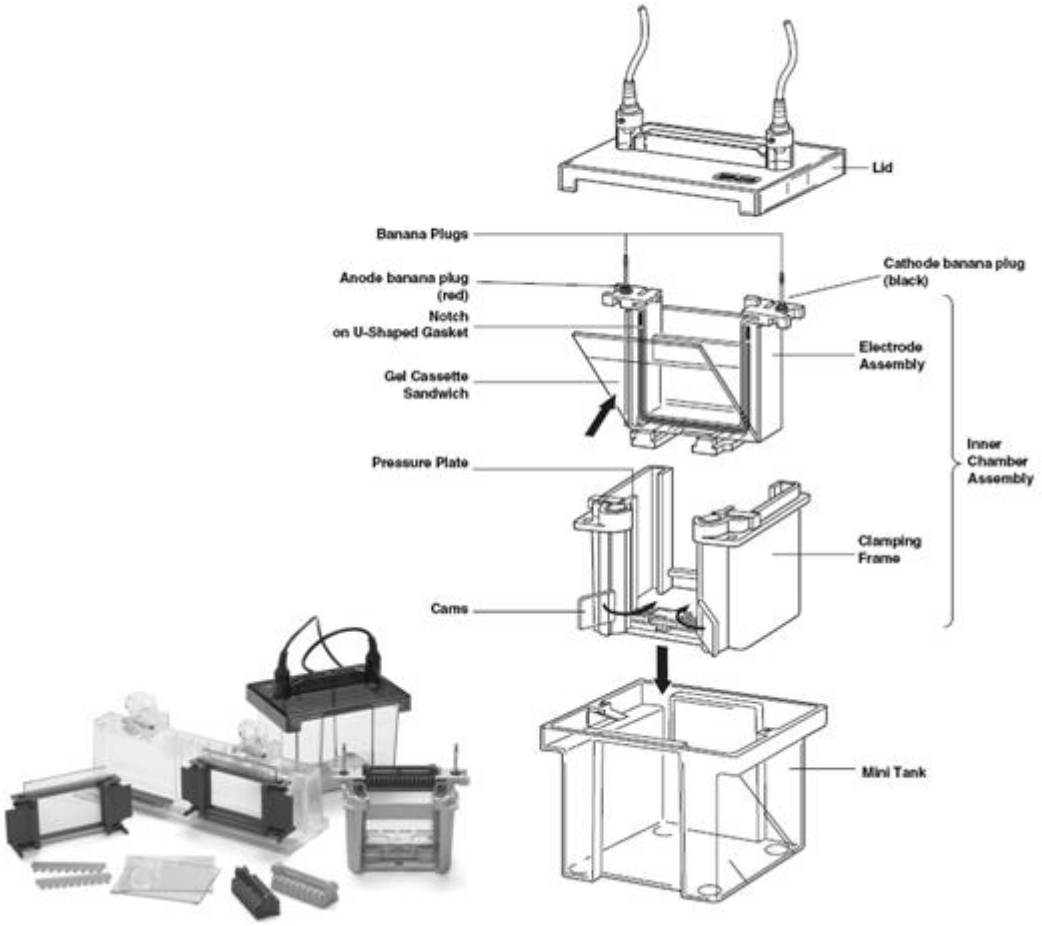

Figure 2.18: The Mini-PROTEAN 3 apparatus (BioRad) was used to run sodium dodecyl sulphate polyacrylamide gel electrophoresis (SDS-PAGE). www3.bio-rad.com/cmc_upload/ Literature/44432/4006157B.pdf (22/01/10).

2.10.1: Casting SDS-PAGE gels

Gels were cast in 1mm width casts. The resolving gel (1.5M Tris-HCL, 10% SDS, Acrylamide/Bis {Severn Biotech}, 10% APS {Sigma}, TEMED {Sigma} and dH_2O) mixture was made up leaving the addition of APS and TEMED until last. Once the APS and TEMED were added the liquid gel was immediately placed into the cast leaving adequate room for the teeth of the comb (to create the loading wells). On top of this

approximately 500µl isobutanol was added to make the gel surface smooth and flat. The gel was left to set at room temperature for 45 minutes. The isobutanol was then poured off and then the gel was rinsed with distilled water. The 4% stacking gel (0.5M Tris-HCL, 10% SDS, Acrylamide/Bis, 10% APS, TEMED and dH_2O) mixture was made up leaving the addition of APS and TEMED until last. This was then placed on top of the set resolving gel. A 1mm, 10 teethed comb was placed in the stacking gel mixture to create wells for the samples. The gel was left to set at room temperature for 45 minutes.

Once the stacking gel had set, the comb was removed and the gels were placed into the electrophoresis tank (BioRad). X1 running buffer solution (25Mm Tris, 192mM glycine and 0.1% {w/v} SDS, pH8.3) was then placed into the tank.

2.10.2: Sample preparation

ECV304 cells were lysed in 25cm^2 flasks (Nunc) with 1ml X2 reducing sample buffer (Appendix) for 4 hours on the work top shaker and then frozen at -20˚C for a minimum of one night. Primary HUVECs were lysed in 24-well plates (Nunc) with 200µl X2 reducing sample buffer for 4 hours on the work top shaker and then frozen at -20˚C for a minimum of 24 hours.

2.10.3: Running samples

50µl of the lysed samples and 21µl of the molecular weight marker (1µl biotinylated SDS-PAGE broad range standard {BioRad} in 20µl reducing sample buffer) were placed in eppendorf tubes and boiled in a water bath for 10 minutes. Once let to cool for approximately 5 minutes, 30µl of the samples were placed in their respective wells in the polyacrylamide gel. The gel was run at 200V constant for 45-50 minutes within X1 running buffer solution (BioRad).

Once samples have ran through the polyacrylamide gel it was removed and placed on transfer (Section 2.11) so that the proteins migrate into a nitrocellulose membrane. The membrane was then labelled and imaged via enhanced chemiluminescence (ECL {Section 2.12}).

2.10.4: Coomassie blue staining of SDS-PAGE gel

Coomassie blue, or coomassie brilliant blue G-250, stain binds non-specifically to nearly all proteins through van der Waal`s force interactions with amino acids such as histidine, arginine, lysine and tyrosine. Coomassie blue staining is used for a number of purposes such as protein concentration determination, via the Bradford protein assay, or visualization of protein bands on SDS-PAGE gels. In this study coomassie blue staining was used to visualize protein bands separated in SDS-PAGE gels.

2.10.4.1: Coomassie blue protocol

The SDS-PAGE gel was removed from the electrophoresis glass plates and placed in fixing solution (Appendix) overnight. The gel was removed from the fixing solution and then submerged in coomassie blue for 60 minutes. The coomassie blue (Appendix) was removed and the gel was washed with de-stain (Appendix) with changes at every 10 minutes until stained protein bands could be observed. The optical densities of the bands were quantified using a densitometer (GS-700 imaging densitometer {BioRad}).

2.11: SDS-PAGE gel transfer

Following SDS-PAGE (Section 2.10) the gel is removed and undergoes an electroblot. The proteins are transferred into a portion of nitrocellulose membrane in the same formation as they were in the gel. The gel transfer mechanism uses the same method as

SDS-PAGE to pull proteins, or nucleic acids, out of the polyacrylamide gel matrix and into the nitrocellulose membrane (Figure 2.19).

Electroblot layout

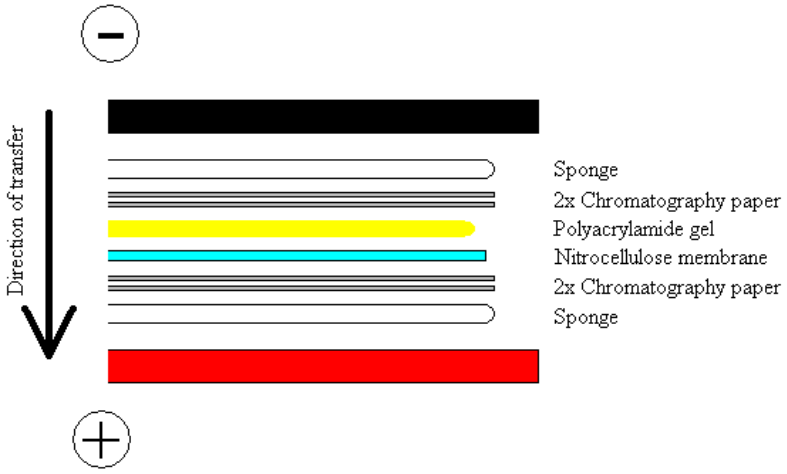

Figure 2.19: Electroblotting layout. Electroblotting is used to pull proteins from a polyacrylamide gel onto a nitrocellulose membrane. The direction of transfer/protein movement is illustrated by black arrow (left). The protein is pulled out of the polyacrylamide gel (yellow) into the nitrocellulose membrane (blue), from a negative to positive charge.

Once in the membrane the sample is accessible to labelling and analysis via a number of methods, such as: fluorescent detection, radioactive detection, colorimetric detection and chemiluminescence. These techniques allow one to view the position and relative concentration of a specific protein.

Transfer apparatus

Figure 2.20: Bio-Rad transfer apparatus. www.bosch.org.au/facilities/molecularbiology/Western Blot/WesternBlot.jpg (23/01/10).

2.11.1: Transfer protocol

After SDS-PAGE the poly acrylamide gel was removed and placed on transfer using the Mini Transblot system form BioRad. The gel was placed in a transfer cassette on top of a porous pad, two pieces of blotting paper and a nitrocellulose transfer membrane (Whatman Protran), in that order (Figure 2.20). Two pieces of blotting paper and then a porous pad were placed on top of the membrane. All components of the transfer construction were previously soaked in transfer buffer (20nM Tris acetate, 0.1% SDS, 20% isopropanol, pH 8.3). The cassette was closed and placed into the transfer tank. An ice block was placed inside the tank along with the cassette and then it was filled to the top with transfer buffer. The power pack was set to run at 220mA constant for 55 minutes.

2.12: Enhanced chemiluminescence

Enhanced chemiluminescence (ECL) is a very sensitive and fast procedure. This method utilises light emitted from an enzymatic reaction to image a protein of choice. After a protein sample has been separated by SDS-PAGE (Section 2.10) and transferred onto a solid support (Section 2.11), the target protein is then labelled either directly or indirectly with an antibody that is conjugated to an enzyme. Horse radish peroxidase (HRP) was used in this study (Table 2.1). The exposure of a luminol based substrate (ECL reagents) to the HRP label causes a light emitting reaction that can be visualized when exposed to high performance chemiluminescence film.

Enhanced chemiluminescence by indirect labelling

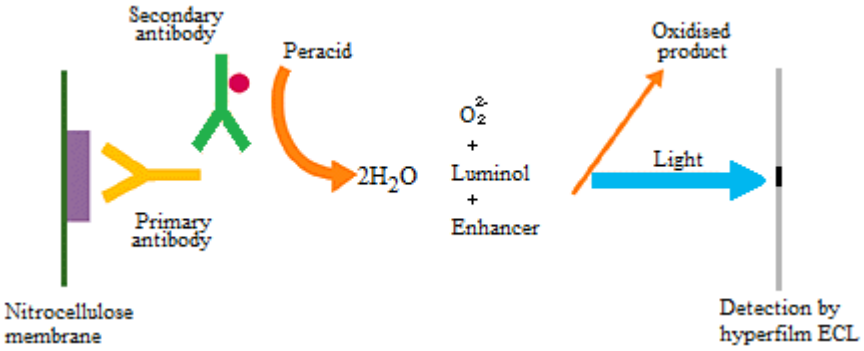

Figure 2.21: Enhanced chemiluminescence (ECL). Indirect labelling. The nitrocellulose membrane was labelled with primary (yellow) and horse radish peroxidise (HRP {red}) conjugated secondary antibody (green). HRP catalyzes the oxidation of luminal and light (blue) is emitted and detected (black) on film (grey). Adapted from: www1.gelifesciences .com/Images/ps/ figure1t.gif (25/01/10).

NF-κB, the downstream transcription factor of the TLR pathway, is held in an inactive form in the cytoplasm by members of the inhibitor of NF-κB (IκB) family. Phosphorylation of IκB leads to IκB polyubiquitylation that labels the NF-κB inhibitor for proteasomal degradation which in turns releases NF-κB from inhibition which can then translocate to the nucleus and upregulate inflammatory genes (Section 1.3.6). Thus the presence of phospho-IκB illustrates the activation of the TLR signalling pathway, demonstrating an immune response. In this study ECL was utilised to image both phospho-IκB and total-IκB. Total-IκB levels were viewed as a control to demonstrate equal loading. Indirect immunofluorescence was used to probe the nitrocellulose membrane where the secondary antibodies were conjugated to HRP.

2.12.1: Labelling the nitrocellulose membrane

The nitrocellulose membrane was removed from transfer and rinsed twice with X1 PBS TWEEN (Appendix) and then placed in blocking buffer (Appendix) on rotary for 1 hour. The membrane was then washed for 1 hour in X1 PBS TWEEN with two rinses

every 15 minutes. The membrane was then placed in low volume containers and were submerged in 9ml 1:1000 of either or Phospho-IKappaB-alpha (Ser 32) rabbit (Cell Signalling technology) or IKappaB-alpha (C-term) mouse (Cell Signalling technology) primary antibodies in X1 PBS TWEEN (Table 2.1). The membrane was left on rotary at room temperature for 4 hours and left in the fridge overnight. The next day the membrane was washed for 30 minutes with X1 PBS TWEEN with two rinses every 15 minutes. The membrane was then placed in low volume containers and was submerged in 9ml 1:2000 HRP-conjugated secondary antibody (DAKO Cytomation) in X1 PBS TWEEN (Table 2.1). The membrane was left on rotary at room temperature for 45 minutes. 30 minutes into the incubation with secondary antibody streptavidin-HRP conjugate (GE Healthcare) 1:1500, was added for 15 minute incubation with the membrane. At 45 minutes after addition of the swine anti-rabbit HRP secondary antibody the membrane was removed and washed for 2 hours in X1 PBS TWEEN with two rinses every 15 minutes. After two hours washing, the membrane was ready for developing by enhanced chemiluminescence (ECL).

2.12.2: ECL protocol

ECL western blotting detection reagents A and B (GE Healthcare) were mixed in a 1:1 ratio (3ml total for one membrane). A dark room was utilised for film processing. Membranes were placed face up on Saran wrap and then covered with the detection reagents. The membranes were then incubated at room temperature for 1 minute. Once the reaction had commenced the membranes were transferred to a fresh piece of Saran wrap, flipped over and wrapped up ensuring only one sheet of Saran wrap was covering the face of the membrane. The membrane was placed in a developing cassette where high performance chemiluminescence film (Hyperfilm^{TM} from GE Healthcare) was

exposed to it. An initial exposure of 2 minutes was performed; film developed, fixed and analysed in order to optimise exposure time (repeated if necessary).

2.12.3: Stripping nitrocellulose membrane

In order to re-probe the membrane with a different primary antibody, it is possible to strip the membrane and reprobe. Submerge in stripping buffer (100mM β-mercaptoethanol, 2% SDS, 62.5mM Tris-HCl, pH 6.7) 10 minutes at 37˚C.

2.13: Transfection

Cell transfection is the introduction of nucleic acids into a cell using non-viral methods. Due to the use of non-viral methods of material transfer the term transformation is also widely accepted. This process can be used for a number of purposes such as to change the protein expression of a cell (upregulate/downregulate) in order to: elucidate its role in cell function, mass produce a protein for therapeutic purposes, mass produce a protein for research purposes or introduce a cell marker to a cell line.

There have been a number of different protocols created in order to transform a cell line; these can be divided into physical and biochemical methods. Physical methods include electroporation where high voltage shock creates temporary holes in the membrane allowing nucleic acid entry, heat shock and micro-injection where material is directly injected into the cell. Biochemical methods include the use of calcium phosphate, DEAE-dextran promoting endocytosis, and liposome mediated introduction of nucleic acids through the formation of lipoplexes which fuse with and enter through the cell membrane.

Transfections can be either transient or stable. With transient transfections the cell phenotype is lost during mitosis, and therefore has a limited effect. In this study the

transient transfection of HUVECs was used. Stable transfections involve the integration of a gene into a cells genome which is then replicated during mitosis, passing on the phenotype to the daughter cells. In this study a number of HEK293 cell lines were used that had been stably transfected to express various desirable phenotypes. The transfection reagent jetPEI™-HUVEC was used in this study for the transfection of primary HUVEC. HUVECS were transformed with CD36 shRNA plasmids in order to knockdown their expression by RNA interference (RNAi). The jetPEI™-HUVEC reagent has been optimized for the transfection of primary human endothelial cells.

2.13.1: RNA interference

RNA interference (RNAi) was first described by Fire and Mello in 1998 who later won The Nobel Prize in Physiology or Medicine 2006[200]. RNAi involves the control of genes at the level of RNA. In this study HUVECS were transformed with TLR2, TLR4 and CD36 shRNA plasmid DNA in order to knockdown their expression. The plasmid is transcribed producing shRNA, this is processed by the Dicer class of RNase III enzymes into siRNA, removing the hairpin and leaving a two nucleotide long 3' overhang. The siRNA is then bound by siRNA-induced silencing complex (siRISC) which has an RNase component (argonaute), which is activated and sets about degrading one of the siRNA strands. The strand left intact, with RISC attached, is complimentary to and binds endogenous target mRNA. This complex not only prevents translation of the mRNA but also when bound the RNAse component of RISC leads to cleavage and degradation of the target mRNA (Figure 2.22).

Gene silencing by RNAi

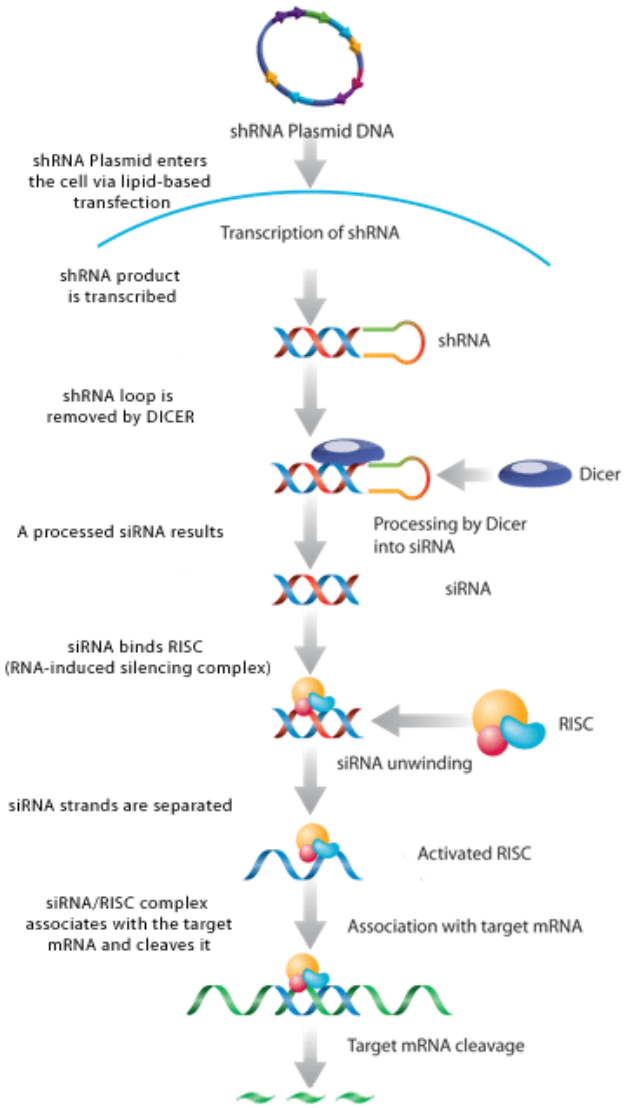

Figure 2.22: Gene silencing by siRNA. Transfection of shRNA plasmid DNA into a mammalian cell leads to the cleavage and degradation of the target mRNA causing knockdown of gene expression.www.scbt.com/sv/images/en/gene_silencers/shrna_plasmids.png (27/01/10).

2.13.2: Plasmid purification

The purification of the CD36 plasmids required a number of steps. Initially these were transformed into the competent *E.coli* strain, *E.coli* GT116. The transformed cells were expanded and lysed. The plasmids were then purified from the lysate and then concentrated and sterilised.

2.13.2.1: Transfection of *E.coli* GT116 cells

5µl of plasmid encoding CD36 shRNA {Santa Cruz} was added to 100µl of competent *E.coli* GT116 cells (Autogen Bioclear). These were gently mixed and incubated on wet ice for 30 minutes. Cells were heat shocked for 60 seconds at 42ºC in a heat block, and immediately placed back on wet ice for 2 minutes. 500µl Luria broth (Appendix) was added to the transformed cells and then these were incubated at 37ºC for 60 minutes at 125RPM. 100µl of transformed cells were then plated on Puromycin (10µg/ml) incorporated agar. Plates were left to grow overnight in an incubator shaker at 37ºC at 125RPM.

2.13.2.2: DNA isolation

Sterile conditions were practiced throughout this procedure. Eight separate colonies were selected with toothpicks from transfected cell agar plates and placed in different 25ml vials of Puromycin (10µg/ml) incorporated luria broth. These were grown overnight 37ºC at 125RPM. The 25ml transformed cells were spun at 1880g 4ºC for 10 minutes to pellet the cells. The resulting supernatant was poured off, removing as much as possible with minimal disruption of the pellet. The pellet was re-suspended in 400µl STET buffer (Appendix). The cells were transferred into a sterile 1.5ml eppendorf tube. 10µl of lysozyme (50mg/ml {Sigma}) was added and the sample was then immediately boiled for 60 seconds. The eppendorf tube was then placed on wet ice for 5 minutes. The tube was spun for 30 minutes at 135g RT and the resulting pellet removed and discarded. 5µl of RNase A (20µg/ml {Sigma}) was placed in the supernatant and then the tube was incubated at 42ºC for 30 minutes. 500µl of phenol was added, the mixture vortexed and then spun for 15 minutes at 135g RT. The upper aqueous phase was removed and placed in a 1.5ml sterile eppendorf tube. 500µl of chloroform lisoamyl

alcohol was added, the mixture vortexed and spun for 15 minutes at 135g RT. The upper aqueous phase was removed and placed in a 1.5ml sterile eppendorf tube. 20µl of 2M NaAc and 1000µl of ethanol was added to the tube. The sample was then stored at -80ºC overnight. The following day the tube was spun for 20 minutes at 135g RT and the upper aqueous phase discarded. Another spin of 1 minute at 135g RT was performed and any supernatant removed. The DNA pellet was re-suspended in 80µl sterile dH_2O. Plasmids were stored at -20ºC.

2.13.3: Agarose gel electrophoresis

Agarose gel electrophoresis is used to separate nucleic acids according to size. Agarose is a polysaccharide that forms an inert matrix that can be used as a sieve like medium through which molecules may be separated. Application of voltage across the horizontal gel pulls the negatively charged nucleic acids towards the anode. Smaller molecules have an advantage due to their size and thus will move furthest through the gel toward the positive terminal.

Agarose gel cell

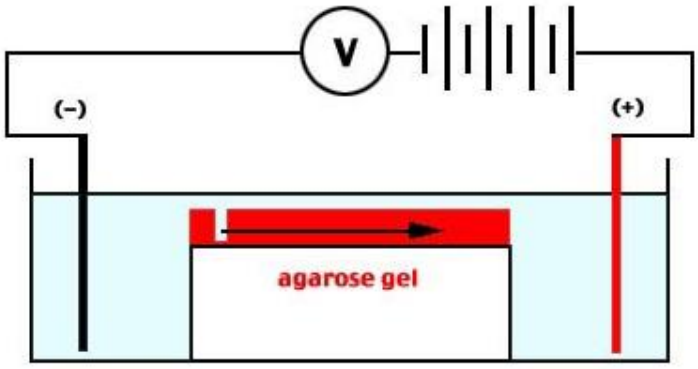

Figure 2.24: Diagram illustrating an agarose gel unit. The nucleic acids run horizontally (arrow) through the agarose gel (grey). www.icampus.ucl.ac.be/courses/SBIM2520/document/genemol/electrophorese/southern1.jpg (28/01/10).

Agarose gel electrophoresis was used in this study in order to assess the purity of the plasmid preparations.

2.13.3.1: Agarose gel electrophoresis protocol

A 1% agarose w/v gel was set in a gel cast. A comb was submerged into the liquid gel at one end to create wells for loading samples. The gel was left to set for 45 minutes. The comb was removed and the gel was placed in the running tank. The tank was topped up with ELFO running buffer (Appendix), covering the gel. 10µl of the sample was mixed with 5µl ELFO loading buffer (Appendix) and then pipetted into a well. 5µl of the 1Kb DNA ladder (New England BioLabs {500µg/ml}) was mixed with 10µl ELFO loading buffer and then pipetted into a well. Samples were run at 100V until dye nearly runs off gel. Bands were observed using a Stratagene eagle eye UV imager.

2.13.3.2: Plasmid digestion

To ensure double bands observed on agarose gels were oligomers not impurities the plasmids were digested prior to running the agarose gel. Known restriction sites were utilised. In this study HIND III digestion was performed. During digestion the plasmids would become linear and the oligomers would dissociate. An agarose gel of a pure digested plasmid sample produces one solid band on the imaged gel.

2.13.3.2.1: HIND III digestion

To an eppendorf tube, 5µl plasmid, 2µl ELFO loading buffer, 12µl dH_2O and 1µl HIND III enzyme (New England BioLabs) were added. This was left for 1 hour at 37˚C. The sample was then run on an agarose gel (Section 2.13.3.1).

2.13.4: HUVEC transfection

HUVEC cells were transfected with CD36 silencing plasmids. Transfected cells were stimulated as normal in order to elucidate their role in the HUVEC immune response.

2.13.4.1: Cell seeding

For optimal transfection efficiency HUVECs were required at 50-60% confluency for this procedure. 24 hours prior to transfection a confluent 24 well plate of HUVEC was split into two plates using M199 (GIBCO) and RPMI 1640 (GIBCO) medium (v/v), supplemented with 30% foetal calf serum (FCS {Biosera}). Cells were incubated for 18 hours at 37˚C with 5% CO_2 in a humidified atmosphere.

2.13.4.2: Preparation of CD36 plasmids

Plasmid, 4µl, was diluted in 50µl NaCl 150mM, vortexed and then spun down briefly. Separately 8µl of jetPEI™-HUVEC was then diluted in 50µl NaCl 150mM, vortexed and spun down briefly. The jetPEI™-HUVEC/NaCl was then immediately added to the plasmid/NaCl mixture. This was then vortexed and spun down briefly. The mixture was incubated at room temperature for 30 minutes prior to transfection.

2.13.4.3: HUVEC Transfection with CD36 plasmid

Cells were washed with 500µl X1 PBS. 200µl of DMEM-1000 (GIBCO) supplemented with 2% FCS (Biosera) was then added to each well. 100µl of the plasmid/jetPEI™-HUVEC mixture was then added to each well. The plate was gently shaken and then incubated at 37˚C with 5% CO_2 in a humidified atmosphere for 4 hours. After the incubation the transfection medium was removed and then replaced with selection media containing the appropriate antibiotic (Medium 200/30% FCS/10µg/ml Puromycin). Cells were left in the selection medium for 24 hours. Receptor expression assay and stimulations were carried out at 24 hours in 200µl SFM (GIBCO).

2.14: Lipid raft disruption

The plasma membrane of mammalian cells is discontinuous in that it contains microdomains that are involved in the recruitment and concentration of molecules

concerned with cellular signalling. These sphingolipid and cholesterol-enriched microdomains are known as lipid rafts, and have been shown to be essential for a number of cellular signalling cascades. Lipid rafts allow the congregation of receptors, co-receptors and their signal transduction machinery required for an appropriate signal in response to a stimulus. For this reason the disruption of lipid rafts can be used to knockdown a group of cellular signalling cascades to elucidate the role of their up-stream receptors in the detection of certain ligands.

Lipid raft disruption can be achieved by using raft-disrupting drugs, such as Nystatin or methyl-beta-cyclodextrin (MCD). Nystatin and MCD have been shown to disorder receptors, co-receptors and their signal transduction machinery[201]. Nystatin is a fungal metabolite that binds membrane cholesterol and disrupts raft integrity[202]. MCD works by disrupting protein associations with lipid rafts[203]. In this study, PRR signalling was disrupted in ECV 304 and primary HUVEC lines using Nystatin.

2.14.1: Lipid raft disruption protocol

Primary HUVECs seeded in 24 well plates (NUNC) were washed with 1ml sterile X1 PBS then placed in 500µl SFM (GIBCO). Nystatin (60µg/ml {Sigma}) was added. The cells were left to incubate at 37°C in a 5% CO_2 in a humidified atmosphere for 10 minutes. Immediately after the incubation the cells were washed and then stimulated.

HUVECs seeded in 8 well glass slides (Lab-Tek™ Chamber Slide™ System) were washed with 500µl sterile X1 PBS then placed in 200µl SFM. Nystatin (60µg/ml) was added. The cells were left to incubate at 37°C in a 5% CO_2 in a humidified atmosphere for 10 minutes. Immediately after the incubation the cells were stimulated. Nystatin cytotoxcity was analysed using the trypan blue viability test (Section 2.4).

2.15: Affinity chromatography

Affinity chromatography is a technique which uses reversible biospecific reactions that allows the purification, extraction and separation of biologically active material. This techniques was introduced in 1968 by Cuatrecasas, Wilchek and Anfinsen who illustrated the rapid and complete purification of staphylococcal nuclease, a-chymotrypsin and carboxypeptidase A[204]. Specific properties of biomolecues such as charge, hydrophobicity and ligand specificity are utilised in order to selectively bind them from a sample. A selection tool specific for the unique property of the protein of choice is coupled to an insoluble chromatography matrix. When the sample is passed through the matrix the protein is sequestered from the crude mixture. The interaction between the target protein and ligand is reversible as to allow the collection of the protein on elution of the column. Elution buffers reverse the biospecific interaction between the ligand and chromatography matrix allowing collection of the ligand. Ligands used in affinity chromatography include antibodies, metal ions, enzymes, hormones and nucleic acids.

Examples of affinity chromatography techniques

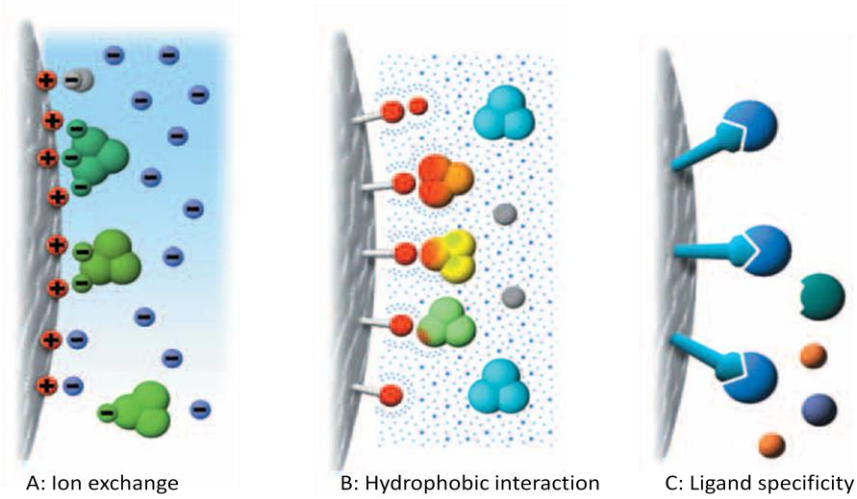

Figure 2.25: Affinity chromatography. Allows purification of a biologically active material from a crude sample using specific properties such as; (A) charge (B) hydrophobicity and (C0 ligand specificity. Affinity Chromatography, Principles and Methods. Amersham biosciences. 18-1022-29 (07/01/10).

2.15.1: His-tagged protein purification

Immobilized metal ion affinity chromatography (IMAC) using HisTrap™ HP columns (GE Healthcare) was used for the purification and concentration of HSP70. IMAC works on the basis that immobilized metal ions (Co^{2+}, Ni^{2+}, Cu^{2+} and Zn^{2+}) have preferential binding of certain protein properties. These properties can be native or introduced into the protein in the form of a tag. Ni^{2+} has a high affinity for histidine (His) residues. HSP70 is a His-tagged fusion protein which enhances its selection from the crude sample mixture. In this study HisTrap™ HP columns pre-packed with Nickel (Ni) Sepharose™ High Performance were used for HSP70 w-t purification. HisTrap™ HP columns allow easy high performance purification of His tagged proteins.

HisTrap™ HP columns

Figure 2.26: HisTrap™ HP 1-ml and 5-ml columns. HisTrap columns are used for the purification of histidine-tagged proteins. www4.gelifesciences.com/aptrix/upp01077.nsf/Content/Products?OpenDocument&ModuleId= 165701 (07/01/10).

The crude sample mixture is passed into the equilibrated column which has been pre-packed with Ni Sepharose™ High Performance. Native and marker His groups have a high affinity for, and reversibly bind to, the immobilized metal ion. Elution buffer containing an excess of imidazole is passed through the column which displaces the His-tag from the Ni^{2+} ion releasing the His-tagged protein.

His-tagged protein purification

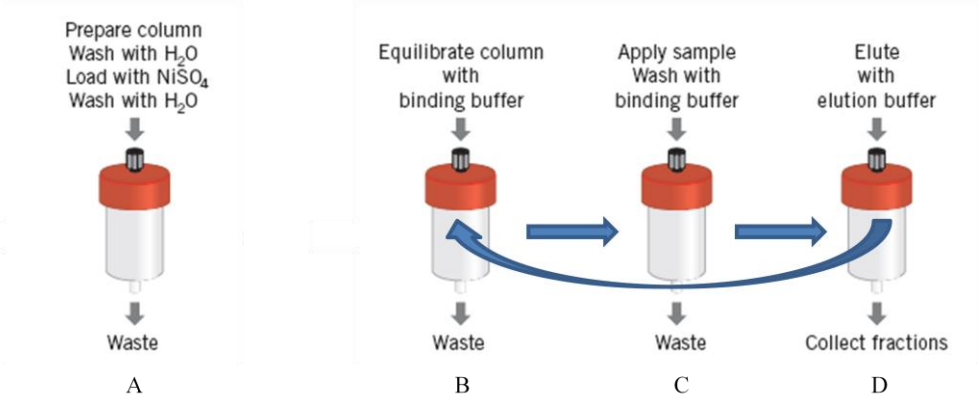

Figure 2.27: His-tagged protein purification using a HisTrap™ HP column. Ni is immobilized on the Sepharose matrix (A). The column is equilibrated (B), the sample is passed through the column and the His tag reversibly binds to the immobilised Ni ions (C), elution buffer containing imidazole breaks this interaction and releases the His-tagged protein (D). http://fachschaft.biochemtech.uni-halle.de/downloads/chromatography/affchr.pdf (07/01/10).

2.15.1.1: Expression and extraction of heat shock protein 70

In sterile glass vials 25µl ampicillin (Fisher BioReagents) was added to 25ml luria broth (Appendix) creating selection media. *E.coli* GT116 (Autogen Bioclear) colonies expressing HS70 ({Kindly supplied by Professor C. Lingwood of the University of Toronto}), and thus ampicillin resistance, were selected from a pre-cultured agar plate with a tooth pick. The tooth pick was then vigorously stirred and dropped into the luria broth vial. The vial was then placed into a 37ºC rotatory incubator at 130RPM overnight. Two larger luria broths were prepared by adding 500µl ampicillin (Fisher BioReagents) and 250µl IPTG (Fisher BioReagents) into autoclaved (180ºC) 500ml luria broth glass bottles. Half the 25ml luria broth *E.coli* GT116 culture was then poured into each of the second stage 500ml luria broths. The broths were then placed into a 37ºC rotatory incubator at 130RPM for 5 hours. The 500ml broths were then centrifuged at 4970g in a 4ºC centrifuge for 20 minutes. The pellets were re-suspended in 10ml lysis buffer (Appendix) and placed in 50ml tubes, the centrifuge container was washed out with a

further 10ml lysis buffer and this was also added to the 50ml tube. The lysed *E.coli* GT116 cells were then frozen (-20ºC) and thawed 6 times. Tubes were vortexed vigorously between freezing and thawing. The tubes were then centrifuged at 735g in a 4ºC centrifuge for 60 minutes. The supernatant was placed in a sterile 50ml tube. The pellet was discarded. The supernatant was purified using HisTrap™ HP Columns (GE Healthcare).

2.15.1.2: Heat shock protein 70 purification

Binding buffer (5ml {Appendix}) was passed through the HisTrap™ HP 1ml Columns (GE Healthcare) using a sterile 5ml syringe, the waste was discarded. 2mls of HSP70 lysate was then passed into the column at 1 ml/minute and left to incubate for 2 minutes. 5ml binding buffer (Appendix) was then passed through the column, the waste was discarded. 4mls elution buffer (Appendix) was then passed through the column, the elution was collected in sterile glassware. This process was repeated until all lysate had been passed through the column. Purified HSP70 w-t was collected and stored in sterile glassware at pH7 at 4ºC. Concentration was determined via spectrophotometry.

2.16: Protein concentration

To concentrate purified proteins 10kDa cut off Centriprep centrifuge concentrators (Amicon) were utilised. Centriprep concentrators consist of two tubes, one housed in the other (Figure 2.30). The base of the internal tube has a permeable membrane that allows molecules through which are 10kDa or smaller, retaining the protein in the external tube. During centrifugation the centrifugal force pushes anything that is ≤10kDa through the membrane into the internal tube. The sample remains in the

exterior tube whilst the waste runs through the membrane into the internal tube and is discarded.

Centriprep concentrators

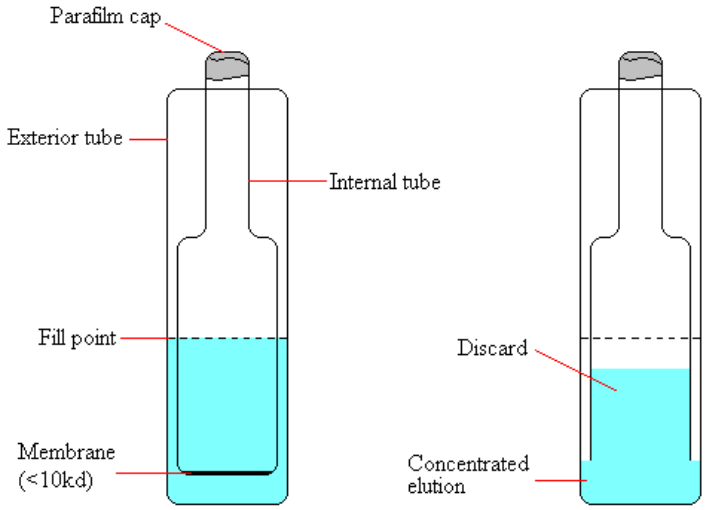

Figure 2.30: Centriprep concentrators. During centrifugation (735g 4ºC for 40 minutes) the centrifugal force pushes anything that is ≤10kDa through the cut off membrane into the internal tube. Internal tube = waste. External tube = purified sample.

2.16.1: Centriprep protocol

Sterile 10kDa cut off Centriprep concentrators (Amicon) were filled to the "fill point" (Figure 2.30) with purified sample. The concentrators were then placed in the centrifuge and spun at 735g for 40 minutes at 4ºC. The content of the internal tube was discarded. The content of the exterior tube was placed back into the original elution and any precipitate re-suspended. This process was repeated until approximately 1-2ml of purified and concentrated protein remained. Sterile X1 PBS was used for buffer exchange with the protein sample. X1 PBS was filled to the "fill point" and the Centriprep concentrator was spun at 735g for 40 minutes at 4ºC. This was performed three times with an end sample of approximately 1-2ml. Protein concentration was determined by spectrophotometry.

2.17: Endotoxin removal

Bacterial endotoxin contamination has proven a big problem in research, especially in the field of immunology. When expressing a protein in an *E.coli* strain, for example, endotoxin from the bacteria can easily contaminate the purified product. Any cell stimulations performed with the contaminated protein will have a double effect of the protein itself and the contaminant, producing invalid data. To avoid this problem endotoxin can be removed by either: ultra-filtration, ion exchange chromatography, two phase extraction or ligand specificity chromatography. In this study the Profos EndoTrap® blue 10 (Hycult Biotechnology) protocol was used to remove endotoxin from purified protein samples, this assay utilizes ligand specificity chromatography.

Profos EndoTrap® blue is an affinity matrix that is designed to remove bacterial endotoxins from aqueous solutions, even at low endotoxin concentrations. Pre-packed columns have the EndoTrap blue ligand covalently bound to beaded agarose. The EndoTrap blue ligand is highly specific for bacterial endotoxin and has very low non-specific binding, giving high sample yields free of endotoxin.

EndoTrap kit

Figure 2.31: Profos EndoTrap® blue 10 (Hycult Biotechnology) kit. Bacterial endotoxin is removed from aqueous solution by ligand specific affinity chromatography. www.jki.co.jp/ (08/01/10).

2.17.1: Endotoxin removal protocol

Profos EndoTrap® blue 10 assay columns (Hycult Biotechnology) were firstly regenerated. 3X the column volume of regeneration buffer (Hycult Biotechnology) was passed through the column and the elution discarded, this step was repeated. 3X the column volume of equilibration buffer (Hycult Biotechnology) was passed through the column and the elution discarded, this step was repeated. 1X the column volume of sample was passed into the column; the elute was collected in sterile glassware. 3X the column volume of equilibration buffer was then passed through the column and collected in the same sterile glassware. Endotoxin free sample was re-concentrated in sterile Centriprep concentrators (Section 2.16), to a final volume of 1-2mls.

2.18: Animal model

Animal models used in animal testing include both non-vertebrates and vertebrates. Non-vertebrates include the widely used *Drosophila melanogaster* and *Caenorhabditis elegans*. Vertebrates include animals such as mice, rats, guinea pigs, cats, dogs, fish, amphibians, larger domestic species such as pigs, goats, equines and primates including new and old world monkeys.

In the selection of a model organism for a specific experiment a number of factors have to be considered. Preliminary *in vitro* data should be used to help select the model. Animal models can come in a number of varieties where they can be tailored for a specific experiment. Animals can be out-bred, in-bred, mutants or transgenic. Out-bred animals ("stocks") are from closed undefined genetic colonies. These have good fertility, large litter sizes, are easy to mate, have a good growth curve and are usually relatively cheap. Inbred mice ("strains") are compromised in these factors. However, their benefit is that they are ~99% homozygous as a result of ≥20 generations of brother sister inbreeding. Mutant animals are an out-bred stock with a mutant gene, these are

tricky to breed and maintain. Dominant and recessive mutations can have a number of effects, such as infertility and high birth mortality. Transgenic mice have had foreign DNA permanently incorporated into their genome resulting in, for example, the knock-out (KO) of genes. These mice often require high levels of maintenance. For example, animals whose immune system is compromised may require a germ free environment.

In this study the out-bred CD-1 male mouse was selected for an animal model of sepsis. AMD3100 and HSP70 were tested for their ability to reduce inflammation and lethal shock in the murine model of sepsis, by protecting or potentially reversing the progression of lethal sepsis in mice.

2.18.1: The CD-1 mouse

This study utilised out-bred CD-1 male mice at 6-8 weeks to produce an animal model of sepsis: as advised by Professor Mervyn Singer and Dr. Richard Hotchkiss who both have well established endotoxin CD-1 mouse models of sepsis. Mice were also selected for their good fertility, good growth curve, large litter size and the ease at which they can be bred.

The CD-1 mouse

Figure 2.32: The CD-1 mouse. In this study the CD-1 mouse was selected as an animal model of sepsis. They have good fertility, a good growth curve, a large litter size and are easy to breed. www.criver.com/ENUS/PRODSERV/BYTYPE/RESMODOVER/RESMOD/Pages/CD1Mouse.aspx (02/02/10).

LPS, AMD3100 and HSP70 were administered via intraperitoneal injection.

2.18.2: Intraperitoneal injection

Intraperitoneal (i.p) injection is the injection of a substance into the peritoneal cavity. This allows large amounts to be injected producing a massive and rapid systemic immune response. The procedure is relatively quick and easy which reduces any stress and damage that may be caused to the animal. Reducing these factors also increases result validity and reliability.

The mouse is restrained so that its head was facing away and downward with its abdomen exposed (Figure 2.33), this allows the intestines to be under less pressure to reduce chance of internal damage. The needle is inserted, at a 30˚ angle, close to the midline on the animals right side horizontally in-line with the knees to a depth of 5mm (Figure 2.33). Injection to the right side places the needle at the sight of the small intestines: again reducing risk of internal damage for the needle is less likely to hit smaller structures.

Intraperitoneal injection

Figure 2.33: Intraperitoneal (i.p) injection administered to a mouse. The needle is inserted at a 30˚ angle, close to the midline on the animals right side horizontally in-line with the knees. www.bu.edu/research/compliance/lacu/lacf/sop/injection-techniques/intraperitoneal.shtml (02/02/10).

2.18.3: Injected substance concentration determination

The concentrations of substances to be injected were determined with preliminary experiments. In order to determine whether HSP70 or AMD3100 protects against meningococcal septic shock, a mouse model had to be developed. The septic shock mouse model was designed to have 100% mortality at 24 hours post LPS administration. HSP70 and AMD3100 were tested to find optimum concentrations for protection against LPS endotoxin induced septic shock.

2.18.3.1: Determination of LPS concentration for sepsis model

Male CD-1 mice (6-8 weeks) were randomly grouped (5-10 mice per group) and injected by intraperitoneal (i.p) injection with different concentrations (50, 60, 70, 80mg/Kg) of *E.coli* 055 LPS (List Biological Laboratories) using a sterile 1ml syringe (BD Plastipak™ {Becton Dickinson}) with a 25 GA1 0.5x25mm needle (BD Microlance™ 3 {Becton Dickinson}). The syringe was prepared with the correct volume of *E.coli* 055 LPS to be administered. The mouse was then restrained so that its head was facing away and downward with its abdomen exposed (Figure 2.33). The needle was inserted, at a 30˚ angle, close to the midline on the animals right side horizontally in line with the knees to a depth of 5mm (Figure 2.33). The needle was withdrawn and the mouse returned to the cage.

Once the optimum concentration of LPS required to induce septic shock and death at 24 hours was determined, it was kept constant throughout the *in vivo* inhibition studies.

2.18.3.1.1: Induction of sepsis in the CD-1 mouse

Intraperitoneal (i.p) injection of *E.coli* 055 LPS (60mg/kg) was administered to the CD-1 mouse (male 6-8 weeks) using a sterile 1ml syringe (BD Plastipak™ {Becton Dickinson}) with a 25 GA1 0.5x25mm needle (BD Microlance™ 3 {Becton Dickinson}). The syringe was prepared with the correct volume of LPS, relative to mouse weight, to be administered. The mouse was then restrained so that its head was facing away and downward with its abdomen exposed (Figure 2.33). The needle was inserted, at a 30˚ angle, close to the midline on the animal's right side horizontally in line with the knees to a depth of 5mm (Figure 2.33). The needle was withdrawn and the mouse returned to the cage.

2.18.3.2: Determination of optimal HSP70 and AMD3100 concentration

In order to determine the optimum concentration of HSP70 (Kindly supplied by Professor C.Lingwood of the University of Toronto) and AMD3100 (Sigma) that was needed to protect mice from LPS-induced septic shock, mice were administered different concentrations (100, 200, 300, 500 and 1000µg/mouse**)** of either and HSP70 or AMD3100 by i.p injection 1 hour before LPS administration. Blood (50µl) was collected at certain time points after LPS administration (0, 2, 4, 6, 8 hours) from the tail vein of mice. The level of TNF-α and IL-1β in the serum was determined using the CBA system (Section 2.8.2.2).

2.18.3.2.1: *In vivo* testing of HSP70 and AMD3100

I.p injection of HSP70 and AMD3100 was administered to the CD-1 mouse (male 6-8 weeks) using a sterile 1ml syringe (BD Plastipak™ {Becton Dickinson}) with a 25 GA1 0.5x25mm needle (BD Microlance™ 3 {Becton Dickinson}). The syringe was prepared

with the correct volume of HSP70 or AMD3100 to be administered. The mouse was then restrained so that its head was facing away and downward with its abdomen exposed (Figure 2.33). The needle was inserted, at a 30˚ angle, close to the midline on the animals right side horizontally in-line with the knees to a depth of 5mm (Figure 2.33). The needle was withdrawn and the mouse returned to the cage.

2.18.4: Cytokine analysis of blood samples

Blood samples (50µl) were collected at determined time points before and after LPS administration. Samples were centrifuged at 132g for 30 minutes and the serum removed. Mouse Inflammation cytokine bead array (CBA) system (Becton Dickinson) was used in order to determine cytokine concentration (Section 2.8.2.2).

2.19: Statistical analysis

Statistical analysis was performed using SPSS (Statistical Package for the Social Sciences) software version 15.0 (SPSS Inc.). Two sets of data were compared using a two tailed, paired t-test. In this study a p-value of less than 0.05 ($p<0.05$) was considered significant. Throughout this thesis, * = $p<0.05$.

Chapter 3:

Results

3.1: ECV inflammatory response

Vascular endothelial cells line the lumen of arteries where they are subject to challenge from circulating ligands. These cells are considered to be responsible for the initial steps in the inflammatory process of atherogenesis. The increased cytokine release caused by the activation, due to atherosclerosis-associated ligands, in vascular endothelial cells is thought to instigate the multi-step process of plaque formation. TLRs have been suggested as the source of the inflammatory response, but the precise triggers are not fully understood. This study was set out to fully characterise the ligand(s) that trigger PRRs and the subsequent inflammatory response leading to atherogenesis.

This study utilised human ECV304 (Section 2.2.2) cells to elucidate PRR associations with atherosclerosis-associated ligands, and their ability to induce inflammatory cytokine release. This study investigated the role of endogenous lipoproteins, bacterial products and combinations of these to analyze their capability of initiating atherogenesis by activation of an innate immune response in vascular endothelial cells.

3.1.1: PRR association with endogenous LDL

In order to determine which PRRs are involved in the recognition of endogenous/host lipoproteins over time, ECV304 cells were stimulated for 30, 60 and 120 minutes with human endogenous LDL and its oxidised derivatives mmLDL and oxLDL (Section 2.6). For concentrations see Section 2.5. All stimulations were carried out in 25cm^2 flasks in SFM (GIBCO) (Section 2.5.1). The cell surface receptors TLR1, TLR2, TLR4, TLR6, CD36 and CD14 were labelled via indirect immunofluorescence (Section 2.7.2) and analyzed by flow cytometry (Section 2.8.2.1).

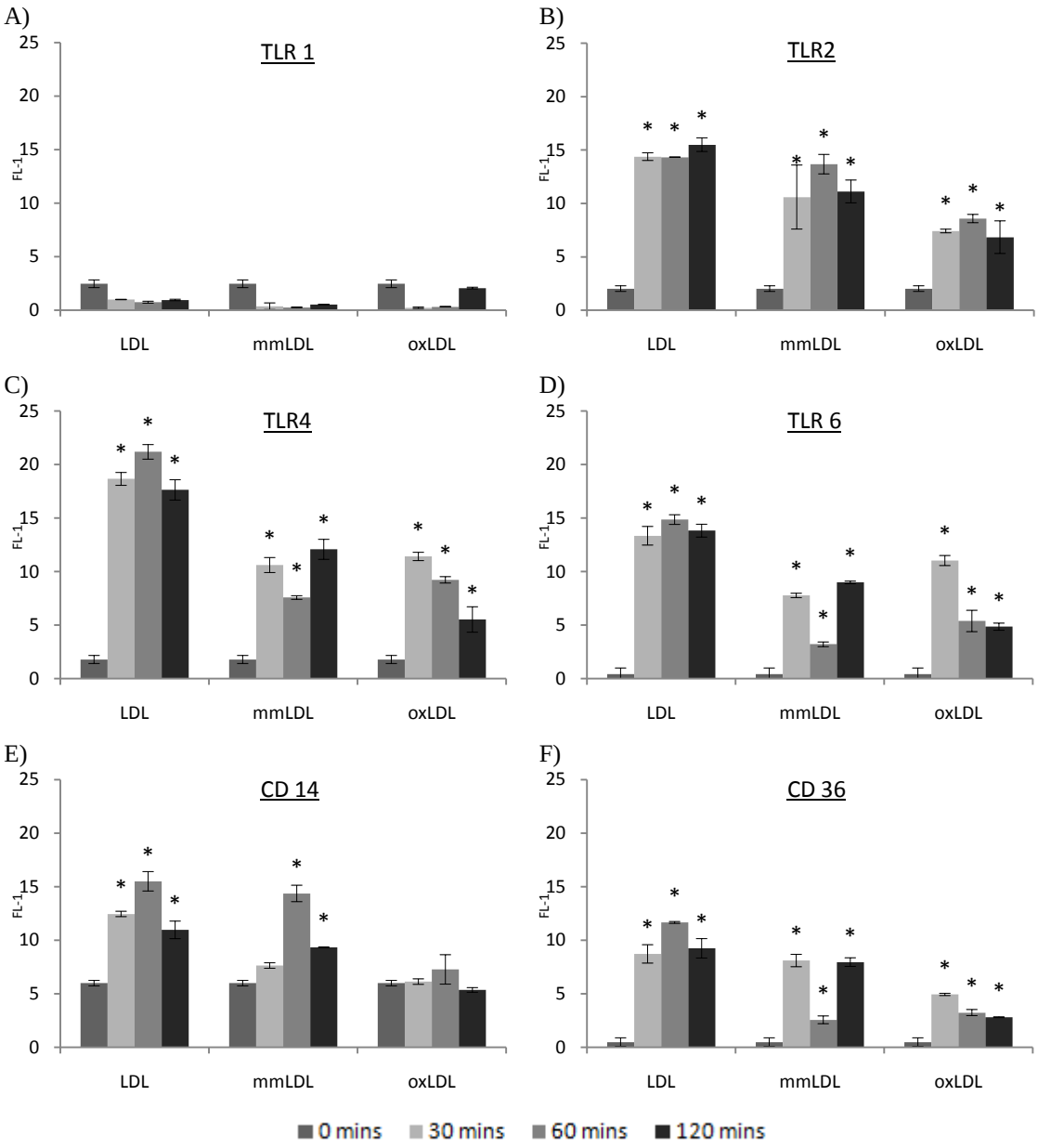

Figure 3.1.1: Cell surface receptor expression of: A) TLR1, B) TLR2, C) TLR4, D) TLR6, E) CD14 and F) CD36, on human ECV304 cells after stimulation with LDL and its oxidised derivatives, mmLDL and oxLDL, over time (0, 30, 60 and 120 minutes). Cells were fixed and labelled with a primary antibody against the receptor of interest, followed by an appropriate secondary antibody conjugated to FITC. Fluorescence was measured on a FACSCalibur (Becton Dickinson), counting 10,000 cells per sample, not gated. Data represents mean, ± standard deviation, n=3. *Indicates statistically significant ($p<0.05$) upregulation of receptor expression in comparison to unstimulated cells (Section 2.19).

LDL and its derivatives mmLDL and oxLDL all caused upregulation of TLR2, TLR4, TLR6, CD14 and CD36 expression on ECV304 cells (Figure 3.1.1B/C/D/E/F). There was no upregulation of TLR1 observed (Figure 3.1.1A). The lipoprotein that caused the

greatest upregulation of PRRs, causing the largest response, was LDL. oxLDL was the least effective at causing upregulation of PRRs. At 60 minutes TLR4, TLR6, CD14 and CD36 expression was ≤50% for oxLDL in comparison to LDL (Figure 3.1.1C/D/E/F). Interestingly these results were the reverse to what was expected. Many studies have shown that oxLDL is the associated LDL derivative in atherogenesis, thus presumably the most immunostimulatory. Due to its inability to cause a large upregulation of PRRs in comparison to LDL and mmLDL it was hypothesised that this inability itself may allow oxLDL to have a chronic inflammatory effect, by avoiding clearance, characteristic of atherosclerosis.

3.1.1.1: Inflammatory response to endogenous LDL

Since endogenous lipoproteins were found to modulate the expression of PRRs, the next step in this study was to examine the release of cytokines (the inflammatory mediators) caused by ECV304 lipoprotein stimulation to see whether PRR expression mimics the inflammatory response induced in vascular endothelial cells. Out of the inflammatory cytokines analysed (IL-1β, IL-6, IL-8, IL-10, IL-12p70 and TNF), only the release of IL-6 and IL-8 were significantly increased.

ECV304 cells were stimulated for 30, 60 and 120 minutes with human endogenous LDL and its oxidised derivatives mmLDL and oxLDL (Section 2.6). For concentrations see Section 2.5. All stimulations were carried out in 25cm^2 flasks in SFM (Section 2.5.1). The SFM was collected post stimulation for cytokine analysis using the Human Inflammation BD™ cytometric bead array system (Section 2.8.2.2).

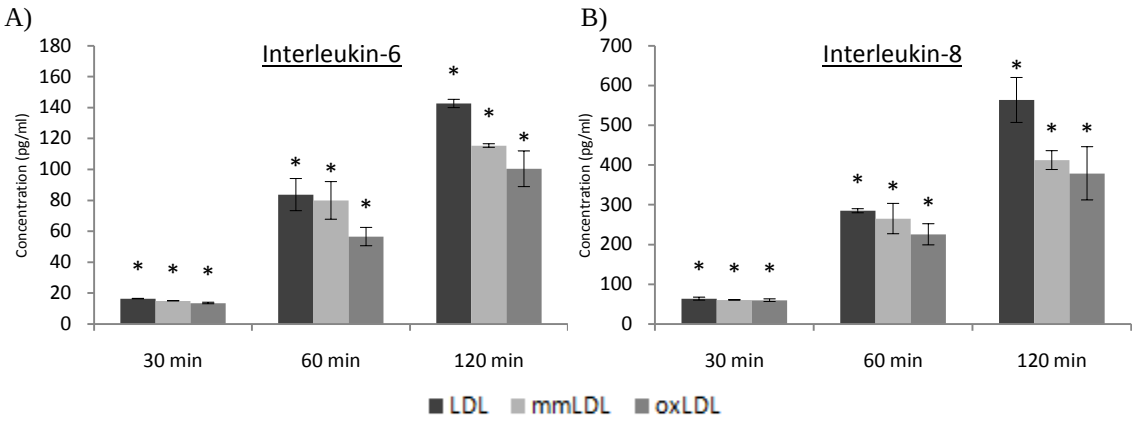

Figure 3.1.2: A) Interleukin-6 and B) interleukin-8 release from human ECV304 cells after stimulation with human LDL and its oxidised derivatives mmLDL and oxLDL, over time (30, 60 and 120 minutes). Interleukin-6 and interleukin-8 were measured in the cell supernatant using a flow cytometric cytokine bead array system (Becton Dickinson). Negatives subtracted. Data represents mean, ± standard deviation, n=2. *Indicates statistically significant ($p<0.05$) increase in cytokine release in comparison to unstimulated cells (Section 2.19).

As expected the cytokine release (Figure 3.1.2) does mimic the PRR expression (Figure 3.1.1). IL-6 (Figure 3.1.2A) and IL-8 (Figure 3.1.2B) were significantly upregulated. Their release increased over time to 120 minutes. IL-8 release was far greater than that of IL-6, at 120 minutes the IL-8 concentration for LDL was 300% greater than the IL-6 concentration recorded (Figure 3.1.2A/B, LDL). The largest cytokine release was seen when ECV304 cells were stimulated with LDL, oxLDL caused the least. This demonstrates the ability of endogenous lipoproteins to cause an inflammatory response in vascular endothelial cells, and possibly initiating atherogenesis. The same ECV304 cell line was then exposed to known atherogenic bacterial PAMPs.

3.1.2: PRR association with atherosclerosis-associated bacterial ligands

Since endogenous lipoproteins were shown to be able to stimulate an inflammatory response via specific receptors in human vascular endothelial cells, this study proceeded to investigate whether bacterial ligands could also stimulate an inflammatory response in these cells. ECV304 cells were stimulated for 30, 60 and 120 minutes with the bacterial ligands *S.aureus* LTA and LPS from *E.coli* and *P.gingivalis*. For

concentrations see Section 2.5. All stimulations were carried out in 25cm^2 flasks in SFM (GIBCO) (Section 2.5.1). The cell surface receptors (TLR1, TLR2, TLR4, TLR6, CD36 and CD14) were labelled via indirect immunofluorescence (Section 2.7.2) and analyzed by flow cytometry (Section 2.8.2.1).

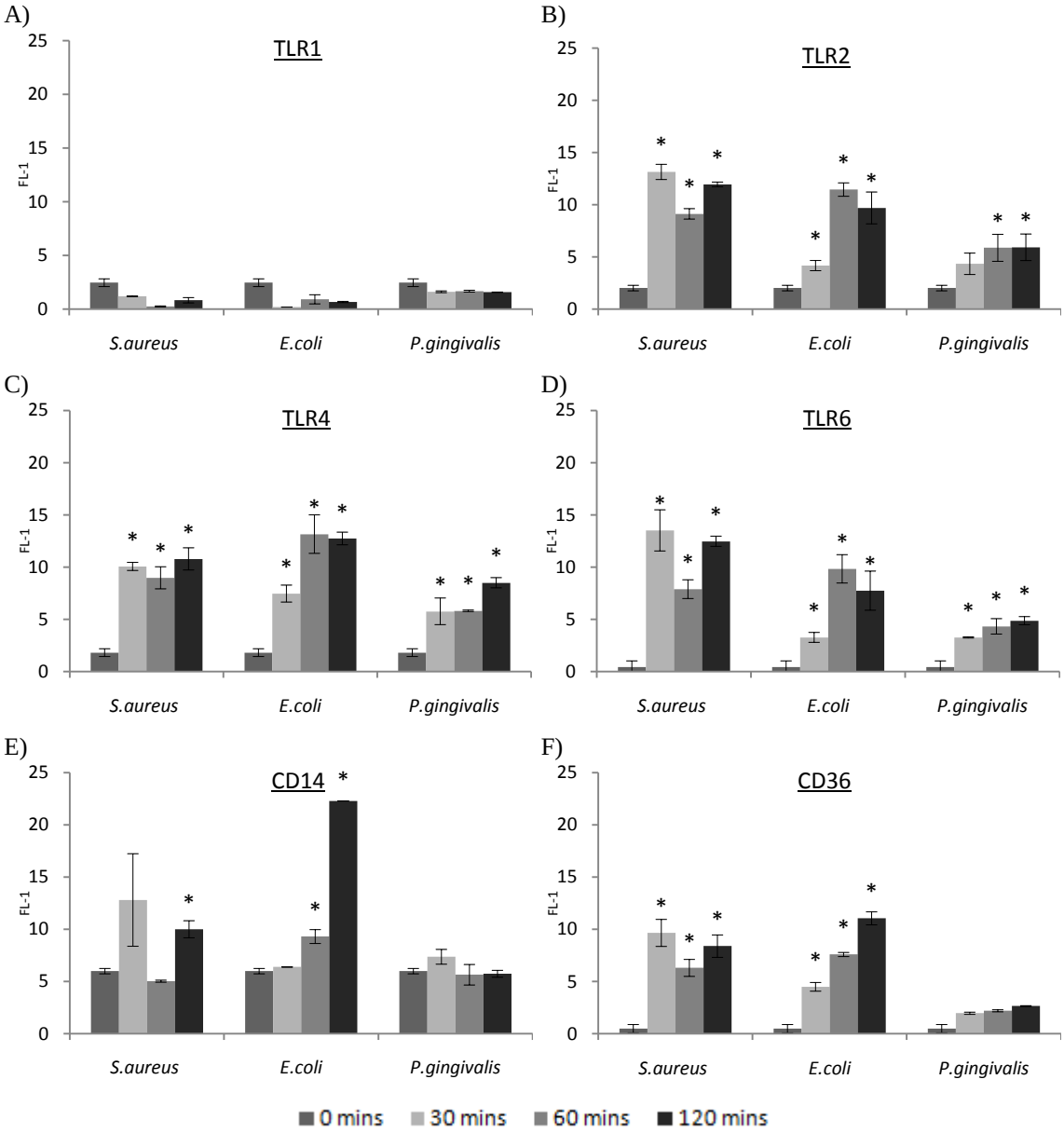

Figure 3.1.3: Cell surface receptor expression of: A) TLR1, B) TLR2, C) TLR4, D) TLR6, E) CD14 and F) CD36 on human ECV304 cells after stimulation with the atherosclerosis-associated bacterial ligands *S.aureus* LTA, *E.coli* LPS and *P.gingivalis* LPS over time (0, 30, 60 and 120 minutes). Cells were fixed and labelled with a primary antibody against the receptor of interest, followed by an appropriate secondary antibody conjugated to FITC. Fluorescence was measured on a FACSCalibur (Becton Dickinson), counting 10,000 cells per sample, not gated. Data represents mean, ± standard deviation, n=3. *Indicates statistically significant ($p<0.05$) upregulation of receptor expression in comparison to unstimulated cells (Section 2.19).

S.aureus LTA, *E.coli* LPS and *P.gingivalis* LPS were capable of upregulating TLR2, TLR4, TLR6, CD14 and CD36 expression on ECV304 cells (Figure 3.1.3B/C/D/E/F). There was no upregulation of TLR1 observed (Figure 3.1.3A). *P.gingivalis* LPS was less effective at upregulating the receptors observed in comparison to *S.aureus* LTA, and *E.coli* LPS. Interestingly the receptor expression profile on ECV304 cells in response to LDL and its derivatives (Figure 3.1.1) have a similar profile to that of the bacterial PAMPs (Figure 3.1.3) with upregulation of TLR2, TLR4, TLR6, CD14 and CD36, but not TLR1. This demonstrates similar responses in this cell line to LDL and bacterial PAMPs.

3.1.2.1: Inflammatory response to atherosclerosis-associated bacterial ligands

Stimulation of ECV304 with atherosclerosis-associated bacterial ligands demonstrated that these ligands are able to modulate PRR expression. Therefore the next step in this study was to examine the ECV304 cytokine release caused by *S.aureus* LTA, *E.coli* LPS and *P.gingivalis* LPS to see whether PRR expression mimics the inflammatory response induced in vascular endothelial cells. Here *C.pneumoniae* LPS in addition to *S.aureus* LTA, *E.coli* LPS and *P.gingivalis* LPS was also tested. *C.pneumoniae* LPS, like *P.gingivalis* LPS, is an unconventional TLR2-associated LPS that is strongly linked to atherosclerosis. As found with lipoprotein stimulations ECV304 cells were found to release only IL-6 and IL-8 to a significant degree.

ECV304 cells were stimulated for 30, 60 and 120 minutes with *S.aureus* LTA, *E.coli* LPS, *P.gingivalis* LPS and *C.pneumoniae* LPS. For concentrations see Section 2.5. All stimulations were carried out in 25cm^2 flasks in SFM (GIBCO) (Section 2.5.1). The

SFM was collected post stimulation for cytokine analysis using the Human Inflammation BD™ cytometric bead array system (Section 2.8.2.2).

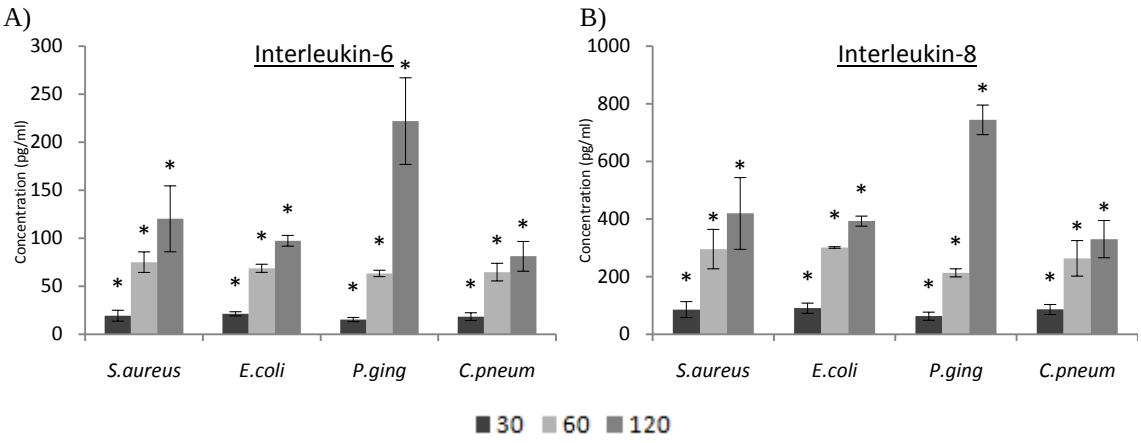

Figure 3.1.4: A) interleukin-6 and B) interleukin-8 release from human ECV304 cells after stimulation with the atherosclerosis-associated bacterial ligands *S.aureus* LTA, *E.coli* LPS, *P.gingivalis* (*P.ging*) LPS and *C.pneumoniae* (*C.pneum*) LPS over time (30, 60 and 120 minutes). IL-6 and IL-8 was measured in the cell supernatant using a flow cytometric cytokine bead array system (Becton Dickinson). Negatives subtracted. Data represents mean, ± standard deviation, n=2. *Indicates statistically significant ($p<0.05$) increase in cytokine release in comparison to unstimulated cells (Section 2.19).

S.aureus LTA, *E.coli* LPS, *P.gingivalis* LPS and *C.pneumoniae* LPS all caused a significant increase in release of IL-6 (Figure 3.1.4A) and IL-8 (Figure 3.1.4B). *P.gingivalis* stimulated IL-6 and IL-8 cytokine release at 120 minutes was greater than the other unconventional LPS from *C.pneumoniae*, 173% and 125% greater respectively.

The similar receptor expression profiles caused by LDL (Figure 3.1.1) and bacterial PAMPs (Figure 3.1.3) may suggest that these ligands are recognised in a similar manner, opening the possibility of interference and/or interactions between them. This study has demonstrated their individual ability to cause vascular endothelial cell activation through increased cytokine release and thus their ability to initiate the inflammatory disorder atherosclerosis (Figure 3.1.2/4). These events however would not

occur uniquely in the vascular system, they would occur in unison. To see whether these ligands have an altered recognition and/or inflammatory response, when exposed to vascular endothelial cells at the same time, I went on to test the ECV304 cell line with combined stimulations. The cells were exposed to an endogenous lipoprotein and a bacterial PAMP one after the other. The combined stimulations were designed to simulate a high cholesterol state, a known risk factor, prior to infection. This is the sequence of events that would take place in the human vascular system.

3.1.3: PRR association with endogenous LDL and bacterial ligand combined

The combined stimulations involved a 60 minute pre-incubation with an endogenous lipoprotein (human LDL and its oxidised derivatives, mmLDL} and oxLDL) and then further 60 minute stimulation with the bacterial ligand (*S.aureus* LTA, *E.coli* LPS and *P.gingivalis* LPS). For concentrations see Section 2.5. All stimulations were carried out in 25cm^2 flasks in SFM (GIBCO) (Section 2.5.1). The cell surface receptors (TLR1, TLR2, TLR4, TLR6, CD36 and CD14) were labelled via indirect immunofluorescence (Section 2.7.2) and analyzed by flow cytometry (Section 2.8.2.1).

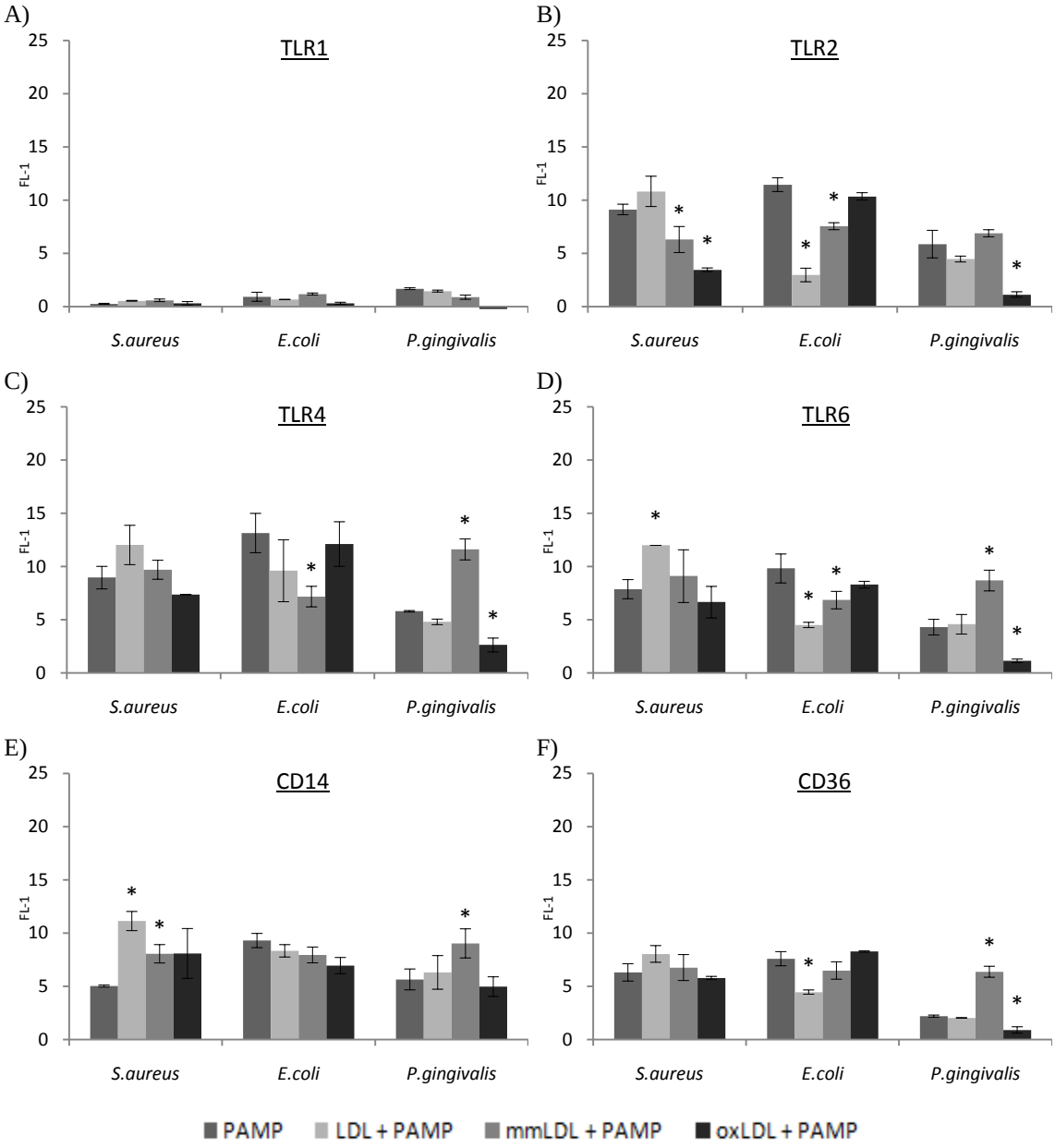

Figure 3.1.5: Cell surface receptor expression of: A) TLR1, B) TLR2, C) TLR4, D) TLR6, E) CD14 and F) CD36 on human ECV304 cells after 60 minute stimulation with the atherosclerosis-associated bacterial ligands *S.aureus* LTA, *E.coli* LPS or *P.gingivalis* LPS with pre-incubation (60 minute) with human LDL or either of its oxidised derivatives mmLDL and oxLDL. Cells were fixed and labelled with a primary antibody against the receptor of interest, followed by an appropriate secondary antibody conjugated to FITC. Fluorescence was measured on a FACSCalibur (Becton Dickinson), counting 10,000 cells per sample, not gated. Data represents mean, ± standard deviation, n=3. *Indicates statistically significant ($p<0.05$) difference in receptor expression in combined stimulations in comparison to PAMP alone (Section 2.19).

Pre-incubation with LDL reduced receptor expression in the case of the TLR4 agonist *E.coli* LPS with particular emphasis on TLR2 (Figure 3.1.5B) and TLR6 (Figure 3.1.5D)

which were reduced by 75% and 54% respectively in comparison to stimulation with *E.coli* LPS alone (Figure 3.1.5B/C). Pre-incubation with LDL had little or no effect on the TLR2 agonists *S.aureus* LTA and *P.gingivalis* LPS. Pre-incubation with mmLDL had a similar effect to LDL pre-incubation but to a lesser extent. With LDL pre-incubation the *E.coli* LPS induced receptor expression was reduced but this had little or no effect on the TLR2 agonists. The effect of pre-incubation with oxLDL seemed to mirror that of LDL pre-incubation. Although having little or no effect on CD14 (Figure 3.1.5E) or CD36 (Figure 3.1.5F) receptor expression the cell surface expression of TLR2, TLR4 and TLR6 (Figure 3.1.5B/C/D) were reduced. Of particular interest is their target receptor TLR2 whose expression was reduced dramatically by oxLDL pre-incubation (Figure 3.1.5B). TLR2 expression observed for *S.aureus* LTA exposure alone dropped by 63% when the cells were pre-incubated with oxLDL (Figure 3.1.5B). The same scenario gave an 81% reduction in TLR2 expression in the case of *P.gingivalis* LPS (Figure 3.1.5B). TLR4, TLR6 and CD36 (Figure 3.1.5C/D/E) expression due to *P.gingivalis* LPS stimulation were also reduced dramatically when vascular cells were pre-incubated with oxLDL. oxLDL pre-incubation had little or no effect on CD14 and CD36 (Figure 3.1.5E/F) expression with *S.aureus* LTA stimulation.

The reduction of receptor expression on the vascular endothelial cell surface suggests immunosuppression, a dampening of the immune response, which would agree with previous studies. It was hypothesised that this dampening of the immune system by endogenous lipoproteins could be allowing circulating bacteria to cause a chronic infection where their clearance is not performed effectively. The chronic nature of such an infection could lead to atherosclerosis, where a low level inflammatory state could enhance the environment for plaque formation. To see whether the modulation of

receptor expression caused by lipoprotein pre-incubation had the same effect on the release of inflammatory mediators the supernatant was collected from these stimulations and assayed for cytokine concentrations.

3.1.3.1: Inflammatory response to endogenous LDL and bacterial ligand combined

Cytokine analysis was performed on combined stimulations to see whether PRR expression mimics the inflammatory response produced. *C.pneumoniae* LPS was tested in addition to *S.aureus* LTA, *E.coli* LPS and *P.gingivalis* LPS. *C.pneumoniae* LPS, like *P.gingivalis* LPS, is an unconventional TLR2-associated LPS that is strongly related with atherosclerosis. As found with lipoprotein stimulations ECV304 cells were found to release only IL-6 and IL-8 to a significant degree.

ECV304 cells were subject to 60 minute pre-incubation with an endogenous lipoprotein (human LDL and its oxidised derivatives mmLDL and oxLDL) and then further 60 minute stimulation with the bacterial ligand (*S.aureus* LTA, *E.coli* LPS, *P.gingivalis* LPS or *C.pneumoniae* LPS). For concentrations see Section 2.5. All stimulations were carried out in 25cm^2 flasks in SFM (GIBCO) (Section 2.5.1). The SFM was collected post stimulation for cytokine analysis using the Human Inflammation BD™ cytometric bead array system (Section 2.8.2.2).

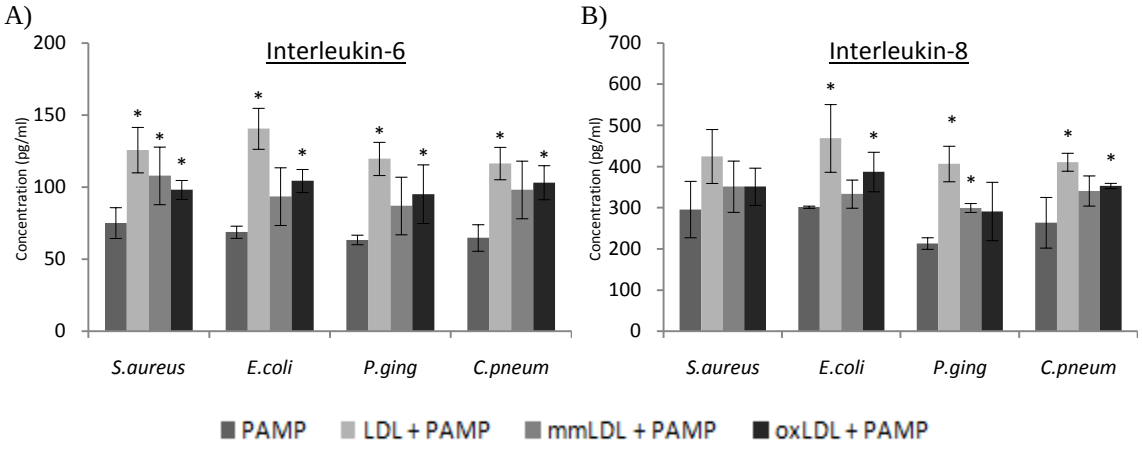

Figure 3.1.6: A) interleukin-6 and B) interleukin-8 release from human ECV304 cells after 60 minute stimulation with the atherosclerosis-associated bacterial ligands *S.aureus* LTA, *E.coli* LPS, *P.gingivalis* (*P.ging*) LPS or *C.pneumoniae* (*C.pneum*) LPS with pre-incubation (60 minutes) with human LDL or either of its oxidised derivatives, mmLDL oxLDL. IL-6 AND IL-8 was measured in the cell supernatant using a flow cytometric cytokine bead array system (Becton Dickinson). Negatives subtracted. Data represents mean, ± standard deviation, n=3. *Indicates statistically significant ($p<0.05$) increase in cytokine release in combined stimulations in comparison to PAMP alone (Section 2.19).

Interestingly the cytokine results are quite dissimilar to the receptor expression alterations observed. The combined stimulations saw an increased cytokine release in the human vascular endothelial cells (Figure 3.1.6) even though this study observed reduced PRR expression in a number of cases (Figure 3.1.5). LDL pre-incubation seemed to cause the greatest cytokine increase. mmLDL and oxLDL were lesser immunostimulatory in comparison.

3.1.4: Conclusions

- TLR2, TLR4, TLR6, CD14 and CD36 are potentially stimulated by atherosclerosis-associated ligands in the vascular system.
- Endogenous lipoproteins are capable of initiating a response in human ECV304 cells. The strongest immunostimulant of the lipoproteins is LDL, and the least is oxLDL. The association of oxLDL with atherosclerosis may be due to its low stimulatory nature preventing its clearance thus allowing chronic inflammation characteristic of atherogenesis.
- IL-6 and IL-8 are the predominant inflammatory cytokines released by human ECV304 cells in response to atherosclerosis-associated ligands.
- Although lipoprotein pre-incubation reduces cell surface PRR expression the cytokine concentration released increases. This could indicate alternate/disrupted receptor trafficking and/or cellular signalling.

3.2: HUVEC inflammatory response

Previous experimentation with the immortalised human ECV304 cell line showed upregulation of PRRs in the response to atherosclerosis-associated ligands. Lipoprotein pre-incubation was shown to be able to reduce ECV304 cell surface TLR expression, but conversely increase the concentration of IL-6 and IL-8 release. The next step in this study was to perform these experiments in a primary human vascular endothelial cell line, a more representative model. Cytokine induced expression of cell surface molecules has been shown to vary between vascular endothelial cells, be it primary or immortilised[205]. These discrepancies could arise from transformation procedures or the vascular bed of origin of the primary cell. The role of endogenous lipoproteins, bacterial products and combinations of these to analyze their capability of initiating atherogenesis by activation of cytokine release from primary HUVECs (Section 2.2.3) was investigated. The induced inflammatory response was quantified by cytokine analysis.

3.2.1: HUVEC inflammatory response to atherosclerosis-associated ligands

HUVECs were subject to 60 minute stimulation with human LDL, mmLDL, oxLDL, *S.aureus* LTA, *E.coli* LPS, *P.gingivalis* LPS or *C.pneumoniae* LPS. For concentrations see Section 2.5. All stimulations were carried out in 24 well plates in SFM (GIBCO) (Section 2.5.2). The SFM was collected post stimulation for cytokine analysis using the Human Inflammation BD™ cytometric bead array system (Section 2.8.2.2). Out of the inflammatory cytokines analysed (IL-1β, IL-6, IL-8, IL-10, IL-12p70 and TNF), only the release of IL-6 and IL-8 were significantly increased.

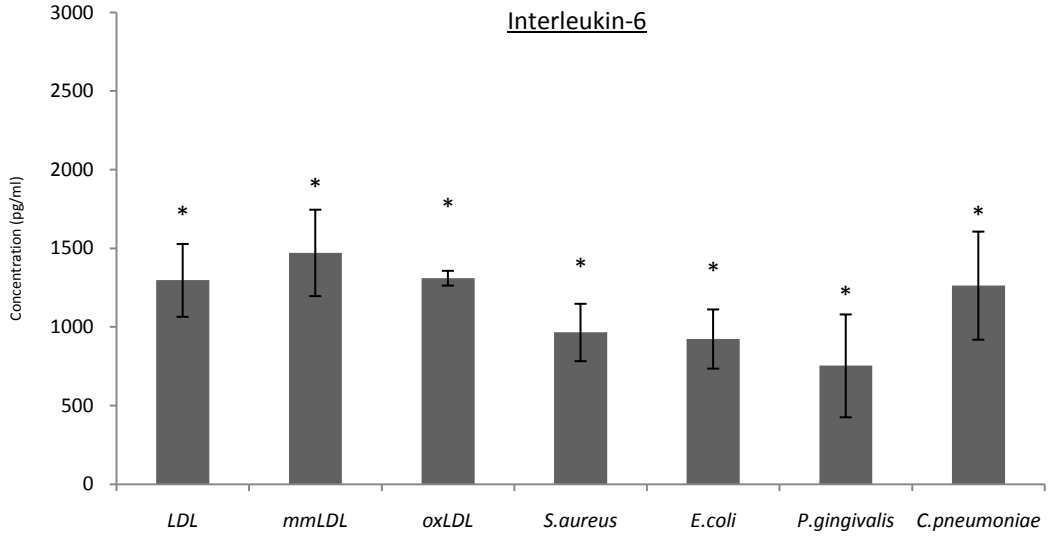

Figure 3.2.1: Interleukin-6 release from primary HUVECs in response to LDL, mmLDL, oxLDL, *S.aureus* LTA, *E.coli* LPS, *P.gingivalis* LPS and *C.pneumoniae* LPS. IL-6 was measured in the cell supernatant using a flow cytometric cytokine bead array system (Becton Dickinson). Negatives subtracted. Data represents mean, ± standard deviation, n=3. *Indicates statistically significant ($p<0.05$) increase in interleukin-6 release in comparison to unstimulated cells (Section 2.19).

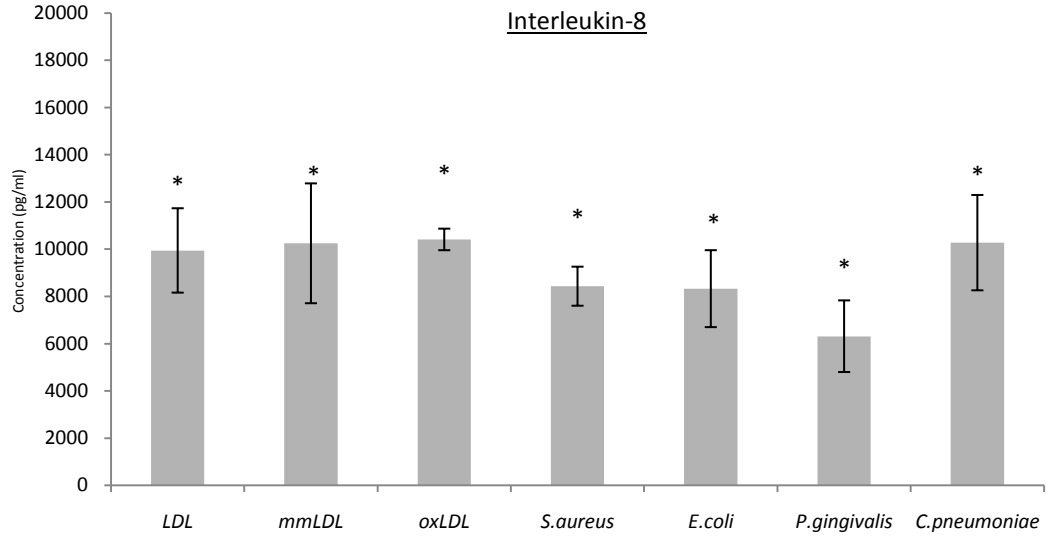

Figure 3.2.2: Interleukin-8 (IL-8) release from primary HUVECs in response to LDL, mmLDL, oxLDL, *S.aureus* LTA, *E.coli* LPS, *P.gingivalis* LPS and *C.pneumoniae* LPS. IL-8 was measured in the cell supernatant using a flow cytometric cytokine bead array system (Becton Dickinson). Negatives subtracted. Data represents mean, ± standard deviation, n=3. *Indicates statistically significant ($p<0.05$) increase in interleukin-8 release in comparison to unstimulated cells (Section 2.19).

As observed with ECV304 cells (Figure 3.1.2/4), lipoprotein and bacterial stimulation of HUVECs caused significant upregulation of only IL-6 and IL-8 out of the inflammatory cytokines screened for (Figure 3.2.1/2). HUVEC cytokine release was far greater than that recorded with ECV304 cells. The 60 minute HUVEC *S.aureus* LTA stimulation (Figure 3.2.2) induced ~27X more IL-8 than the same stimulation with ECV304 cells (Figure 3.1.4). The ability of LDL, mmLDL and oxLDL to induce IL-6 and IL-8 release differs between ECV304 and HUVECs. In the HUVEC cell line all lipoproteins gave a similar response (Figure 3.2.1/2) whilst in ECV304 cells LDL was the strongest immunostimulant and oxLDL the least (Figure 3.1.2). HUVECs (Figure 3.2.1/2) respond to *S.aureus* LTA, *E.coli* LPS and *P.gingivalis* LPS in a similar manner as ECVs (Figure 3.1.4) at 60 minutes where *S.aureus* LTA and *E.coli* LPS cause a similar response whilst *P.gingivalis* LPS is not as stronger a stimulant. *C.pneumoniae* LPS appears to be more immunostimulatory, relative to other ligands, in the primary HUVECs.

As observed with ECV304 cells IL-6 and IL-8 concentrations released were highly dissimilar, however this was much more apparent in the HUVECs. The 60 minute ECV304 cell *S.aureus* LTA stimulation gave IL-8 concentrations that were ~4X greater than IL-6 (Figure 3.1.4), the same stimulation in HUVECs gave IL-8 concentrations that were ~9X greater than IL-6 (Figure 3.2.1/2).

3.2.1.2: HUVEC NF-κB activation in response to atherosclerosis-associated ligands

TLRs act upstream of NF-κB activation. TLR signalling pathways have been shown to ultimately result in the release of NF-κB from its endogenous inhibitor which

subsequently causes its nuclear translocation that leads to the transcription of inflammatory cytokines (Section 1.3.6)[119].

In order to determine whether single stimulations with endogenous lipoproteins and bacterial products lead to a NF-κB-driven transcription response, HUVECs were subject to 60 minute stimulation with human LDL, mmLDL, oxLDL, *S.aureus* LTA, *E.coli* LPS, *P.gingivalis* LPS or *C.pneumoniae* LPS. For concentrations see Section 2.5. All stimulations were carried out in 24 well plates in SFM (GIBCO) (Section 2.5.2). The medium was removed and the HUVECs were lysed with 200µl X2 reducing sample buffer for 4 hours on the work top shaker and frozen (-20˚C) for a minimum of 24 hours (Section 2.10.2). Samples were separated using SDS-PAGE (Section 2.10.3) and then transferred onto a nitrocellulose membrane (Section 2.11.1). The membrane was probed using phospho-IKappaB-alpha or IKappaB-alpha (Section 2.12.1) monoclonal antibodies followed by the appropriate secondary antibody conjugated to horse radish peroxidase (HRP {Section 2.1}). Membranes were imaged via enhanced chemiluminescence (Section 2.12.2).

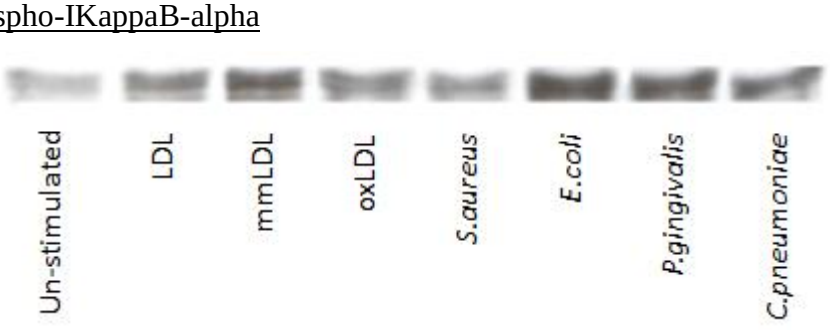

Figure 3.2.3: Western blot of phospho-IKappaB-alpha from lysates of unstimulated HUVECs and those exposed to the atherosclerosis-associated ligands: LDL, mmLDL, oxLDL, *S.aureus* LTA, *E.coli* LPS, *P.gingivalis* LPS and *C.pneumoniae* LPS. Lysates were separated by sodium dodecyl sulphate polyacrylamide gel electrophoresis and transferred onto a nitrocellulose membrane. The membrane was probed for phospho-IKappaB-alpha specific mAb followed by the appropriate secondary antibody conjugated to HRP and imaged via enhanced chemiluminescence.

NF-κB activation was evident in all single stimulations (Figure 3.2.3). *E.coli* and *P.gingivalis* LPS stimulations seemed to have produced the most pronounced NF-κB activation, compared to all other stimulations. As a control the membrane was probed for total-IκB (IKappaB-alpha) which demonstrated equal loading (data not shown), suggesting that the increase in the density of the band for NF-κB activation in response to *E.coli* and *P.gingivalis* LPS is specific.

3.2.2: Inflammatory response to bacterial ligand with lipoprotein pre-incubation

The next step in this study was to pre-incubate HUVECs with lipoprotein before bacterial stimulus. The combined stimulations were designed to simulate a high cholesterol state, a known risk factor for atherosclerosis, prior to infection. This is the hypothesised sequence of events that would take place in the human vascular system. HUVECs were subject to 60 minute pre-incubation with an endogenous lipoprotein (human LDL or its oxidised derivatives mmLDL and oxLDL) and then further 60 minute stimulation with the bacterial ligand (*S.aureus* LTA, *E.coli* LPS, *P.gingivalis* LPS and *C.pneumoniae* LPS). For concentrations see Section 2.5. All stimulations were carried out in 24 well plates in SFM (GIBCO) (Section 2.5.2). The SFM was collected post stimulation for cytokine analysis using the Human Inflammation BD™ cytometric bead array system (Section 2.8.2.2).

Combined stimulations involved a 60 minute pre-incubation with an endogenous lipoprotein and then further 60 minute stimulation with the bacterial ligand to simulate the sequence of events that would take place in the human vascular system. Similarly to previous findings, only interleukin-6 and interleukin-8 concentrations were significantly increased.

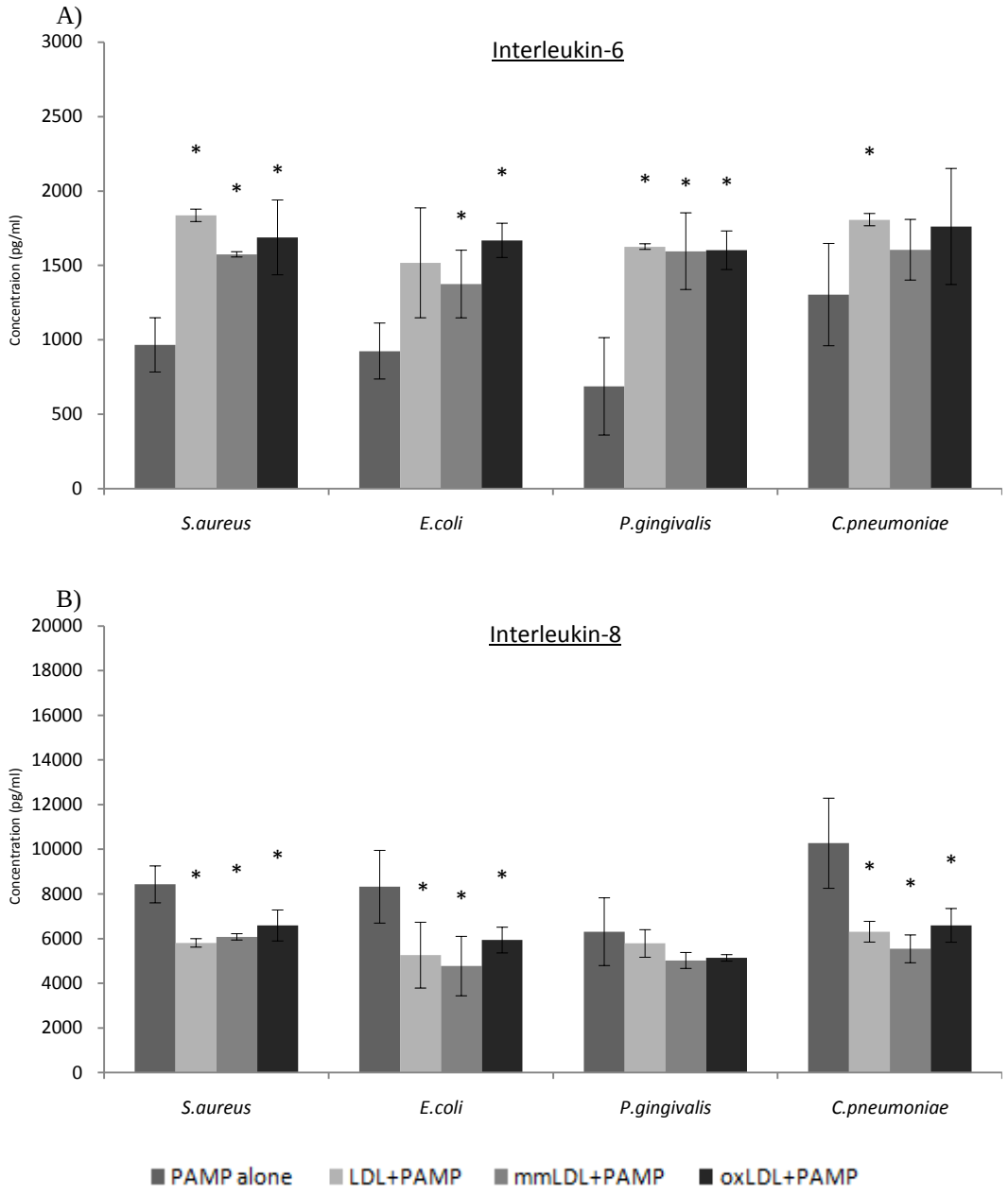

Figure 3.2.4: Interleukin-6 (A) and interleukin-8 (B) release from primary HUVECs after 60 minute stimulation with the atherosclerosis-associated bacterial ligands *S.aureus* LTA, *E.coli* LPS, *P.gingivalis* LPS or *C.pneumoniae* LPS with pre-incubation (60 minutes) with human LDL or either of its oxidised derivatives mmLDL and oxLDL. IL-6 and IL-8 were measured in the cell supernatant using a flow cytometric cytokine bead array system (Becton Dickinson). Negatives subtracted. Data represents mean, ± standard deviation, n=3. *Indicates statistically significant ($p<0.05$) difference in cytokine release in combined stimulations in comparison to PAMP alone (Section 2.19).

HUVEC IL-6 levels in response to *S.aureus* LTA, *E.coli* LPS and *P.gingivalis* LPS (Figure 3.2.1) were increased significantly when combined with endogenous lipoprotein pre-incubation (Figure 3.2.4A), as observed with the immortalised ECV304 cell line

(Figure 3.1.6A). LDL, mmLDL and oxLDL pre-incubations all had a similar effect on HUVEC IL-6 in response to bacterial ligands (Figure 3.2.4A).

HUVEC IL-8 release in response to *S.aureus* LTA, *E.coli* LPS, *P.gingivalis* LPS and *C.pneumoniae* LPS with endogenous lipoprotein pre-incubation (Figure 3.2.4B) contrasted that observed with ECV304 cells (Figure 3.1.6B). HUVEC IL-8 release decreased when the cells were pre-incubated with lipoprotein prior to *S.aureus* LTA, *E.coli* LPS, and *C.pneumoniae* LPS stimulation (Figure 3.2.4B). The opposite of this was observed with the ECV304 cells where lipoprotein pre-incubation augmented the response (Figure 3.1.6). The greatest decrease was observed with *C.pneumoniae* LPS versus *C.pneumoniae* LPS with pre-incubation with mmLDL where a 36% decrease in IL-8 concentration was observed (Figure 3.2.4B). This illustrates an immunoprotective role of lipoproteins where they may have the ability to influence cellular immune response to bacterial infection.

3.2.2.1: HUVEC NF-κB activation response to atherosclerosis-associated ligands

In order to determine whether the combination of endogenous lipoproteins and bacterial products can lead to NF-κB-driven transcription response, HUVECs were subject to 60 minute pre-incubation with an endogenous lipoprotein (human LDL or its oxidised derivatives mmLDL and oxLDL) and then further 60 minute stimulation with the bacterial ligand (*S.aureus* LTA, *E.coli* LPS, *P.gingivalis* LPS or *C.pneumoniae* LPS). For concentrations see Section 2.5. All stimulations were carried out in 24 well plates in SFM (GIBCO) (Section 2.5.2). The medium was removed and the HUVECs were lysed with 200µl X2 reducing sample buffer for 4 hours on the work top shaker and frozen (-20˚C) for a minimum of 24 hours (Section 2.10.2). Samples were separated using

sodium dodecyl sulphate polyacrylamide gel electrophoresis (Section 2.10.3) and then transferred onto a nitrocellulose membrane (Section 2.11.1). The membrane was probed for phospho-IKappaB-alpha or IKappaB-alpha (Section 2.12.1). Membranes were imaged via enhanced chemiluminescence (Section 2.12.2).

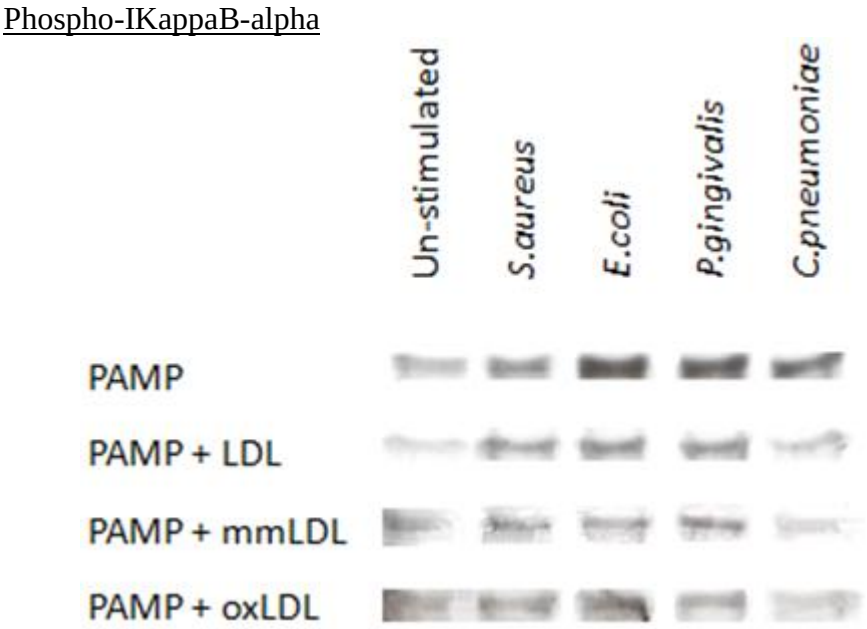

Figure 3.2.5: Western blot of phospho-IKappaB-alpha from lysates of unstimulated HUVECs and those after 60 minute stimulation with bacterial ligands *S.aureus* LTA, *E.coli* LPS, *P.gingivalis* LPS or *C.pneumoniae* LPS alone (PAMP) and bacterial ligand with 60 minute pre-incubation with human LDL (PAMP + LDL) or either of its oxidised derivatives, mmLDL (PAMP + mmLDL) and oxLDL (PAMP + oxLDL). Lysates were separated by sodium dodecyl sulphate polyacrylamide gel electrophoresis and transferred onto a nitrocellulose membrane. The membrane was probed for phospho-IKappaB-alpha specific mAb followed by the appropriate secondary antibody conjugated to HRP and imaged via enhanced chemiluminescence.

NF-κB activation decreases when HUVECs are pre-incubated with lipoprotein prior to *E.coli* LPS, *P.gingivalis* LPS and *C.pneumoniae* LPS (Figure 3.2.5). This effect was most evident for *C.pneumoniae*. The western blot mirrors the cytokine results obtained for IL-8 (Figure 3.2.4B) but not for IL-6 (Figure 3.2.4A). As a control the membrane was probed for total-IκB (IKappaB-alpha) which demonstrated equal loading (data not shown

3.2.3: Inflammatory response to altered combined stimulations

Since this study had already demonstrated that lipoprotein pre-incubation of human vascular endothelial cells altered their inflammatory response to the bacterial ligands *S.aureus* LTA, *E.coli* LPS, *P.gingivalis* LPS and *C.pneumoniae* LPS, this study proceeded to investigate whether the sequence of introducing these ligands into the system would further affect the inflammatory response.

Human vascular endothelial cells were either incubated with an endogenous lipoprotein (human LDL or its oxidised derivatives mmLDL and oxLDL) for 60 minutes prior to the addition of bacterial products (*S.aureus* LTA, *E.coli* LPS, *P.gingivalis* LPS or *C.pneumoniae* LPS) for 60 minutes, incubated with bacterial products for 60 minutes prior to the addition of the lipoprotein for 60 minutes or the lipoproteins and bacterial products were added to the HUVECs at the same time for 60 minutes. For concentrations see Section 2.5. All stimulations were carried out in 24 well plates in SFM (GIBCO) (Section 2.5.2). The SFM was collected post stimulation for cytokine analysis using the Human Inflammation BD™ cytometric bead array system (Section 2.8.2.2).

Pre-incubation with LDL and its derivatives, mmLDL and oxLDL, gave similar results in the three different double stimulation protocols. For this reason only the results for oxLDL have been displayed, the LDL associated with atherosclerosis and one that would most feasibly exist *in vivo*. Again, only interleukin-6 and interleukin-8 concentrations were significantly increased.

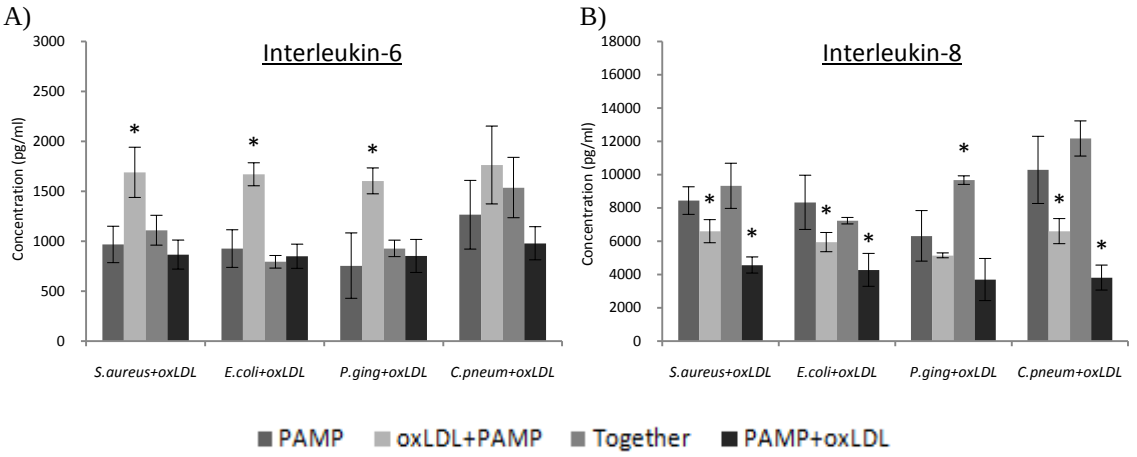

Figure 3.2.6: A) interleukin-6 and B) interleukin-8 release from primary HUVECs in response to a 60 minute stimulation with the atherosclerosis-associated bacterial ligands *S.aureus* LTA, *E.coli* LPS, *P.gingivalis* (*P.ging*) LPS or *C.pneumoniae* (*C.pneum*) LPS alone (PAMP) or with either oxLDL pre-incubation (oxLDL+PAMP), stimulation of oxLDL and PAMP simultaneously (Together) or addition of oxLDL after PAMP stimulation (PAMP+oxLDL). IL-6 and IL-8 were measured in the cell supernatant using a flow cytometric cytokine bead array system (Becton Dickinson). Negatives subtracted. Data represents mean, ± standard deviation, n=3. *Indicates statistically significant ($p<0.05$) difference in cytokine release in combined stimulations in comparison to PAMP alone (Section 2.19).

Pre-incubation of HUVECs with oxLDL prior to exposure to bacterial products augmented IL-6 release (Figure 3.2.6A, oxLDL+PAMP). Increases of 75% for *S.aureus* LTA, 80% for *E.coli* LPS, 133% for *P.gingivalis* LPS and 35% for *C.pneumoniae* LPS in IL-6 release were observed when cells were pre-incubated with oxLDL in comparison to PAMP alone. Variation of IL-6 release was least for *C.pneumoniae* LPS (Figure 3.2.6A). Incubation of the ligands when added simultaneously gave a slight increase in IL-6 release when the TLR2 agonists (*S.aureus* LTA, *P.gingivalis* LPS and *C.pneumoniae* LPS) were added to the HUVECs with oxLDL (Figure 3.2.6A, Together). When the bacterial product was added prior to oxLDL a reduction in IL-6 release, in comparison to single stimulation (PAMP), was seen for *S.aureus* LTA, *E.coli* LPS and more substantially *C.pneumoniae* LPS (Figure 3.2.6A, PAMP+oxLDL).

As explained in Section 3.2.2, IL-8 release decreased when the cells were pre-incubated with low density lipoprotein in comparison to single bacterial stimulations. This was more apparent for the PAMP+oxLDL combined stimulation where decrease in IL-8 release was ~2X greater than that observed when HUVECs were pre-incubated with oxLDL (Figure 3.2.6B, oxLDL+PAMP). When HUVECs were incubated with oxLDL and bacterial product together another discrepancy between the TLR2 and TLR4 ligands was highlighted. Increase in IL-8 concentrations were observed when the TLR2 agonists (*S.aureus* LTA, *P.gingivalis* LPS and *C.pneumoniae* LPS) were added to HUVECs in unison with oxLDL whilst the same stimulation protocol decreased IL-8 release when *E.coli* LPS was stimulated alongside oxLDL (Figure 3.2.6B, Together)

The altered responses observed from the three different double stimulation protocols signify altered activation of the endothelial cell line. This shows that the sequence of events leading to HUVEC activation can have a profound effect on the cellular response and thus inflammation in the vascular system. The altered level of activation between these stimulations demonstrates that there must be some kind of interaction between these ligands, and/or their receptors, affecting their recognition by endothelial cells.

3.2.4: Conclusions

- LDL, mmLDL, oxLDL, *S.aureus* LTA, *E.coli* LPS, *P.gingivalis* LPS and *C.pneumoniae* LPS all cause activation of NF-κB in HUVECs.
- Lipoprotein pre-incubation of HUVECs causes a reduction in NF-κB.
- HUVECs and ECV304 cells have different inflammatory responses to ligands. ECV304 may not be a representative model of inflammation.
- IL-6 and IL-8 are the predominant inflammatory cytokines released by HUVECs in response to atherosclerosis-associated ligands.
- IL-6 is upregulated when HUVECs are pre-treated with LDL, mmLDL and oxLDL. This is in compliance with the ECV304 data.
- IL-8 is downregulated when HUVECs are pre-treated with LDL, mmLDL and oxLDL. This contrasts with ECV304 data.
- Ratios of IL-6 and IL-8 alter between different combined stimulation protocols. This may indicate alternate receptor trafficking and/or cellular signalling.
- The altered responses observed from the three different double stimulation protocols signify altered activation of the endothelial cell line, suggesting that the sequence of events leading to HUVEC activation can have a profound effect on the cellular response and thus inflammation in the vascular system.

3.3: Lipid raft dependant signalling

Lipid rafts provide the necessary microenvironment in order for certain specialised signalling events to take place. It has recently been found that components of the innate immune system concentrate in lipid rafts in order to facilitate signal transduction[130,131].

This study investigated whether membrane partitioning and lipid rafts play a role in the innate immune activation observed in atherosclerosis. In order to investigate the importance of lipid raft formation, the disruption of lipid rafts was used. Disruption of lipid rafts can be utilised in order to knockdown cellular signalling cascades to elucidate the role of up-stream receptors in the detection of certain ligands.

Lipid raft disruption in primary HUVECs was achieved with the use of the drug Nystatin. Once rafts were disrupted cells were subjected to stimulations with lipoproteins, bacterial products as well as combinations of these to analyze the effect of the disruption of lipid rafts. The inflammatory response was quantified by cytokine release.

3.3.1: Lipid raft dependant signalling to atherosclerosis-associated ligands

HUVEC lipid rafts were disrupted by addition of Nystatin (60µg/ml) 10 minutes prior to cell simulation (Section 2.14). HUVECs were then subject to 60 minute stimulation with human LDL, mmLDL, oxLDL, *S.aureus* LTA, *E.coli* LPS, *P.ging* LPS or *C.pneumoniae* LPS (Section 2.5). All stimulations were carried out in 24 well plates in SFM (GIBCO) (Section 2.5.2). The SFM was collected post stimulation for cytokine analysis (IL-1β, IL-6, IL-8 IL-10, IL-12p70, TNF) using the Human Inflammation BD™ cytometric bead array system (Section 2.8.2.2).

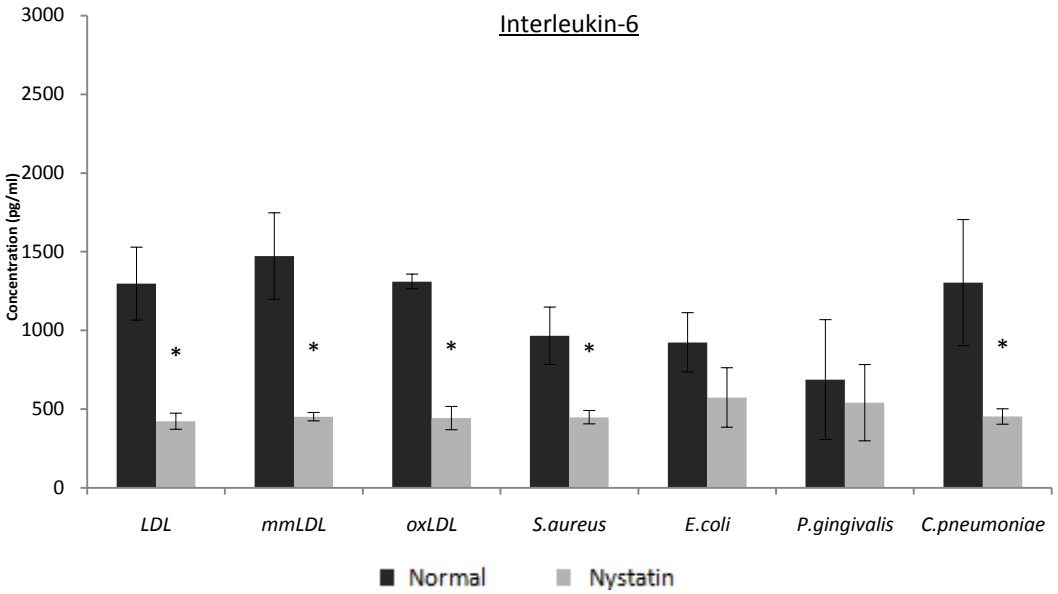

Figure 3.3.1: Comparison of interleukin-6 release from primary HUVECs with intact (Normal/Dark grey) and disrupted (Nystatin/Light grey) lipid rafts in response to LDL, mmLDL, oxLDL, *S.aureus* LTA, *E.coli* LPS, *P.gingivalis* LPS and *C.pneumoniae* LPS IL-6 and IL-8 were measured in the cell supernatant using a flow cytometric cytokine bead array system (Becton Dickinson). Negatives subtracted. Data represents mean, ± standard deviation, n=2. *Indicates statistically significant ($p<0.05$) difference in interleukin-6 release between nystatin treated and corresponding controls (Section 2.19).

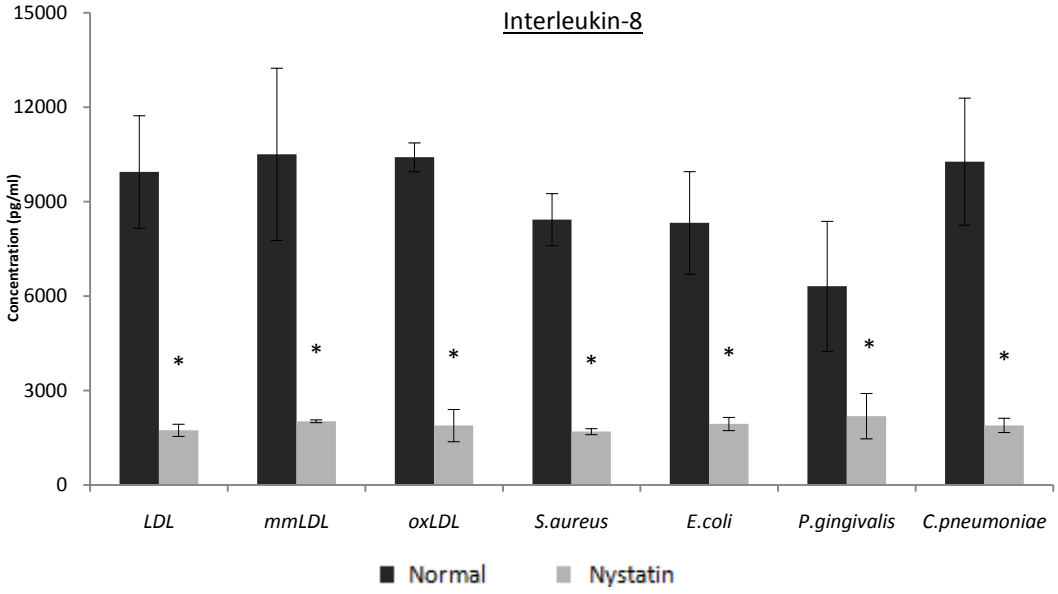

Figure 3.3.2: Comparison of interleukin-8 release from primary HUVECs with intact (Normal/Dark grey) and disrupted (Nystatin/Light grey) lipid rafts in response to LDL, mmLDL, oxLDL, *S.aureus* LTA, *E.coli* LPS, *P.gingivalis* LPS and *C.pneumoniae* LPS IL-6 and IL-8 were measured in the cell supernatant using a flow cytometric cytokine bead array system (Becton Dickinson). Negatives subtracted. Data represents mean, ± standard deviation, n=2. *Indicates statistically significant ($p<0.05$) difference in interleukin-8 release between nystatin treated and corresponding controls (Section 2.19).

HUVECs that were pre-treated with the raft disrupting agent Nystatin showed a significant reduction in cytokine release in response to lipoprotein and bacterial ligands in comparison to untreated cells (Figure 3.3.1/2). Nystatin did not affect cell viability as tested by trypan blue incorporation. All stimulations were modified by raft disruption to give similar low level cytokine profiles (Figure 3.3.1/2). These data indicate the requirement for lipid rafts for the induction of effective cytokine release. The data would suggest that the receptors involved in the recognition of these ligands (TLR2, TLR4, TLR6, CD14 and CD36) are lipid raft dependant.

3.3.2: Lipid raft dependant signalling to bacterial ligand with lipoprotein pre-incubation

Since the data suggested that the innate immune recognition of atherosclerosis-associated ligands is lipid-raft dependent, this study proceeded to investigate whether this is the case when PRRs are challenged with combinations of endogenous lipoproteins and bacterial ligands.

HUVEC lipid rafts were disrupted by addition of Nystatin 10 minutes prior to cell simulation (Section 2.14). HUVECs were then subject to 60 minute pre-incubation with an endogenous lipoprotein (human LDL or its oxidised derivatives, mmLDL and oxLDL) and then further 60 minute stimulation with the bacterial ligand (*S.aureus* LTA, *E.coli* LPS, *P.gingivalis* LPS and *C.pneumoniae* LPS) (Section 2.5). All stimulations were carried out in 24 well plates in SFM (GIBCO) (Section 2.5.2). The SFM was collected post stimulation for cytokine analysis using the Human Inflammation BD™ cytometric bead array system (Section 2.8.2.2).

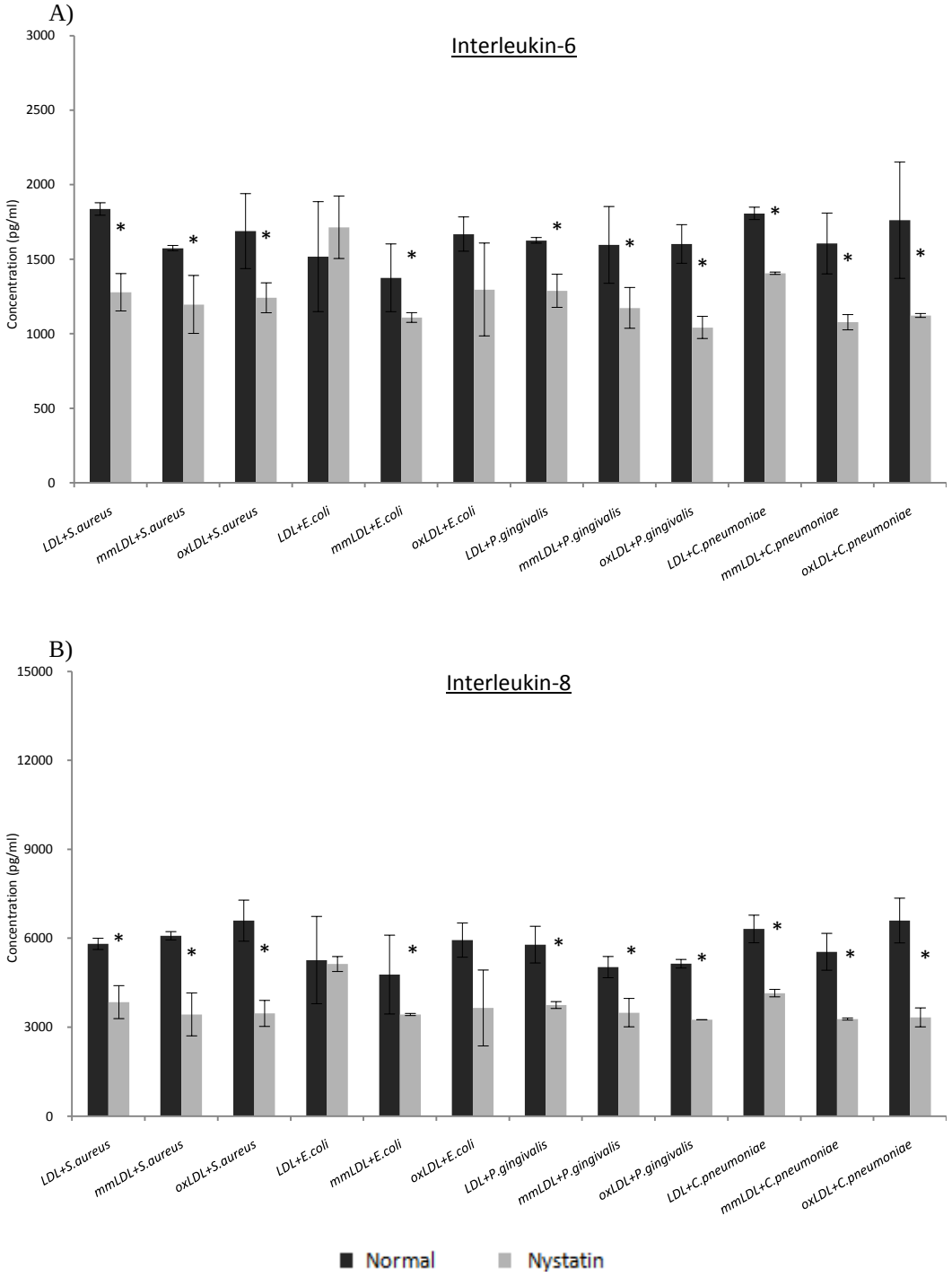

Figure 3.3.3: A) interleukin-6 and B) interleukin-8 release comparison from primary HUVECs after 60 minute stimulation with the atherosclerosis associate bacterial ligands *S.aureus* LTA, *E.coli* LPS, *P.gingivalis* LPS or *C.pneumoniae* LPS with pre-incubation (60 minutes) with human LDL or either of its oxidised derivatives, mmLDL and oxLDL with intact (dark grey) and disrupted (light grey) lipid rafts by the use of Nystatin. IL-6 and IL-8 were measured in the cell supernatant using a flow cytometric cytokine bead array system (Becton Dickinson). Negatives subtracted. Data represents mean, ± standard deviation, n=3. *Indicates statistically significant ($p<0.05$) difference in cytokine release between nystatin treated and corresponding controls (Section 2.19).

Lipid raft disruption had a lesser effect on the double stimulations (Figure 3.3.3) in comparison to single stimulations (Figure 3.3.1/2); the reduction in cytokine release was reduced. Activation of the HUVECs still showed lipid raft dependence. Perhaps the ability of lipoprotein and bacterial ligand to form complexes enhances somehow their recognition, possibly by involving non-raft resident receptors and thus reducing requirement for lipid rafts.

3.3.3: Lipid raft dependant localisation and trafficking of receptors

Lipid raft dependence has been shown in TLR signalling cascades. This study has shown that the disruption of lipid rafts reduces cellular response to endogenous lipoproteins, invading pathogens and combinations of these products. Results indicate the necessity of TLR signalling in the response to these products and points to their possible contribution to the inflammatory disorder of atherosclerosis. To try to understand in more detail the effect of lipid raft disruption on cellular activation this study employed confocal microscopy to view receptor localisation and trafficking with various stimuli in intact and lipid raft disrupted HUVECs.

3.3.3.1: Lipid raft dependant PRR localisation and trafficking

HUVECs were seeded on collagen treated 8 well glass slides (Section 2.9.1). Lipid raft disruption was performed by adding Nystatin (60µg/ml) directly to the slide 10 minutes prior to cell stimulation (Section 2.14). The cells were stimulated directly on the slide in 200µl SFM (GIBCO) (Section 2.5.3). Intact HUVECs and Nystatin treated HUVECs were subject to single (lipoprotein or bacterial PAMP) and combined (lipoprotein pre-incubation then bacterial PAMP exposure) stimulations. Single stimulations involved 60 minute incubation with LDL, mmLDL, oxLDL, *S.aureus* LTA, *E.coli* LPS, *P.gingivalis* LPS or *C.pneumoniae* LPS (Section 2.5). Combined stimulations involved 60 minute

pre-incubation with an endogenous lipoprotein (LDL, mmLDL or oxLDL) and then further 60 minute stimulation with the bacterial ligand (*S.aureus* LTA, *E.coli* LPS, *P.gingivalis* LPS and *C.pneumoniae* LPS) (Section 2.5). Both direct and indirect immunofluorescence techniques (Section 2.7) were used to label primary HUVECs on 8 well glass slides (Section 2.9.2). Slides were viewed using a Zeiss LSM 510 META confocal microscope with a 1.4 NA 63x Zeiss objective, used in conjunction with Zeiss LSM 2.5 analysis software (Section 2.9).

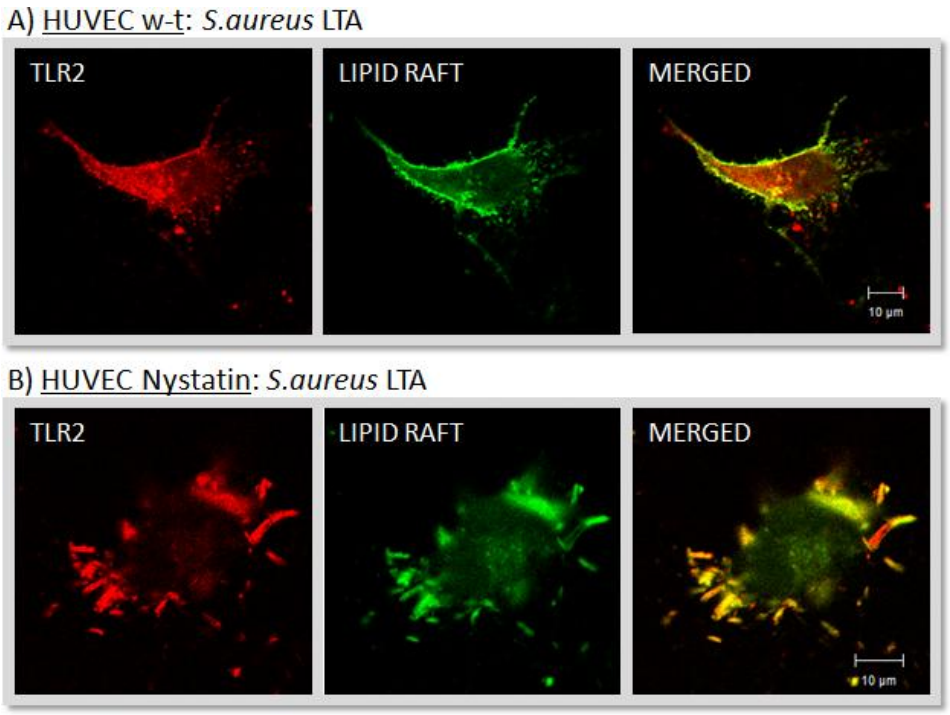

Figure 3.3.4: Cellular distribution of TLR2 (Red) in relation to Lipid rafts (Green) in intact HUVECs (A) and HUVECs treated with Nystatin (B) which have been stimulated with *S.aureus* LTA (60 minutes). The cells were stimulated with the different ligands in the presence and absence of Nystatin. They were subsequently fixed and labelled with the corresponding primary antibody against the receptor of interest, followed by an appropriate secondary antibody. Lipid rafts were labelled using cholera-toxin-FITC. Images were acquired using a Zeiss LSM 510 META confocal microscope with a 1.4 NA 63x Zeiss objective, used in conjunction with Zeiss LSM 2.5 analysis software. The image is a representative from a number of independent experiments.

TLR2 is located in lipid rafts in both intact HUVECs (Figure 3.3.4A) and HUVECs treated with Nystatin (Figure 3.3.4B) when subject to *S.aureus* LTA. In the intact raft image there is evidence of TLR2 localisation in areas other than lipid rafts, this is not apparent with lipid raft disrupted HUVECs (Figure 3.3.4A).

In order to determine which sub-cellular organelles TLR2 might be targeted to this study proceeded to investigate the colocalisation of TLR2 with different organelles in response to its ligand, *S.aureus* LTA.

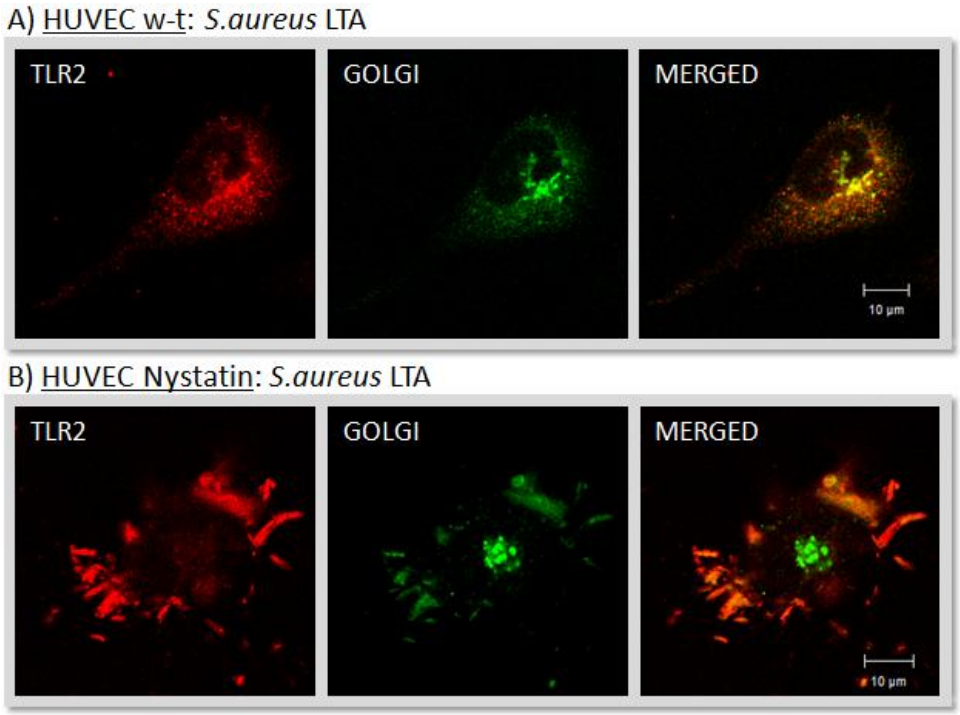

Figure 3.3.5: Cellular distribution of TLR2 (Red) in relation to Golgi (Green) in intact HUVECs (A) and HUVECs treated with Nystatin (B) which have been stimulated with *S.aureus* LTA (60 minutes). The cells were stimulated with *S.aureus* in the presence and absence of Nystatin. They were subsequently fixed and labelled with the corresponding primary antibody against the receptor of interest, followed by an appropriate secondary antibody. Lipid rafts were labelled using cholera-toxin-FITC. Images were acquired using a Zeiss LSM 510 META confocal microscope with a 1.4 NA 63x Zeiss objective, used in conjunction with Zeiss LSM 2.5 analysis software. The image is representative of a number of independent experiments.

TLR2 was found to be targeted to the Golgi in response to *S.aureus* LTA in intact HUVECs (Figure 3.3.5A). This association was completely lost when lipid rafts were disrupted (Figure 3.3.5B).

Lipid raft disruption had similar effects for each stimulation protocol including combined stimulations (Figure 3.3.6/7). Nystatin treatment shows obvious distortion of lipid raft morphology and disruption of TLR trafficking.

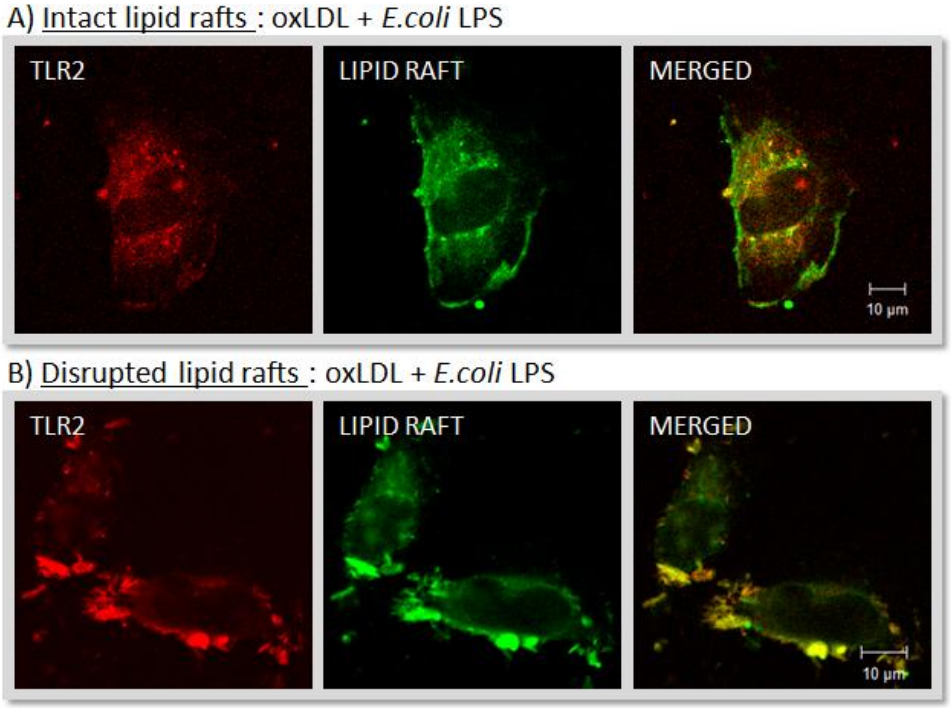

Figure 3.3.6: Cellular distribution of TLR2 (Red) in relation to Lipid rafts (Green) in intact HUVECs (A) and HUVECs treated with Nystatin (B) which have been stimulated with *E.coli* LPS with pre-incubation (60 minutes) with oxLDL. The cells were stimulated with the different ligands in the presence and absence of Nystatin. They were subsequently fixed and labelled with the corresponding primary antibody against the receptor of interest, followed by an appropriate secondary antibody. Lipid rafts were labelled using cholera-toxin-FITC. Images were acquired using a Zeiss LSM 510 META confocal microscope with a 1.4 NA 63x Zeiss objective, used in conjunction with Zeiss LSM 2.5 analysis software. The image is representative of a number of independent experiments.

The association of TLR2 and lipid raft in intact HUVECs is less obvious in the *E.coli* stimulation with oxLDL pre-incubation (Figure 3.3.6A) in comparison to *S.aureus* LTA stimulation of intact HUVECs (Figure 3.3.4 A). This displays the altered response of the cells as would be expected. However, as observed with *S.aureus* LTA stimulation of lipid raft disrupted HUVECs (Figure 3.3.4B), TLR2 is located in lipid rafts in Nystatin treated HUVECs (Figure 3.3.6B).

Investigation of the colocalisation of TLR2 with different organelles in response to *E.coli* stimulation with oxLDL pre-incubation revealed the importance of lipid rafts in the targeting not only to the Golgi but also other cellular compartments such as endosomes.

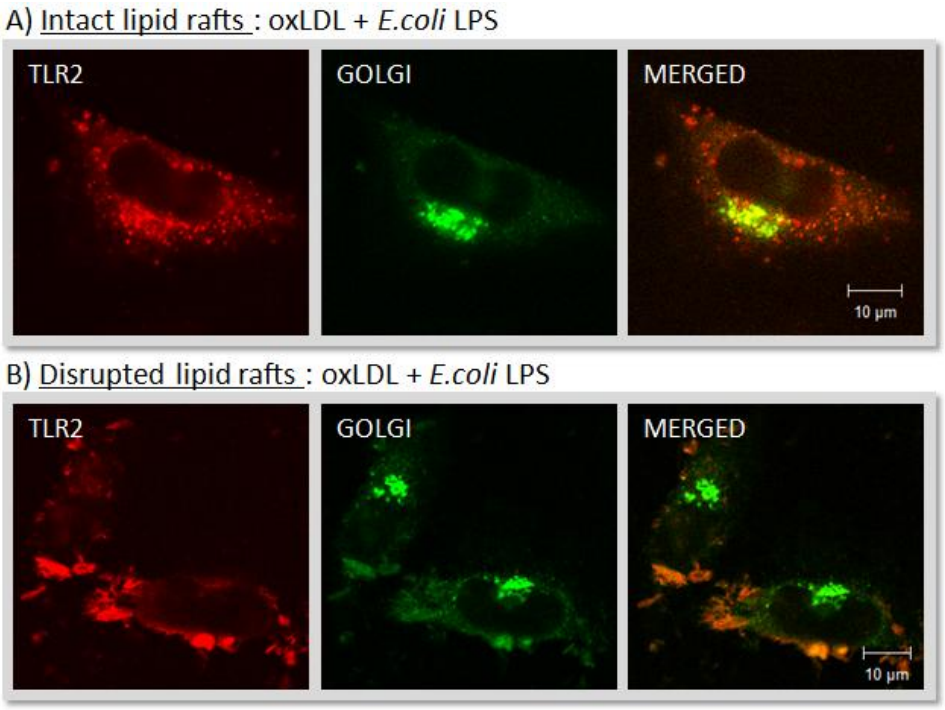

Figure 3.3.7: Cellular distribution of TLR2 (Red) in relation to Golgi (Green) in intact HUVECs (A) and HUVECs treated with Nystatin (B) which have been stimulated with *E.coli* LPS with pre-incubation (60 minutes) with oxLDL. The cells were stimulated in the presence and absence of Nystatin. They were subsequently fixed and labelled with the corresponding primary antibody against the receptor of interest, followed by an appropriate secondary antibody. Lipid rafts were labelled using cholera-toxin-FITC. Images were acquired using a Zeiss LSM 510 META confocal microscope with a 1.4 NA 63x Zeiss objective, used in conjunction with Zeiss LSM 2.5 analysis software. The image is representative of a number of independent experiments.

TLR2 was found to be targeted to the Golgi in response to *E.coli* stimulation with oxLDL pre-incubation in intact HUVECs (Figure 3.3.7A). This association was completely lost when lipid rafts were disrupted (Figure 3.3.7B).

The disturbance of cellular signalling due to lipid raft disruption is caused through altered trafficking of receptors. Lipid rafts are not only required for the formation of heterotypic receptor complexes but are also important for receptor internalization and targeting to locations such as the Golgi and endosomes. These images show the requirement of lipid rafts for appropriate TLR targeting and signalling.

3.3.4: Recruitment of TLR2 to lipid rafts following bacterial stimulation with lipoprotein pre-incubation

Confocal data demonstrated that TLR2 is recruited within lipid rafts upon stimulation by its ligands. Since it has been previously demonstrated that *H.pylori* and *P.gingivalis* LPS-induced cellular activation is mediated within lipid rafts[206], this study proceeded to investigate whether lipid rafts play a role in activation in response to lipoproteins and lipoprotein/bacterial product combinations. Lipid raft recruitment of receptors in response to lipoproteins and lipoprotein/bacterial product combinations was analysed using FRET (Section 2.9.4).

3.3.4.1: Lipid raft recruitment of TLR2

FRET experiments between TLR2 and GM-1 ganglioside (a lipid raft-associated lipid) were performed before and after HUVEC single stimulation with lipoprotein (human LDL or its oxidised derivatives, mmLDL and oxLDL), bacterial products (*S.aureus* LTA, *E.coli*, *P.gingivalis* or *C.pneumoniae* LPS) or combined stimulations involving 60 minute pre-incubation with an endogenous lipoprotein (LDL, mmLDL, or oxLDL) and then further 60 minute stimulation with the bacterial ligand (*S.aureus* LTA, *E.coli* LPS, *P.gingivalis* LPS or *C.pneumoniae* LPS) (Section 2.5). TLR2 molecules were labelled with Cy3-TL2.1 and GM-1 ganglioside was labelled with Cy5-cholera toxin. FRET was measured in terms of dequenching of donor fluorescence after complete photobleaching of the acceptor fluorophore (Section 2.9.4). Fluorescence was quantified using a Zeiss LSM 510 META confocal microscope with a 1.4 NA 63x Zeiss objective, used in conjunction with Zeiss LSM 2.5 analysis software (Section 2.9).

The energy transfer efficiency in this system was tested using a positive control, i.e. energy transfer between mAbs to different epitopes on CD14 molecules, showing that the maximum energy transfer efficiency (E%) was 38 ± 1.0. A negative control between

Cy3-CD14 and Cy5-W6/32 (mAb specific for major histocompatibility complex class I) was also used, which revealed no significant energy transfer (7 ± 1.2).

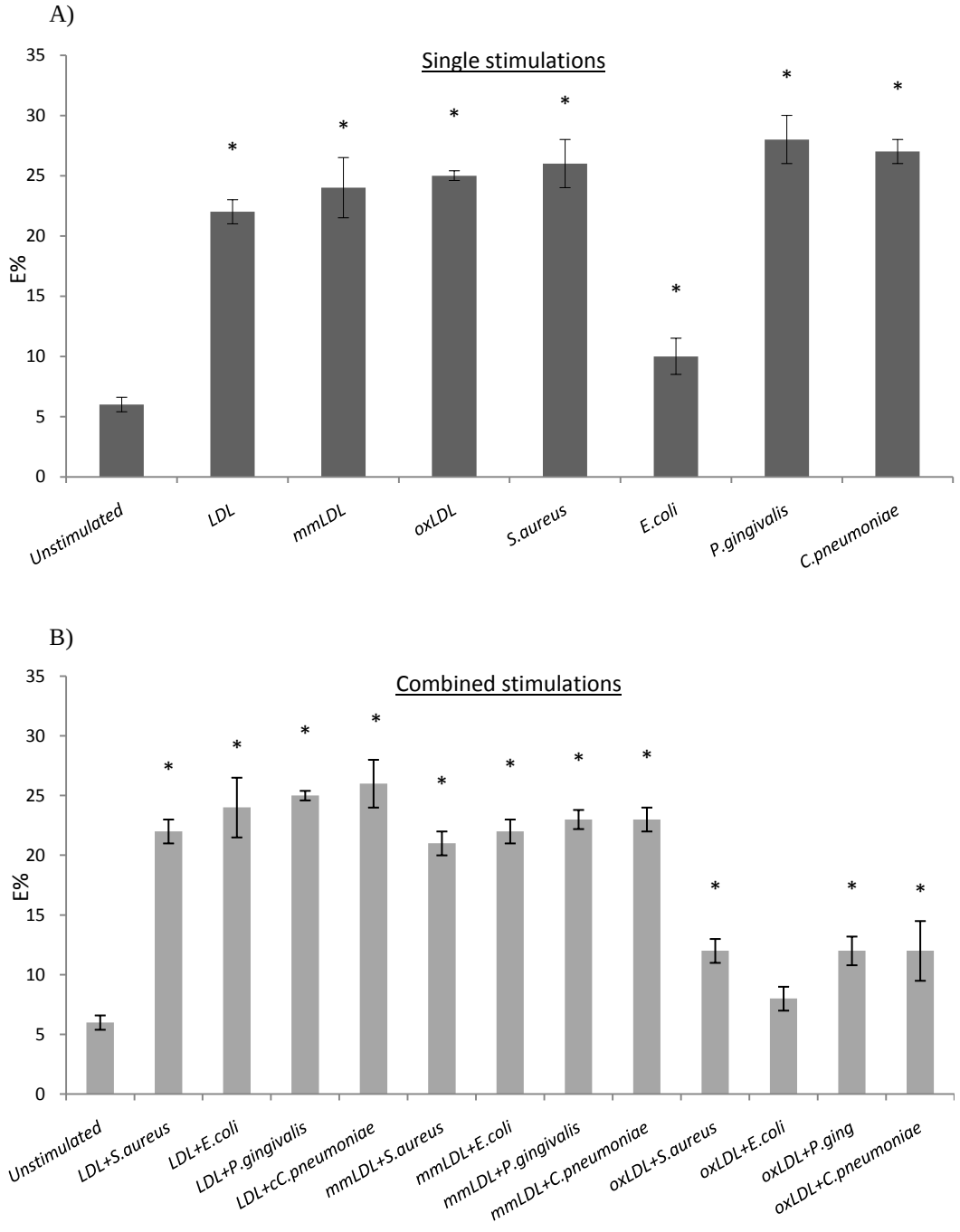

Figure 3.3.8: HUVEC TLR2 lipid raft recruitment in response to (A) single stimulation with lipoprotein (LDL, mmLDL, or oxLDL) and bacterial stimulations (*S.aureus* LTA, *E.coli* LPS, *P.gingivalis* LPS or *C.pneumoniae* LPS) or (B) combinations of bacterial products with either LDL, mmLDL, or oxLDL. Energy transfer between TLR2 (Cy3) and lipid raft (Cy5-cholera toxin) was measured from the increase in donor (Cy3) fluorescence after acceptor (Cy5) photobleaching. Data represents mean, ± standard deviation, n=3. *Indicates statistically significant ($p<0.05$) increase in recruitment of TLR2 to lipid rafts in the stimulated protocols in comparison to unstimulated controls (Section 2.19).

It was shown that lipoproteins (LDL, mmLDL and oxLDL) as well as *S.aureus* LTA, *P.gingivalis* LPS and *C.pneumoniae* LPS could recruit TLR2 in lipid rafts (Figure 3.3.8A). Similarly, combinations of these bacterial products with either LDL or mmLDL induce the recruitment of TLR2 within lipid rafts (Figure 3.3.8B). In contrast, although *S.aureus, P.gingivalis* and *C.pneumoniae* on their own can engage and recruit TLR2 to lipid rafts, when either PAMP was combined with oxLDL their ability to do so was greatly impaired (Figure 3.3.8B).

3.3.5: Receptor associations with and within lipid rafts

It has been previously shown that human vascular endothelial cell activation by *H.pylori* and *P.gingivalis* LPS is mediated through TLR2, is lipid-raft dependent and requires the formation of heterotypic receptor complexes comprising of TLR2, TLR1, CD36 and CD11b/CD18. Therefore this study proceeded to investigate whether similar or different activation clusters on human vascular endothelial cells are formed following exposure to lipoproteins and combinations of lipoproteins with bacterial products. This study proceeded to measure FRET between TLR2 and different receptor molecules that have been implicated in TLR2-dependent activation (TLR1, TLR6 and CD36).

3.3.5.1: Lipoprotein/bacterial product-induced receptor clusters

FRET experiments between TLR2 and TLR1, TLR6 and CD36 when HUVECs were exposed to lipoprotein (human LDL or its oxidised derivatives, mmLDL and oxLDL), bacterial products (*S.aureus* LTA, *E.coli* LPS, *P.gingivalis* LPS or *C.pneumoniae* LPS) or combined stimulations involving 60 minute pre-incubation with an endogenous lipoprotein (LDL, mmLDL or oxLDL) and then further 60 minute stimulation with the bacterial ligand (*S.aureus* LTA, *E.coli* LPS, *P.gingivalis* LPS and *C.pneumoniae* LPS) (Section 2.5). TLR2 molecules were labelled with Cy3-TL2.1 whilst TLR1, TLR6 and

CD36 were labelled with Cy5. FRET was measured in terms of dequenching of donor fluorescence after complete photobleaching of the acceptor fluorophore (Section 2.9.4). Energy transfer between TLR2-Cy3 and the various Cy5-labelled molecules was measured using a Zeiss LSM 510 META confocal microscope with a 1.4 NA 63x Zeiss objective, used in conjunction with Zeiss LSM 2.5 analysis software (Section 2.9).

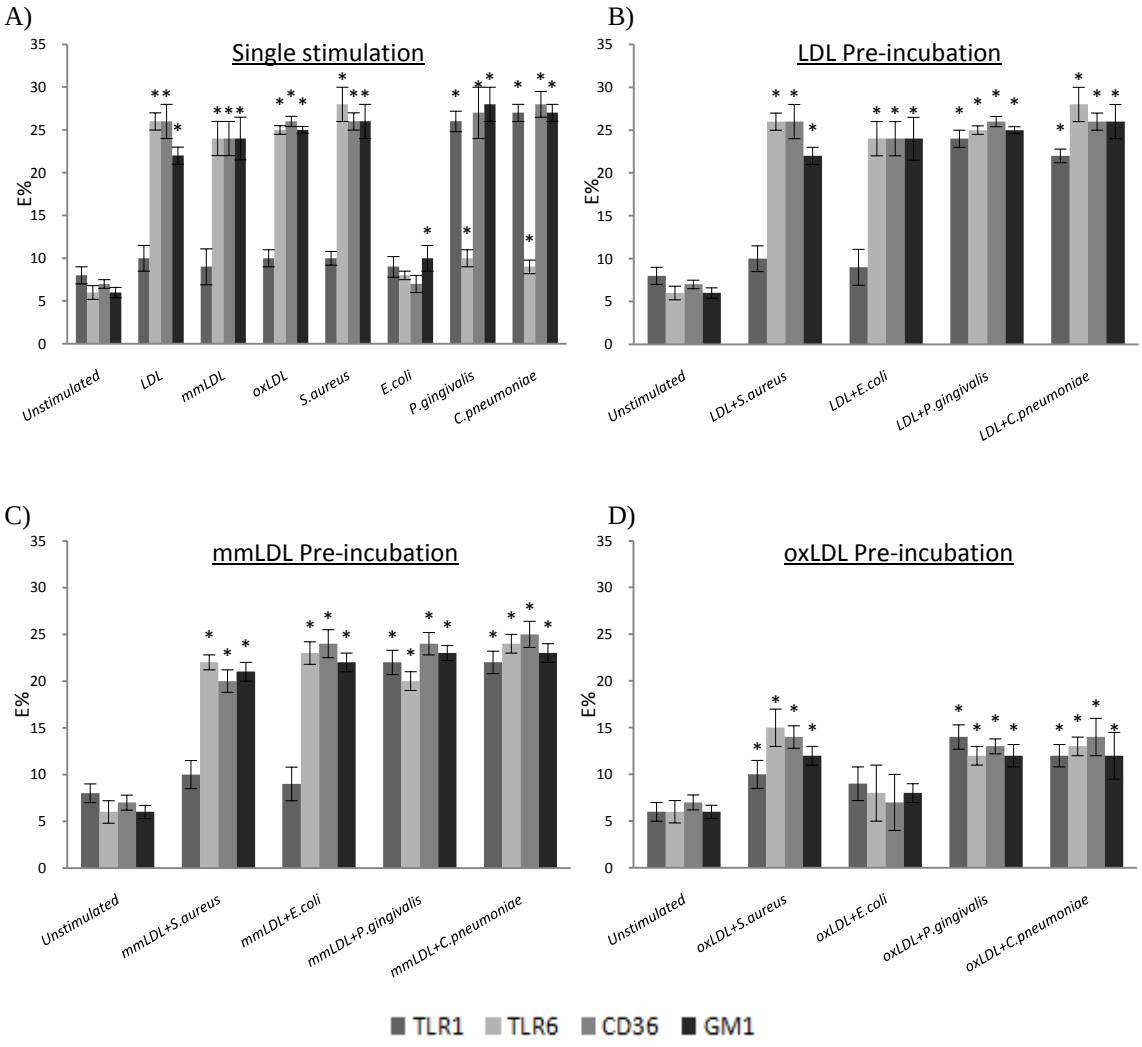

Figure 3.3.9: HUVEC TLR2 heterotypic associations in response to lipoproteins, bacterial products or combinations of both. Human vascular endothelial cells were stimulated with lipoprotein (LDL, mmLDL, or oxLDL) (A), bacterial PAMP (*S.aureus* LTA, *E.coli* LPS, *P.gingivalis* LPS or *C.pneumoniae* LPS) (A) or combinations of bacterial products with either LDL (B), mmLDL (C), or oxLDL (D). Energy transfer between TLR2 (Cy3) and the different receptors (Cy5) was measured from the increase in donor (Cy3) fluorescence after acceptor (Cy5) photobleaching. Data represents mean, ± standard deviation, n=3. *Indicates statistically significant ($p<0.05$) increase in association of TLR2 with the corresponding receptor in the stimulated protocols in comparison to unstimulated controls (Section 2.19).

TLR2 was found not to associate with TLR1, TLR6 or CD36 prior to stimulation (Figure 3.3.9A). It was shown that TLR2 associates with TLR6 and CD36 after lipoprotein (LDL, mmLDL or oxLDL), as well as *S.aureus* LTA stimulation (Figure 3.3.9A). Interestingly, *P.gingivalis* LPS and *C.pneumoniae* LPS triggered the formation of TLR1, TLR2 and CD36 receptor clusters, demonstrating that they induce the formation of slightly different activation cluster from *S.aureus* LTA (Figure 3.3.9A). *E.coli* LPS stimulation alone caused no association of receptors with TLR2 (Figure 3.3.9A). Combinations of lipoproteins with *P.gingivalis* LPS or *C.pneumoniae* LPS induce the association of TLR2 with TLR1, TLR6 and CD36 (Figure 3.3.9B/C/D), suggesting that *P.gingivalis* and *C.pneumoniae* LPS engage TLR2/TLR1 heterodimers whereas lipoproteins induce TLR2/TLR6/CD36 associations forming a larger cumulative cluster consisting of all receptors. TLR1 was not associated with any double stimulations with *E.coli* LPS Figure (3.3.9B/C/D) nor was it associated with LDL and mmLDL pre-incubation with *S.aureus* LTA (Figure 3.3.9B/C). Interestingly, oxLDL pre-incubation reduced TLR2 associations with TLR1, TLR2, CD36 and lipid raft in all PAMP stimulations (Figure 3.3.9D) in comparison to PAMP alone (Figure 3.3.9A). *S.aureus*, *P.gingivalis* and *C.pneumoniae* induced receptor associations with TLR2 were reduced by around 40-50% when HUVECs were pre-incubated with oxLDL (Figure 3.3.9D).

3.3.6: Conclusions

- TLRs are involved in the recognition of endogenous lipoproteins and bacterial products that are associated with atherosclerosis.
- Lipid raft disruption prevents appropriate trafficking of receptors modulating cellular response to ligands. Lipid rafts are important for receptor internalization and targeting to compartments such as endosomes and organelles such as the Golgi.
- Lipid rafts are involved in the recognition of atherosclerosis-associated ligands.
- Double stimulation of lipoprotein with bacterial PAMP reduces the requirement for lipid rafts.
- Single stimulations with lipoproteins (LDL, mmLDL or oxLDL) as well as *S. aureus* LTA, *P.gingivalis* LPS and *C.pneumoniae* LPS recruit TLR2 in lipid rafts.
- Combined stimulus of PAMP with either LDL or mmLDL induces the recruitment of TLR2 within lipid rafts.
- oxLDL pre-incubation reduces recruitment of TLR2 to lipid rafts.
- *S.aureus* LTA and lipoprotein (LDL, mmLDL or oxLDL) stimulation cause the association of TLR2, TLR6 and CD36 in lipid rafts.
- *P.gingivalis* and *C.pneumoniae* LPS induce the formation of a slightly different activation cluster in lipid rafts including TLR2, TLR1 and CD36.
- Combinations of lipoproteins with *P.gingivalis* LPS or *C.pneumoniae* LPS induce the association of TLR2, TLR1, TLR6 and CD36. This suggests the possibility that different receptor clusters are bought together to form a larger cluster, resulting in altered signalling, relevant for the present ligands.

3.4: Elucidation of receptor significance

The upregulation of PRRs, as observed in plaque by Edfeldt *et al*. (2002)[8], has been mimicked in this study using ligands thought to be involved in atherogenesis. Cytokine release has been observed to coincide with this upregulation, but individual TLR involvement has not been deciphered. Previous studies have strongly associated TLR2, TLR4 and CD36 with atherosclerosis. These findings combined with data from this study directed the next step in this research to elucidate the individual role of these receptors in atherogenesis.

3.4.1: Transfected HEK293 response

Although the role of TLR2 and TLR4 in the recognition of lone PAMPs is recognized, their role in combinatorial stimulations with atherosclerosis-associated ligands, more importantly lipoproteins and bacterial products, is not. To elucidate the individual role of TLR2 and TLR4 in the initiation of atherosclerosis, transformed HEK293 cells expressing either TLR2 (HEK TLR2) or TLR4 (HEK TLR4) were utilised. HEK293 wild-type (HEK w-t) cells do not express cell surface receptors, thus the transformation of these allows tailored protein expression.

3.4.1.1: HEK inflammatory response to atherosclerosis-associated ligands

In order to investigate which TLRs might play a role in lipoprotein and lipoprotein/bacterial product activation of human vascular endothelial cells, transfected cell lines were used. HEK cells transfected with either TLR2, or TLR4/MD2 were utilised. Either HEK TLR2 or HEK TLR4 cells were subject to 60 minute stimulation with human LDL, mmLDL, oxLDL, *S.aureus* LTA, *E.coli* LPS, *P.gingivalis* LPS or *C.pneumoniae* LPS (Section 2.5). All stimulations were carried out in 24 well plates in

SFM (GIBCO) (Section 2.5.2). The SFM was collected post stimulation for cytokine analysis using the Human Inflammation BD™ cytometric bead array system (Section 2.8.2.2). Out of the inflammatory cytokines analysed (IL-1β, IL-6, IL-8, IL-10, IL-12p70 and TNF, only the release IL-8 was significantly increased.

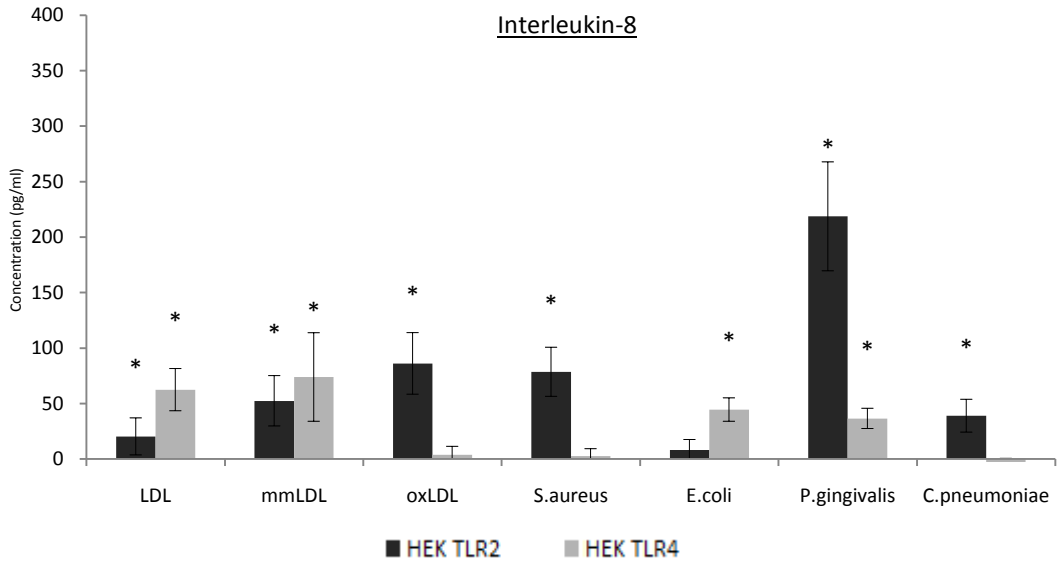

Figure 3.4.1: Interleukin-8 release from HEK TLR2 (dark grey) and HEK TLR4 (light grey) in response to LDL, mmLDL, oxLDL, *S.aureus* LTA, *E.coli* LPS, *P.gingivalis* LPS and *C.pneumoniae* LPS. IL-8 was measured in the cell supernatant using a flow cytometric cytokine bead array system (Becton Dickinson). Negatives (HEK wild-type) subtracted. Data represents mean, ± standard deviation, n=3. *Indicates statistically significant ($p<0.05$) increase in interleukin-8 release in comparison to HEK wild-type (Section 2.19).

HEK TLR2 and HEK TLR4 cell lines were both capable of generating a response to LDL and mmLDL, but only HEK TLR2 cells were able to generate a significant response to oxLDL (Figure 3.4.1). HEK TLR4 gave a stronger response to LDL and mmLDL than HEK TLR2, the opposite to what was observed with oxLDL. *S.aureus* LTA, a TLR2 agonist, was detected by HEK TLR2 but not HEK TLR4, results as expected. *E.coli* LPS, a TLR4 agonist, induced cytokine release from the HEK TLR4 cell line (Figure 3.4.1). A negligible response was seen in the HEK TLR2 cell line to

E.coli LPS (Figure 3.4.1). The results obtained for the unconventional LPS bacterial ligands of *P.gingivalis* and *C.pneumoniae* confirmed their recognition primarily through TLR2 and not the endotoxin receptor TLR4. *P.gingivalis* LPS was capable of inducing a response in both HEK TLR2 and, to a lesser extent, HEK TLR4 cells (Figure 3.4.1). *C.pneumoniae* LPS only induced a response in the HEK TLR2 cell line verifying unconventional signalling (Figure 3.4.1).

3.4.1.2:HEK inflammatory response to bacterial ligand with lipoprotein pre-incubation

In order to determine whether TLR2 or TLR4 is involved in the inflammatory response to combinations of endogenous lipoproteins and bacterial ligands, I proceeded to stimulate HEK cells transfected with the corresponding receptor with the various ligands. Either HEK TLR2 or HEK TLR4 cells were subject to 60 minute pre-incubation with an endogenous lipoprotein (human LDL or its oxidised derivatives mmLDL and oxLDL) and then further 60 minute stimulation with the bacterial ligand (*S.aureus* LTA, *E.coli* LPS, *P.gingivalis* LPS or *C.pneumoniae* LPS) (Section 2.5). All stimulations were carried out in 24 well plates in SFM (GIBCO) (Section 2.5.2). The SFM was collected post stimulation for cytokine analysis using the Human Inflammation BD™ cytometric bead array system (Section 2.8.2.2). Again only interleukin-8 concentrations were significantly increased.

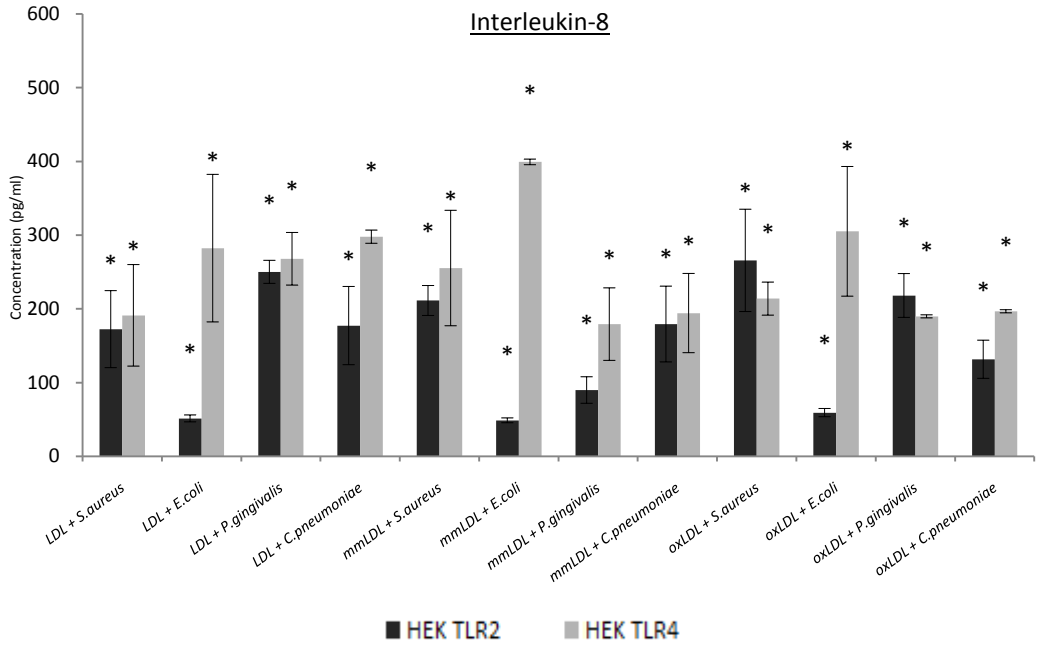

Figure 3.4.2: Interleukin-8 release from HEK TLR2 (dark grey) and HEK TLR4 (light grey) after 60 minute stimulation with the atherosclerosis-associated bacterial ligands *S.aureus* LTA, *E.coli* LPS, *P.gingivalis* LPS or *C.pneumoniae* LPS with pre-incubation (60 minutes) with human LDL or either of its oxidised derivatives, mmLDL and oxLDL. IL-8 was measured in the cell supernatant using a flow cytometric cytokine bead array system (Becton Dickinson). Negatives (HEK wild-type) subtracted. Data represents mean, ± standard deviation, n=3. *Indicates statistically significant ($p<0.05$) increase in interleukin-8 release in comparison to HEK wild-type (Section 2.19).

Both HEK TLR2 and HEK TLR4 were capable of increased cytokine release in response to all combined stimulations (Figure 3.4.2). Interestingly, although oxLDL and *C.pneumoniae* LPS single stimulations were very poor at causing IL-8 release from the HEK TLR4 cell line, when these were simultaneously exposed to HEK TLR4 cells a significant IL-8 response was observed (Figure 3.4.3). This would suggest that pre-exposure to lipoproteins enhances sensitivity to bacterial ligands, or that bacterial ligand exposure increases sensitivity to lipoproteins, through TLR4. This effect is apparent for all stimulations with HEK TLR4 cells, where pre-incubation with LDL, mmLDL and oxLDL enhanced the cytokine response to atherosclerotic bacterial ligands (Figure 3.4.4). Similar results were obtained for HEK TLR2 but to a much lesser extent. Pre-incubation of HEK TLR2 cells with LDL and oxLDL and then subsequent *P.gingivalis* LPS exposure had little or no effect on IL-8 release (Figure 3.4.3). Pre-incubation with mmLDL reduced the HEK TLR2 response to *P.gingivalis* LPS (Figure 3.4.3).

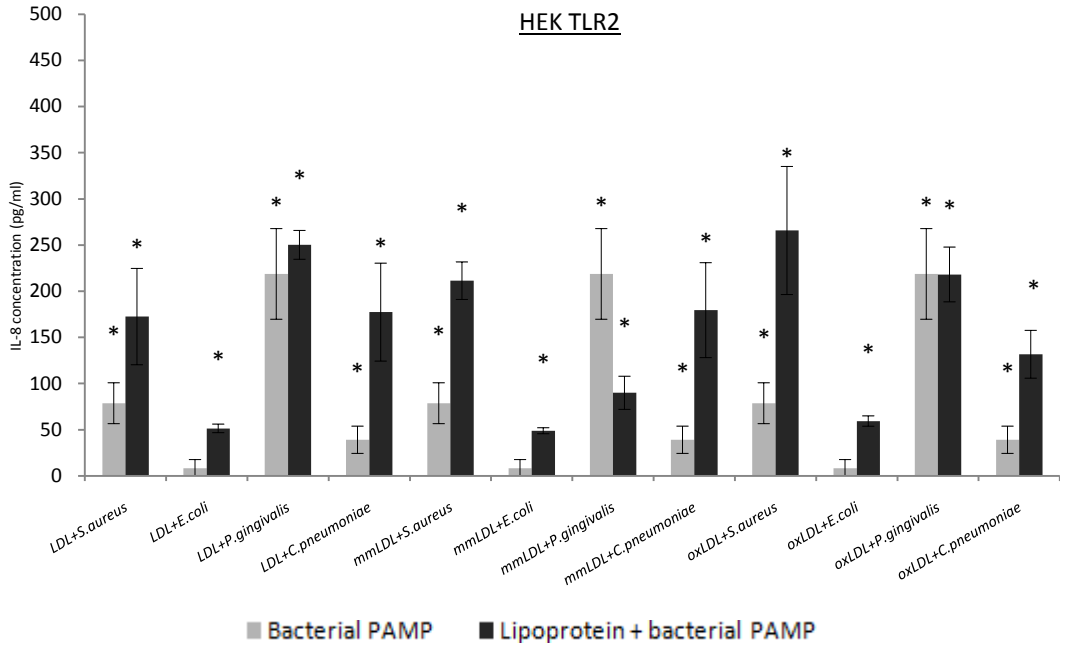

Figure 3.4.3: IL-8 release from HEK TLR2 cells after 60 minute incubation with bacterial PAMP (*S.aureus* LTA, *E.coli* LPS, *P.gingivalis* LPS or *C.pneumoniae* LPS) alone (light grey) and 60 minute incubation with bacterial PAMP (*S.aureus* LTA, *E.coli* LPS, *P.gingivalis* LPS or *C.pneumoniae* LPS) with 60 minute pre-incubation with either human LDL, mmLDL or oxLDL (dark grey). IL-8 was measured in the cell supernatant using a flow cytometric cytokine bead array system (Becton Dickinson). Negatives (HEK wild-type) subtracted. Data represents mean, ± standard deviation, n=3. *Indicates statistically significant ($p<0.05$) increase in IL-8 release in comparison to HEK w-t (Section 2.19).

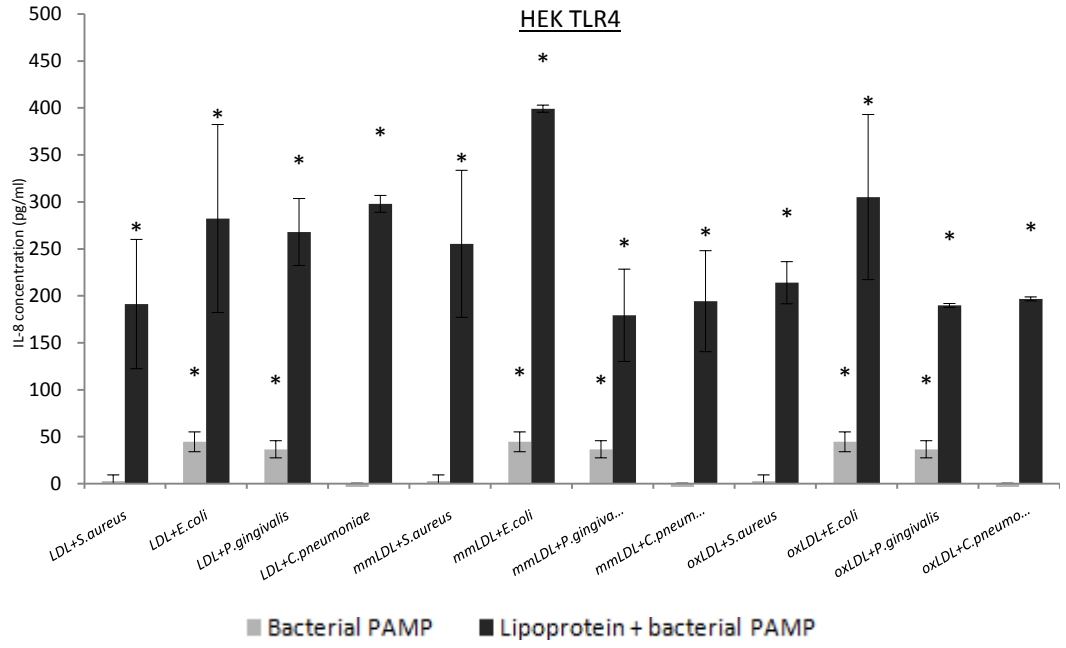

Figure 3.4.4: IL-8 release from HEK TLR4 cells after 60 minute incubation with bacterial PAMP (*S.aureus* LTA, *E.coli* LPS, *P.gingivalis* LPS or *C.pneumoniae* LPS) alone (light grey) and 60 minute incubation with bacterial PAMP (*S.aureus* LTA, *E.coli* LPS, *P.gingivalis* LPS or *C.pneumoniae* LPS) with 60 minute pre-incubation with either human LDL, mmLDL or oxLDL) (dark grey). IL-8 was measured in the cell supernatant using a flow cytometric cytokine bead array system (Becton Dickinson). Negatives (HEK wild-type) subtracted. Data represents mean, ± standard deviation, n=3. *Indicates statistically significant ($p<0.05$) increase in IL-8 release in comparison to HEK w-t (Section 2.19).

3.4.2: CD36 silencing on HUVECs

The accumulation of lipid laden macrophages (foam cells) is a major characteristic of plaque formation. CD36 SR is expressed on macrophages where it binds modified lipids[173] and is involved in their internalization causing dysregulation of cellular function resulting in foam cell formation[102]. Previous data in this study has shown upregulation of CD36 on endothelial cells in response to LDL, mmLDL, oxLDL and bacterial products associated with atherosclerosis resulting in cytokine release (Section 3.1). It was of interest in this study to elucidate the contribution of CD36 SR in the immune response to these ligands.

CD36 expression on primary HUVECs was silenced by transfection with CD36 psiRNA. Reduction in expression was confirmed by direct immunofluorescence and flow cytometry (data not shown). I investigated the role of endogenous lipoproteins, bacterial products and combinations of these to analyze their capability of activating an innate immune response in CD36 silenced primary HUVECs.

3.4.2.1: CD36 purification

CD36 psiRNA was transformed into a competent *E.coli* strain (*E.coli* GT116), which was expanded and lysed (Section 2.13.2.1). The plasmids were then purified from the lysate, concentrated and sterilised (Section 2.13.2.2). To check purity of the plasmid preparations 10µl of the sample was run on a 1% w/v agarose gel at 100V for 45 minutes (Section 2.13.3.1).

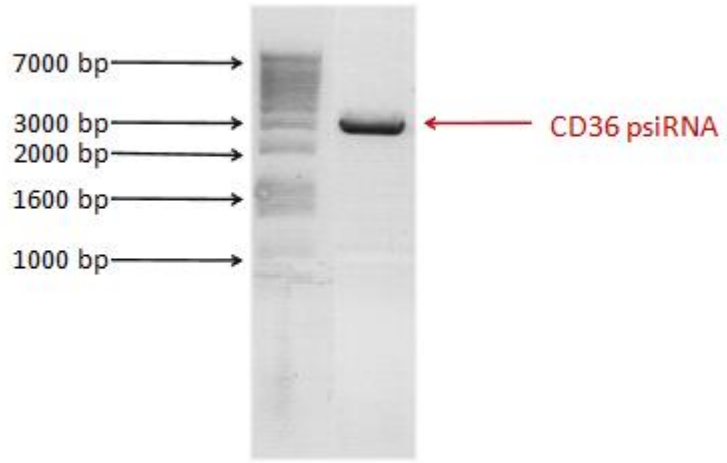

Image 3.4.1: Agarose gel of purified CD36 psiRNA. The plasmid is approximately 3000bp. The positions of the 1Kb DNA ladder fragments are indicated on the left. The plasmid sample was run on a 1% w/v agarose gel for 45 minutes at 100V. Bands were observed using a Stratagene eagle eye UV imaging system. (Colour inverted).

Agarose gel analysis of the purified plasmid samples revealed a single band representing CD36 plasmid illustrating a very high level of purity (Image 3.4.1).

3.4.2.2: CD36 silenced HUVEC response to atherosclerosis-associated ligands

Cellular expression of CD36 was reduced by transfecting HUVEC cells with CD36 shRNA (60% reduction in CD36 expression was achieved) (Section 2.13.4.3). Silenced cells were stimulated 24 hours post transfection. CD36 silenced HUVECs were subject to 60 minute stimulation with human LDL, oxLDL, *S.aureus* LTA, *E.coli* LPS or *P.gingivalis* LPS (Section 2.5). All stimulations were carried out in 24 well plates in SFM (GIBCO) (Section 2.5.2). The SFM was collected post stimulation for cytokine analysis using the Human Inflammation BD™ cytometric bead array system (Section 2.8.2.2). Out of the inflammatory cytokines analysed (IL-1β, IL-6, IL-8, IL-10, IL-12p70 and TNF), only the release of IL-6 and IL-8 were significantly increased.

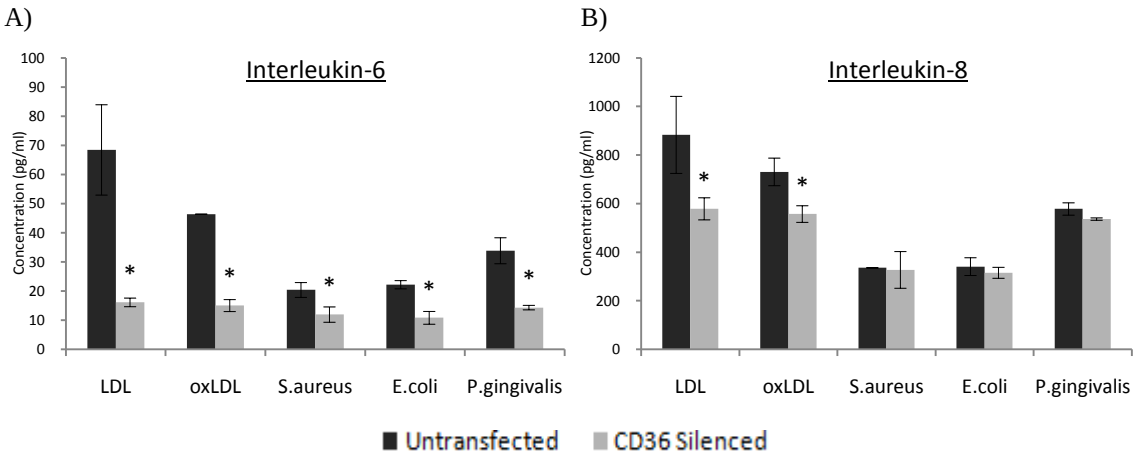

Figure 3.4.5: Interleukin-6 (A) and interleukin-8 (B) release from untransfected HUVECs (dark grey) and CD36 silenced HUVECs (light grey) in response to LDL, mmLDL, oxLDL, *S.aureus* LTA, *E.coli* LPS and *P.gingivalis* LPS. Interleukin-6 and interleukin-8 were measured in the cell supernatant using a flow cytometric cytokine bead array system (Becton Dickinson). Negatives subtracted. Data represents mean, ± standard deviation, n=3. *Indicates statistically significant ($p<0.05$) decrease in cytokine release from CD36 silenced cells in comparison to untransfected controls (Section 2.19).

The silencing of CD36 reduced the IL-6 release from HUVECs in response to endogenous and exogenous ligands (Figure 3.4.5A). LDL and oxLDL induced IL-6 release from CD36 silenced HUVECS was reduced by 76% and 68% respectively in comparison to that observed from wild-type cells (Figure 3.4.5A). This illustrates CD36 as a lipoprotein receptor favouring LDL over oxLDL. CD36 silenced HUVEC IL-6 release was also less responsive to PAMPs, the greatest reduction seen with *P.gingivalis* which was diminished by ~50% (Figure 3.4.5A).

As observed with previous data, IL-8 did not follow the same pattern of release as IL-6. CD36 silenced HUVECs had a reduced IL-8 release (Figure 3.4.5B) in response to LDL and oxLDL, but lesser a reduction as observed with IL-6 release (Figure 3.4.5A). The transfected cells had little or no difference in the IL-8 response observed with *S.aureus* LTA, *E.coli* LPS and *P.gingivalis* LPS stimulation in comparison to wild-type cells (Figure 3.4.5B).

3.4.2.3:CD36 silenced HUVEC response to bacterial ligand stimulation with lipoprotein pre-incubation

The absence of CD36 was shown to affect the inflammatory response to atherosclerosis-associated ligands. Thus I proceeded to investigate whether the presence of CD36 was also significant for the inflammatory response to combinations of endogenous lipoproteins and bacterial ligands. Cellular expression of CD36 was reduced by transfection of the HUVEC cell line with CD36 psiRNA (60% reduction in CD36 expression was achieved) (Section 2.13.4.3). Silenced cells were stimulated 24 hours post transfection. HUVECs were subject to 60 minute pre-incubation with an endogenous lipoprotein (human LDL or oxLDL) and then further 60 minute stimulation with the bacterial ligand (*S.aureus* LTA, *E.coli* LPS or *P.gingivalis* LPS) (Section 2.5). All stimulations were carried out in 24 well plates in SFM (GIBCO). The SFM was collected post stimulation for cytokine analysis using the Human Inflammation BD™ cytometric bead array system (Section 2.8.2.2). As found with the single stimulations of CD36 silenced HUVECs, only the release of IL-6 and IL-8 were significantly increased.

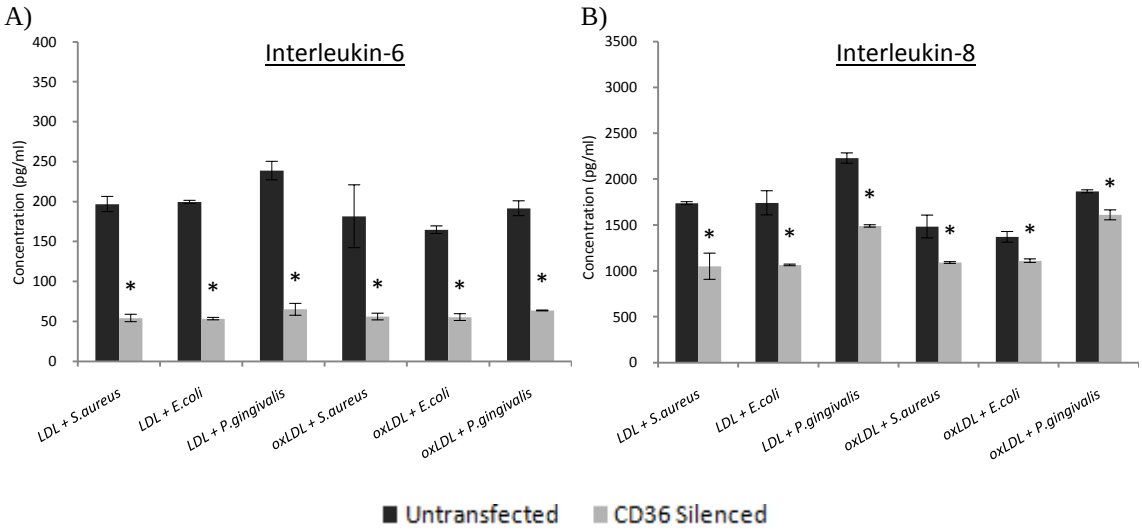

Figure 3.4.6: Interleukin-6 (A) and interleukin-8 (B) release from untransfected HUVECs (dark grey) and CD36 silenced HUVECs (light grey) after 60 minute stimulation with the atherosclerosis-associated bacterial ligands *S.aureus* LTA, *E.coli* LPS or *P.gingivalis* LPS with pre-incubation (60 minutes) with human LDL or oxLDL. IL-6 and IL-8 were measured in the cell supernatant using a flow cytometric cytokine bead array system (Becton Dickinson). Negatives subtracted. Data represents mean, ± standard deviation, n=3. *Indicates statistically significant ($p<0.05$) decrease in cytokine release from CD36 silenced cells in comparison to untransfected controls (Section 2.19).

Both the IL-6 and IL-8 response to all double stimulations were reduced in CD36 transfected HUVECs in comparison to wild-type HUVECs (Figure 3.4.6). The reduction in IL-6 (Figure 3.4.6A) release was greater than that observed with IL-8 (Figure 3.4.6B). These results show the significance of CD36 in the cellular response to these combined stimulations.

CD36 has been shown to form clusters with other receptors in lipid rafts. An association of TLR2/1 and CD36 has been observed in response to *P.gingivalis* LPS[51]. The ability of CD36 SR to form such clusters with TLRs presents the possibility of cross talk, or some kind of interference. When lipoproteins and bacterial products are exposed to cells at the same time they may compete/interact with the same receptor cluster in lipid rafts. This could give rise to the modulation of cellular response to bacterial products caused by lipoproteins that has been observed in this study.

3.4.3: Conclusions

- LDL and mmLDL can signal through TLR2 and TLR4. oxLDL is only recognised through TLR2.
- *S.aureus* LTA and *C.pneumoniae* LPS are recognised through TLR2. *P.gingivalis* LPS is recognised by TLR2 and to a lesser extent TLR4. *E.coli* LPS is only recognised by TLR4.
- The increased cytokine release in response to bacterial ligands (*S.aureus* LTA, *E.coli* LPS and *C.pneumoniae* LPS) that was observed when cells were pre-incubated with lipoprotein occurs through TLR2 and TLR4. This is most apparent through TLR4.
- Pre-incubation of HEK TLR2 cells with LDL and oxLDL and then subsequent *P.gingivalis* LPS exposure had little or no effect on IL-8 release. Pre-incubation with mmLDL reduced the HEK TLR2 response to *P.gingivalis* LPS.
- CD36 is involved in the recognition of lipoproteins, preferentially binding LDL over oxLDL.
- CD36 has no effect on IL-8 release from HUVECs in response to bacterial ligands but is involved in IL-6 release.
- CD36 is involved in IL-6 and IL-8 release when lipoprotein and bacterial product were combined, suggesting a greater involvement in bacterial recognition when lipoproteins are present.

3.5: PRR association and trafficking

The initial recognition of the enormous range of varied foreign ligands that can invade our bodies requires our innate immune system to react quickly and accordingly for their fast and efficient removal. The immune response to a specific ligand is tailored not only by recognition by a specific PRR, but also by the associations caused between these receptors allowing precise identification. In atherosclerosis this response has become dysregulated causing chronic inflammation leading to plaque formation and associated clinical outcomes. Increased PRR expression has been shown in the atherosclerotic plaque, and associations between these in response to various ligands is well established. This study is concerned with the effects that circulating LDL has on this tailored response to bacterial ligands. It is becoming apparent that the presence of LDL and its derivatives prior to bacterial infection may have the effect of altering cellular response to a ligand, through disruption of the appropriate PRR associations normally tailored for such a pathogen.

When cells were pre-incubated with lipoprotein prior to bacterial stimulation the cytokine release, PRR expression and pattern of receptor associations were altered. In this study FRET analysis has shown that oxLDL incubation prior to bacterial exposure reduced the recruitment of TLR2 to lipid rafts in comparison to bacterial stimulation alone. These data highlight the possible effect of circulating lipids. Work continued on these associations using confocal microscopy to image their cell surface interaction, internalization and intracellular trafficking. I also imaged the localisation of the intracellular TLR signalling adapter MyD88 to investigate whether the localisation of this molecule is altered in response to the presence of lipoprotein.

3.5.1: Pattern recognition receptor distribution in unstimulated HUVECs

Initially the intracellular distribution of the PRRs in question was investigated in unstimulated HUVEC cells. HUVECs were seeded on collagen treated 8 well glass slides (Section 2.9.1). Both direct and indirect immunofluorescence (Section 2.7) techniques were used to label primary HUVECs on the 8 well glass slides (Section 2.9.2). Slides were viewed using a Zeiss LSM 510 META confocal microscope with a 1.4 NA 63x Zeiss objective, used in conjunction with Zeiss LSM 2.5 analysis software (Section 2.9). Localisation was quantified using Costes' method in ImageJ version 1.43 with the JACoP plugin (Section 2.9.3).

Unstimulated

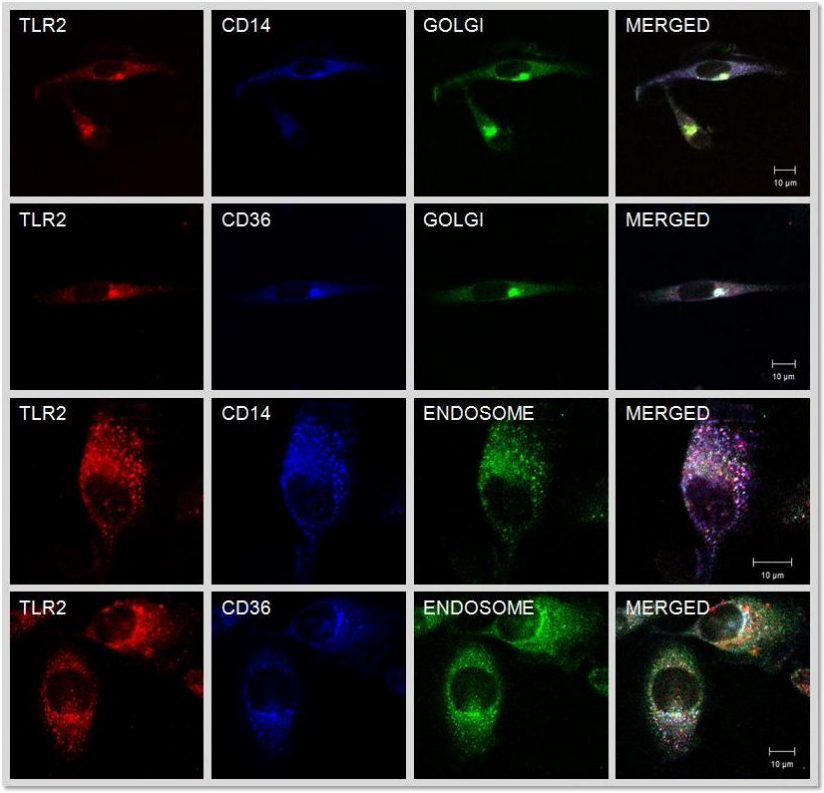

Figure 3.5.1: Cellular distribution of TLR2 (Red {Alexa555}), CD36 (Blue {Cy5}) and CD14 (Blue {Cy5}) in relation to Golgi (Green {FITC}) and endosomes (Green {FITC}) in unstimulated HUVECs. The cells were fixed and labelled via immunofluorescence. Images were acquired using a Zeiss LSM 510 META confocal microscope with a 1.4 NA 63x Zeiss objective, used in conjunction with Zeiss LSM 2.5 analysis software. The images are representative of a number of independent experiments. Localisation was quantified using Costes' method in ImageJ version 1.43 with the JACoP plugin. Scale bar, 10µm.

In unstimulated HUVECs (Figure 3.5.1) TLR2, CD14 and CD36 localise to the Golgi (r{obs} 0.844, 0.860 and 0.923 respectively) and endosomes (r{obs} 0.729, 0.771 and 0.799 respectively). TLR2, CD14 and CD36 have a preference for the Golgi with respective r{obs} values being 16.4% 11.5% and 15.5% greater than those obtained for association with endosomal compartments (Figure 3.5.1).

3.5.1.1: PRR association with lipid rafts in unstimulated cells

In order to determine PRR association with lipid rafts in unstimulated cells, HUVECs were seeded on collagen treated 8 well glass slides (Section 2.9.1). The cells were stimulated directly on the slide in 200µl SFM (Section 2.5.3). Both direct and indirect immunofluorescence (Section 2.7) techniques were used to label primary HUVECs on 8 well glass slides (Section 2.9.2). Slides were viewed using a Zeiss LSM 510 META confocal microscope with a 1.4 NA 63x Zeiss objective, used in conjunction with Zeiss LSM 2.5 analysis software (Section 2.9). Localisation was quantified using Costes' method in ImageJ version 1.43 with the JACoP plugin (Section 2.9.3).

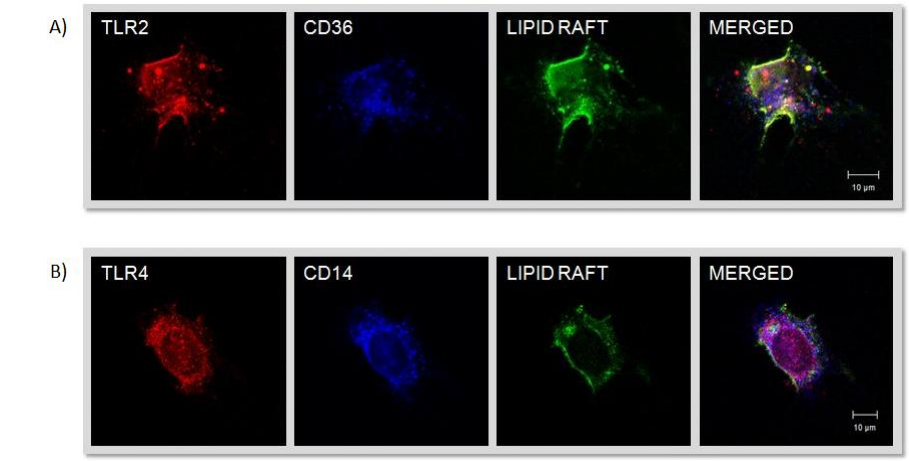

Figure 3.5.2: Cellular distribution of: A) TLR2 (Red {Alexa555}) and CD36 (Blue {Cy5}) in relation to lipid rafts (Green {Cholera-toxin-FITC}) and B) TLR4 (Red {Cy3}) and CD14 (Blue {Cy5}) in relation to lipid rafts (Green {Cholera-toxin-FITC}) in unstimulated HUVECs. The cells were fixed and labelled via immunofluorescence. Images were acquired using a Zeiss LSM 510 META confocal microscope with a 1.4 NA 63x Zeiss objective, used in conjunction with Zeiss LSM 2.5 analysis software. The images are representative of a number of independent experiments. Localisation was quantified using Costes' method in ImageJ version 1.43 with the JACoP plugin. Scale bar, 10µm.

In the unstimulated HUVECs (Figure 3.5.2), TLR2 had a weak association with lipid rafts whilst TLR4 did not (r{obs} 0.519 and 0.495 respectively). The SR CD36 was not associated with lipid rafts (r{obs} 0.494). It was found that CD14 localised weakly with the lipid raft in unstimulated HUVECs (r{obs} 0.547).

3.5.2: Intracellular HUVEC receptor targeting in response to *S.aureus* LTA and *S.aureus* LTA lipoprotein combined stimulations

It has previously been shown that TLR2 is targeted to the Golgi apparatus in response to *S.aureus* LTA[207,208]. This study was set out to investigate the intracellular targeting of PRRs involved in atherosclerosis in response to *S.aureus* LTA, as well as in response to combined stimulations with *S.aureus* LTA and low density lipoprotein.

HUVECs were seeded on collagen treated 8 well glass slides (Section 2.9.1). The cells were stimulated directly on the slide in 200µl SFM (Section 2.5.3). HUVECs were subject to *S.aureus* LTA, *S.aureus* LTA with LDL pre-incubation or *S.aureus* LTA with oxLDL pre-incubation (Section 2.5). Both direct and indirect immunofluorescence (Section 2.7) techniques were used to label primary HUVECs on 8 well glass slides (Section 2.9.2). Slides were viewed using a Zeiss LSM 510 META confocal microscope with a 1.4 NA 63x Zeiss objective, used in conjunction with Zeiss LSM 2.5 analysis software (Section 2.9). Localisation was quantified using Costes' method in ImageJ version 1.43 with the JACoP plugin (Section 2.9.3).

S.aureus LTA

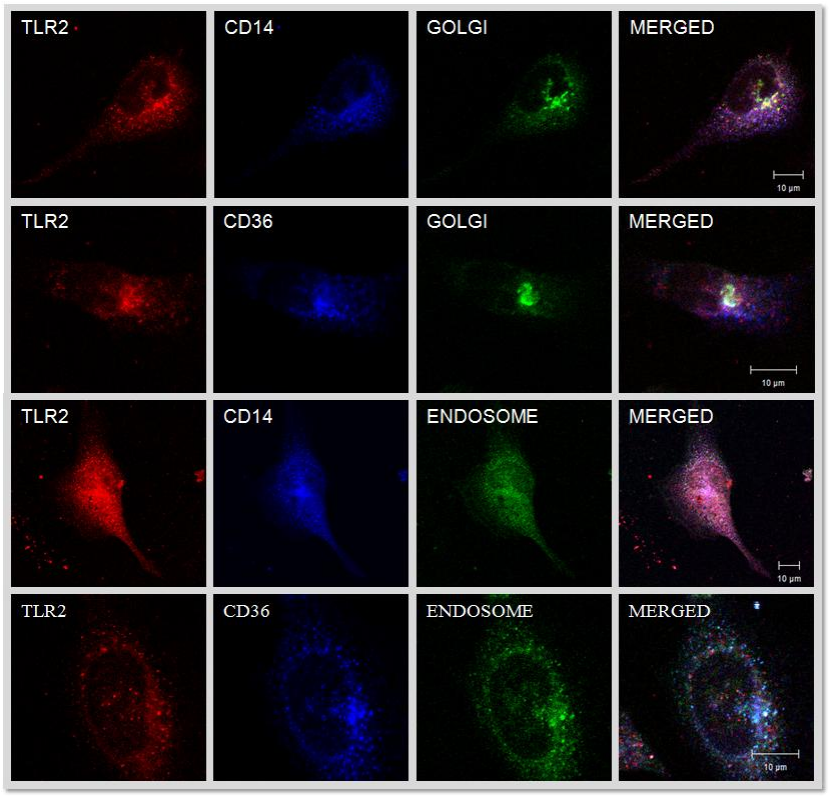

Figure 3.5.3: Cellular distribution of TLR2 (Red {Alexa555}), CD36 (Blue {Cy5}) and CD14 (Blue {Cy5}) in relation to Golgi (Green {FITC}) and endosomes (Green {FITC}) in HUVECs that have been stimulated with *S.aureus* LTA (60 minutes). The cells were subsequently fixed and labelled via immunofluorescence. Images were acquired using a Zeiss LSM 510 META confocal microscope with a 1.4 NA 63x Zeiss objective, used in conjunction with Zeiss LSM 2.5 analysis software. The images are representative of a number of independent experiments. Localisation was quantified using Costes' method in ImageJ version 1.43 with the JACoP plugin. Scale bar, 10µm.

Following stimulation of HUVECs with *S.aureus* LTA (Figure 3.5.3) the receptors TLR2, CD14 and CD36 were shown to reside in both the Golgi (r{obs} 0.667, 0.687 and 0.709 respectively) and endosomes (r{obs} 0.646, 0.820 and 0.721 respectively). CD14, in contrast to the unstimulated cell (Figure 3.5.1), was more strongly associated with the endosome in comparison to the Golgi (Figure 3.5.3). Both TLR2 and CD36 were now equally distributed between the Golgi and endosomes in comparison to unstimulated cells where a preference for the Golgi was observed (Figure 3.5.3).

LDL + *S.aureus* LTA

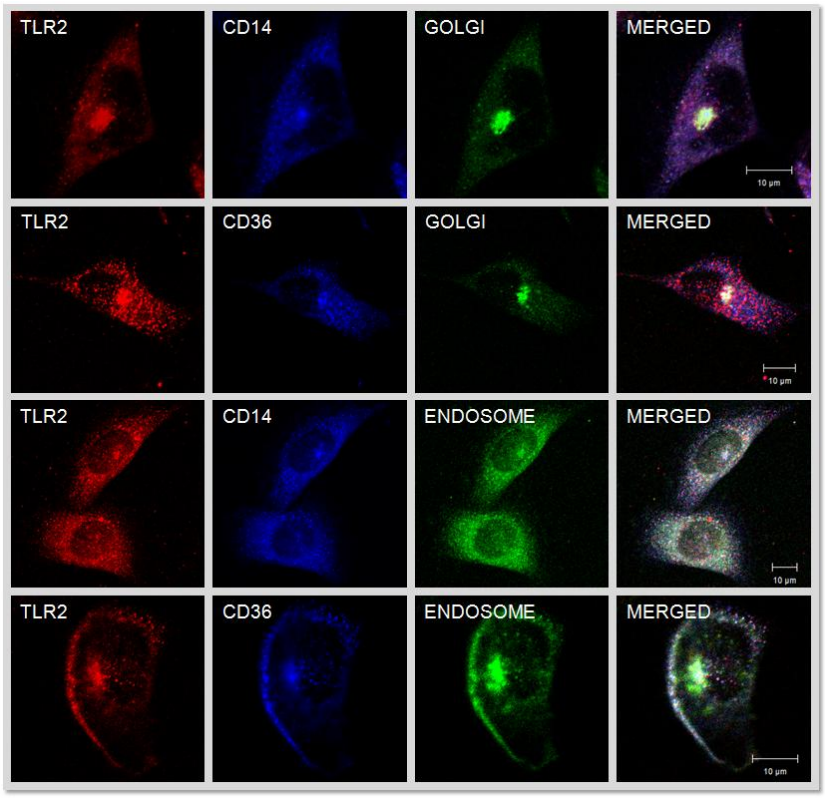

Figure 3.5.4: Cellular distribution of TLR2 (Red {Alexa555}), CD36 (Blue {Cy5}) and CD14 (Blue {Cy5}) in relation to Golgi (Green {FITC}) and endosomes (Green {FITC}) in HUVECs that have been pre-incubated with LDL (60 minutes) and then stimulated with *S.aureus* LTA (60 minutes). The cells were subsequently fixed and labelled via immunofluorescence. Images were acquired using a Zeiss LSM 510 META confocal microscope with a 1.4 NA 63x Zeiss objective, used in conjunction with Zeiss LSM 2.5 analysis software. The images are representative of a number of independent experiments. Localisation was quantified using Costes' method in ImageJ version 1.43 with the JACoP plugin. Scale bar, 10µm.

As with *S.aureus* LTA stimulation, when HUVECs were pre-incubated with LDL prior to *S.aureus* LTA exposure (Figure 3.5.4) the receptors TLR2, CD14 and CD36 were shown to reside in both the Golgi (r{obs} 0.689, 0.750 and 0.702 respectively) and endosomes (r{obs} 0.771, 0.856 and 0.848 respectively). PRRs were more strongly associated with endosomes than the Golgi. Stimulation with a combination of *S.aureus* and LDL promoted PRRs targeting to the endosomes.

oxLDL + *S.aureus* LTA

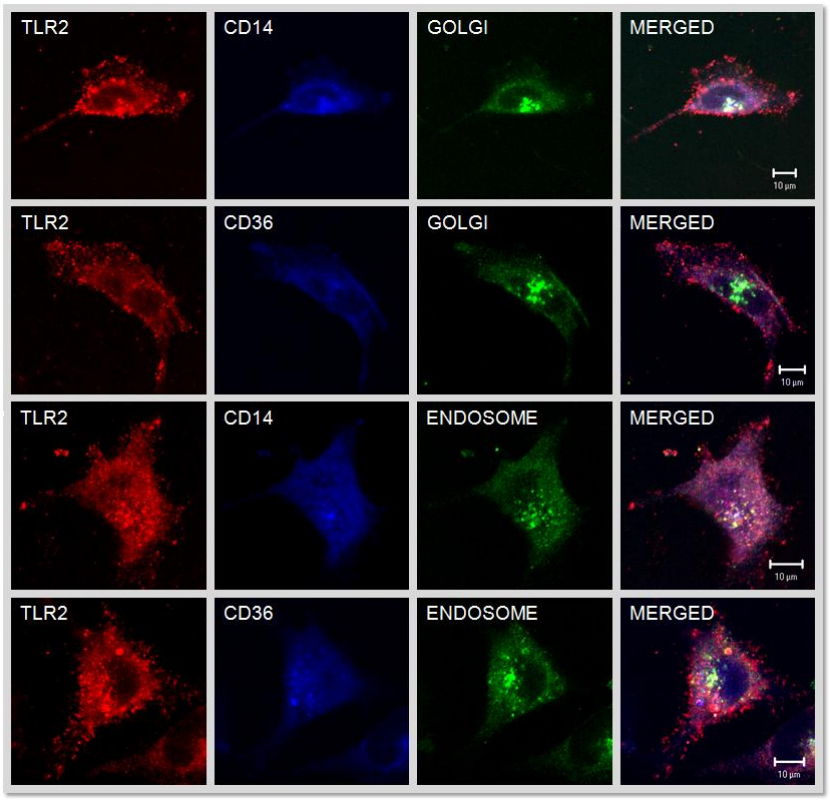

Figure 3.5.5: Cellular distribution of TLR2 (Red {Alexa555}), CD36 (Blue {Cy5}) and CD14 (Blue {Cy5}) in relation to Golgi (Green {FITC}) and endosomes (Green {FITC}) in HUVECs that have been pre-incubated with oxLDL (60 minutes) and then stimulated with *S.aureus* LTA (60 minutes). The cells were subsequently fixed and labelled via immunofluorescence. Images were acquired using a Zeiss LSM 510 META confocal microscope with a 1.4 NA 63x Zeiss objective, used in conjunction with Zeiss LSM 2.5 analysis software. The images are representative of a number of independent experiments. Localisation was quantified using Costes' method in ImageJ version 1.43 with the JACoP plugin. Scale bar, 10µm.

TLR2, CD14 and CD36 were shown to reside in both the Golgi (r{obs} 0.545, 0.718 and 0.653 respectively) and endosomes (r{obs} 0.608, 0.700 and 0.668 respectively) when HUVECs were pre-incubated with oxLDL prior to *S.aureus* LTA stimulation (Figure 3.5.5). Both TLR2 and CD36 were preferentially localised to the endosomes (Figure 3.5.5). Although TLR2 was observed in the Golgi and mainly in the endosomes, it is apparent from the confocal image that it is targeted to another distinct cellular compartment when cells are pre-incubated with oxLDL, possibly in lysosomes (Figure 3.5.5).

3.5.2.1:PRR lipid raft association in response to *S.aureus* LTA and *S.aureus* LTA lipoprotein combined stimulations

Lipid rafts have been shown to constitute platforms on the plasma membrane where signalling is concentrated. It has been shown that TLRs cluster within lipid rafts from where they signal. In this study I set out to investigate the involvement of lipid rafts in the internalization and targeting of PRRs involved in atherosclerosis.

HUVECs were seeded on collagen treated 8 well glass slides (Section 2.9.1). The cells were stimulated directly on the slide in 200µl SFM (GIBCO) (Section 2.5.3). HUVECs were subject to *S.aureus* LTA, *S.aureus* LTA with LDL pre-incubation or *S.aureus* LTA with oxLDL pre-incubation (Section 2.5). Both direct and indirect immunofluorescence (Section 2.7) techniques were used to label primary HUVECs on 8 well glass slides (Section 2.9.2). Slides were viewed using a Zeiss LSM 510 META confocal microscope with a 1.4 NA 63x Zeiss objective, used in conjunction with Zeiss LSM 2.5 analysis software (Section 2.9). Localisation was quantified using Costes' method in ImageJ version 1.43 with the JACoP plugin (Section 2.9.3).

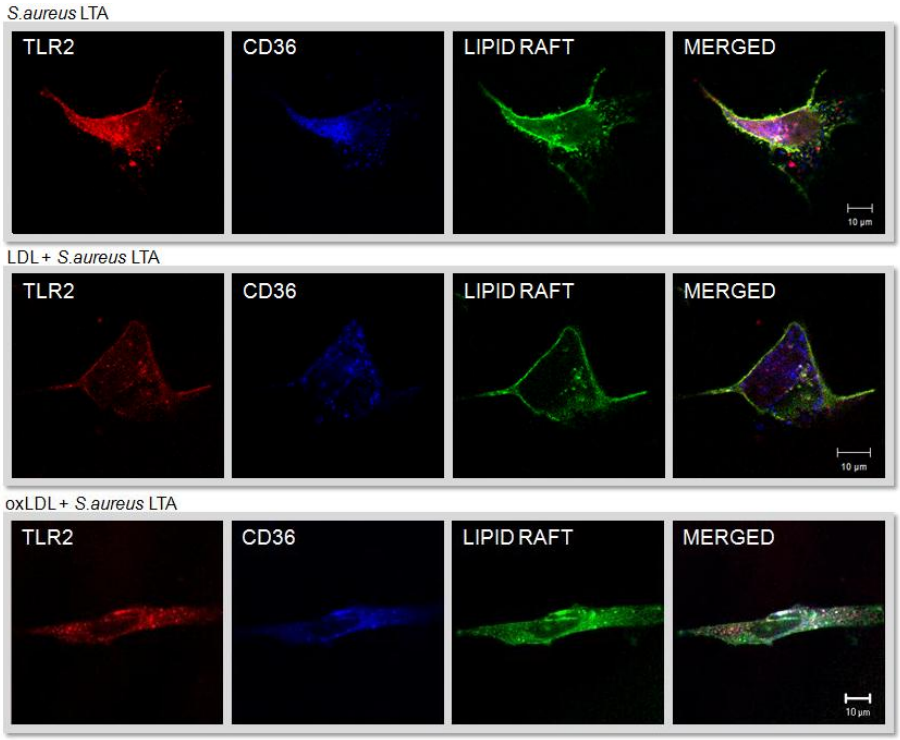

Figure 3.5.6: Cellular distribution of TLR2 (Red {Alexa555}) and CD36 (Blue {Cy5}) in relation to lipid rafts (Green {Cholera-toxin-FITC}) in HUVECs that have been stimulated with *S.aureus* LTA alone or *S.aureus* LTA with LDL or oxLDL pre-incubation. The cells were subsequently fixed and labelled via immunofluorescence. Images were acquired using a Zeiss LSM 510 META confocal microscope with a 1.4 NA 63x Zeiss objective, used in conjunction with Zeiss LSM 2.5 analysis software. The images are representative from a number of independent experiments. Localisation was quantified using Costes' method in ImageJ version 1.43 with the JACoP plugin. Scale bar, 10µm.

TLR2 is present in lipid rafts of HUVECs stimulated with *S.aureus* LTA (r{obs} 0.699. Figure 3.5.6, *S.aureus* LTA) and, to a lesser extent, *S.aureus* LTA with LDL pre-incubation (r{obs} 0.570. Figure 3.5.6, LDL + *S.aureus* LTA). This association is lost when HUVECs were pre-treated with oxLDL (r{obs} 0.430, Figure 3.5.6. oxLDL + *S.aureus* LTA). CD36 SRs weakly associate with lipid rafts with *S.aureus* LTA stimulation (r{obs} 0.523. Figure 3.5.6, *S.aureus* LTA), this is lost when cells were pre-incubated with LDL (r{obs} 0.453. Figure 3.5.6, LDL + *S.aureus* LTA). However, when cells were pre-treated with oxLDL prior to *S.aureus* LTA (Figure 3.5.6. oxLDL + *S.aureus* LTA) it was shown that CD36 was recruited to lipid rafts (r{obs} 0.601). This data suggests oxLDL pre-incubation may modulate the immune response, as observed with the cytokine data, by diminishing the ability of a cell to recognise a PAMP by

reducing cell surface expression of receptors, such as TLR2. While on the other hand, recruiting SRs such as CD36 to lipid rafts, in order to internalize the oxidized lipid.

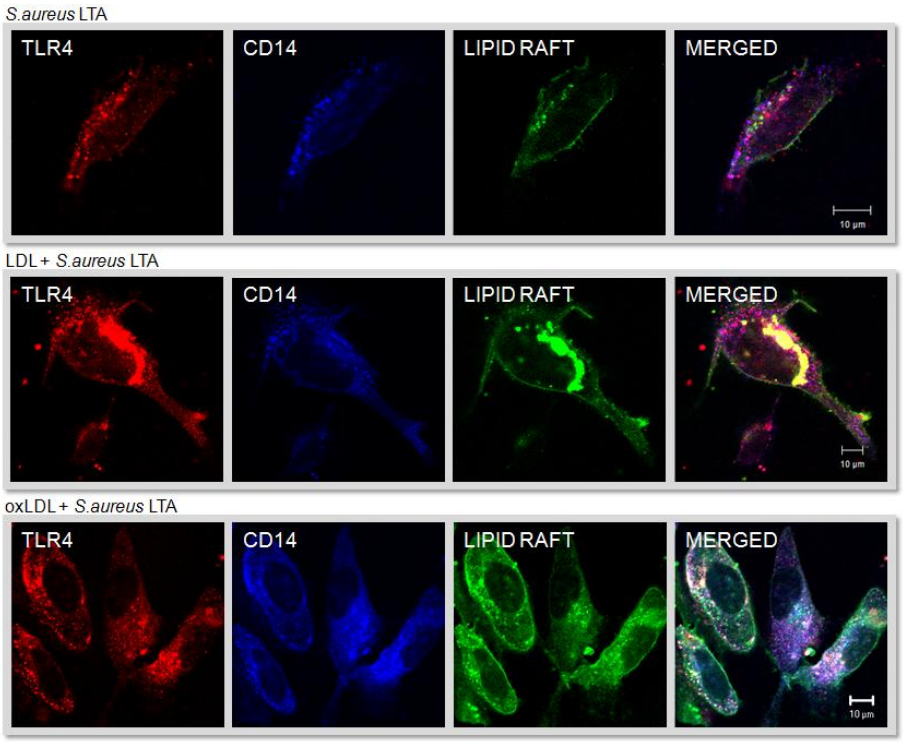

Figure 3.5.7: Cellular distribution of TLR4 (Red {Cy3}) and CD14 (Blue {Cy5}) in relation to lipid rafts (Green {Cholera-toxin-FITC}) in HUVECs that have been stimulated with *S.aureus* LTA alone or *S.aureus* LTA with LDL or oxLDL pre-incubation. The cells were subsequently fixed and labelled via immunofluorescence. Images were acquired using a Zeiss LSM 510 META confocal microscope with Zeiss LSM software. The images are representative of a number of independent experiments. Localisation was quantified with Costes' method in ImageJ (v1.43) with JACoP plugin. Scale bar, 10µm.

S.aureus LTA causes a weak association of TLR4 and CD14 with lipid rafts (r{obs} 0.517 and 0.516 respectively. Figure 3.5.7. *S.aureus* LTA). Pre-incubation with LDL causes strong recruited of TLR4 to lipid rafts (r{obs} 0.815. Figure 3.5.7. LDL + *S.aureus* LTA). *S.aureus* stimulation with oxLDL pre-incubation (Figure 3.5.7. oxLDL + *S.aureus* LTA) causes TLR4 and CD14 recruitment to lipid rafts (r{obs} 0.637 and 0.744 respectively).

The recruitment of MyD88 to lipid rafts in HUVECs in response to *S.aureus* LTA alone was reduced by 25% when cells were pre-incubated with oxLDL (data not shown).

A): *S.aureus* LTA

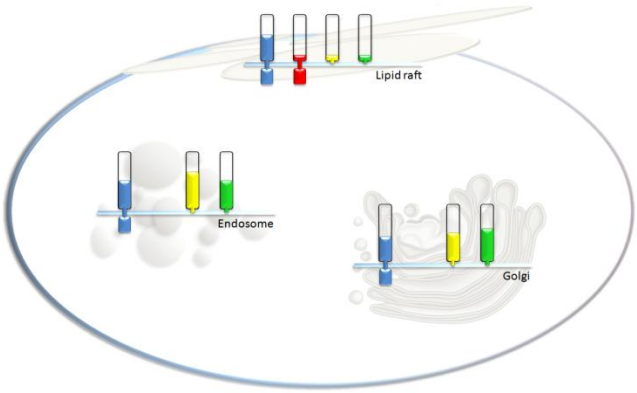

B): LDL + *S.aureus* LTA

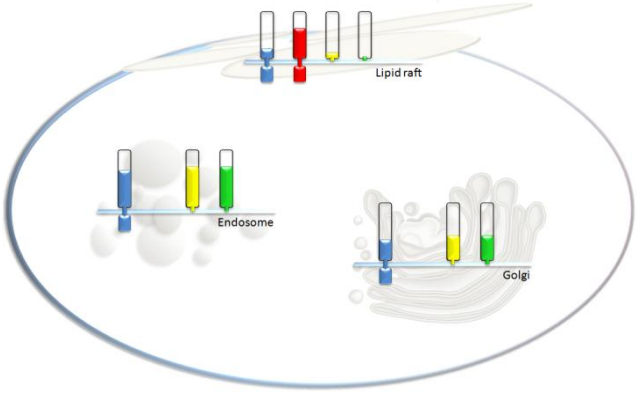

C): oxLDL + *S.aureus* LTA

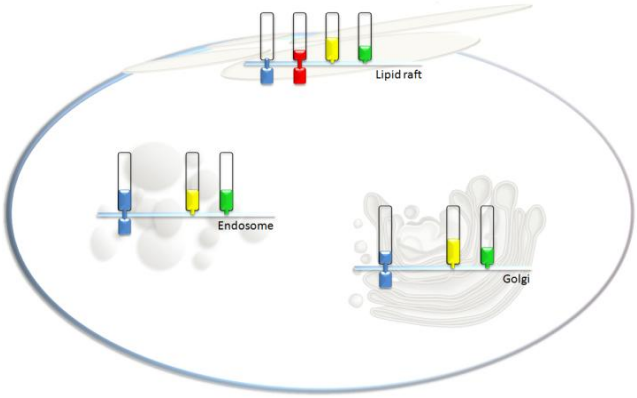

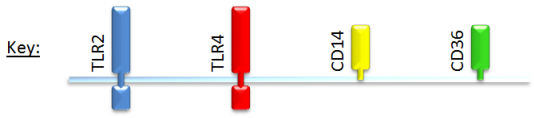

Figure 3.5.8: Schematic diagrams of the cellular distribution of TLR2 (Blue), CD14 (Green) and CD36 (Yellow) in relation to endosomes and the Golgi, and the cellular distribution of TLR2, TLR4 (Red), CD14 and CD36 in relation to lipid rafts in response to *S.aureus* LTA (A), *S.aureus* LTA with LDL pre-incubation (B) and *S.aureus* LTA with oxLDL pre-incubation (C). Note: The presence of TLR4 in endosomes and the Golgi was not imaged. Extracellular domain colour fill represents localisation determined by r{obs}.

3.5.3: Intracellular PRR receptor targeting in response to *E.coli* LPS and *E.coli* LPS lipoprotein combined stimulations

To investigate the intracellular PRR receptor targeting in response to *E.coli* LPS and *E.coli* LPS lipoprotein combined stimulations, HUVECs were seeded on collagen treated 8 well glass slides (Section 2.9.1). These were subject to *E.coli* LPS or *E.coli* LPS with either LDL or oxLDL pre-incubation (Section 2.5) directly on the slide in 200µl SFM (Section 2.5.3). Both direct and indirect immunofluorescence (Section 2.7) was used to label primary HUVECs on 8 well glass slides (Section 2.9.2). Slides were viewed using a Zeiss LSM 510 META confocal microscope with Zeiss LSM software (Section 2.9). Localisation quantified using Costes' method in ImageJ (Section 2.9.3).

E.coli LPS

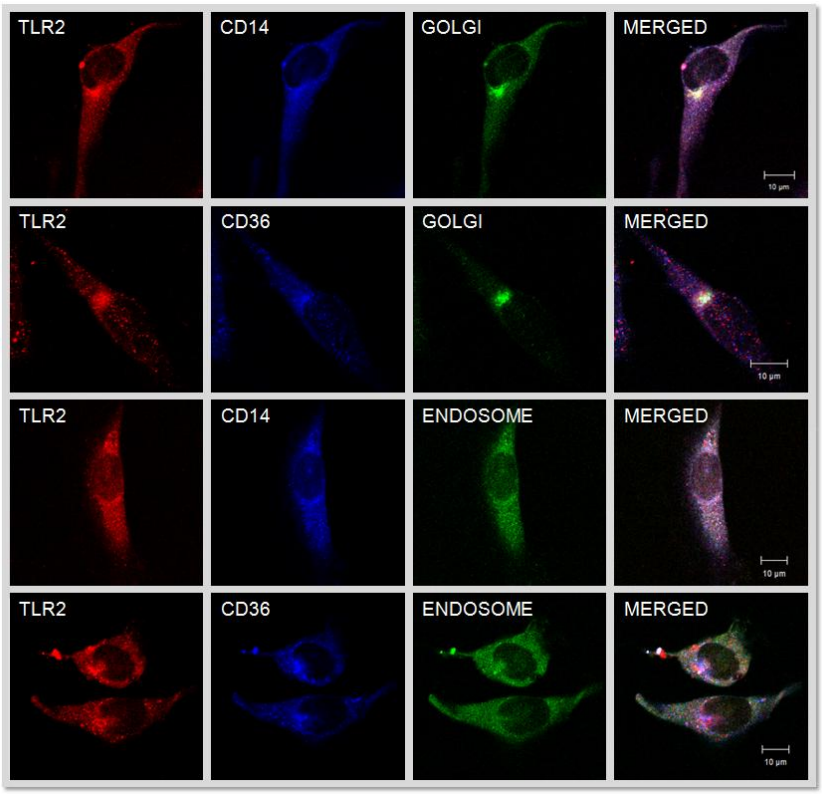

Figure 3.5.9: Cellular distribution of TLR2 (Red {Alexa555}), CD36 (Blue {Cy5}) and CD14 (Blue {Cy5}) in relation to Golgi (Green {FITC}) and endosomes (Green {FITC}) in HUVECs that have been stimulated with *E.coli* LPS (60 minutes). The cells were subsequently fixed and labelled via immunofluorescence. Images were acquired using a Zeiss LSM 510 META confocal microscope with a 1.4 NA 63x Zeiss objective, used in conjunction with Zeiss LSM 2.5 analysis software. The images are representative of a number of independent experiments. Localisation was quantified using Costes' method in ImageJ version 1.43 with the JACoP plugin. Scale bar, 10µm.

In HUVECs stimulated with *E.coli* LPS (Figure 3.5.9) the receptors TLR2, CD14 and CD36 were seen to localise with the Golgi (r{obs} 0.659, 0.842 and 0.677 respectively) and endosomes (r{obs} 0.814, 0.851 and 0.844 respectively). Both TLR2 and CD36 were more concentrated in the endosomes (Figure 3.5.9).

LDL + *E.coli* LPS

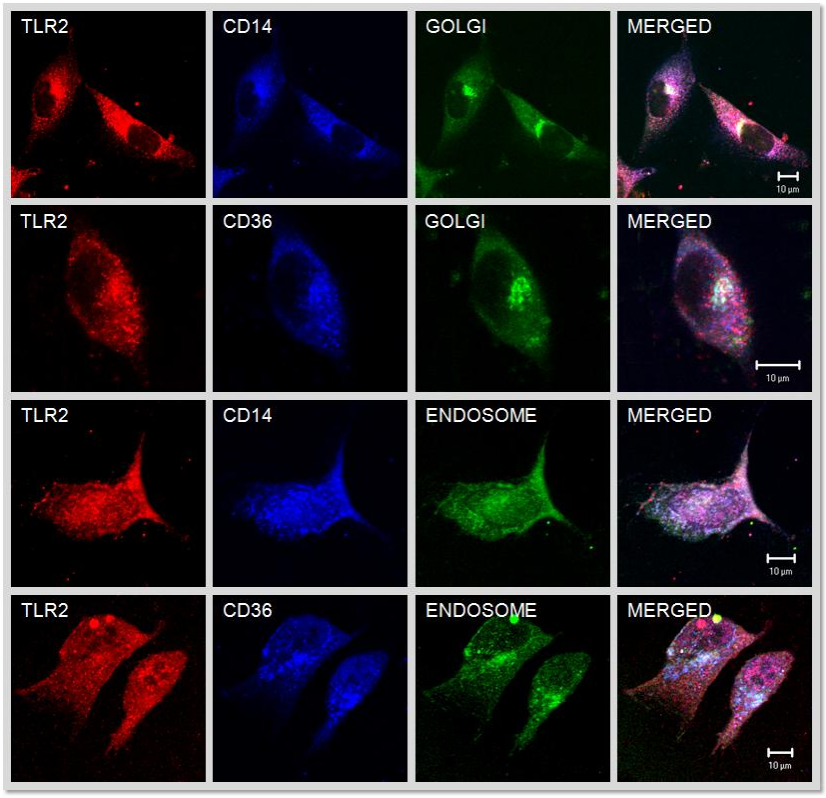

Figure 3.5.10: Cellular distribution of TLR2 (Red {Alexa555}), CD36 (Blue {Cy5}) and CD14 (Blue {Cy5}) in relation to Golgi (Green {FITC}) and endosomes (Green {FITC}) in HUVECs that have been pre-incubated with LDL (60 minutes) and then stimulated with *E.coli* LPS (60 minutes). The cells were subsequently fixed and labelled via immunofluorescence. Images were acquired using a Zeiss LSM 510 META confocal microscope with a 1.4 NA 63x Zeiss objective, used in conjunction with Zeiss LSM 2.5 analysis software. The images are representative of a number of independent experiments. Localisation was quantified using Costes' method in ImageJ version 1.43 with the JACoP plugin. Scale bar, 10µm.

LDL incubation prior to *E.coli* LPS stimulation reduces TLR2 and CD36 targeting to the endosomes in comparison to *E.coli* LPS stimulation alone (Figure 3.5.10). For TLR2 and CD36 localisation with endosomal compartments the r{obs} values obtained

for *E.coli* LPS stimulation drop by 17% and 23% respectively when cells are pre-incubated with LDL. TLR2 and CD36 localise in both the Golgi and endosome (Figure 3.5.10). CD14 is mainly located in the endosome (r{obs} 0.842) but is also found in the Golgi (r{obs} 0.782) (Figure 3.5.10).

oxLDL + *E.coli* LPS

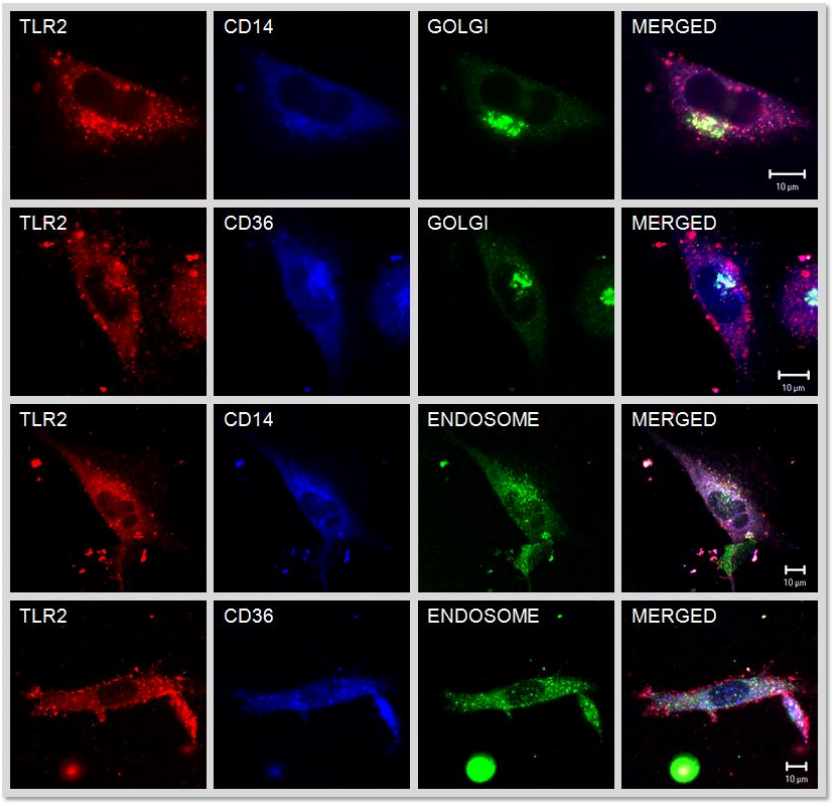

Figure 3.5.11: Cellular distribution of TLR2 (Red {Alexa555}), CD36 (Blue {Cy5}) and CD14 (Blue {Cy5}) in relation to Golgi (Green {FITC}) and endosomes (Green {FITC}) in HUVECs that have been pre-incubated with oxLDL (60 minutes) and then stimulated with *E.coli* LPS (60 minutes). The cells were subsequently fixed and labelled via immunofluorescence. Images were acquired using a Zeiss LSM 510 META confocal microscope with a 1.4 NA 63x Zeiss objective, used in conjunction with Zeiss LSM 2.5 analysis software. The images are representative of a number of independent experiments. Localisation was quantified using Costes' method in ImageJ version 1.43 with the JACoP plugin. Scale bar, 10µm.

When HUVECs were pre-treated with oxLDL prior to *E.coli* LPS (Figure 3.5.11), the localisation of TLR2 with the Golgi (r{obs} 0.573) and endosomes (r{obs} 0.547) was reduced in comparison to *E.coli* LPS and *E.coli* LPS with LDL pre-incubation stimulations. It is apparent that TLR2 is targeted to other distinct cellular compartments,

possibly to lysosomes (Figure 3.5.11). Both CD14 and CD36 were targeted to the Golgi (r{obs} 0.677 and 0.666 respectively) (Figure 3.5.11). However, although CD14 was targeted to the endosomes (r{obs} 0.701) it was found that oxLDL pre-incubation prevents CD36 targeting to the endosomes (r{obs} 0.396) (Figure 3.5.11). It is clear that oxLDL greatly disrupts trafficking and targeting of receptors in response to *E.coli* LPS.

3.5.3.1:PRR association with lipid rafts in response to *E.coli* LPS and *E.coli* LPS lipoprotein combined stimulations

The role of lipid rafts in cellular signalling and the internalization and targeting of PRRs is well documented. PRRs have been shown to concentrate in these cell membrane domains resulting in intracellular signalling. In this study I set out to investigate whether lipid rafts play a role in the internalization and targeting of PRRs involved in atherosclerosis in response to *E.coli* LPS, and whether lipoprotein pre-incubation has an effect on this.

HUVECs were seeded on collagen treated 8 well glass slides (Section 2.9.1). The cells were stimulated directly on the slide in 200µl SFM (GIBCO) (Section 2.5.3). HUVECs were subject to *E.coli* LPS, *E.coli* LPS with LDL pre-incubation or *E.coli* LPS with oxLDL pre-incubation (Section 2.5). Both direct and indirect immunofluorescence (Section 2.7) techniques were used to label primary HUVECs on 8 well glass slides (Section 2.9.2). Slides were viewed using a Zeiss LSM 510 META confocal microscope with a 1.4 NA 63x Zeiss objective, used in conjunction with Zeiss LSM 2.5 analysis software (Section 2.9). Localisation was quantified using Costes' method in ImageJ version 1.43 with the JACoP plugin (Section 2.9.3).

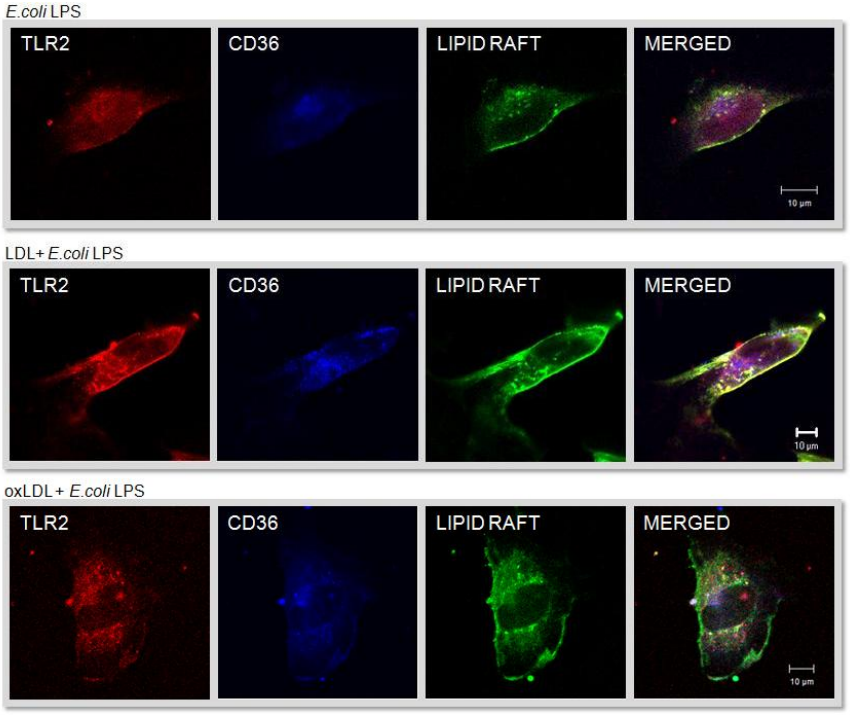

Figure 3.5.12: Cellular distribution of TLR2 (Red {Alexa555}) and CD36 (Blue {Cy5}) in relation to lipid rafts (Green {Cholera-toxin-FITC}) in HUVECs that have been stimulated with *E.coli* LPS alone or *E.coli* LPS with LDL or oxLDL pre-incubation. The cells were subsequently fixed and labelled via immunofluorescence. Images were acquired using a Zeiss LSM 510 META confocal microscope with a 1.4 NA 63x Zeiss objective, used in conjunction with Zeiss LSM 2.5 analysis software. The images are representative of a number of independent experiments. Localisation was quantified using Costes' method in ImageJ version 1.43 with the JACoP plugin. Scale bar, 10µm.

HUVEC stimulation with *E.coli* LPS (Figure 3.5.12, *E.coli* LPS) results in mild recruitment of TLR2 and CD36 to lipid rafts (r{obs} 0.656 and 0.656 respectively). When cells are pre-incubated with LDL prior to *E.coli* LPS (Figure 3.5.12, LDL + *E.coli* LPS) the recruitment of TLR2 to lipid rafts is increased (r{obs} 0.790) whilst CD36 is reduced (r{obs} 0.560) in comparison to *E.coli* LPS alone (Figure 3.5.12, *E.coli* LPS). When cells were pre-incubated with oxLDL prior to *E.coli* LPS (Figure 3.5.12, oxLDL + *E.coli* LPS) the recruitment of the SR CD36 to lipid rafts was increased (r{obs} 0.730), whilst TLR2 raft recruitment decreased (r{obs} 0.555) in comparison to *E.coli* LPS alone (Figure 3.5.12, *E.coli* LPS).

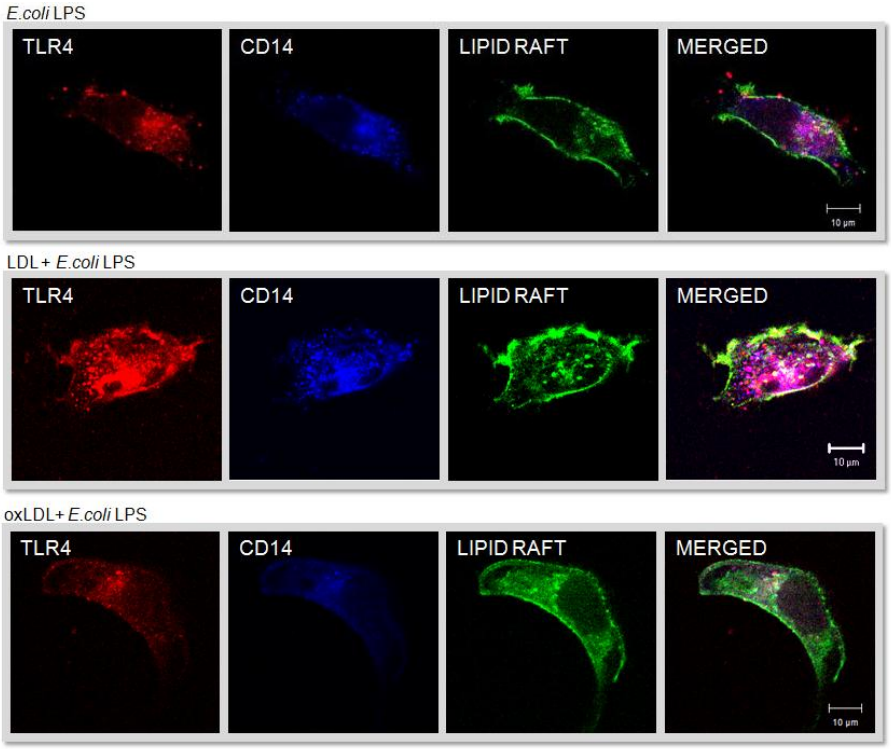

Figure 3.5.13: Cellular distribution of TLR4 (Red {Cy3}) and CD14 (Blue {Cy5}) in relation to lipid rafts (Green {Cholera-toxin-FITC}) in HUVECs that have been stimulated with *E.coli* LPS alone or *E.coli* LPS with LDL or oxLDL pre-incubation. The cells were subsequently fixed and labelled via immunofluorescence. Images were acquired using a Zeiss LSM 510 META confocal microscope with a 1.4 NA 63x Zeiss objective, used in conjunction with Zeiss LSM 2.5 analysis software. The images are representative from a number of independent experiments. Localisation was quantified using Costes' method in ImageJ version 1.43 with the JACoP plugin. Scale bar, 10µm.

TLR4 and to a greater extent CD14 can be seen in lipid rafts in response to *E.coli* LPS (r{obs} 0.505 and 0.564 respectively) (Figure 3.5.13, *E.coli* LPS). Pre-incubation with LDL prior to *E.coli* LPS (Figure 3.5.13, LDL + *E.coli* LPS) reduced TLR4 and CD14 recruitment to lipid rafts. When cells are pre-incubated with oxLDL and then stimulated with *E.coli* LPS (Figure 3.5.13, oxLDL + *E.coli* LPS) both TLR4 and CD14 are recruited to lipid rafts (r{obs} 0.617 and 0.780 respectively).

When HUVECs were pre-incubated with oxLDL prior to *E.coli* LPS stimulation the lipid raft recruitment of MyD88 was reduced by 26% in comparison to *E.coli* LPS alone (data not shown).

A): *E.coli* LPS

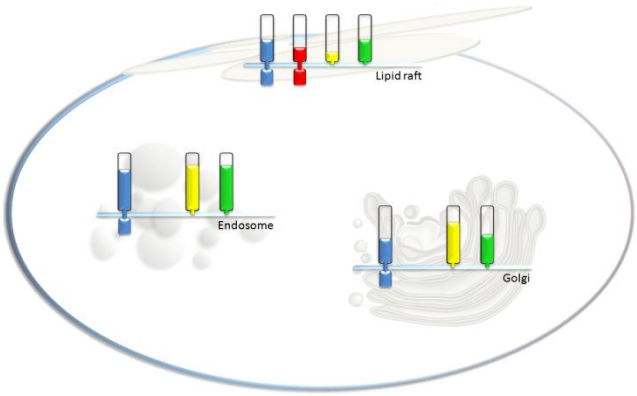

B): LDL + *E.coli* LPS

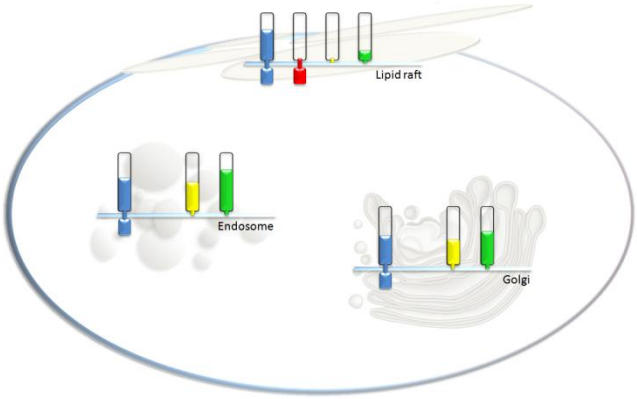

C): oxLDL + *E.coli* LPS

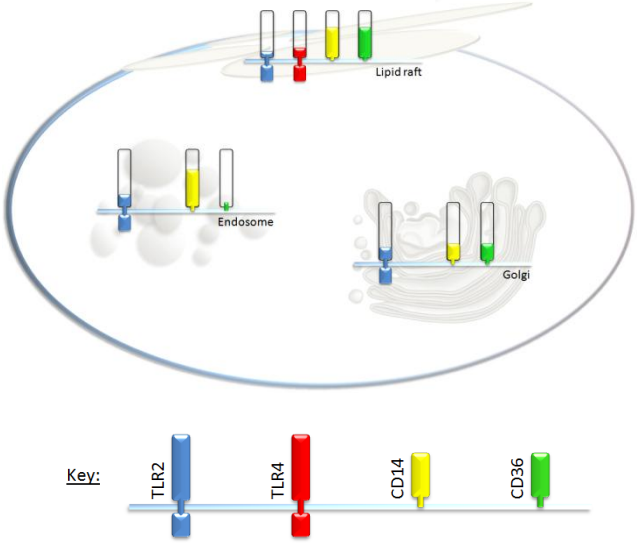

Figure 3.5.14: Schematic diagrams of the cellular distribution of TLR2 (Blue), CD14 (Green) and CD36 (Yellow) in relation to endosomes and the Golgi, and the cellular distribution of TLR2, TLR4 (Red), CD14 and CD36 in relation to lipid rafts in response to *E.coli* LPS (A), *E.coli* LPS with LDL pre-incubation (B) and *E.coli* LPS with oxLDL pre-incubation (C). Note: The presence of TLR4 in endosomes and the Golgi was not imaged. Extracellular domain colour fill represents localisation determined by r{obs}.

3.5.4: Intracellular PRR targeting in response to *P.gingivalis* LPS and *P.gingivalis* LPS lipoprotein combined stimulations

To investigate the intracellular PRR targeting in response to *P.gingivalis* LPS and *P.gingivalis* LPS lipoprotein combined stimulations, HUVECs were seeded on 8 well glass slides (Section 2.9.1). Cells were subject to *P.gingivalis* LPS and *P.gingivalis* LPS with either LDL or oxLDL pre-incubation (Section 2.5) directly on the slide in 200µl SFM (Section 2.5.3). Both direct and indirect immunofluorescence (Section 2.7) were used to label HUVECs on 8 well glass slides (Section 2.9.2). Slides were viewed using a Zeiss LSM 510 META confocal microscope, used with Zeiss LSM software (Section 2.9). Localisation was quantified using Costes' method in ImageJ (Section 2.9.3)

<u>*P.gingivalis* LPS</u>

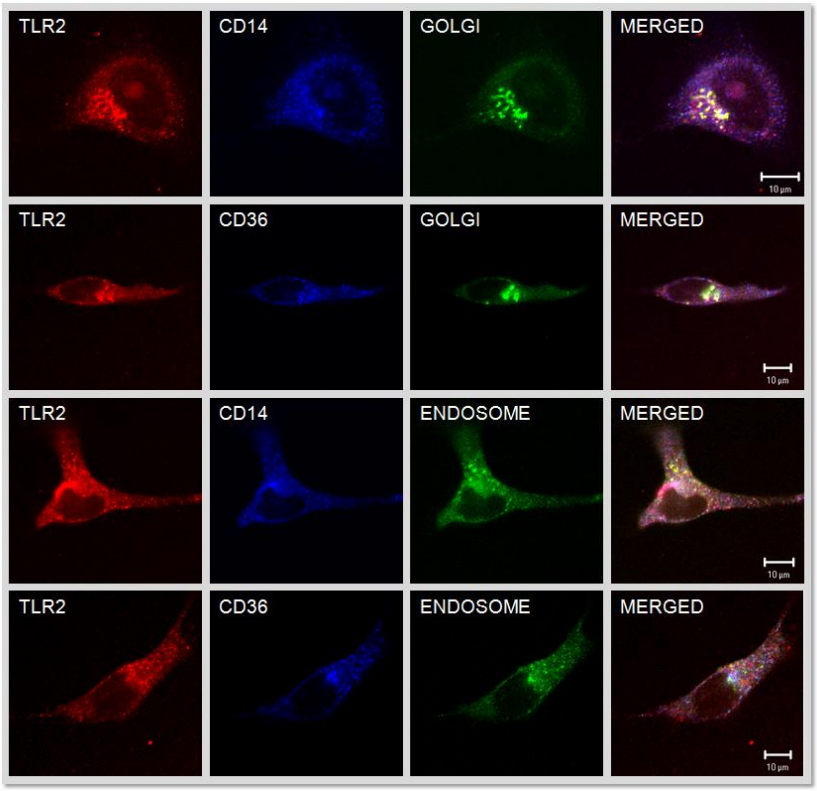

Figure 3.5.15: Cellular distribution of TLR2 (Red {Alexa555}), CD36 (Blue {Cy5}) and CD14 (Blue {Cy5}) in relation to Golgi (Green {FITC}) and endosomes (Green {FITC}) in HUVECs that have been stimulated with *P.gingivalis* LPS (60 minutes). The cells were subsequently fixed and labelled via immunofluorescence. Images were acquired using a Zeiss LSM 510 META confocal microscope with a 1.4 NA 63x Zeiss objective, used in conjunction with Zeiss LSM 2.5 analysis software. The images are representative of a number of independent experiments. Localisation was quantified using Costes' method in ImageJ version 1.43 with the JACoP plugin. Scale bar, 10µm.

When HUVECs were stimulated with *P.gingivalis* LPS (Figure 3.5.15) the receptors TLR2, CD14 and CD36 were shown to reside in both the Golgi (r{obs} 0.685, 0.641 and 0.747 respectively) and endosomes (r{obs} 0.650, 0.800 and 0.737 respectively). Results show that CD14 was preferentially targeted to endosomes.

LDL + *P.gingivalis* LPS

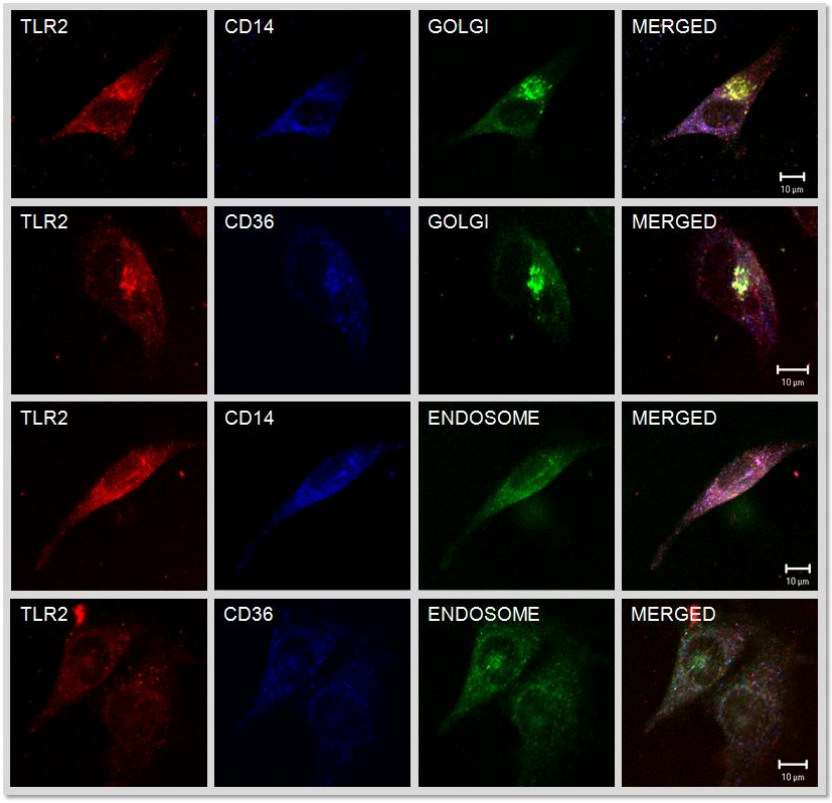

Figure 3.5.16: Cellular distribution of TLR2 (Red {Alexa555}), CD14 (Blue {Cy5}) and CD36 (Blue {Cy5}) in relation to Golgi (Green {FITC}) and endosomes (Green {FITC}) in HUVECs that have been pre-incubated with LDL (60 minutes) and then stimulated with *P.gingivalis* LPS (60 minutes). The cells were subsequently fixed and labelled via immunofluorescence. Images were acquired using a Zeiss LSM 510 META confocal microscope with a 1.4 NA 63x Zeiss objective, used in conjunction with Zeiss LSM 2.5 analysis software. The images are representative of a number of independent experiments. Localisation was quantified using Costes' method in ImageJ version 1.43 with the JACoP plugin. Scale bar, 10µm.

When HUVECs were pre-incubated with LDL prior to *P.gingivalis* LPS (Figure 3.5.16) the recruitment of CD14 and CD36 to the Golgi (r{obs} 0.607 and 0.652 respectively) and endosomal compartments (r{obs} 0.651 and 0.600 respectively) was reduced in comparison to *P.gingivalis* LPS stimulation alone (Figure 3.5.15). This was also

apparent for TLR2 localisation with the Golgi (r{obs} 0.588). The r{obs} value obtained for TLR2 localisation with endosomal compartments indicates little or no colocalisation.

oxLDL + *P.gingivalis* LPS

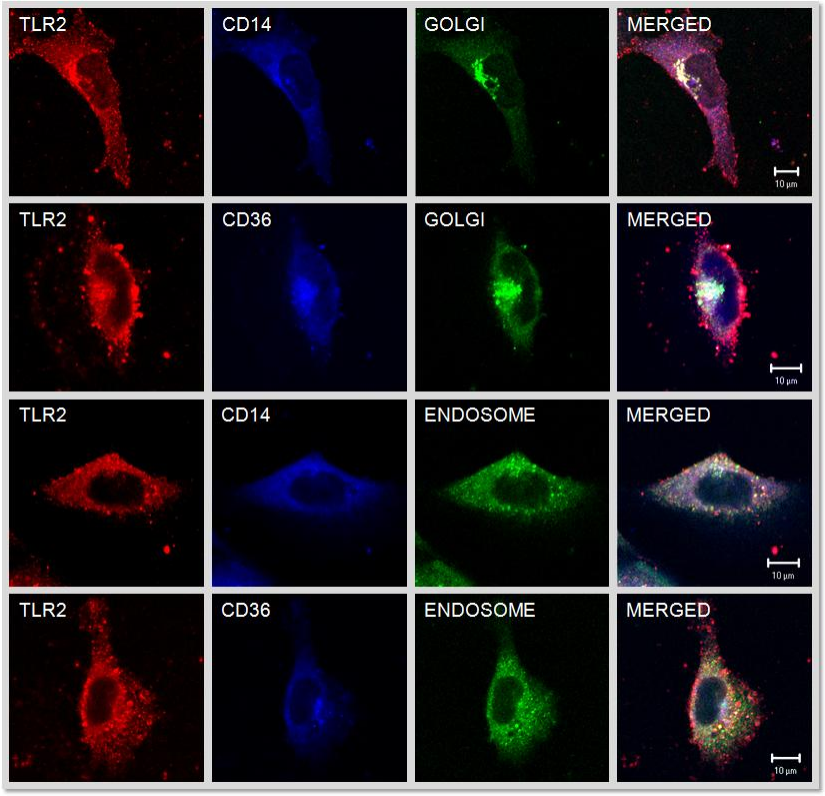

Figure 3.5.17: Cellular distribution of TLR2 (Red {Alexa555}), CD36 (Blue {Cy5}) and CD14 (Blue {Cy5}) in relation to Golgi (Green {FITC}) and endosomes (Green {FITC}) in HUVECs that have been pre-incubated with oxLDL (60 minutes) and then stimulated with *P.gingivalis* LPS (60 minutes). The cells were subsequently fixed and labelled via immunofluorescence. Images were acquired using a Zeiss LSM 510 META confocal microscope with a 1.4 NA 63x Zeiss objective, used in conjunction with Zeiss LSM 2.5 analysis software. The images are representative of a number of independent experiments Localisation was quantified using Costes' method in ImageJ version 1.43 with the JACoP plugin. Scale bar, 10µm.

When HUVECs were pre-incubated with oxLDL and then further stimulated with *P.gingivalis* LPS (Figure 3.5.17), the receptors TLR2, CD14 and CD36 were shown to reside in both the Golgi (r{obs} 0.577, 0.647 and 0.793 respectively) and endosomes (r{obs} 0.682, 0.790 and 0.694 respectively). Data shows that TLR2 and CD14 are

preferentially located within endosomal compartments rather than the Golgi. The opposite was found for CD36.

3.5.4.1:PRR lipid raft association in response to *P.gingivalis* LPS and *P.gingivalis* LPS lipoprotein combined stimulations

Lipid rafts have been shown to concentrate PRRs involved in cellular signalling. In this study I set out to investigate whether these rafts play a role in the internalization and targeting of PRRs involved in atherosclerosis in response to *P.gingivalis* LPS. This study also investigated the effect of lipoprotein pre-incubation on the internalization and targeting of receptors in response to this bacterial ligand.

HUVECs were seeded on collagen treated 8 well glass slides (Section 2.9.1). The cells were stimulated directly on the slide in 200µl SFM (Section 2.5.3). HUVECs were subject to *P.gingivalis* LPS, *P.gingivalis* LPS with LDL pre-incubation or *P.gingivalis* LPS with oxLDL pre-incubation (Section 2.5). Both direct and indirect immunofluorescent labelling (Section 2.7) techniques were used to label primary HUVECs on 8 well glass slides (Section 2.9.2). Slides were viewed using a Zeiss LSM 510 META confocal microscope with a 1.4 NA 63x Zeiss objective, used in conjunction with Zeiss LSM 2.5 analysis software (Section 2.9). Localisation was quantified using Costes' method in ImageJ version 1.43 with the JACoP plugin (Section 2.9.3).

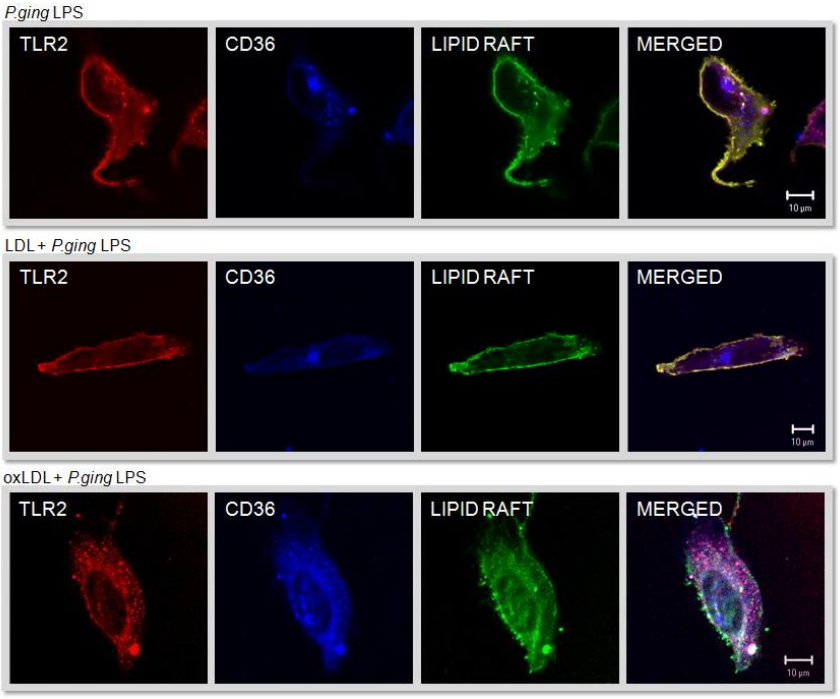

Figure 3.5.18: Cellular distribution of TLR2 (Red {Alexa555}) and CD36 (Blue {Cy5}) in relation to lipid rafts (Green {Cholera-toxin-FITC}) in HUVECs that have been stimulated with *P.gingivalis* LPS alone or *P.gingivalis* LPS with LDL or oxLDL pre-incubation. The cells were subsequently fixed and labelled via immunofluorescence. Images were acquired using a Zeiss LSM 510 META confocal microscope with a 1.4 NA 63x Zeiss objective, used in conjunction with Zeiss LSM 2.5 analysis software. The images are representative of a number of independent experiments. Localisation was quantified using Costes' method in ImageJ version 1.43 with the JACoP plugin. Scale bar, 10µm.

In HUVECs, TLR2 is strongly associated with lipid rafts (r{obs} 0.872) following *P.gingivalis* LPS exposure (Figure 3.5.18, *P.gingivalis* LPS). This reflects the unconventional nature of this LPS. CD36 was not shown to associate with lipid rafts (r{obs} 0.444) following *P.gingivalis* LPS exposure (Figure 3.5.18, *P.gingivalis* LPS). When cells were pre-incubated with LDL prior to *P.gingivalis* LPS (Figure 3.5.18, LDL + *P.gingivalis* LPS) both TLR2 (r{obs} 0.958) and CD36 (r{obs} 0.648) were associated with lipid rafts. As seen with oxLDL pre-incubation with *E.coli* LPS (Figure 3.5.12, oxLDL + *E.coli* LPS), the pre-incubation of HUVECs with oxLDL prior to bacterial PAMP reduces TLR2 recruitment to lipid rafts. In this case TLR2 lipid raft recruitment (r{obs} 0.483) was abolished due to oxLDL pre-incubation (Figure 3.5.18, oxLDL + *P.gingivalis* LPS). CD36 however, was still recruited to lipid rafts (r{obs}

0.682) in this stimulation. These data show that the "normal" response a cell produced in response to *P.gingivalis* LPS is disrupted by the presence of oxLDL.

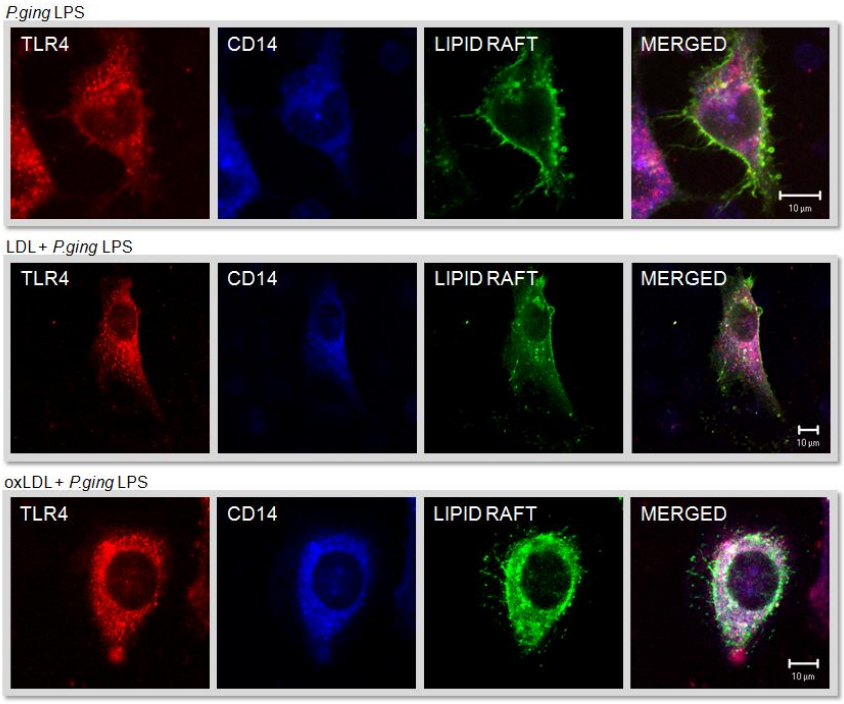

Figure 3.5.19: Cellular distribution of TLR4 (Red {Cy3}) and CD14 (Blue {Cy5}) in relation to lipid rafts (Green {Cholera-toxin-FITC}) in HUVECs that have been stimulated with *P.gingivalis* LPS alone or *P.gingivalis* LPS with LDL or oxLDL pre-incubation. The cells were subsequently fixed and labelled via immunofluorescence. Images were acquired using a Zeiss LSM 510 META confocal microscope with a 1.4 NA 63x Zeiss objective, used in conjunction with Zeiss LSM 2.5 analysis software. The images are representative of a number of independent experiments. Localisation was quantified using Costes' method in ImageJ version 1.43 with the JACoP plugin. Scale bar, 10µm.

TLR4 had a low level of association with lipid rafts (r{obs} 0.573) when cells were incubated with *P.gingivalis* LPS alone (Figure 3.5.19, *P.gingivalis* LPS). No significant recruitment of CD14 to lipid rafts was observed. When HUVECs were pre-incubated with LDL (Figure 3.5.19, LDL + *P.gingivalis* LPS), both TLR4 and CD14 were observed to associate with lipid rafts (r{obs} 0.620 and 0.585 respectively). oxLDL pre-incubation (Figure 3.5.19, oxLDL + *P.gingivalis* LPS) increased CD14 recruitment to lipid rafts (r{obs} 0.762) in comparison to *P.gingivalis* LPS alone (Figure 3.5.19, *P.gingivalis* LPS) and *P.gingivalis* LPS with LDL pre-incubation (Figure 3.5.19, LDL +

P.gingivalis LPS). The pre-incubation of HUVECs with oxLDL (Figure 3.5.19, oxLDL + *P.gingivalis* LPS) reduced TLR4 lipid raft recruitment (r{obs} 0.595) in comparison to LDL pre-incubation (Figure 3.5.19, LDL + *P.gingivalis* LPS).

The recruitment of MyD88 to HUVEC lipid rafts in response to *P.gingivalis* alone was reduced by 25% when cells were pre-incubated with oxLDL (data not shown).

A): *P.gingivalis* LPS

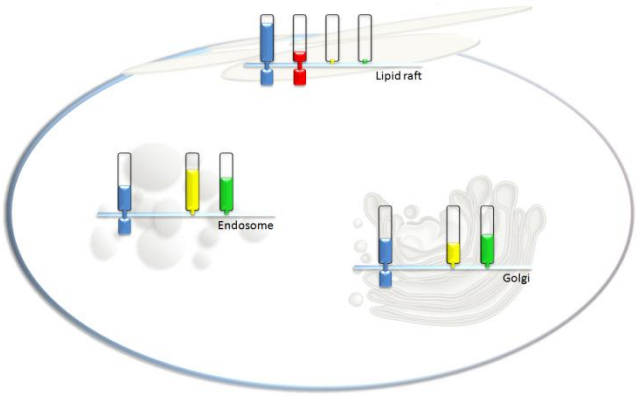

B): LDL + *P.gingivalis* LPS

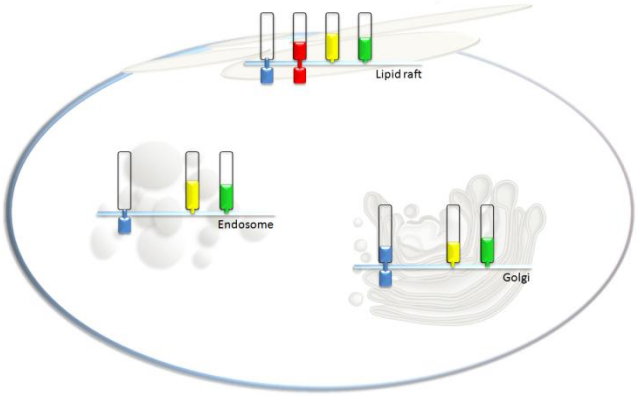

C): oxLDL + *P.gingivalis* LPS

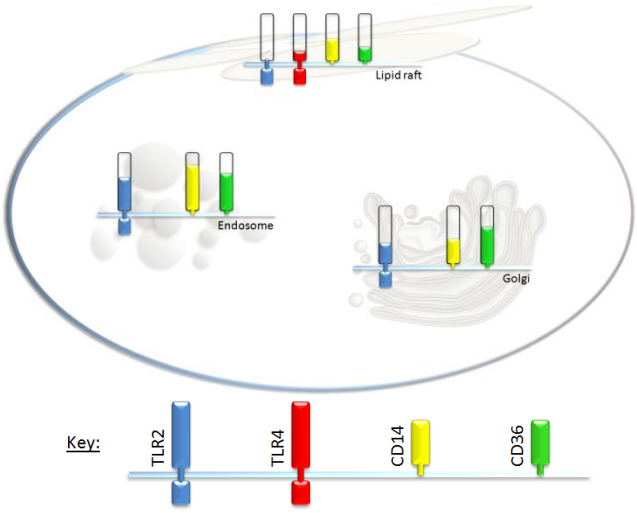

Figure 3.5.20: Schematic diagrams of the cellular distribution of TLR2 (Blue), CD14 (Green) and CD36 (Yellow) in relation to endosomes and the Golgi, and the cellular distribution of TLR2, TLR4 (Red), CD14 and CD36 in relation to lipid rafts in response to *P.gingivalis* LPS (A), *P.gingivalis* LPS with LDL pre-incubation (B) and *P.gingivalis* LPS with oxLDL pre-incubation (C). Note: The presence of TLR4 in endosomes and the Golgi was not imaged. Colour fill of extracellular domain represents localisation determined by r{obs}.

3.5.4: Conclusions

- LDL pre-incubation can significantly alter receptor targeting in response to bacterial ligands.
- LDL reduces TLR4 recruitment, but increases TLR2 recruitment, to lipid rafts when combined with the TLR4 agonist *E.coli* in comparison to PAMP alone.
- LDL reduces TLR2 recruitment, but increases TLR4 recruitment, to lipid rafts when combined with the TLR2 agonists *S.aureus* and *P.gingivalis* in comparison to PAMP alone.
- oxLDL reduces TLR2 and TLR4 lipid raft recruitment when combined with *S.aureus*, *E.coli* and *P.gingivalis* in comparison to PAMP alone.
- oxLDL increases lipid raft recruitment of CD14 and CD36 when combined with *S.aureus*, *E.coli* and *P.gingivalis* in comparison to PAMP alone.
- oxLDL incubation prior to *S.aureus* and *E.coli* stimulation reduces targeting of TLR2, CD14 and CD36 to endosomes and the Golgi in comparison to PAMP alone.
- oxLDL seems to alter the targeting of TLRs in response to bacterial ligands. TLR2 is targeted to other distinct cellular compartments, possibly lysosomes.
- oxLDL alters preferential targeting of TLR2 from Golgi to endosomes in comparison to *S.aureus* or *P.gingivalis* alone.
- The recruitment of MyD88 to lipid rafts in HUVECs in response to *S.aureus*, *E.coli* and *P.gingivalis* alone was reduced by 25%, 26% and 25% respectively, when cells were pre-incubated with oxLDL. MyD88 interaction with TLR2 is unaffected. Signalling may be occurring from compartments other that lipid rafts.

3.6: *In vivo* control of the inflammatory response

This study demonstrates the inflammatory nature of atherosclerosis and the involvement of PRRs of the innate immune system in this disease. The control/dampening of this inflammatory disorder could prove to be of therapeutic benefit. If one could stop, reverse, or better still prevent the dysregulated inflammation seen in the atheromatous plaque, tens of thousands of lives could be improved and saved in the U.K alone. Such intervention would free up millions of pounds greatly benefiting other areas within the National Health Service.

Work in this study including lipid raft disruption (Section 3.3), silencing experiments on primary HUVECs (Section 3.4.2) and work on transfected HEK cells expressing known TLR patterns (Section 3.4.1), has shown the importance of PRRs in orchestrating an appropriate response to atherosclerotic exogenous and endogenous ligands. This work has shown that the disruption of innate immune receptor complexes directed at atherosclerotic ligands causing a reduction in the inflammatory response, could have therapeutic potential. This study went on to explore the blocking of the endogenous and microbial sensing apparatus *in vivo* to determine the beneficial effects, if any, of TLR directed therapeutics in the prevention of atherosclerosis.

Taking into account "The three R's" of *in vivo* testing (replacement, reduction and refinement), this study initially established and tested on a reliable mouse model of inflammation. In this model, *in vitro* blockers of innate immunity established in the lab of Dr. K. Triantafilou (University of Sussex) were analysed for their potential in treating this disease prior to testing in an atherosclerotic mouse model, which require more lengthy and complex protocols. The *in vitro* blockers of inflammation tested in this

study were HSP70 and AMD3100. A mouse model of sepsis, an often fatal over reaction of the immune system, was concluded appropriate for the testing of these anti-inflammatory molecules.

Sepsis is caused by a systemic hyper-inflammatory response which involves the over secretion of pro-inflammatory mediators, such as TNF-α, IL-1β and migration inhibitory factor (MIF) in response to bacteria or bacterial products, such as LPS. It has recently been shown that pharmacological inhibition of endotoxin responses can be achieved by targeting TLR4 and MD2[209]. Clinical trials are starting to test the efficacy of TLR4 antagonists, such as E5564 (Eritoran), in sepsis and septic shock[210]. A double-blind placebo-controlled human study recently demonstrated that the TLR4 antagonist Eritoran could block the effects of endotoxin in human volunteers[211]. These studies show that immune-modulation can be achieved by targeting the receptors of the innate immune system and that this is transferable to human subjects, demonstrating the potential that mediators of the inflammatory disease atherosclerosis could have.

3.6.1: Establishing the sepsis model

Male CD-1 out-bred mice (6-8 weeks) were randomly grouped (5-10 mice per group) and injected by intraperitoneal (i.p) injection (Section 2.18.2) with varied concentrations (50, 60, 70, 80mg/Kg) of *E.coli* 055 LPS (List Biological Laboratories) using a sterile 1ml syringe (BD Plastipak™) with a 25 GA1 0.5x25mm needle (BD Microlance™ 3).

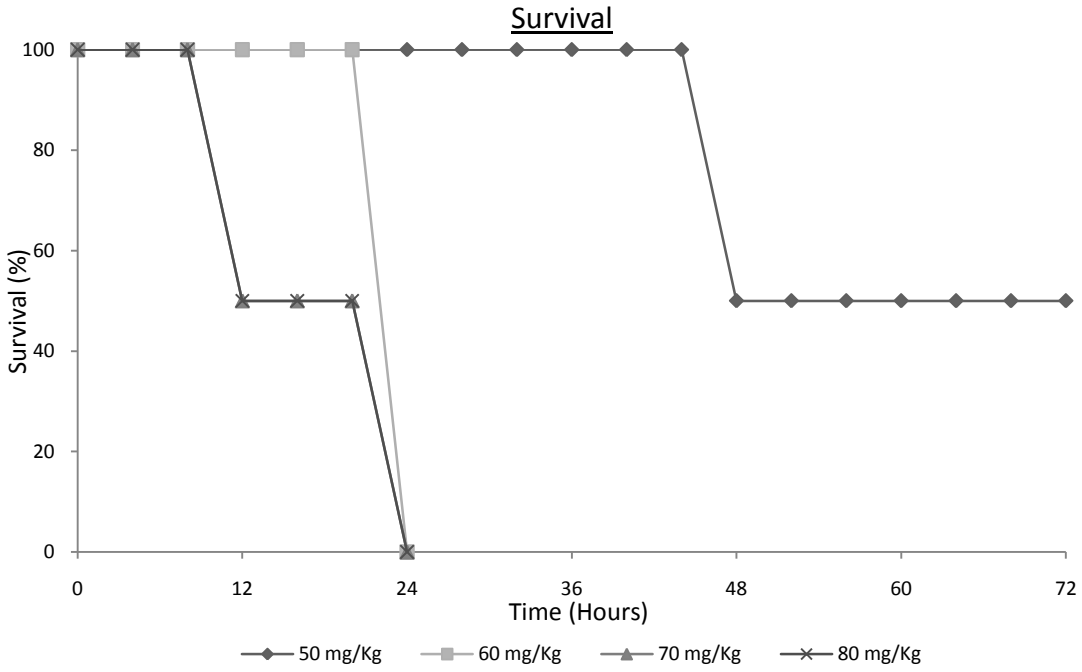

Figure 3.6.1: Determination of LPS-induced sepsis mouse model. Male CD-1 mice (6-8 weeks) were randomly grouped (5-10 mice per group) and injected by intraperitoneal (i.p) injection with varied concentrations (50, 60, 70, 80mg/Kg) of *E.coli* 055 LPS. Survival was recorded every 4 hours.

LPS-induced death was observed for LPS concentrations of 60, 70 and 80mg/Kg (Figure 3.6.1). When 50mg/Kg was administered 100% survival at 72 hours was recorded. 70 and 80mg/Kg LPS terminated the mice too early. 60mg/Kg showed 100% survival up to 24 hours when the mice succumbed to the infection. For these reasons 60mg/Kg was chosen for the sepsis mouse model in this study.

3.6.2: Heat shock protein 70

Infection along with many other cellular stresses or damage causes the production of HSPs. Their main function has been found to be concerned with assisting the cell to carry on with normal tasks, primarily by helping proteins fold[139]. More recently the role of HSPs as endogenous modulators of the innate immune response have been explored.

A possible cardioprotective role of HSP70 has been shown through studies demonstrating an increased resistance of transgenic mice which over express HSP70 to ischemic injury[143,144]. This work is supported by patient studies demonstrating a positive correlation between elevated HSP70 levels and low CAD risk[145]. Triantafilou (2008)[141] has shown that the use of exogenous HSP70 can inhibit LPS-induced inflammatory responses in monocytes demonstrating its potential as a therapeutic agent for many disorders. It was demonstrated that HSP70 has the ability of reducing expression of TLRs 2, 4, 6, 7, 8 and 9, diminishing cellular immune capabilities. This study has established the role of TLRs in the onset of atherosclerosis and thus their modulation is of great interest. If TLR expression can be reduced, weakening the inflammatory response to atherosclerotic ligands, so could the extent of this inflammatory disorder.

In this study the *in vivo* immunomodulatory effects of HSP70 was investigated. The effect of HSP70 on cytokine levels and survival in our established sepsis model (Section 3.6.1) were analyzed to explore the possibility of using HSP70 as a therapeutic agent for atherosclerosis. HSP70 toxicity was tested.

3.6.2.1: HSP70 decreases LPS-induced mortality

Intraperitoneal (i.p) injection (Section 2.18.2) of HSP70 at 500µg/mouse (Kindly supplied by Professor C.Lingwood of the University of Toronto) was administered to the CD-1 mouse (out-bred male 6-8 weeks) using a sterile 1ml syringe (BD Plastipak™) with a 25 GA1 0.5x25mm needle (BD Microlance™ 3) at 1 hour pre-LPS administration (Section 2.18.3.1.1) or 1, 2, 4 and 6 hours post-LPS administration. Mice were closely monitored every 4 hours for 72 hours, survival was recorded.

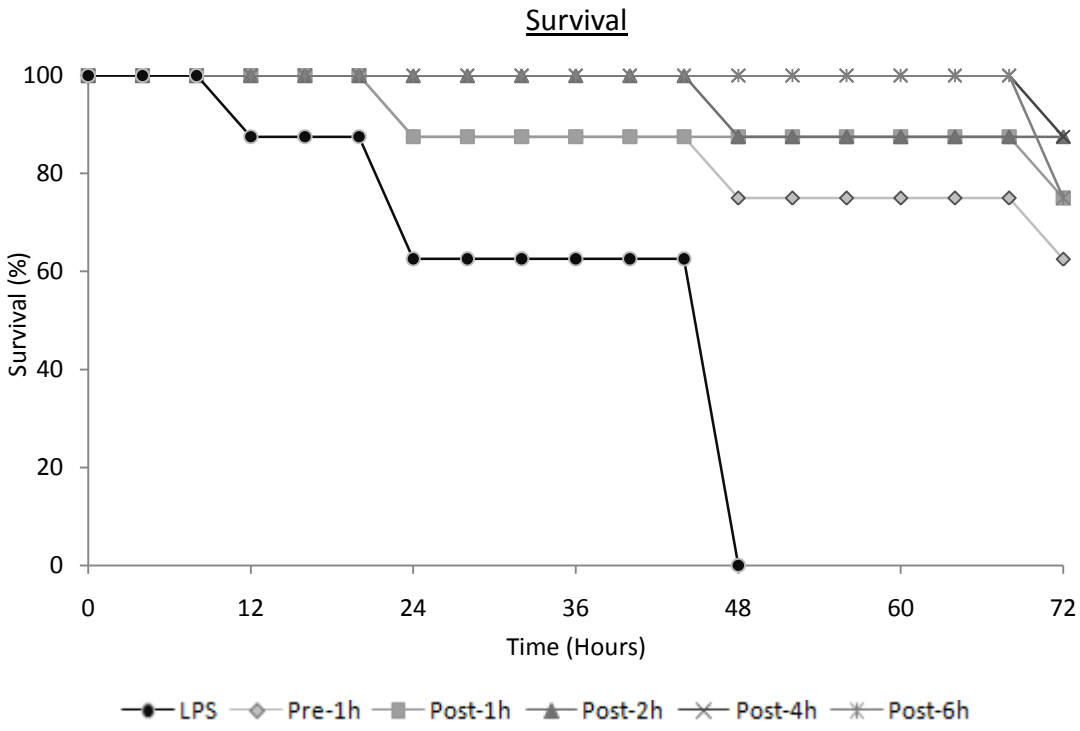

Figure 3.6.2: Survival of LPS-induced septic shock in CD-1 mice through administration of HSP70. CD-1 mice (out-bred male 6-8 weeks) were administered a lethal dose of LPS (60mg/kg) by intraperitoneal (i.p) injection. Mice were treated with HSP70 (500µg/mouse) 1 hour before LPS administration (Pre-1h) or 1, 2, 4 and 6 hours after LPS administration (Post-1/2/4/6h). Control mice (LPS) were not treated with HSP70. Mice were monitored every 4 hours.

Over the 72 hour observation period, all HSP70 treatment protocols conferred survival (Figure 3.6.2). HSP70 treatment 1 hour prior to LPS (Pre-1h) administration was the least successful protocol with 62.5% survival at 72 hours (Figure 3.6.2). HSP70 was most effective when administered post-1, 2, 4 and 6 hours to LPS administration giving 75%, 87.5%, 87.5% and 75% survival respectively (Figure 3.6.2). These data show that administration of HSP70 at 2-4 hours post infection would be most beneficial.

3.6.2.2: HSP70 inhibits LPS-induced inflammatory responses

Intraperitoneal (i.p) injection of HSP70 at 500µg/mouse (kindly supplied by Professor C.Lingwood of the University of Toronto) was administered to the CD-1 mouse (out-bred male 6-8 weeks) using a sterile 1ml syringe (BD Plastipak™) with a 25 GA1 0.5x25mm needle (BD Microlance™ 3) at 1 hour pre-LPS administration (Section 2.18.3.1.1) or 1, 2, 4 and 6 hours post-LPS administration. Blood (50µl) was collected at time points (0, 2, 4, 6, 8 and 12 hours) after LPS administration from the tail vein of the mice. Inflammatory cytokine levels in the serum were determined using a cytokine bead array (CBA) system obtained from Becton Dickinson (Section 2.8.2.2).

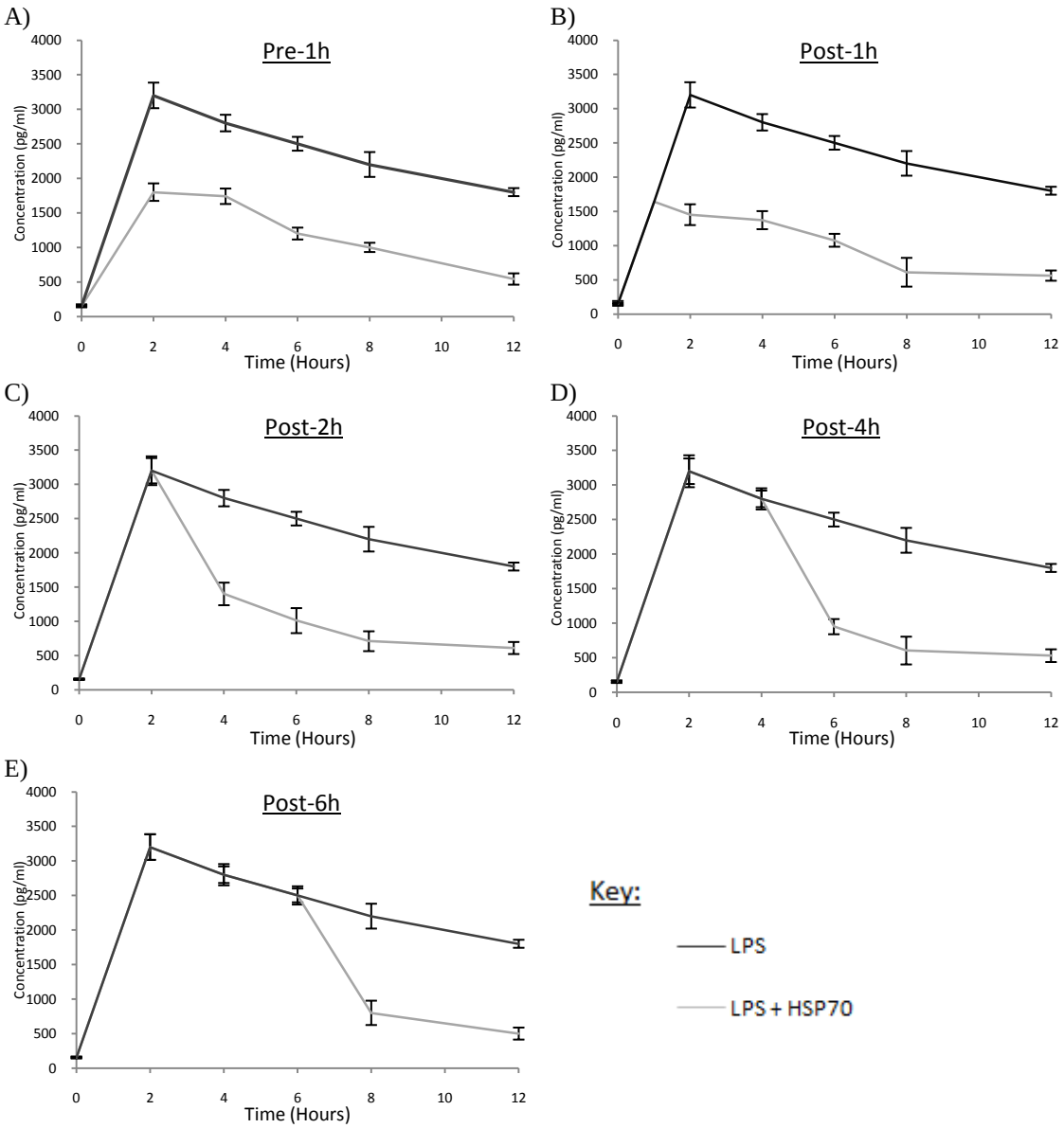

Figure 3.6.3: Comparison of TNF-α concentration in blood samples taken from CD-1 mice at 0, 2, 4, 6, 8 and 12 hours between LPS control and HSP70 treated LPS sepsis induced mice. HSP70 was administered 1 hour previous to LPS (Pre-1h {A}), 1 hour post-LPS (Post-1h {B}), post-2h (C), post-4h (D) and post-6h (E). CD-1 mice (out-bred male 6-8 weeks) were administered a lethal dose of LPS (60mg/kg) by intraperitoneal (i.p) injection. Mice were treated with HSP70 (500µg/mouse) at times stated. Control mice (LPS) were not treated with HSP70. 50µl tail vein blood was collected at each stated time point. Inflammatory cytokine levels in the serum were determined using a cytokine bead array (CBA) system obtained from Becton Dickinson. Data represents mean, ± standard deviation, n=2.

Blood samples taken from mice in the HSP70 pre-treated and post-treated protocols at different time points after LPS administration showed a significant reduction of plasma TNF-α concentration (Figure 3.6.3A-E). This data illustrates HSP70 as an effective

immune-modulator with the capability of reducing cytokine levels in response to infection through reducing TLR expression. All HSP70 administration protocols achieved TNF-α concentrations at 12 hours of ≤34% of the control untreated sepsis model (Figure 3.6.3A-E).

3.6.3: AMD3100 octahydrochloride

Another potential therapeutic for atherosclerosis is AMD3100 octahydrochloride (AMD 3100). AMD3100 is a CXCR4 antagonist that was previously, but unfortunately unsuccessfully, explored for its potential in HIV treatment[148]. CXCR4 is a chemokine receptor that belongs to the seven transmembrane domain G-protein-coupled receptor family. The expression of CXCR4 has been shown to increase after exposure to bacterial products[151]. In response to LPS, CXCR4 co-clusters with TLR4 and other receptors forming the "LPS-sensing apparatus". The formation of this cluster was found to be responsible for triggering LPS-induced responses[69]. Triantafilou *et al*. (2008)[69] have shown that, along with TLR4, CXCR4 co-clusters with other LPS receptors such as CD55, HSP70, HSP90 and CD11b/CD18 in human monocytes and human endothelial cells following LPS stimulation. AMD3100 was found to inhibit these CXCR4 heterotypic associations with LPS receptors, such as TLR4, suggesting that AMD3100 inhibits the formation of the "LPS-sensing" apparatus (Dr. K. Triantafilou {unpublished data}).

TLR4 is the major component of the LPS-sensing apparatus. The disruption of this cluster would greatly attenuate TLR4 function. The involvement of TLR4 in the sensing of pro-atherogenic ligands makes it an interesting target for the prevention of this disease. Inhibition of the ability to respond to exogenous, thus potentially endogenous, ligands could have great therapeutic potential. AMD3100 was explored as a novel drug

for the treatment and prevention of atherosclerosis through the inhibition of signalling through TLR4. AMD3100 toxicity was tested.

3.6.3.1: AMD3100 decreases LPS-induced mortality

Intraperitoneal (i.p) injection (Section 2.18.2) of AMD3100 (500µg/mouse {Sigma}) was administered to the CD-1 mouse (out-bred male 6-8 weeks) using a sterile 1ml syringe (BD Plastipak™) with a 25 GA1 0.5x25mm needle (BD Microlance™ 3) at 1 hour pre-LPS administration (Section 2.18.3.1.1) or 1, 2, 4 and 6 hours post-LPS administration. Mice were closely monitored every 4 hours for 72 hours, survival was recorded.

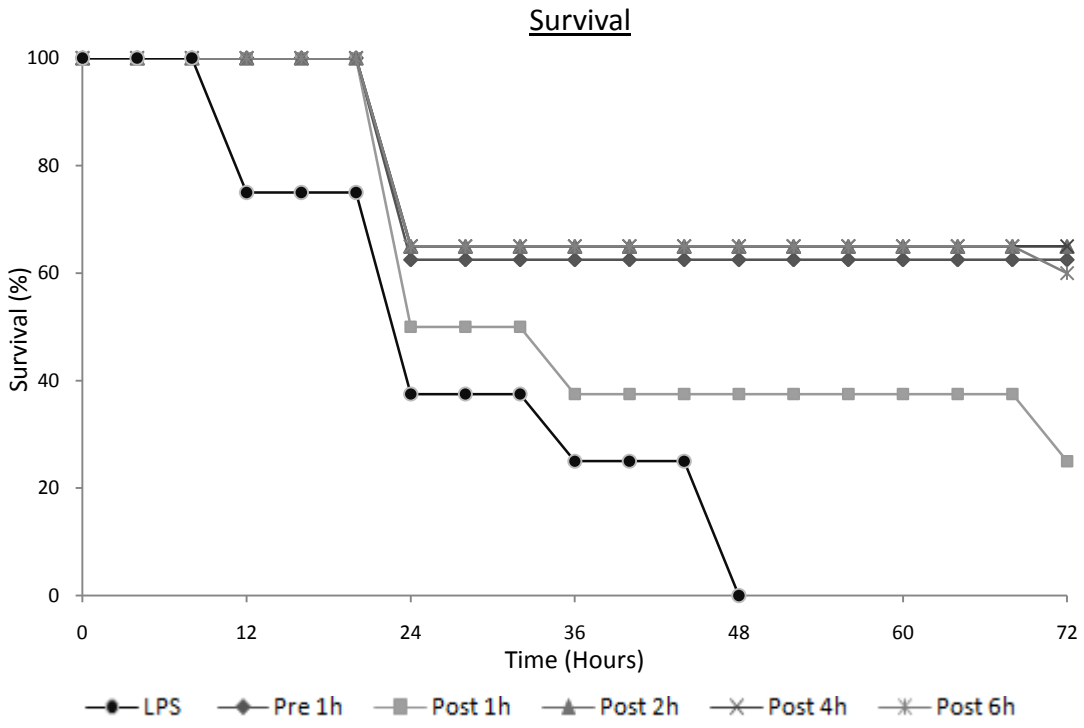

Figure 3.6.4: Survival of LPS-induced septic shock in CD-1 mice through administration of AMD3100. CD-1 mice (out-bred male 6-8 weeks) were administered a lethal dose of LPS (60mg/kg) by intraperitoneal (i.p) injection. Mice were treated with AMD3100 (500µg/mouse) 1 hour before LPS administration (Pre-1h) or 1, 2, 4 and 6 hours after LPS administration (Post-1/2/4/6h). Control mice (LPS) were not treated with AMD3100. Mice were monitored every 4 hours.

A significant decrease in sepsis-induced mortality was found when AMD3100 was administered. Notably, over the 72 hour observation period 62.5% of the 1 hour pre-treated mice (Figure 3.6.4, Pre-1h) survived, whereas all untreated mice (Figure 3.6.4, LPS) died by 48 hours after LPS administration. AMD3100 conferred 25% protection against endotoxic shock when applied 1 hour after LPS injection (Figure 3.6.4, Post-1h). AMD3100 was more protective when administered 2, 4 or 6 hours post-LPS injection conferring 65% protection when administered either 2 hours (Figure 3.6.4, Post 2h) or 4 hours (Figure 3.6.4, Post 4h) after LPS injection and 60% protection if administered 6 hours (Figure 3.6.4, Post 6h) after injection.

3.6.3.2: AMD3100 inhibits LPS-induced inflammatory responses

Intraperitoneal (i.p) injection of AMD3100 (500µg/mouse {Sigma}) was administered to the CD-1 mouse (out-bred male 6-8 weeks) using a sterile 1ml syringe (BD Plastipak™) with a 25 GA1 0.5x25mm needle (BD Microlance™ 3) at 1 hour pre-LPS administration (Section 2.18.3.1.1) or 1, 2, 4 and 6 hours post-LPS administration. Blood (50µl) was collected at time points (0, 2, 4, 6, 8 and 12 hours) after LPS administration from the tail vein of the mice. Inflammatory cytokine levels in the serum were determined using a cytokine bead array (CBA) system obtained from Becton Dickinson (Section 2.8.2.2).

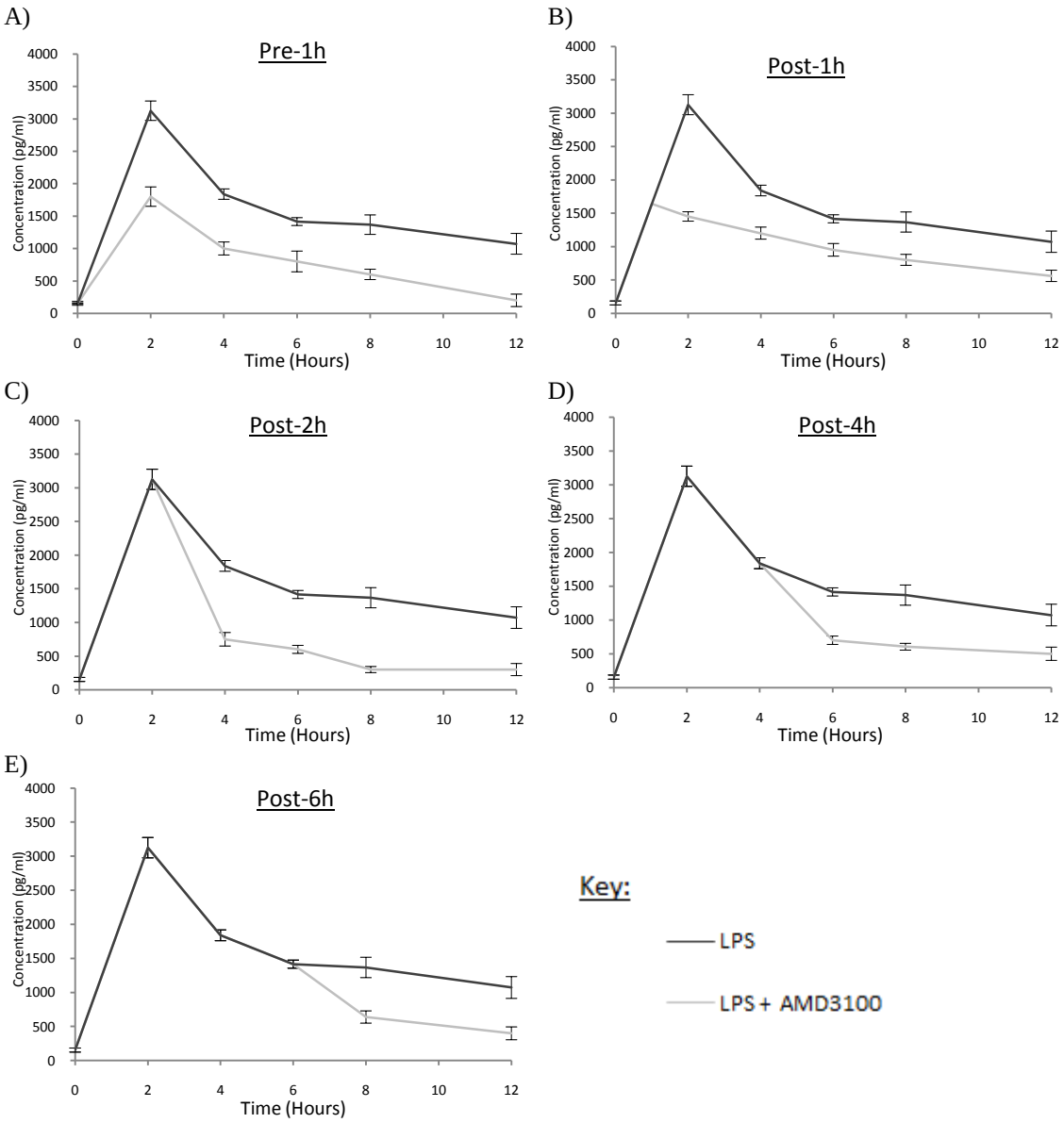

Figure 3.6.5: Comparison of TNF-α concentration in blood samples taken from CD-1 mice at 0, 2, 4, 6, 8 and 12 hours between LPS control and AMD3100 treated LPS sepsis induced mice. AMD3100 was administered 1 hour previous to LPS (Pre-1h {A}), 1 hour post-LPS (Post-1h {B}), post-2h (C), post-4h (D) and post-6h (E). CD-1 mice (out-bred male 6-8 weeks) were administered a lethal dose of LPS (60mg/kg) by intraperitoneal (i.p) injection. Mice were treated with AMD3100 (500µg/mouse) at times stated. Control mice (LPS) were not treated with AMD3100. 50µl tail vein blood was collected at each stated time point. Inflammatory cytokine levels in the serum were determined using a cytokine bead array (CBA) system obtained from Becton Dickinson. Data represents mean, ± standard deviation, n=2.

Analysis of blood samples taken from mice either pre-treated or post-treated with AMD3100 at different time points after LPS administration showed a significant

reduction of plasma cytokine concentrations. Treatment with AMD3100 1 hour prior to LPS (Figure 3.6.5, Pre-1h) injection significantly reduced cytokine levels in comparison to the control, giving the lowest levels of TNF-α at 72 hours in comparison to other protocols tested (Figure 3.6.5, Post-1h/Post-2h/Post-4h/Post-6h). Interestingly, it seems that similarly to the survival studies (Figure 3.6.4), administration of AMD3100 at 2 hours (Figure 3.6.5, Post-2h), 4 hours (Figure 3.6.5, Post-4h) or 6 hours (Figure 3.6.5, Post-6h) after LPS administration is more beneficial than administration after 1 hour post-LPS injection (Figure 3.6.5, Post-1h). Plasma cytokine concentration was lower in the mice that received AMD3100 later than 1 hour after LPS administration. This data indicates optimal time points at which AMD3100 should be employed.

3.6.4: Conclusions

- HSP70 administration before and after LPS exposure significantly reduces the release of inflammatory cytokines reducing mortality.
- Treatment of mice with HSP70 2-4 hours after the induction of sepsis gave the lowest mortality.
- HSP70 has great potential as an immunomodulator in atherosclerosis, through reducing the dysregulated inflammation of the vascular wall.
- AMD3100 reduces inflammatory cytokine levels in the sepsis model when administered before and after LPS injection.
- Injection of AMD3100 at 1 hour before or 2, 4 and 6 hours after LPS gave ≥60% survival in the sepsis model. AMD3100 injection one hour after sepsis induction only gave 25% survival. Therefore treatment should be given at one hour prior or no earlier than 2 hours post infection.
- AMD3100 is capable of reducing inflammatory processes to the point of rescuing mice from septic shock. The prospect of using AMD3100 to modulate the inflammatory disorder of atherosclerosis is promising.

Chapter 4:

Discussion

4.1: Atherosclerosis: An inflammatory disorder

Atherosclerosis is one of the largest contributors of mortality in the Western world. This multi-factorial disease is characterized by the formation of plaques in medium and large arterial blood vessel walls, which can lead to vascular occlusion resulting in tissue damage such as myocardial infarction. There are many factors that have been associated with atherosclerosis over the years including smoking, hypercholesterolemia, high plasma concentrations of LDL, low plasma concentrations of HDL, hypertension, lack of exercise, diabetes mellitus, obesity and autoimmune diseases such as rheumatoid arthritis and systemic lupus erythematosus[6,7,212]. When the atherosclerotic plaque was analyzed, interestingly it was found that a number of components of the innate immune system were upregulated in comparison to normal artery[8,9]. The view that atherosclerosis is due to an inflammatory disorder is now at the forefront of atherosclerosis research.

Edfeldt *et al*. (2002)[8] revealed augmented expression of members of the TLR family in the atherosclerotic plaque. TLRs are germ-line encoded PRRs of the innate immune system that have evolved to be able to recognize PAMPs that are present on all pathogens. PAMPs range from flagellin of flagella to ssRNA. PAMP recognition through TLRs causes the activation of intracellular signalling cascades that ultimately cause the release of inflammatory mediators. The field of TLR research is relatively new with the first human Toll being discovered in 1997 by Medzhitov & Janeway[40]. The role of TLRs in pathogen recognition and disease is ever expanding as our knowledge of their function increases, making them exciting therapeutic targets. The discovery of augmented TLR expression in the atherosclerotic plaque sparked much speculation as to why and how this has come about. Within the last decade a role for

TLRs in atherosclerosis has been shown through a number of *in vitro* and *in vivo* studies on mice and humans.

Much evidence exists supporting a role for infection in plaque development. A large population study has demonstrated that chronic infections, such as those of the respiratory system, urinary tract and gums, are associated with an increased risk of atherosclerotic plaque development[213]. Atherosclerosis-associated exogenous ligands include *P.gingivalis*, *H.pylori*, *C.pneumoniae*, HSV, CMV and EBV[18-25,172,214-216]. Endogenous ligands are also implicated in atherogenesis. LDL can undergo oxidative modification under physiological conditions[98]. The oxidation of LDL seems to have the effect of turning this molecule from "self" to "non-self". oxLDL is bound by CD36 SRs on macrophages and is engulfed which can lead to foam cell formation, a major component of the atherosclerotic plaque[73,101,102]. Interestingly it was found that the immunization of mice with oxLDL reduces atherosclerotic lesion development[27,28]. Similarly, a decreased probability of patients experiencing a second MI was attributed to vaccination against influenza[7].

As mentioned, atherosclerosis is now widely accepted to be due to an inflammatory disorder. However, oxLDL has been implicated in this disease for many years. Whilst some studies have given oxLDL an immunogenic role, linking endogenous ligands and inflammation, others have pointed to an immunosuppressive role. oxLDL has been shown to be immunogenic[99] and being capable of causing upregulation of TLR4[100] on human monocyte-derived macrophages. On the other hand, OxPAPC, one of the oxidative epitopes of oxLDL, has been shown to inhibit LPS signalling via the competitive binding of the adapter molecules CD14, MD2 and LBP which are required

for effective LPS recognition through TLR4[103,153]. A protective role of oxLDL to TLR2 and TLR4 ligands has been shown[103,104].

This study was interested in the interaction between exogenous and endogenous atherosclerosis-associated ligands, with emphasis on PRRs of the innate immune system. Although individually the role of these ligands in atherosclerosis has been investigated, the cellular effect of the interaction between host lipoproteins and bacterial PAMPs, and the consequence of this on the immune response, has not.

In this study the functional significance of PRR associations and signalling in response to atherosclerosis-associated endogenous and exogenous ligands and the alterations that may be caused to these events when ligands are present at the same time was investigated. The atherosclerosis-associated ligands assayed include human endogenous LDL and its oxidised derivatives mmLDL and oxLDL, LTA from *S.aureus* and LPS from *E.coli*, *P.gingivalis* and *C.pneumoniae*.

4.2: Stimulations with single ligands

This study utilised immortalised human ECV304 cells to elucidate PRR expression and associations in response to atherosclerosis-associated ligands. Furthermore ECV304 cells and primary HUVEC inflammatory cytokine release in response to atherosclerosis-associated ligands was analysed.

Initially PRR expression on ECV304 cells was investigated in response to endogenous lipoproteins and bacterial products via indirect immunofluorescence and flow cytometry. It was shown that LDL and its derivatives mmLDL and oxLDL as well as

LTA from *S.aureus* and LPS from *E.coli* and *P.gingivalis* all caused upregulation of TLR2, TLR4, TLR6, CD14 and CD36 expression on ECV304 cells. Increased TLR1 expression was not observed in any stimulation. Augmented TLR expression has previously been observed in the atherosclerotic plaque in comparison to a normal artery[8,167]. In particular the significant upregulation of TLRs 1, 2 and 4 on endothelial cells and macrophages was shown in plaques obtained from patients who have undergone a carotid endarterectomy[8]. The absence of TLR1 expression in the ECV304 cell line differs from that previously found in the plaque. This could indicate an additional *in vivo* source, other than what was assayed, of vascular endothelial cell activation. The lack of involvement of TLR1 but involvement of TLR6 suggests the TLR2/TLR6 heterodimer is primarily involved in the recognition of atherosclerosis-associated ligands in the ECV304 cell line, not the TLR2/TLR1 heterodimer.

When looking at LDL and its oxidised derivatives the greatest PRR upregulation was observed with LDL, with oxLDL giving the lowest ECV304 cell surface receptor expression. Under physiological conditions "self" LDL can undergo oxidative modification forming "non-self" oxLDL[98]. oxLDL has been implicated in atherosclerosis and its role in foam cell formation has been well documented. CD36 SRs expressed on macrophages bind such modified lipids and are involved in their endocytic internalization which, if dysregulated, can result in foam cell formation[73,101,102]. The lower PRR expression observed in this study on ECV304 cells in response to oxLDL in comparison to LDL may illustrate the endocytosis of "non-self" oxLDL reducing cell surface expression rather than a lower ligand immunogenicity. In contrast to this data Xu *et al*. (2001)[100] demonstrated that oxLDL, but not native LDL, causes increased expression of TLR4 on human monocyte-derived macrophages. It is

hypothesized this gives the "self"/"non-self" discrimination. This study however, has shown that both "self" and "non-self" LDL are capable of inducing TLR2, TLR4, TLR6, CD14 and CD36 expression in endothelial cells but to different degrees. TLR4, like CD36, has been shown to be involved in the uptake of modified LDL. Miller *et al*. (2009)[170] showed a reduction in uptake of mmLDL in macrophages of mice that were TLR4 deficient. Oxidatively modified LDL has been shown to be more resistant to lysosomal degradation[217], which leads to its intracellular accumulation in macrophages causing foam cell formation. The reduced expression of receptors that was observed in response to oxLDL in comparison to LDL may represent oxLDL holding internalised receptors in intracellular compartments, decreasing the possible cell surface PRR expression. LDL that is targeted to lysosomes may be cleared effectively allowing receptors to be recycled back to the membrane surface. Data from this study demonstrates that endothelial cells react to LDL and its oxidized counterparts by increasing receptors involved in their uptake, ultimately resulting in their increased endocytosis.

Cell surface expression of TLR2, TLR4, TLR6, CD14 and CD36 are augmented in ECV304 cells in response to LTA from *S.aureus* and LPS from *E.coli* and *P.gingivalis*. At 60 minutes *P.gingivalis* was notably less capable at increasing TLR2, TLR4, TLR6, and CD36 expression. This suggests *P.gingivalis* is the least immunogenic of the tested atherosclerosis-associated ligands, which may permit the establishment of an infection. Although LTA from *S.aureus*[53] and LPS from *P.gingivalis*[51] are TLR2 agonists the upregulation of TLR4 was observed. Similarly, although LPS from *E.coli*[61] is a well documented TLR4 agonist, TLR2 upregulation was observed. This data does not assume a role for these receptors in signalling. This data could suggest that ligands for

one TLR could in fact upregulate TLRs that may not be specifically involved in the recognition of the present ligand. This could indicate that ECV304 cells may not only sensitize to the ligand present but this interaction increases their overall immunogenic competence. Such a scenario would exacerbate plaque formation, for endothelial cells could become sensitized to ligands that may be present in low concentrations, but previously tolerated, increasing further cellular immune output in the vascular wall.

To see whether PRR expression mimics the inflammatory response induced in vascular endothelial cells in response to atherosclerosis-associated ligands, this study went on to look at cytokine release. Formation of the TLR/ligand complex causes homo/hetero-dimerization of TLRs resulting in activation of the intracellular TIR domains causing production of intracellular signalling cascades. Bjorkbacka *et al*. (2004)[159] demonstrated the involvement of intracellular TLR signalling in atherosclerosis by showing reduced plaque area in *ApoE*$^{-/-}$*MyD88*$^{-/-}$ mice in comparison to *ApoE*$^{-/-}$*MyD88*$^{+/+}$ mice. MyD88 is an intracellular TLR signalling adapter protein, which is required for TLR signalling, apart from TLR3 signalling. These intracellular cascades result in the release of NF-κB from its endogenous inhibitor and subsequent nuclear translocation that leads to the transcription of inflammatory cytokines, which modulate the inflammatory and antiviral response[119]. Inflammatory cytokine levels were measured in the cell supernatant using a flow cytometric cytokine bead array system. Cytokine analysis of ECV304 cells and HUVECs in response to modified and native LDL gave a notable increase in IL-6 and IL-8 levels in comparison to unstimulated cells. It is known that OxPAPC, a major active component of modified LDL, is capable of stimulating endothelial cells[99]. Both IL-6[185] and IL-8[218] have been implicated in the multi-factorial disease atherosclerosis. Profumo *et al*. (2008)[185] have shown increased expression of the pro-inflammatory

cytokines TNF-α, IFN-γ, IL-1β, IL-6 and the anti-inflammatory cytokines IL-4 and IL-10 in the peripheral blood of patients with atherosclerosis. Levels of the chemokine IL-8 have been associated with increased risk of future coronary artery disease and plaque instability[219,220]. Data from this work demonstrate that endogenous LDL alone may be capable of causing the chronic inflammation observed in atherosclerosis.

Interestingly in ECV304 cells native "self" LDL was more immunogenic that "non-self" oxLDL at 60 and 120 minutes. This discrepancy was not observed to a significant degree in the HUVEC cell line where each LDL ligand gave similar increased IL-6 and IL-8 responses in comparison to unstimulated cells. One would expect that the recognition of "non-self" ligands would cause augmented cytokine response in endothelial cells in comparison to "self" molecules. The reduced cell surface PRR expression that was observed may indicate internalisation of oxLDL which could have the effect of reducing cell surface signalling, in effect reducing a cell's immune capabilities. Such a process would suggest that internalisation of "non-self" ligands could have an immunosuppressive action, a form of immunoregulation. The immunosuppression of this ligand could shed light on its strong association with the inflammatory disorder causing atherosclerosis. The suppression of an appropriate immune response generated towards it, through reduced PRR expression and reduced cytokine release, may attenuate its clearance allowing chronic low level inflammation.

Overall this study demonstrates that the ECV304 cell line and HUVECs are capable of recognising and responding to LDL and its oxidised derivatives mmLDL and oxLDL, as well as bacterial ligands such as LTA from *S.aureus* and LPS from *E.coli*, *P.gingivalis* and *C.pneumoniae*. TLRs were found to be upregulated in response to the ligands in

both cell lines tested. In the ECV304 cell line the upregulation of TLR2, TLR4, TLR6, and CD36 expression mimicked the release of IL-6 and IL-8, whereas in HUVECs all ligands triggered a similar response. Interestingly, LDL was found to be more immunogenic in the ECV304 cells than its oxidized derivative (oxLDL), whereas in HUVECs all lipoproteins triggered a similar response, suggesting a cell-type specific response to these ligands.

4.3: Stimulations with combined ligands

Although the involvement of atherosclerosis-associated ligands has been widely investigated, the modulation that these ligands may have on one another has not. With the great likelihood of the existence of these ligands in unison, their effect on one another must be elucidated. Lipid emulsions have been shown to mop up LPS and LTA with the effect of reducing the inflammatory response *in vitro* and *in vivo*[221,222]. Also, as mentioned, lipid binding to LTA and LPS has been demonstrated in the lab of Dr. K. Triantafilou (University of Sussex. Mouratis *et al*. {submitted}). OxPAPC has been shown to inhibit LPS-induced MCP-1 and IL-8 release in HAECs[104]. As well as interacting with the ligand, modified LDL is thought to sequester signalling adapters. It has been proposed that OxPAPC causes inhibition of LPS signalling through the competitive binding of CD14, MD2 and LBP; the upstream adapter molecules in LPS signalling[103,153]. However, it has also been shown that *E.coli* LPS binding is enhanced by OxPAPC pre-incubation, suggesting greater complexity to lipoprotein regulation than adapter sequestration[104]. This “lipid immunoregulation” has been shown to be restricted to TLRs 2 and 4[153], through which atherosclerosis-associated bacteria signal. Whether endogenous LDL and/or its oxidised counterparts could have the same effect on atherosclerosis-associated bacteria was investigated.

PRR expression on ECV304 cells in response to combinations of endogenous lipoproteins with bacterial products was analysed via indirect immunofluorescence and flow cytometry. The combined stimulations were designed to simulate high plasma concentrations of LDL, a known risk factor of atherosclerosis, prior to infection. ECV304 cells and HUVECs were pre-incubated with LDL and its oxidised forms prior to bacterial exposure. This is the sequence of events that would most feasibly take place in the human vascular system. Furthermore, ECV304 cell and HUVEC inflammatory cytokine release in response to combinatorial stimulations was investigated using a flow cytometric cytokine bead array system.

It was found that LDL pre-incubation reduces cell surface receptor expression in response to the TLR4 agonist LPS from *E.coli* in the ECV304 cell line in comparison to PAMP alone. Pre-incubation with oxLDL reduces cell surface receptor expression in response to the TLR2 agonists LTA from *S.aureus* and LPS from *P.gingivalis* in the ECV304 cell line in comparison to PAMP alone. This data demonstrates that lipoprotein pre-incubation, a plausible *in vivo* scenario, can alter the typical pattern of cell surface receptor expression in response to a particular pathogen. Reduction in PRR expression would be expected to represent a diminished cellular response which would support an inhibitory role for LDL and its oxidised forms as shown in previous studies. oxLDL is most likely to exist *in vivo*, this reduces TLR2 expression which would suggest a reduction in the recognition of TLR2 bacterial ligands allowing chronic infection.

The capability of combinatorial stimulations of endogenous lipoproteins with bacterial products at initiating atherogenesis through activation of an innate immune response in ECV304 cells and HUVECs was analyzed. The inflammatory response induced in

vascular endothelial cells was determined by measuring cytokine levels in the cell supernatant using a flow cytometric cytokine bead array system and also western blots probing for phospho-IκB.

When ECV304 cells were pre-incubated with lipoprotein the inflammatory response was increased, this does not seem to mirror receptor TLR expression observed in the double stimulations which shows in the majority of cases reduced expression. This suggests that cellular signalling is occurring from areas other than the cell surface. Internalised receptors could be signalling from intracellular compartments. All pre-incubations with LDL, mmLDL and oxLDL and subsequent exposure to either LTA from *S.aureus* or LPS from *E.coli*, *P.gingivalis* and *C.pneumoniae* gave increased IL-6 and IL-8 concentrations in comparison to PAMP alone. Both IL-6 and IL-8 remained the predominant cytokines released from ECV304 cells. Pre-incubation with LDL caused the greatest increase in IL-6 and IL-8 serum concentrations in comparison to PAMP alone, whilst mmLDL and oxLDL pre-incubation gave similar results. This data indicates no immunoprotective role of LDL and its oxidised derivatives in ECV304 cells to atherosclerosis-associated bacteria, but further exacerbation of the immune response in the vascular wall contrary to previous research. An increased sensitivity to bacterial ligands when endogenous lipoprotein is present could perhaps clear an infection more efficiently preventing chronic inflammation, which may be atheroprotective. This study does however support a lesser immunostimulatory role of mmLDL and oxLDL when exposed to cells prior to bacterial PAMP in comparison to LDL. Discrepancies highlighted earlier in this work between immortalised ECV304 cells line and the primary HUVECs led us on to run these experiments in the primary cell line.

Similar results were obtained for the HUVEC cell line with regards to IL-6 levels released in response to the combinatorial stimulations, where attenuated release with pre-incubations with LDL, mmLDL or oxLDL prior to *S.aureus* LTA, *E.coli* LPS, *P.gingivalis* LPS or *C.pneumoniae* LPS in comparison to bacterial stimulation alone. There was no significant difference between the different LDL pre-incubations; these augmented the response to similar degrees. However, the release of the chemokine IL-8 differed in the HUVEC cell line in comparison to ECV304 cells in response to combined stimulations. In the combinatorial stimulations of LDL, mmLDL or oxLDL with *S.aureus* LTA, *E.coli* LPS and *C.pneumoniae* LPS the IL-8 serum concentrations were significantly reduced. This data obtained in the primary HUVEC cell line supports a role for LDL, mmLDL and oxLDL in the reduction of the response through reduced IL-8 release. Western blot for phospho-IκB demonstrated a reduction in NF-κB activation when cells were pre-incubated with lipoprotein, which would explain the reduced IL-8 response observed. Reduced release of the chemokine IL-8 would reduce the chemotaxis of immune cells, such as monocytes, to the site of infection (plaque). Such a scenario may also allow chronic infection.

Oxidised phospholipids have been shown to bind the adapter molecules CD14, MD-2 and LBP attenuating TLR4 signalling[103]. Data from this study demonstrates reduced *E.coli* LPS recognition in HUVECs, when LDL is present, supporting this. However, this does not explain the reduced signalling through TLR2. This studies data suggests a similar scenario may hamper TLR2 signalling, where adapter molecules may be sequestered by components of LDL and its modified counterparts. One such scenario could involve CD36. CD36 SR binds oxLDL, these receptors are involved in macrophage lipoprotein internalisation resulting in the formation of foam

cells[72,73,101,102]. Since CD36 is utilised in receptor clusters formed in response to TLR2 ligands, the binding of oxLDL to CD36 and its subsequent internalisation may reduce the abundance of CD36 for bacterial detection. This could cause a reduced sensitivity of cells to TLR2 ligands, in much the same manner as oxidised phospholipids attenuate LPS-induced responses by binding signalling adapter molecules.

Mouratis *et al*. (University of Sussex, submitted) have shown that lipids can bind LPS and LTA. Such findings may suggest complexes of lipid and PAMPs exist in the system. However, experiments where HAECs were rinsed after pre-incubation with modified lipoprotein still demonstrate reduced IL-8 response when exposed to *E.coli* LPS in comparison to *E.coli* LPS alone, suggesting regulation at the cell surface[104].

Together these data suggest immunoregulation of lipids could occur in solution and at the cell surface. My data demonstrates an ability of LDL, mmLDL and oxLDL to selectively dampen the release of the chemokine IL-8 in HUVECs, in response to TLR2 and TLR4 agonists. Western blot analysis of stimulated cell lysate has revealed reduced NF-κB activation when lipoprotein is present. These results indicate that high levels of LDL in a native or oxidised form can mask a pathogenic ligand reducing cellular response for its destruction and removal. The dampening of the cytokine release may allow infections to continue for sustained periods of time producing low-level chronic inflammation characteristic of atherosclerosis.

4.4: Is inflammation affected by the "sequence" of events?

To begin to determine the manner of this immunoregulation I investigated whether the sequence of introducing these ligands into the system would manipulate the

inflammatory response. Cells were either exposed to LDL, mmLDL or oxLDL at the same time as the bacterial PAMP (LTA from *S.aureus* or LPS from *E.coli*, *P.gingivalis* or *C.pneumoniae*) or after bacterial exposure. These results were compared with the data from the lipoprotein incubations prior to bacterial PAMP exposure. Again, alternate results were obtained for IL-6 and IL-8. IL-6 levels in response to *S.aureus*, *E.coli*, *P.gingivalis* and *C.pneumoniae* were increased when cells were pre-incubated with lipoprotein as described. However, when lipoprotein and PAMP were exposed to HUVECs simultaneously or lipoprotein after PAMP, this augmented IL-6 release was lost and levels similar to that observed with PAMP alone were recorded. Both pre- and post-incubation with lipoprotein, in relation to PAMP exposure, gave diminished IL-8 response in comparison to bacterial PAMP alone. Competitive binding of TLR signalling adapters can be used to explain why I saw a dampened IL-8 response in HUVECs when oxLDL is added prior to PAMP[103]. However the increased IL-6 release that was observed in these same stimulations does not fit this theory. The diminished IL-8 response in comparison to bacterial PAMP alone in stimulations where PAMP was exposed to the cells prior to lipoprotein could also occur through the competitive binding of adapter molecules. This does however provoke interest when thinking of drug targets for this disease, due to the practicality of intervention. When lipoprotein and PAMP were exposed to HUVECs at the same time an increased IL-6 and IL-8 response was seen in relation to PAMP alone with the exception of oxLDL with *E.coli* LPS. Perhaps here oxLDL has not had sufficient time to competitively inhibit TLR2 and/or TLR4 signalling, or the PAMP has a higher affinity for the adapter molecules.

4.5: Lipid rafts in atherosclerosis

Lipid rafts are islands of highly ordered saturated lipids and cholesterol present in a fluid disordered bilayer of largely unsaturated lipids of the cell membrane. These domains have been shown to act as platforms for the concentration and oligomerization of mediators of the innate immune system, in order to facilitate signal transduction across the membrane[130,131]. In this study the role of lipid rafts in the activation of the innate immune response that was observed in HUVECs in response to atherosclerosis-associated ligands was investigated.

Lipid raft disruption was achieved by incubating HUVECs with 60µg/ml Nystatin for ten minutes prior to stimulation. It was found that HUVEC activation via single stimulations with atherosclerosis-associated ligands required lipid rafts. Both IL-6 and IL-8 serum concentrations were reduced in response to LDL, mmLDL, oxLDL, *S.aureus* LTA, *E.coli* LPS, *P.gingivalis* LPS and *C.pneumoniae* LPS. This supports previous work by Triantafilou *et al*. (2002)[201] who demonstrate reduced LPS-induced TNF-α secretion in human monocytes on lipid raft disruption. Impaired cytokine release due to lipid raft disruption has also been demonstrated in response to Pam_3CSK_4, a synthetic bacterial lipoprotein that signals through TLR2/1[223], which is also in compliance with my data. Zeng *et al*. (2003)[224] have shown that oxLDL is endocytosed in a lipid raft-dependant manner via CD36, suggesting a role for lipid rafts in foam cell formation as well as cell signalling. Combined stimulations where HUVECs were pre-incubated with LDL, mmLDL or oxLDL prior to *S.aureus* LTA, *E.coli* LPS, *P.gingivalis* LPS and *C.pneumoniae* LPS were also found to be lipid raft dependant. The reduction in IL-6 and IL-8 concentration was significant in the combined stimulations, but was observed to a lesser extent than seen with the lipoprotein or

bacterial single stimulation. This data suggests that double stimulations are less dependent on lipid rafts for signal transduction. Perhaps the ability of lipoprotein derived lipids and bacterial ligands to form complexes may reduce their dependence on lipid rafts. A lipid/PAMP complex may act as a scaffold by interacting with a greater number of receptors bringing them together for signal transduction, much like the lipid raft.

Confocal microscopy revealed the importance of lipid rafts in the HUVEC innate immune mechanisms. Immunofluorescent labelling of PRRs and cellular compartments of HUVECs grown on microscope slides demonstrated that the altered cellular signalling due to lipid raft disruption that was observed is likely caused through altered trafficking of receptors. The trafficking and targeting of receptors in relation to the Golgi and lipid rafts was viewed. HUVEC slides were treated with Nystatin as before, and then stimulated and then labelled with fluorescent antibodies. *S.aureus* LTA was capable of causing recruitment of TLR2 to lipid rafts and the Golgi as observed using confocal microscopy. When Nystatin was used to disrupt lipid rafts on HUVECs, which were then subsequently stimulated with *S.aureus* LTA, any TLR2 association with the Golgi was lost. The loss of TLR association with the Golgi observed here was apparent for all stimulations in this study, including combined lipoprotein and PAMP stimulations. It was found that lipid rafts are essential for receptor internalization and targeting to compartments such as endosomes and organelles such as the Golgi. This is in compliance with Zeng *et al*. (2003)[224] who demonstrate that oxLDL is endocytosed from the cell membrane in a lipid raft-dependant manner.

4.6: Receptor associations in response to endogenous lipoproteins and bacterial ligands

To observe the recruitment of TLR2 to lipid rafts in HUVECs in response to atherosclerosis-associated ligands, FRET was utilised. TLR2 molecules were labelled with Cy3-TL2.1 and GM-1 ganglioside, a raft-associated lipid, was labelled with Cy5-cholera toxin. This technique allows one to quantify associations between fluorescently labelled molecules if they are ≤10nm apart. The significant recruitment of TLR2 to lipid rafts on HUVECs in response to LDL, mmLDL, oxLDL, *S.aureus* LTA, *P.gingivalis* LPS and *C.pneumoniae* LPS was shown. There was little recruitment of TLR2 to lipid rafts seen with *E.coli* LPS. To see whether lipoprotein pre-incubation affects TLR2 recruitment to lipid rafts FRET was performed on combinatorial HUVEC stimulation experiments. It was found that LDL and mmLDL pre-incubation gave little change to the recruitment of TLR2 to lipid raft domains in comparison to *S.aureus* LPS, *P.gingivalis* LPS and *C.pneumoniae* LPS alone. LDL and mmLDL pre-incubation caused TLR2 association with lipid rafts when combined with *E.coli* LPS. However, oxLDL pre-incubation prior to *S.aureus* LTA, *P.gingivalis* LPS and *C.pneumoniae* LPS exposure was found to significantly reduce TLR2 recruitment to lipid rafts by ≥50%, even though the ligands separately were capable of causing significant TLR2 recruitment. The ability of oxLDL pre-incubation to reduce IL-8 release in HUVECs may be explained by its ability to reduce TLR2 recruitment to lipid rafts. Similarly, Walton *et al.* (2003)[104] found that the LPS-induced recruitment of TLR4 and MD-2 to caveolar membrane compartments is reduced when OxPAPC is present reducing cellular response. It seems that oxLDL may disrupt the interaction between lipid rafts and PRRs, as observed with caveolar and TLR4 and MD-2. Previous data in this study illustrates the importance of lipid rafts in cellular response to atherosclerosis-associated

ligands. This data demonstrates that oxLDL can distort the interaction between TLR2 and lipid rafts with the effect of modulating cellular response to a PAMP, through reduction of IL-8. I then went on to explore whether the reduced recruitment of TLR2 to lipid rafts, due to the presence of oxLDL, affects its heterotypic associations with other receptors of the innate immune system.

FRET experiments were performed with HUVECs to quantify the interaction between TLR2 and its associated receptors TLR1, TLR6 and CD36 in response to atherosclerosis-associated ligands and combinations thereof. TLR2 was labelled with Cy3-TL2.1 whilst TLR1, TLR6 and CD36 were labelled with Cy5. In unstimulated cells it was found that there was no association between these receptors. In response to LDL, mmLDL and oxLDL a TLR2/TLR6/CD36 receptor cluster was formed in lipid rafts, this was also the case for *S.aureus* LTA. It was found that the unconventional LPS molecules from *P.gingivalis* and *C.pneumoniae* caused a lipid raft-associated TLR2/TLR1/CD36 receptor cluster. This data agrees with that demonstrating receptor clusters incorporating TLR2/TLR1/CD36 and CD11b/CD18 in human vascular endothelial cells in response to the atherosclerosis-associated bacteria *P.gingivalis* and *H.pylori*[51]. *E.coli* LPS caused no association of receptors with TLR2.

When HUVECs were pre-incubated with LDL, mmLDL and oxLDL the receptor clusters formed in response to further bacterial stimulation were altered in comparison to PAMP alone, with the exception of *S.aureus* LTA. The double stimulations had an additional effect on the receptor cluster. For example, *P.gingivalis* LPS and *C.pneumoniae* LPS similarly cause a TLR2/TLR1/CD36 cluster, when HUVECs were pre-incubated with either LDL, mmLDL or oxLDL (which all cause a

TLR2/TLR6/CD36 cluster) a receptor cluster of TLR2/TLR1/TLR6/CD36 was observed in lipid rafts. This may indicate the recruitment of two separate clusters to the lipid raft, or the interaction of a larger number of receptors in a more complex cluster on the HUVEC cell surface causing the disruption to cellular signalling observed. This data could explain the reduced requirement for lipid rafts that was shown for combined stimulations in raft disrupted HUVECs. Interestingly, it was observed that oxLDL pre-incubation dramatically reduced, and in the case of *E.coli* LPS almost abolished, TLR2 interaction with TLR1, TLR6, CD36 and the lipid raft. Again, although oxLDL is capable of causing a lipid raft-associated TLR2/TLR6/CD36 cluster, when combined with a bacterial PAMP any TLR2 association is dramatically diminished. In the case of *S.aureus* LTA, *P.gingivalis* LPS and *C.pneumoniae* LPS single stimulations in comparison to these combined with oxLDL the TLR2 association with either TLR1, TLR6 or CD36 are reduced by around 40-50%, as seen with the recruitment of TLR2 to the lipid raft. This data suggests that a reduction in receptor association due to oxLDL requires the presence of a bacterial PAMP; oxLDL alone does not dampen TLR2 associations with PRRs or lipid rafts.

TLR2 expression, recruitment to lipid rafts and heterotypic associations in response to oxLDL pre-incubations begins to shed light on the immune modulation observed. My data indicates that TLR2 is involved in the recognition of atherosclerosis-associated oxLDL, *S.aureus* LTA, *P.gingivalis* LPS and *C.pneumoniae* LPS. Previous studies have shown an involvement of TLR2 in plaque development such as that of Madan *et al*. (2008)[160] who demonstrated that *ApoE*$^{+/-}$*Tlr2*$^{-/-}$ mice had reduced cytokine levels and lesion size in comparison to *ApoE*$^{+/-}$*Tlr2*$^{+/+}$ mice when fed on a high fat diet, or when subject to *P.gingivalis*. Similar studies have also demonstrated a role for TLR4 in

atherosclerosis. The genetic deficiency of TLR4 in the atherosclerosis prone *ApoE*$^{-/-}$ mouse resulted in reduced total lesion area in comparison to control wild-type TLR4 *ApoE*$^{-/-}$ mice, when both were fed on a high-cholesterol diet[152]. To elucidate further the involvement of TLR2 and TLR4 in atherosclerosis, and the modulation that endogenous lipoprotein has on their ligand recognition, HEK293 cells expressing either TLR2 or TLR4 were employed.

4.7: TLR2, TLR4 and CD36 in atherosclerosis

Results obtained from experiments on transfected HEK293 cells demonstrate a preference of LDL and oxLDL for TLR4 and TLR2 respectively. Mullick *et al.* (2005)[161] demonstrated that atherosclerosis prone *Ldlr*$^{-/-}$ mice that do not express TLR2 (*Ldlr*$^{-/-}$*Tlr2*$^{-/-}$) have reduced lesion size in comparison to *Ldlr*$^{-/-}$ mice expressing TLR2 (*Ldlr*$^{-/-}$*Tlr2*$^{+/+}$) in the absence of any exogenous agonist. This study indicates an endogenous activator of plaque formation, signalling through TLR2. My data suggests that the endogenous activator of atherosclerosis speculated by Mullick *et al*. is oxLDL. mmLDL seems to signal though both TLR2 and TLR4, this could indicate a heterogeneous mixture.

Here this study confirms the unconventional signalling of the LPS molecules from *P.gingivalis* and *C.pneumoniae,* which were capable of causing augmented cytokine release in HEK293 cells expressing TLR2 (HEK TLR2) but not in HEK TLR4 cells. As expected the prototypic Gram-positive PAMP *S.aureus* LTA and Gram-negative PAMP *E.coli* LPS were shown to signal through TLR2 and TLR4 respectively.

Both HEK TLR2 and HEK TLR4 were capable of mounting a response to all combined stimulations. When HEK TLR2 and HEK TLR4 cells were pre-incubated with lipoprotein and then subsequently stimulated with a bacterial ligand the immune response, in the form of IL-8 release, was enhanced with the exception of *P.gingivalis* LPS with mmLDL in HEK TLR2 cells. This data conflicts with previous data obtained with HUVECs in this study, which showed a protective role of oxLDL. The difference in findings could be solely due to the cell line or may indicate that the protective role of oxLDL acts via a mechanism involving receptors on HUVECs that were not present on the HEK cell line, such as CD36. One ligand could have an adapter role for the other much like CD14 in LPS recognition. For example, oxLDL could enhance TLR2 binding of *S.aureus*. However, this theoretical role may be reduced in HUVECs by the sequestration of the "adapter" ligand by cellular receptors, such as CD36, that are not found on HEK cells. Lipoproteins may enhance PAMP recognition but when CD36 is present, for example, the lipoprotein is bound and internalized, possibly with PAMP, as a form of immune regulation.

A dramatic difference between single and combined stimulations was seen in the HEK TLR4 cell line. For example, HEK TLR4 exposure to either oxLDL or *C.pneumoniae* LPS was very poor at causing IL-8 release, although when these were simultaneously exposed to HEK TLR4 cells a significant IL-8 response was observed. A role for TLR4 in atherosclerosis was shown by Michelsen *et al*. (2004)[152] who demonstrated reduced total lesion area, reduced macrophage infiltration and reduced monocyte chemotactic protein-1 (MCP-1) serum concentrations in the *ApoE*$^{-/-}$*TLR4*$^{-/-}$ mouse in comparison to control *ApoE*$^{-/-}$*TLR4*$^{+/+}$ mice. My data suggests that lipoproteins enhance cellular sensitivity to bacterial ligands in HEK TLR4 cells.

To explore the individual role of CD36 in atherosclerosis, silencing technology to reduce CD36 cell surface expression on primary endothelial cells was employed. CD36 expression on primary HUVECs was silenced by transfection with CD36 psiRNA plasmid.

CD36 silencing reduced the cellular response to both LDL and oxLDL indicating the requirement of CD36 in lipoprotein binding. CD36 SR expressed on macrophages has been shown to bind oxLDL, where it is engulfed leading to foam cell formation[73,101,102]. Data from this study suggests that CD36 is also involved in the binding of native LDL. Interestingly it was found that CD36 favoured LDL over oxLDL. A greater reduction in IL-6 and IL-8 concentrations were observed in CD36 silenced HUVECs in response to LDL in comparison to oxLDL. CD36 silenced HUVEC IL-6 concentrations were also lower in response to *S.aureus* LTA, *E.coli* LPS and *P.gingivalis* LPS demonstrating its involvement in PAMP recognition. The greatest reduction was seen with *P.gingivalis* LPS where a reduction of ~50% in IL-6 serum concentration was observed in comparison to wild-type HUVECs. CD36 associates with TLR2[173]. These findings support previous FRET data and other studies demonstrating CD36 involvement in the receptor cluster formed in response to *P.gingivalis* LPS shown as TLR2/TLR1/CD36[51] and *S.aureus* LTA shown as TLR2/TLR6/CD36[208]. IL-8 concentrations released by CD36 silenced and wild-type HUVECs in response to bacterial products were unaffected. These results show that CD36 is important in the generation of a response via IL-6 for both lipoprotein and bacterial stimuli. This data also highlights that CD36 is involved in lipoprotein-induced but not bacterial-induced IL-8 release. When cells were pre-incubated with lipoprotein, both IL-6 and IL-8 serum concentrations were reduced in CD36 silenced HUVECs in comparison to wild-type HUVECs. The reduction of IL-6

was greater than that observed with IL-8. There was no significant difference between cytokine reductions between different lipoprotein pre-incubations. My data demonstrates the involvement of CD36 in the inflammatory response generated towards atherosclerosis-associated ligands and combinations thereof.

Data obtained in this study from HEK293 cells and CD36 silenced HUVECs has demonstrated the involvement of TLR2, TLR4 and CD36 in the recognition of atherosclerosis-associated ligands and combinations of these. By manipulating receptor expression, varied levels of response were observed. The reason for the locality of atheroma development is speculated to be due to differential expression of TLRs throughout the vascular system, or due to disturbed flow. Pryshchep *et al*. (2008)[168] illustrated heterogeneous TLR expression in the subclavian, mesenteric, iliac, and temporal arteries. On the other hand, the increased susceptibility to plaque initiation has been attributed to disturbed blood flow in the artery which creates shear stresses that adversely affects the biology of the arterial wall[169]. My data has shown that differential PRR expression does indeed affect cellular response to atherosclerosis-associated ligands. As shown by Pryshchep *et al*. (2008)[168], heterogeneous expression of TLRs in human arteries exists. This study would support that plaque formation is attributed to differential expression of TLRs throughout the vascular system and suggests that this is also true for adapters of the TLR family, such as CD36.

Not only has this study implicated the involvement of TLR2, TLR4 and CD36 in atherosclerosis, but it has also established that lipid raft-associated receptor clusters formed in response to bacterial stimulation are altered when cells are pre-incubated with lipoprotein. This has the effect of modifying cellular response, in the form of cytokine

release. FRET data from my study has illustrated that pre-incubation with oxLDL reduces TLR2 recruitment to lipid rafts and the association of TLR2 with receptors such as TLR1, TLR6 and CD36. To image the altered fate of the receptors observed in this study, triple label confocal microscopy was employed.

4.8: Intracellular trafficking and targeting in response to endogenous lipoproteins and bacterial ligands

Cell surface receptor associations allow a tailored response to an invading pathogen. The inflammatory response in atherosclerosis seems to have become dysregulated allowing chronic inflammation characteristic of this disease. My data has shown that circulating lipoprotein can disrupt the regular cellular response tailored for a specific bacterial ligand by altering PRR expression, PRR localisation, NF-κB activation and cytokine release. FRET data from this study has shown oxLDL pre-incubation causes reduced association of TLR2 with lipid rafts and reduced heterotypic associations of TLR2 with TLR1, TLR6 and CD36, suggesting altered trafficking and targeting of PRRs. Thus this study proceeded to employ triple label confocal microscopy in order to image the effect of lipoprotein pre-incubation on PRR associations, trafficking and targeting in the primary HUVEC cell line in response to atherosclerosis-associated bacterial ligands and combinations of these. In addition the TLR signalling adapter MyD88 was labelled to image the localisation of TLR signalling in these different situations.

Confocal imaging uncovered that PRR targeting and localisation in response to bacterial PAMP was indeed altered when cells were pre-incubated with lipoprotein. Confocal microscopy of HUVECs stimulated with oxLDL alone demonstrated high accumulation

of CD36 and TLR2 in endosomes (data not shown). It has been previously demonstrated that oxLDL causes CD36 internalisation into endosomal structures, which is supported by oxLDL single stimulation images in this study[224]. The pre-incubation of HUVECs with oxLDL prior to *S.aureus* LTA altered TLR2, CD14 and CD36 localisation in comparison to *S.aureus* LTA stimulation alone. TLR2, CD14 and CD36 targeting to the Golgi and endosomal compartments, that was observed with *S.aureus* LTA single stimulation, was significantly reduced when oxLDL was present.

In addition to reducing the PRR intracellular targeting to the Golgi and endosomal compartments, oxLDL seemed to target TLR2 to distinct cellular compartment other than the Golgi or endosomes. It is possible that these distinct cellular compartments may be lysosomes. Although this study did not have enough time to verify this, Itabe *et al*. (2000)[225] have demonstrated lysosomal accumulation of oxLDL derived products, thus suggesting that the distinct cellular compartments that are being observed are most likely lysosomes. Itabe *et al*. (2000) show that the oxLDL derived OxPC colocalised with lysosomal markers in murine macrophages. oxLDL products targeted to lysosomes may be TLR2 bound resulting in the lysosomal expression of TLR2. Interestingly, I did not observe any of these distinct compartments when cells were pre-incubated with LDL. This may be due to the fact that LDL targeted to lysosomes can be cleared effectively, whereas oxidatively modified LDL has been shown to be more resistant to lysosomal degradation than native LDL[217], a theory behind oxLDL accumulation in foam cells. Taking together the effective clearance of LDL from lysosomes and the reduced binding of TLR2 with LDL in comparison to oxLDL, one would not expect high levels of lysosomal accumulation of TLR2 bound LDL.

In contrast to oxLDL, LDL pre-incubation of HUVECs prior to stimulation with bacterial ligands had little effect on the intracellular targeting of PRRs in comparison to bacterial single stimulation, suggesting that only its fully oxidatively modified derivative alters PRR targeting.

The presence of oxidized lipoprotein within a cellular compartment would suggest room for error. Bacteria/oxLDL complexes being internalised together may somehow disrupt trafficking and normal processing of the bacterial products in intracellular compartments along with their associated PRRs with an atherogenic outcome. Not only would this altered trafficking affect the accumulation of lipoprotein within a cell, leading to foam cell formation, but it would disrupt the signalling emanating from the PRRs.

This study also shows altered localisation of MyD88 when cells were exposed to oxLDL. The recruitment of MyD88 to lipid rafts on HUVECs in response to *S.aureus* LTA, *E.coli* LPS and *P.gingivalis* LPS alone was reduced by 25%, 26% and 25% respectively when cells were pre-incubated with oxLDL. This may cause reduction in NF-κB activation, as observed. However, oxLDL did not significantly reduce the association between MyD88 and TLR2 when exposed to HUVEC prior to PAMP. This suggests that TLR signalling may occur from compartments other than lipid rafts when lipoprotein and PAMP are present. Intracellular signalling through cell surface receptors may lack conventional regulation allowing dysregulated inflammation.

4.9: Current therapeutic interventions

Currently, statins are used widely by physicians to prevent events such as stroke or heart attack. These drugs are HMG-CoA reductase inhibitors resulting in reduced cholesterol

synthesis and increased LDL receptor (LDLR) expression on liver cells, further reducing cholesterol levels by increased uptake of LDL. A number of trials have demonstrated how effective statins are at reducing LDL cholesterol with the effect of reducing intima media thickness, myocardial infarction, stroke, by-pass graft atherosclerosis and overall mortality[226-229]. The success of these drugs is reflected in their use in huge numbers in healthcare today. It has been shown that statin therapy also has the effect of reducing inflammatory markers such as CRP[229,230], thus suggesting that the secret of their success could lie in their targeting of the inflammatory response.

It is believed that the observation of reduced inflammation may begin to be able to explain the pleiotropic effects observed with statin therapy. The reversal of atherosclerosis with aggressive lipid lowering (REVERSAL)[229] trial demonstrated CRP level reductions of 36% in CAD patients after 18 months treatment with 80mg Pravastatin daily. Reduced CRP levels in response to statins were also demonstrated in the Pravastatin inflammation/CRP evaluation study (PRINCE)[231], supporting their anti-inflammatory effect. Rosenson *et al*. (1999)[232] demonstrated a 31% and 26% reduction in TNFα and IL-6 levels respectively in hypercholesterolemic patients after administration of 40mg Pravastatin per day for 7 weeks. Here, Rosenson speculates that reduced plasma lipoproteins would free up PAMPs, thus increasing inflammatory markers when individuals are treated with statins. His results along with others demonstrate the reverse of this, possibly allowing chronic infection. This study demonstrates an immunoregulatory role of oxLDL, as do others. It could be suggested that the removal of this immunoregulatory LDL may allow effective clearing of chronic infections, rather than allow one to persist. The effective clearing of chronic infections would have the effect of reduced inflammatory markers such as IL-6 and CRP, as

observed in these statin trials. The use of statins may disrupt the delicate environmental niche utilised by atherosclerosis-associated bacteria for survival and proliferation. A naturally occurring niche enhanced by the Western life style.

4.10: PRR-based therapeutic interventions

It seems that for a future therapeutic intervention to be successful the inflammatory response triggered either by the endogenous lipoproteins, bacterial pathogens or combinations of both must be targeted. With the discovery of PRRs as central to the inflammatory response in atherosclerosis, the potential to reduce or even inhibit this inflammation seems more achievable.

Throughout this study it has been shown that the disruption of innate immune receptor complexes by the presence of lipoprotein can dysregulate the inflammatory response generated towards a PAMP; possibly leading to atherosclerosis. oxLDL exposure has been shown to reduce PRR cell surface expression with the effect of reducing cellular release of the chemotactic cytokine IL-8 in response to a PAMP. Atherosclerosis is an inflammatory disorder; a reduction in inflammation would be thought to be advantageous. However, whether this reduced inflammation caused by oxLDL is atheroprotective is unclear. On one hand, the inflammation is reduced which would decrease infiltration of immune cells into the arterial intima reducing the chance of plaque formation. On the other hand, a reduction in inflammation through disrupting cellular response to a PAMP may allow colonisation of a pathogen by, in effect, masking its presence.

It is hypothesised that the modulation of this immune response could have therapeutic potential. A number of studies have shown that the deficiency of components of innate

TLR signalling in mice, such as MyD88[159], TLR2[160,161] and TLR4[152], is atheroprotective. This study went on to explore the blocking of the endogenous and microbial sensing apparatus *in vivo* to determine the possible beneficial effects of TLR directed therapeutics in the prevention of atherosclerosis. A male CD-1 out-bred mouse model of sepsis was used to test previously established *in vitro* blockers of innate immunity. The sepsis mouse model was chosen for it displays an over-reaction of the innate immune response, producing dysregulated inflammation, with a short and clear end point. This model has been used in a large number of studies and has proved fruitful in the production of drugs transferable to human subjects. The analysis of these *in vitro* blockers in the sepsis mouse model would determine their efficacy in inflammation reduction so that this study can go on to test these in a more delicate model of atherosclerosis.

The *in vitro* established blockers of inflammation tested in this study for their potential in the treatment of atherosclerosis included HSP70 and AMD3100. Dr. K. Triantafilou (University of Sussex) has demonstrated the ability of HSP70 and AMD3100 at modulating the innate mechanisms. HSP70 has been shown to reduce the expression of TLRs 2, 4, 6, 7, 8 and 9, diminishing cellular immune capabilities. Exogenous HSP70 has been shown to inhibit LPS-induced inflammatory responses in monocytes[141]**.** AMD3100 has been shown to inhibit the formation of the "LPS-sensing apparatus" reducing cellular response to LPS (Triantafilou *et al*. {unpublished data}). These molecules were tested for their efficacy in the prevention of inflammation and ultimately mortality in an *in vivo* model of sepsis. Therapy that is capable of dampening or terminating the inflammation seen in atherosclerosis after the condition has been discovered is of greatest interest, for practically this is when plaques are discovered. In this study these immunomodulators were mainly tested after the induction of

inflammation/sepsis in the mouse model in order to analyze their immune regulatory capabilities.

Intraperitoneal injection of HSP70 was found to be very effective at decreasing sepsis-induced mortality in CD-1 male mice. HSP70 administration after LPS exposure gave better survival rates than HSP70 treatment prior to the induction of sepsis. HSP70 was most effective at preventing septic shock when injected 2 and 4 hours post-sepsis induction, where 87.5% survival was observed at 72 hours. Blood sample concentrations of TNF-α, IL-12, IFN-γ and IL-10 were all reduced in mice treated with HSP70 in comparison to those that were not. At 12 hours all HSP70 administration protocols achieved TNF-α concentrations between 27-34% of the control untreated sepsis model. Although post 2 and 4 hour i.p injection of HSP70 conferred better survival rates this was not necessarily reflected in cytokine levels. However, the reduction for each protocol was significant none the less, and all achieved survival.

AMD3100 was found to be effective at conferring survival in sepsis induced CD-1 male mice. This molecule was not as successful as HSP70. Interestingly AMD3100, like HSP70, was most effective when administered 2 and 4 hours post LPS administration. AMD3100 injection at 2 and 4 hours post-LPS gave 65% survival at 72 hours. Post-1 hour administration of AMD3100 was the least successful giving 25% survival at 72 hours.

These two molecules can clearly modulate the innate immune response. HSP70 has a more general effect by lowering all TLRs rather than just attenuating TLR4 signalling as performed by AMD3100. Therefore, both seem excellent candidates in order to be tested in an atherosclerotic mouse model in the future.

4.11: Concluding remarks

Atherosclerosis is a multi-factorial disease that is characterized by the formation of plaques in arterial blood vessel walls. Early stages of plaque formation are asymptomatic allowing them to grow insidiously increasing an individual's risk of stroke or heart attack, unbeknown to them. Once considered a lipid storage defect, atherosclerosis is now widely accepted to be due to a chronic inflammatory disorder. Inflammation from innate immune mechanisms are implicated in atherogenesis and plaque disruption. TLRs have been suggested as the initiators of the inflammatory response, but the precise triggers are not fully understood. Triggers, which have been suggested include hypercholesterolemia, modified lipoproteins and infections with bacterial pathogens such as *C.pneumoniae* or *P.gingivalis*.

Previous studies have implicated microbial products in the initiation and/or promotion of the inflammatory process in atherosclerosis. My data shows for the first time that specific microbial ligands synergize with host-derived lipoproteins for induction of dysregulated inflammatory responses, which are dependent on interactions with TLR-centred receptor clusters in membrane lipid rafts. This study has focused on the emerging role of the innate immune system in atherosclerosis, and has uncovered TLRs as fundamental culprits of this multi-factorial disease. Future therapy designed for this disorder will unquestionably involve the manipulation of TLR signalling.

4.11.1: Proposed model

Based on the findings of this study, a model for the initiation of atherosclerosis is proposed. In this model elevated levels of low density lipoprotein, such as oxLDL, make us prone to mount a chronic pro-inflammatory response to a bacterial pathogen if subsequently infected. Inflammation characteristic of atherosclerosis. TLR2 seems to be the central receptor involved in vascular endothelial cell activation in atherosclerosis, recognising both endogenous and exogenous atherosclerosis-associated ligands. Therefore, disease progression could be due to low-level chronic inflammatory responses triggered by microbial infections via TLR2 with engagement of LDL derived endogenous ligands, resulting in the formation of atherosclerotic lesions.

An example based on this studies findings proposed in this model is LPS from *P.gingivalis*, a bacteria associated with increased risk of atherosclerosis. It has been found that a lipid emulsion can mop up LPS and LTA with effect of reducing the inflammatory response *in vitro* and *in vivo*[233,234]. For this reason one may hypothesize that a complex of LPS or LTA with lipid could exist in the system. Both lipid and PAMP are recognised by PRRs that exist on the cell surface. PAMP via TLR and lipid via the well described CD36 SR[173]. Data from this study, supporting that from others, demonstrates lipid raft-associated receptor complexes formed in response to challenge by factors associated with atherosclerosis can contain a number of PRRs including associations between TLR2/1 and CD36; receptors that bind *P.gingivalis* LPS and oxLDL respectively[51]. As shown in this study and by others, LPS from *P.gingivalis* is unconventional in that it signals through a receptor complex containing TLR2/1 and CD36, not the TLR4 endotoxin receptor, in a lipid raft dependant manner[51,235,236]. Given this, one would reasonably expect an LDL/LPS composite to bind the same lipid raft linked receptor complex, in a foursome bound formation, where ligands and receptors

all interact (Figure 4.1). This may causes the dysregulation observed at the cell surface, as previously suggested[104]. The subsequent targeting of receptor/ligand, signalling and processing of these factors, when in concert, must be distorted; as observed in this study.

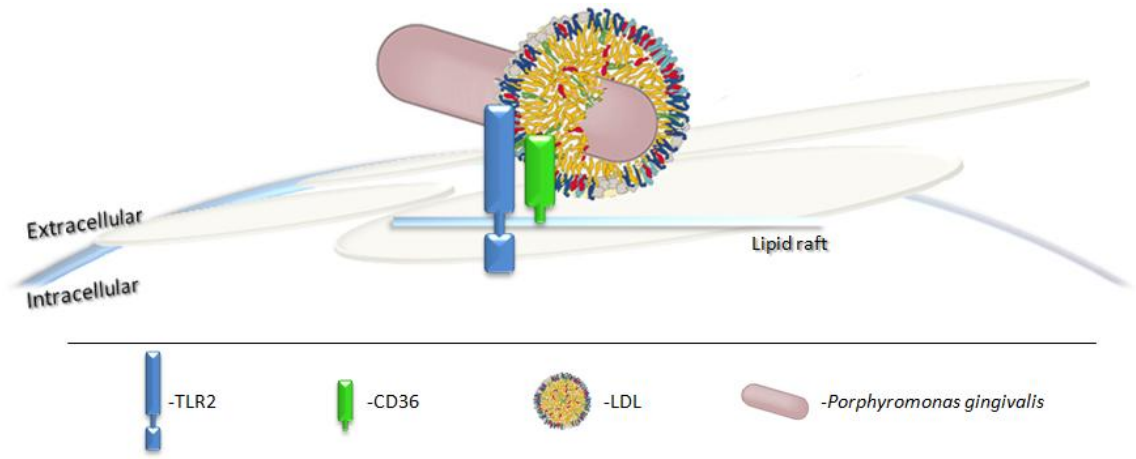

Figure 4.1: Hypothetical model of LPS/oxLDL and receptor cluster interactions: *P.gingivalis* (purple) binds TLR2 (blue)/CD36 (green) receptor complex. oxLDL (yellow) is bound by CD36 SR (green). TLR2/CD36 is localised to lipid rafts (labelled). Hypothesis: oxLDL/LPS bind the same receptor complex, which contains TLR2 (LPS) and CD36 (oxLDL) in a foursome bound formation resulting in the disruption of ligand processing and cellular signalling.

4.12: Future work

- Elucidate the component of oxLDL that produces the effects on innate immune signalling to bacterial PAMPs observed in this study.
- Look at the cause of combined stimulations on macrophages and whether this may lead to foam cell formation.
- Elucidate the therapeutic potential of HSP70 and AMD3100 in atherosclerosis, through *in vitro* experimentation on primary HUVECs exposed to endogenous lipoprotein and bacterial combined stimuli, with the inclusion of either HSP70 or AMD3100.
- If HSP70 and AMD3100 demonstrate potential *in vitro*, then these will be tested on C57BL/6 mice that lack a functional LDL receptor (*Ldlr*$^{-/-}$). Further exposure of these mice with atherosclerosis associated bacteria may prove to be an excellent model to investigate interventions of atherosclerosis explored in this study.

References

Reference List

1. Allender.S *et al.* European Cardiovascular Disease Statistics 2008. *European Heart Network* (2008).

2. Hangartner,J.R., Charleston,A.J., Davies,M.J. & Thomas,A.C. Morphological characteristics of clinically significant coronary artery stenosis in stable angina. *Br. Heart J.* **56**, 501-508 (1986).

3. Libby,P. Molecular bases of the acute coronary syndromes. *Circulation* **91**, 2844-2850 (1995).

4. Hansson,G.K. & Libby,P. The immune response in atherosclerosis: a double-edged sword. *Nat. Rev. Immunol.* **6**, 508-519 (2006).

5. Kiechl,S. *et al.* Chronic infections and the risk of carotid atherosclerosis: prospective results from a large population study. *Circulation* **103**, 1064-1070 (2001).

6. Ross,R. Atherosclerosis--an inflammatory disease. *N. Engl. J. Med.* **340**, 115-126 (1999).

7. Naghavi,M. *et al.* Association of influenza vaccination and reduced risk of recurrent myocardial infarction. *Circulation* **102**, 3039-3045 (2000).

8. Edfeldt,K., Swedenborg,J., Hansson,G.K. & Yan,Z.Q. Expression of toll-like receptors in human atherosclerotic lesions: a possible pathway for plaque activation. *Circulation* **105**, 1158-1161 (2002).

9. Jonasson,L., Holm,J., Skalli,O., Bondjers,G. & Hansson,G.K. Regional accumulations of T cells, macrophages, and smooth muscle cells in the human atherosclerotic plaque. *Arteriosclerosis* **6**, 131-138 (1986).

10. ANITSCHKOW,N. [On the morphodynamics of coronary sclerosis of the heart.]. *Acta Pathol. Microbiol. Scand.* **49**, 426-432 (1960).

11. Fabricant,C.G., Fabricant,J., Litrenta,M.M. & Minick,C.R. Virus-induced atherosclerosis. *J. Exp. Med.* **148**, 335-340 (1978).

12. Lehr,H.A. *et al.* Immunopathogenesis of atherosclerosis: endotoxin accelerates atherosclerosis in rabbits on hypercholesterolemic diet. *Circulation* **104**, 914-920 (2001).

13. Rifai,N. & Ridker,P.M. Proposed cardiovascular risk assessment algorithm using high-sensitivity C-reactive protein and lipid screening. *Clin. Chem.* **47**, 28-30 (2001).

14. Ridker,P.M. *et al.* Rosuvastatin to prevent vascular events in men and women with elevated C-reactive protein. *N. Engl. J. Med.* **359**, 2195-2207 (2008).

15. Kiechl,S. *et al.* Chronic infections and the risk of carotid atherosclerosis: prospective results from a large population study. *Circulation* **103**, 1064-1070 (2001).

16. Mayr,M., Kiechl,S., Willeit,J., Wick,G. & Xu,Q. Infections, immunity, and atherosclerosis: associations of antibodies to Chlamydia pneumoniae, Helicobacter pylori, and cytomegalovirus with immune reactions to heat-shock protein 60 and carotid or femoral atherosclerosis. *Circulation* **102**, 833-839 (2000).

17. Mayr,M. *et al.* Increased risk of atherosclerosis is confined to CagA-positive Helicobacter pylori strains: prospective results from the Bruneck study. *Stroke* **34**, 610-615 (2003).

18. Sasu,S., LaVerda,D., Qureshi,N., Golenbock,D.T. & Beasley,D. Chlamydia pneumoniae and chlamydial heat shock protein 60 stimulate proliferation of human vascular smooth muscle cells via toll-like receptor 4 and p44/p42 mitogen-activated protein kinase activation. *Circ. Res.* **89**, 244-250 (2001).

19. Kuo,C.C. *et al.* Chlamydia pneumoniae (TWAR) in coronary arteries of young adults (15-34 years old). *Proc. Natl. Acad. Sci. U. S. A* **92**, 6911-6914 (1995).

20. Schumacher,A. *et al.* Positive Chlamydia pneumoniae serology is associated with elevated levels of tumor necrosis factor alpha in patients with coronary heart disease. *Atherosclerosis* **164**, 153-160 (2002).

21. Danesh,J., Wong,Y., Ward,M. & Muir,J. Chronic infection with Helicobacter pylori, Chlamydia pneumoniae, or cytomegalovirus: population based study of coronary heart disease. *Heart* **81**, 245-247 (1999).

22. Hajishengallis,G., Martin,M., Schifferle,R.E. & Genco,R.J. Counteracting interactions between lipopolysaccharide molecules with differential activation of toll-like receptors. *Infect. Immun.* **70**, 6658-6664 (2002).

23. Miyamoto,T. *et al.* Pathogen-accelerated atherosclerosis occurs early after exposure and can be prevented via immunization. *Infect. Immun.* **74**, 1376-1380 (2006).

24. Gibson,F.C., III, Yumoto,H., Takahashi,Y., Chou,H.H. & Genco,C.A. Innate immune signaling and Porphyromonas gingivalis-accelerated atherosclerosis. *J. Dent. Res.* **85**, 106-121 (2006).

25. Roth,G.A. *et al.* Infection with a periodontal pathogen increases mononuclear cell adhesion to human aortic endothelial cells. *Atherosclerosis* **190**, 271-281 (2007).

26. Wright,S.D. *et al.* Infectious agents are not necessary for murine atherogenesis. *J. Exp. Med.* **191**, 1437-1442 (2000).

27. Zhou,X., Caligiuri,G., Hamsten,A., Lefvert,A.K. & Hansson,G.K. LDL immunization induces T-cell-dependent antibody formation and protection against atherosclerosis. *Arterioscler. Thromb. Vasc. Biol.* **21**, 108-114 (2001).

28. Caligiuri,G. *et al.* Phosphorylcholine-targeting immunization reduces atherosclerosis. *J. Am. Coll. Cardiol.* **50**, 540-546 (2007).

29. Fredrikson,G.N., Bjorkbacka,H., Soderberg,I., Ljungcrantz,I. & Nilsson,J. Treatment with apo B peptide vaccines inhibits atherosclerosis in human apo B-100 transgenic mice without inducing an increase in peptide-specific antibodies. *J. Intern. Med.* **264**, 563-570 (2008).

30. Kawai,T. & Akira,S. Pathogen recognition with Toll-like receptors. *Curr. Opin. Immunol.* **17**, 338-344 (2005).

31. Martinon,F. & Tschopp,J. NLRs join TLRs as innate sensors of pathogens. *Trends Immunol.* **26**, 447-454 (2005).

32. Yoneyama,M. *et al.* The RNA helicase RIG-I has an essential function in double-stranded RNA-induced innate antiviral responses. *Nat. Immunol.* **5**, 730-737 (2004).

33. Kang,D.C. *et al.* mda-5: An interferon-inducible putative RNA helicase with double-stranded RNA-dependent ATPase activity and melanoma growth-suppressive properties. *Proc. Natl. Acad. Sci. U. S. A* **99**, 637-642 (2002).

34. Yoshimura,A. *et al.* Cutting edge: recognition of Gram-positive bacterial cell wall components by the innate immune system occurs via Toll-like receptor 2. *J. Immunol.* **163**, 1-5 (1999).

35. Parrillo,J.E. Pathogenetic mechanisms of septic shock. *N. Engl. J. Med.* **328**, 1471-1477 (1993).

36. Brun-Buisson,C. *et al.* Incidence, risk factors, and outcome of severe sepsis and septic shock in adults. A multicenter prospective study in intensive care units. French ICU Group for Severe Sepsis. *JAMA* **274**, 968-974 (1995).

37. Anderson,K.V., Bokla,L. & Nusslein-Volhard,C. Establishment of dorsal-ventral polarity in the Drosophila embryo: the induction of polarity by the Toll gene product. *Cell* **42**, 791-798 (1985).

38. Gay,N.J., Packman,L.C., Weldon,M.A. & Barna,J.C. A leucine-rich repeat peptide derived from the Drosophila Toll receptor forms extended filaments with a beta-sheet structure. *FEBS Lett.* **291**, 87-91 (1991).

39. Lemaitre,B., Nicolas,E., Michaut,L., Reichhart,J.M. & Hoffmann,J.A. The dorsoventral regulatory gene cassette spatzle/Toll/cactus controls the potent antifungal response in Drosophila adults. *Cell* **86**, 973-983 (1996).

40. Medzhitov,R., Preston-Hurlburt,P. & Janeway,C.A., Jr. A human homologue of the Drosophila Toll protein signals activation of adaptive immunity. *Nature* **388**, 394-397 (1997).

41. Rock,F.L., Hardiman,G., Timans,J.C., Kastelein,R.A. & Bazan,J.F. A family of human receptors structurally related to Drosophila Toll. *Proc. Natl. Acad. Sci. U. S. A* **95**, 588-593 (1998).

42. Poltorak,A. *et al.* Defective LPS signaling in C3H/HeJ and C57BL/10ScCr mice: mutations in Tlr4 gene. *Science* **282**, 2085-2088 (1998).

43. Takeuchi,O. *et al.* TLR6: A novel member of an expanding toll-like receptor family. *Gene* **231**, 59-65 (1999).

44. Chuang,T.H. & Ulevitch,R.J. Cloning and characterization of a sub-family of human toll-like receptors: hTLR7, hTLR8 and hTLR9. *Eur. Cytokine Netw.* **11**, 372-378 (2000).

45. Chuang,T. & Ulevitch,R.J. Identification of hTLR10: a novel human Toll-like receptor preferentially expressed in immune cells. Biochim Biophys Acta 1518, 157-161. 2001.
Ref Type: Journal (Full)

46. Slack,J.L. *et al.* Identification of two major sites in the type I interleukin-1 receptor cytoplasmic region responsible for coupling to pro-inflammatory signaling pathways. *J. Biol. Chem.* **275**, 4670-4678 (2000).

47. Chang,Y.C., Madkan,V., Cook-Norris,R., Sra,K. & Tyring,S. Current and potential uses of imiquimod. *South. Med. J.* **98**, 914-920 (2005).

48. Dupont,J. *et al.* A controlled clinical trial comparing the safety and immunogenicity of a new adjuvanted hepatitis B vaccine with a standard hepatitis B vaccine. *Vaccine* **24**, 7167-7174 (2006).

49. Takeda,K., Kaisho,T. & Akira,S. Toll-like receptors. Ann.Rev.Immunol. 21, 335-376. 2003.
Ref Type: Journal (Full)

50. Triantafilou,M. *et al.* Membrane sorting of toll-like receptor (TLR)-2/6 and TLR2/1 heterodimers at the cell surface determines heterotypic associations with cd36 and intracellular targeting. *J Biol Chem* (2006).

51. Triantafilou,M. *et al.* Lipopolysaccharides from atherosclerosis-associated bacteria antagonize TLR4, induce formation of TLR2/1/CD36 complexes in lipid rafts and trigger TLR2-induced inflammatory responses in human vascular endothelial cells. *Cell Microbiol.* **9**, 2030-2039 (2007).

52. Schroder,N.W. *et al.* Lipoteichoic acid (LTA) of Streptococcus pneumoniae and Staphylococcus aureus activates immune cells via Toll-like receptor (TLR)-2, lipopolysaccharide-binding protein (LBP), and CD14, whereas TLR-4 and MD-2 are not involved. *J. Biol. Chem.* **278**, 15587-15594 (2003).

53. Dziarski,R. & Gupta,D. Staphylococcus aureus peptidoglycan is a toll-like receptor 2 activator: a reevaluation. *Infect. Immun.* **73**, 5212-5216 (2005).

54. Lien,E. *et al.* Toll-like receptor 2 functions as a pattern recognition receptor for diverse bacterial products. *J. Biol. Chem.* **274**, 33419-33425 (1999).

55. Lepper,P.M., Triantafilou,M., Schumann,C., Schneider,E.M. & Triantafilou,K. Lipopolysaccharides from *Helicobacter pylori* can act as antagonists for Toll-like receptor 4. *Cellular Microbiol* **7**, 519-528 (2005).

56. Jin,M.S. *et al.* Crystal structure of the TLR1-TLR2 heterodimer induced by binding of a tri-acylated lipopeptide. *Cell* **130**, 1071-1082 (2007).

57. Alexopoulou,L., Holt,A.C., Medzhitov,R. & Flavell,R.A. Recognition of double-stranded RNA and activation of NF-kappaB by Toll-like receptor 3. *Nature* **413**, 732-738 (2001).

58. Groskreutz,D.J. *et al.* Respiratory syncytial virus induces TLR3 protein and protein kinase R, leading to increased double-stranded RNA responsiveness in airway epithelial cells. *J. Immunol.* **176**, 1733-1740 (2006).

59. Kanzler,H., Barrat,F.J., Hessel,E.M. & Coffman,R.L. Therapeutic targeting of innate immunity with Toll-like receptor agonists and antagonists. *Nat. Med.* **13**, 552-559 (2007).

60. Liu,L. *et al.* Structural basis of toll-like receptor 3 signaling with double-stranded RNA. *Science* **320**, 379-381 (2008).

61. Hoshino,K. *et al.* Cutting edge: Toll-like receptor 4 (TLR4)-deficient mice are hyporesponsive to lipopolysaccharide: evidence for TLR4 as the Lps gene product. *J. Immunol.* **162**, 3749-3752 (1999).

62. Schumann,R.R. *et al.* Structure and function of lipopolysaccharide binding protein. *Science* **249**, 1429-1431 (1990).

63. Wright,S.D., Ramos,R.A., Tobias,P.S., Ulevitch,R.J. & Mathison,J.C. CD14, a receptor for complexes of lipopolysaccharide (LPS) and LPS binding protein. *Science* **249**, 1431-1433 (1990).

64. Shimazu,R. *et al.* MD-2, a molecule that confers lipopolysaccharide responsiveness on Toll-like receptor 4. *J. Exp. Med.* **189**, 1777-1782 (1999).

65. da Silva,C.J., Soldau,K., Christen,U., Tobias,P.S. & Ulevitch,R.J. Lipopolysaccharide is in close proximity to each of the proteins in its membrane receptor complex. transfer from CD14 to TLR4 and MD-2. *J. Biol. Chem.* **276**, 21129-21135 (2001).

66. Triantafilou,M. *et al.* Combinational clustering of receptors following stimulation by bacterial products determines lipopolysaccharide responses. *Biochem. J.* **381**, 527-536 (2004).

67. Triantafilou,M. & Triantafilou,K. Heat-shock protein 70 and heat-shock protein 90 associate with Toll-like receptor 4 in response to bacterial lipopolysaccharide. *Biochem. Soc. Trans.* **32**, 636-639 (2004).

68. Triantafilou,K., Triantafilou,M. & Dedrick,R.L. A CD14-independent LPS receptor cluster. *Nat. Immunol.* **2**, 338-345 (2001).

69. Triantafilou,M. *et al.* Chemokine receptor 4 (CXCR4) is part of the lipopolysaccharide "sensing apparatus". *Eur. J. Immunol.* **38**, 192-203 (2008).

70. Burzyn,D. *et al.* Toll-like receptor 4-dependent activation of dendritic cells by a retrovirus. *J. Virol.* **78**, 576-584 (2004).

71. Stewart,C.R. *et al.* CD36 ligands promote sterile inflammation through assembly of a Toll-like receptor 4 and 6 heterodimer. *Nat. Immunol.* **11**, 155-161 (2010).

72. Febbraio,M., Hajjar,D.P. & Silverstein,R.L. CD36: a class B scavenger receptor involved in angiogenesis, atherosclerosis, inflammation, and lipid metabolism. *J. Clin. Invest* **108**, 785-791 (2001).

73. Nicholson,A.C., Frieda,S., Pearce,A. & Silverstein,R.L. Oxidized LDL binds to CD36 on human monocyte-derived macrophages and transfected cell lines. Evidence implicating the lipid moiety of the lipoprotein as the binding site. *Arterioscler. Thromb. Vasc. Biol.* **15**, 269-275 (1995).

74. Gao,B. & Tsan,M.F. Endotoxin contamination in recombinant human heat shock protein 70 (Hsp70) preparation is responsible for the induction of tumor necrosis factor alpha release by murine macrophages. *J. Biol. Chem.* **278**, 174-179 (2003).

75. Kim,H.M. *et al.* Crystal structure of the TLR4-MD-2 complex with bound endotoxin antagonist Eritoran. *Cell* **130**, 906-917 (2007).

76. Hayashi,F. *et al.* The innate immune response to bacterial flagellin is mediated by Toll-like receptor 5. *Nature* **410**, 1099-1103 (2001).

77. Zhang,Z., Louboutin,J.P., Weiner,D.J., Goldberg,J.B. & Wilson,J.M. Human airway epithelial cells sense Pseudomonas aeruginosa infection via recognition of flagellin by Toll-like receptor 5. *Infect. Immun.* **73**, 7151-7160 (2005).

78. Heil,F. *et al.* Species-specific recognition of single-stranded RNA via toll-like receptor 7 and 8. *Science* **303**, 1526-1529 (2004).

79. Diebold,S.S., Kaisho,T., Hemmi,H., Akira,S. & Reis e Sousa. Innate antiviral responses by means of TLR7-mediated recognition of single-stranded RNA. *Science* **303**, 1529-1531 (2004).

80. Gantier,M.P. *et al.* TLR7 is involved in sequence-specific sensing of single-stranded RNAs in human macrophages. *J. Immunol.* **180**, 2117-2124 (2008).

81. Hemmi,H. *et al.* Small anti-viral compounds activate cells via the TLR7 MyD88-dependent signaling pathway. Nat.Immunol. 3, 196-200. 2002.
Ref Type: Journal (Full)

82. Jurk,M. *et al.* Human TLR7 or TLR8 independently confer responsiveness to the antiviral compound R-848. Nat.Immunol. 3, 499-505. 2002.
Ref Type: Journal (Full)

83. Hemmi,H. *et al.* A Toll-like receptor recognizes bacterial DNA. *Nature* **408**, 740-745 (2000).

84. Barton,G.M., Kagan,J.C. & Medzhitov,R. Intracellular localization of Toll-like receptor 9 prevents recognition of self DNA but facilitates access to viral DNA. *Nat. Immunol.* **7**, 49-56 (2006).

85. Coban,C. *et al.* Toll-like receptor 9 mediates innate immune activation by the malaria pigment hemozoin. *J. Exp. Med.* **201**, 19-25 (2005).

86. Zhang,D. *et al.* A toll-like receptor that prevents infection by uropathogenic bacteria. *Science* **303**, 1522-1526 (2004).

87. Akira,S. & Takeda,K. Toll-like receptor signalling. *Nat. Rev. Immunol.* **4**, 499-511 (2004).

88. Beveridge,T.J. Use of the gram stain in microbiology. *Biotech. Histochem.* **76**, 111-118 (2001).

89. Fischer,W., Mannsfeld,T. & Hagen,G. On the basic structure of poly(glycerophosphate) lipoteichoic acids. *Biochem. Cell Biol.* **68**, 33-43 (1990).

90. Fischer,W. Lipoteichoic acid and lipids in the membrane of Staphylococcus aureus. *Med. Microbiol. Immunol.* **183**, 61-76 (1994).

91. Greenberg,J.W., Fischer,W. & Joiner,K.A. Influence of lipoteichoic acid structure on recognition by the macrophage scavenger receptor. *Infect. Immun.* **64**, 3318-3325 (1996).

92. Loppnow,H. *et al.* Lipid A, the immunostimulatory principle of lipopolysaccharides? *Adv. Exp. Med. Biol.* **256**, 561-566 (1990).

93. Raetz,C.R. & Whitfield,C. Lipopolysaccharide endotoxins. *Annu. Rev. Biochem.* **71**, 635-700 (2002).

94. Caroff,M., Karibian,D., Cavaillon,J.M. & Haeffner-Cavaillon,N. Structural and functional analyses of bacterial lipopolysaccharides. *Microbes. Infect.* **4**, 915-926 (2002).

95. Esterbauer,H., Gebicki,J., Puhl,H. & Jurgens,G. The role of lipid peroxidation and antioxidants in oxidative modification of LDL. *Free Radic. Biol. Med.* **13**, 341-390 (1992).

96. Hevonoja,T., Pentikainen,M.O., Hyvonen,M.T., Kovanen,P.T. & Ala-Korpela,M. Structure of low density lipoprotein (LDL) particles: basis for understanding molecular changes in modified LDL. *Biochim. Biophys. Acta* **1488**, 189-210 (2000).

97. Hamilton,J.A., Small,D.M. & Parks,J.S. 1H NMR studies of lymph chylomicra and very low density lipoproteins from nonhuman primates. *J. Biol. Chem.* **258**, 1172-1179 (1983).

98. Palinski,W. *et al.* Low density lipoprotein undergoes oxidative modification in vivo. *Proc. Natl. Acad. Sci. U. S. A* **86**, 1372-1376 (1989).

99. Berliner,J.A., Subbanagounder,G., Leitinger,N., Watson,A.D. & Vora,D. Evidence for a role of phospholipid oxidation products in atherogenesis. *Trends Cardiovasc. Med.* **11**, 142-147 (2001).

100. Xu,X.H. *et al.* Toll-like receptor-4 is expressed by macrophages in murine and human lipid-rich atherosclerotic plaques and upregulated by oxidized LDL. *Circulation* **104**, 3103-3108 (2001).

101. Pluddemann,A., Neyen,C. & Gordon,S. Macrophage scavenger receptors and host-derived ligands. *Methods* **43**, 207-217 (2007).

102. Febbraio,M. *et al.* Targeted disruption of the class B scavenger receptor CD36 protects against atherosclerotic lesion development in mice. *J. Clin. Invest* **105**, 1049-1056 (2000).

103. Bochkov,V.N. *et al.* Protective role of phospholipid oxidation products in endotoxin-induced tissue damage. *Nature* **419**, 77-81 (2002).

104. Walton,K.A. *et al.* Specific phospholipid oxidation products inhibit ligand activation of toll-like receptors 4 and 2. *Arterioscler. Thromb. Vasc. Biol.* **23**, 1197-1203 (2003).

105. Li,D. & Mehta,J.L. Upregulation of endothelial receptor for oxidized LDL (LOX-1) by oxidized LDL and implications in apoptosis of human coronary artery endothelial cells: evidence from use of antisense LOX-1 mRNA and chemical inhibitors. *Arterioscler. Thromb. Vasc. Biol.* **20**, 1116-1122 (2000).

106. Sawamura,T. *et al.* An endothelial receptor for oxidized low-density lipoprotein. *Nature* **386**, 73-77 (1997).

107. Binder,C.J. *et al.* The role of natural antibodies in atherogenesis. *J. Lipid Res.* **46**, 1353-1363 (2005).

108. Bird,D.A. *et al.* Receptors for oxidized low-density lipoprotein on elicited mouse peritoneal macrophages can recognize both the modified lipid moieties and the modified protein moieties: implications with respect to macrophage recognition of apoptotic cells. *Proc. Natl. Acad. Sci. U. S. A* **96**, 6347-6352 (1999).

109. Boullier,A. *et al.* The binding of oxidized low density lipoprotein to mouse CD36 is mediated in part by oxidized phospholipids that are associated with both the lipid and protein moieties of the lipoprotein. *J. Biol. Chem.* **275**, 9163-9169 (2000).

110. Pfeiffer,A. *et al.* Lipopolysaccharide and ceramide docking to CD14 provokes ligand-specific receptor clustering in rafts. *Eur. J. Immunol.* **31**, 3153-3164 (2001).

111. Henneke,P. *et al.* Novel engagement of CD14 and multiple toll-like receptors by group B streptococci. *J. Immunol.* **167**, 7069-7076 (2001).

112. Haziot,A., Tsuberi,B.Z. & Goyert,S.M. Neutrophil CD14: biochemical properties and role in the secretion of tumor necrosis factor-alpha in response to lipopolysaccharide. *J. Immunol.* **150**, 5556-5565 (1993).

113. Kim,J.I. *et al.* Crystal structure of CD14 and its implications for lipopolysaccharide signaling. *J. Biol. Chem.* **280**, 11347-11351 (2005).

114. Haziot,A. *et al.* Resistance to endotoxin shock and reduced dissemination of gram-negative bacteria in CD14-deficient mice. *Immunity.* **4**, 407-414 (1996).

115. Miller,Y.I. *et al.* Minimally modified LDL binds to CD14, induces macrophage spreading via TLR4/MD-2, and inhibits phagocytosis of apoptotic cells. *J. Biol. Chem.* **278**, 1561-1568 (2003).

116. Nicholson,A.C., Febbraio,M., Han,J., Silverstein,R.L. & Hajjar,D.P. CD36 in atherosclerosis. The role of a class B macrophage scavenger receptor. *Ann. N. Y. Acad. Sci.* **902**, 128-131 (2000).

117. Silverstein,R.L. & Febbraio,M. CD36 and atherosclerosis. *Curr. Opin. Lipidol.* **11**, 483-491 (2000).

118. Pearson,A.M. Scavenger receptors in innate immunity. *Curr. Opin. Immunol.* **8**, 20-28 (1996).

119. Akira,S. Toll-like receptors and innate immunity. *Adv. Immunol.* **78**, 1-56 (2001).

120. Oquendo,P., Hundt,E., Lawler,J. & Seed,B. CD36 directly mediates cytoadherence of Plasmodium falciparum parasitized erythrocytes. *Cell* **58**, 95-101 (1989).

121. Gruarin,P. *et al.* CD36 is a ditopic glycoprotein with the N-terminal domain implicated in intracellular transport. *Biochem. Biophys. Res. Commun.* **275**, 446-454 (2000).

122. Pearce,S.F., Wu,J. & Silverstein,R.L. A carboxyl terminal truncation mutant of CD36 is secreted and binds thrombospondin: evidence for a single transmembrane domain. *Blood* **84**, 384-389 (1994).

123. Kabouridis,P.S., Hasan,M., Newson,J., Gilroy,D.W. & Lawrence,T. Inhibition of NF-kappa B activity by a membrane-transducing mutant of I kappa B alpha. *J. Immunol.* **169**, 2587-2593 (2002).

124. Schmitz,M.L. *et al.* Structural and functional analysis of the NF-kappa B p65 C terminus. An acidic and modular transactivation domain with the potential to adopt an alpha-helical conformation. *J. Biol. Chem.* **269**, 25613-25620 (1994).

125. Kawagoe,T. *et al.* Sequential control of Toll-like receptor-dependent responses by IRAK1 and IRAK2. *Nat. Immunol.* **9**, 684-691 (2008).

126. Simons,K. & Ikonen,E. Functional rafts in membranes. *Nature* **387**, 569-570 (1997).

127. Pralle,A., Keller,P., Florin,E.L., Simons,K. & Horber,J.K.H. Sphingolipid-cholesterol rafts diffuse as small entities in the plasma membrane of mammalian cells. *Journal of Cell Biology* **148**, 997-1007 (2000).

128. Harder,T., Scheiffele,P., Verkade,P. & Simons,K. Lipid domain structure of the plasma membrane revealed by patching of membrane components. J Cell Biol 141, 929-942. 1998.
Ref Type: Journal (Full)

129. Anderson,H.A., Hiltbold,E.M. & Roche,P.A. Concentration of MHC class II molecules in lipid rafts facilitates antigen presentation. *Nature Immunology* **1**, 156-162 (2000).

130. Triantafilou,M., Miyake,K., Golenbock,D. & Triantafilou,K. Mediators of the innate immune recognition of bacteria concentrate in lipid rafts and facilitate lipopolysaccharide-induced cell activation. *Journal of Cell Science* **115**, 2603-2611 (2002).

131. Triantafilou,M., Morath,S., Mackie,A., Hartung,T. & Triantafilou,K. Lateral diffusion of Toll-like receptors reveals that they are transiently confined within lipid rafts on the plasma membrane. *J Cell Sci* **117**, 4007-4014 (2004).

132. Triantafilou,M. & Triantafilou,K. Receptor cluster formation during activation by bacterial products. *J. Endotoxin. Res.* **9**, 331-335 (2003).

133. Triantafilou,M. *et al.* Combinational clustering of receptors following stimulation by bacterial products determines lipopolysaccharide responses. *Biochem. J.* **381**, 527-536 (2004).

134. Horner,A.A. *et al.* Immunostimulatory DNA is a potent mucosal adjuvant. *Cell Immunol.* **190**, 77-82 (1998).

135. Horner,A.A. *et al.* Immunostimulatory DNA-based vaccines elicit multifaceted immune responses against HIV at systemic and mucosal sites. *J. Immunol.* **167**, 1584-1591 (2001).

136. Krishnan,J., Lee,G. & Choi,S. Drugs targeting Toll-like receptors. *Arch. Pharm. Res.* **32**, 1485-1502 (2009).

137. Rossignol,D.P. & Lynn,M. TLR4 antagonists for endotoxemia and beyond. *Curr. Opin. Investig. Drugs* **6**, 496-502 (2005).

138. Angus,D.C. *et al.* Epidemiology of severe sepsis in the United States: analysis of incidence, outcome, and associated costs of care. *Crit Care Med.* **29**, 1303-1310 (2001).

139. Ellis,J. Proteins as molecular chaperones. *Nature* **328**, 378-379 (1987).

140. Slavotinek,A.M. & Biesecker,L.G. Unfolding the role of chaperones and chaperonins in human disease. *Trends Genet.* **17**, 528-535 (2001).

141. Triantafilou,M., Sawyer,D., Nor,A., Vakakis,E. & Triantafilou,K. Cell surface molecular chaperones as endogenous modulators of the innate immune response. *Novartis. Found. Symp.* **291**, 74-79 (2008).

142. Chen,H. *et al.* Hsp70 inhibits lipopolysaccharide-induced NF-kappaB activation by interacting with TRAF6 and inhibiting its ubiquitination. *FEBS Lett.* **580**, 3145-3152 (2006).

143. Marber,M.S. *et al.* Overexpression of the rat inducible 70-kD heat stress protein in a transgenic mouse increases the resistance of the heart to ischemic injury. *J. Clin. Invest* **95**, 1446-1456 (1995).

144. Radford,N.B. *et al.* Cardioprotective effects of 70-kDa heat shock protein in transgenic mice. *Proc. Natl. Acad. Sci. U. S. A* **93**, 2339-2342 (1996).

145. Zhu,J. *et al.* Increased serum levels of heat shock protein 70 are associated with low risk of coronary artery disease. *Arterioscler. Thromb. Vasc. Biol.* **23**, 1055-1059 (2003).

146. Wisniewska,M. *et al.* Crystal structures of the ATPase domains of four human Hsp70 isoforms: HSPA1L/Hsp70-hom, HSPA2/Hsp70-2, HSPA6/Hsp70B', and HSPA5/BiP/GRP78. *PLoS. One.* **5**, e8625 (2010).

147. Hatse,S., Princen,K., Bridger,G., De Clercq,E. & Schols,D. Chemokine receptor inhibition by AMD3100 is strictly confined to CXCR4. *FEBS Lett.* **527**, 255-262 (2002).

148. Hendrix,C.W. *et al.* Safety, pharmacokinetics, and antiviral activity of AMD3100, a selective CXCR4 receptor inhibitor, in HIV-1 infection. *J. Acquir. Immune. Defic. Syndr.* **37**, 1253-1262 (2004).

149. Matthys,P. *et al.* AMD3100, a potent and specific antagonist of the stromal cell-derived factor-1 chemokine receptor CXCR4, inhibits autoimmune joint inflammation in IFN-gamma receptor-deficient mice. *J. Immunol.* **167**, 4686-4692 (2001).

150. Lukacs,N.W., Berlin,A., Schols,D., Skerlj,R.T. & Bridger,G.J. AMD3100, a CxCR4 antagonist, attenuates allergic lung inflammation and airway hyperreactivity. *Am. J. Pathol.* **160**, 1353-1360 (2002).

151. Moriuchi,M., Moriuchi,H., Turner,W. & Fauci,A.S. Exposure to bacterial products renders macrophages highly susceptible to T-tropic HIV-1. *J. Clin. Invest* **102**, 1540-1550 (1998).

152. Michelsen,K.S. *et al.* Lack of Toll-like receptor 4 or myeloid differentiation factor 88 reduces atherosclerosis and alters plaque phenotype in mice deficient in apolipoprotein E. *Proc. Natl. Acad. Sci. U. S. A* **101**, 10679-10684 (2004).

153. Erridge,C., Kennedy,S., Spickett,C.M. & Webb,D.J. Oxidized phospholipid inhibition of toll-like receptor (TLR) signaling is restricted to TLR2 and TLR4: roles for CD14, LPS-binding protein, and MD2 as targets for specificity of inhibition. *J. Biol. Chem.* **283**, 24748-24759 (2008).

154. Naderer,O., Suttle,B.A., Arumugham,T., Min,S.S. & Jones,L.S. Society of Critical Care Medicine 35th Critical Care Congress San Francisco, California, USA January 7-11, 2006. 33(12) Abstract Supplement:A174. *Critical Care Medicine* (2006).

155. Naderer,O.J. *et al.* Safety and pharmacokinetics GR270773, a novel antisepsis compound, in septic patients. Critical Care Medicine. 32(12) Supplement:A174, December 2004. *Critical Care Medicine* (2004).

156. Dellinger,R.P. *et al.* Efficacy and safety of a phospholipid emulsion (GR270773) in Gram-negative severe sepsis: results of a phase II multicenter, randomized, placebo-controlled, dose-finding clinical trial. *Crit Care Med.* **37**, 2929-2938 (2009).

157. Piedrahita,J.A., Zhang,S.H., Hagaman,J.R., Oliver,P.M. & Maeda,N. Generation of mice carrying a mutant apolipoprotein E gene inactivated by gene targeting in embryonic stem cells. *Proc. Natl. Acad. Sci. U. S. A* **89**, 4471-4475 (1992).

158. Ishibashi,S. *et al.* Hypercholesterolemia in low density lipoprotein receptor knockout mice and its reversal by adenovirus-mediated gene delivery. *J. Clin. Invest* **92**, 883-893 (1993).

159. Bjorkbacka,H. *et al.* Reduced atherosclerosis in MyD88-null mice links elevated serum cholesterol levels to activation of innate immunity signaling pathways. *Nat. Med.* **10**, 416-421 (2004).

160. Madan,M. & Amar,S. Toll-like receptor-2 mediates diet and/or pathogen associated atherosclerosis: proteomic findings. *PLoS. ONE.* **3**, e3204 (2008).

161. Mullick,A.E., Tobias,P.S. & Curtiss,L.K. Modulation of atherosclerosis in mice by Toll-like receptor 2. *J. Clin. Invest* **115**, 3149-3156 (2005).

162. Arbour,N.C. *et al.* TLR4 mutations are associated with endotoxin hyporesponsiveness in humans. *Nat. Genet.* **25**, 187-191 (2000).

163. Kiechl,S. *et al.* Toll-like receptor 4 polymorphisms and atherogenesis. *N. Engl. J. Med.* **347**, 185-192 (2002).

164. Koch,W., Hoppmann,P., Pfeufer,A., Schomig,A. & Kastrati,A. Toll-like receptor 4 gene polymorphisms and myocardial infarction: no association in a Caucasian population. *Eur. Heart J.* **27**, 2524-2529 (2006).

165. Labrum,R., Bevan,S., Sitzer,M., Lorenz,M. & Markus,H.S. Toll receptor polymorphisms and carotid artery intima-media thickness. *Stroke* **38**, 1179-1184 (2007).

166. Hubacek,J.A. *et al.* C(-260)-->T polymorphism in the promoter of the CD14 monocyte receptor gene as a risk factor for myocardial infarction. *Circulation* **99**, 3218-3220 (1999).

167. Frantz,S. *et al.* Toll4 (TLR4) expression in cardiac myocytes in normal and failing myocardium. *J. Clin. Invest* **104**, 271-280 (1999).

168. Pryshchep,O., Ma-Krupa,W., Younge,B.R., Goronzy,J.J. & Weyand,C.M. Vessel-specific Toll-like receptor profiles in human medium and large arteries. *Circulation* **118**, 1276-1284 (2008).

169. Mullick,A.E. *et al.* Increased endothelial expression of Toll-like receptor 2 at sites of disturbed blood flow exacerbates early atherogenic events. *J. Exp. Med.* **205**, 373-383 (2008).

170. Choi,S.H. *et al.* Lipoprotein accumulation in macrophages via toll-like receptor-4-dependent fluid phase uptake. *Circ. Res.* **104**, 1355-1363 (2009).

171. Kazemi,M.R., McDonald,C.M., Shigenaga,J.K., Grunfeld,C. & Feingold,K.R. Adipocyte fatty acid-binding protein expression and lipid accumulation are increased during activation of murine macrophages by toll-like receptor agonists. *Arterioscler. Thromb. Vasc. Biol.* **25**, 1220-1224 (2005).

172. Grayston,J.T. Background and current knowledge of Chlamydia pneumoniae and atherosclerosis. *J. Infect. Dis.* **181 Suppl 3**, S402-S410 (2000).

173. Hoebe,K. *et al.* CD36 is a sensor of diacylglycerides. *Nature* **433**, 523-527 (2005).

174. Walton,K.A. *et al.* Receptors involved in the oxidized 1-palmitoyl-2-arachidonoyl-sn-glycero-3-phosphorylcholine-mediated synthesis of interleukin-8. A role for Toll-like receptor 4 and a glycosylphosphatidylinositol-anchored protein. *J. Biol. Chem.* **278**, 29661-29666 (2003).

175. Fukumoto,Y. *et al.* Genetically determined resistance to collagenase action augments interstitial collagen accumulation in atherosclerotic plaques. *Circulation* **110**, 1953-1959 (2004).

176. Galis,Z.S., Sukhova,G.K., Lark,M.W. & Libby,P. Increased expression of matrix metalloproteinases and matrix degrading activity in vulnerable regions of human atherosclerotic plaques. *J. Clin. Invest* **94**, 2493-2503 (1994).

177. Uzui,H. *et al.* Increased expression of membrane type 3-matrix metalloproteinase in human atherosclerotic plaque: role of activated macrophages and inflammatory cytokines. *Circulation* **106**, 3024-3030 (2002).

178. Monaco,C. *et al.* Toll-like receptor-2 mediates inflammation and matrix degradation in human atherosclerosis. *Circulation* **120**, 2462-2469 (2009).

179. Barraud,N. *et al.* Involvement of nitric oxide in biofilm dispersal of Pseudomonas aeruginosa. *J. Bacteriol.* **188**, 7344-7353 (2006).

180. Mackman,N., Brand,K. & Edgington,T.S. Lipopolysaccharide-mediated transcriptional activation of the human tissue factor gene in THP-1 monocytic cells requires both activator protein 1 and nuclear factor kappa B binding sites. *J. Exp. Med.* **174**, 1517-1526 (1991).

181. Bea,F. *et al.* Chlamydia pneumoniae induces tissue factor expression in mouse macrophages via activation of Egr-1 and the MEK-ERK1/2 pathway. *Circ. Res.* **92**, 394-401 (2003).

182. Smiley,S.T., King,J.A. & Hancock,W.W. Fibrinogen stimulates macrophage chemokine secretion through toll-like receptor 4. *J. Immunol.* **167**, 2887-2894 (2001).

183. Hodgkinson,C.P., Patel,K. & Ye,S. Functional Toll-like receptor 4 mutations modulate the response to fibrinogen. *Thromb. Haemost.* **100**, 301-307 (2008).

184. Kume,N., Cybulsky,M.I. & Gimbrone,M.A., Jr. Lysophosphatidylcholine, a component of atherogenic lipoproteins, induces mononuclear leukocyte adhesion molecules in cultured human and rabbit arterial endothelial cells. *J. Clin. Invest* **90**, 1138-1144 (1992).

185. Profumo,E. *et al.* Association of intracellular pro- and anti-inflammatory cytokines in peripheral blood with the clinical or ultrasound indications for carotid endarterectomy in patients with carotid atherosclerosis. *Clin. Exp. Immunol.* **152**, 120-126 (2008).

186. Ambrosius,W., Kazmierski,R., Michalak,S. & Kozubski,W. Anti-inflammatory cytokines in subclinical carotid atherosclerosis. *Neurology* **66**, 1946-1948 (2006).

187. Niessner,A. *et al.* Synergistic proinflammatory effects of the antiviral cytokine interferon-alpha and Toll-like receptor 4 ligands in the atherosclerotic plaque. *Circulation* **116**, 2043-2052 (2007).

188. Hansson,G.K., Libby,P., Schonbeck,U. & Yan,Z.Q. Innate and adaptive immunity in the pathogenesis of atherosclerosis. *Circ. Res.* **91**, 281-291 (2002).

189. Barlic,J. & Murphy,P.M. Chemokine regulation of atherosclerosis. *J. Leukoc. Biol.* **82**, 226-236 (2007).

190. Schecter,A.D., Berman,A.B. & Taubman,M.B. Chemokine receptors in vascular smooth muscle. *Microcirculation.* **10**, 265-272 (2003).

191. Boekholdt,S.M. *et al.* IL-8 plasma concentrations and the risk of future coronary artery disease in apparently healthy men and women: the EPIC-Norfolk prospective population study. *Arterioscler. Thromb. Vasc. Biol.* **24**, 1503-1508 (2004).

192. Moreau,M. *et al.* Interleukin-8 mediates downregulation of tissue inhibitor of metalloproteinase-1 expression in cholesterol-loaded human macrophages: relevance to stability of atherosclerotic plaque. *Circulation* **99**, 420-426 (1999).

193. Boutte,Y., Crosnier,M.T., Carraro,N., Traas,J. & Satiat-Jeunemaitre,B. The plasma membrane recycling pathway and cell polarity in plants: studies on PIN proteins. *J. Cell Sci.* **119**, 1255-1265 (2006).

194. Kluge,C. *et al.* Subcellular distribution of the V-ATPase complex in plant cells, and in vivo localisation of the 100 kDa subunit VHA-a within the complex. *BMC. Cell Biol.* **5**, 29 (2004).

195. Bolte,S. & Cordelieres,F.P. A guided tour into subcellular colocalization analysis in light microscopy. *J. Microsc.* **224**, 213-232 (2006).

196. Costes,S.V. *et al.* Automatic and quantitative measurement of protein-protein colocalization in live cells. *Biophys. J.* **86**, 3993-4003 (2004).

197. Wu,P. & Brand,L. Resonance energy transfer: methods and applications. *Anal. Biochem.* **218**, 1-13 (1994).

198. Kenworthy,A.K. & Edidin,M. Distribution of a glycosylphosphatidylinositol-anchored protein at the apical surface of MDCK cells examined at a resolution of <100 A using imaging fluorescence resonance energy transfer. *J. Cell Biol.* **142**, 69-84 (1998).

199. Kenworthy,A.K. & Edidin,M. Imaging fluorescence resonance energy transfer as probe of membrane organization and molecular associations of GPI-anchored proteins. *Methods Mol. Biol.* **116**, 37-49 (1999).

200. Fire,A. *et al.* Potent and specific genetic interference by double-stranded RNA in Caenorhabditis elegans. *Nature* **391**, 806-811 (1998).

201. Triantafilou,M., Miyake,K., Golenbock,D.T. & Triantafilou,K. Mediators of innate immune recognition of bacteria concentrate in lipid rafts and facilitate lipopolysaccharide-induced cell activation. *J. Cell Sci.* **115**, 2603-2611 (2002).

202. Rothberg,K.G. *et al.* Caveolin, a protein component of caveolae membrane coats. *Cell* **68**, 673-682 (1992).

203. Keller,P. & Simons,K. Cholesterol is required for surface transport of influenza virus hemagglutinin. *J. Cell Biol.* **140**, 1357-1367 (1998).

204. Cuatrecasas,P., Wilchek,M. & Anfinsen,C.B. Selective enzyme purification by affinity chromatography. *Proc. Natl. Acad. Sci. U. S. A* **61**, 636-643 (1968).

205. Lidington,E.A., Moyes,D.L., McCormack,A.M. & Rose,M.L. A comparison of primary endothelial cells and endothelial cell lines for studies of immune interactions. *Transpl. Immunol.* **7**, 239-246 (1999).

206. Triantafilou,M. *et al.* Lipopolysaccharides from atherosclerosis-associated bacteria antagonize TLR4, induce formation of TLR2/1/CD36 complexes in lipid rafts and trigger TLR2-induced inflammatory responses in human vascular endothelial cells. *Cell Microbiol* **9**, 2030-2039 (2007).

207. Triantafilou,M. *et al.* Lipoteichoic acid and Toll-like receptor 2 internalization and targeting to the Golgi are lipid-raft dependent. *J Biol Chem* **279**, 40882-40889 (2004).

208. Triantafilou,M. *et al.* Membrane sorting of toll-like receptor (TLR)-2/6 and TLR2/1 heterodimers at the cell surface determines heterotypic associations with CD36 and intracellular targeting. *J. Biol. Chem.* **281**, 31002-31011 (2006).

209. Visintin,A., Halmen,K.A., Latz,E., Monks,B.G. & Golenbock,D.T. Pharmacological inhibition of endotoxin responses is achieved by targeting the TLR4 coreceptor, MD-2. *J Immunol* **175**, 6465-6472 (2005).

210. Lynn,M. *et al.* Blocking of responses to endotoxin by E5564 in healthy volunteers with experimental endotoxemia. *J Infect Dis* **187**, 631-639 (2003).

211. Savov,J.D. *et al.* Toll-like receptor 4 antagonist (E5564) prevents the chronic airway response to inhaled lipopolysaccharide. *Am. J. Physiol Lung Cell Mol. Physiol* **289**, L329-L337 (2005).

212. Kiechl,S. *et al.* Chronic infections and the risk of carotid atherosclerosis: prospective results from a large population study. *Circulation* **103**, 1064-1070 (2001).

213. Kiechl,S. *et al.* Chronic infections and the risk of carotid atherosclerosis: prospective results from a large population study. *Circulation* **103**, 1064-1070 (2001).

214. Mayr,M., Kiechl,S., Willeit,J., Wick,G. & Xu,Q. Infections, immunity, and atherosclerosis: associations of antibodies to Chlamydia pneumoniae, Helicobacter pylori, and cytomegalovirus with immune reactions to heat-shock protein 60 and carotid or femoral atherosclerosis. *Circulation* **102**, 833-839 (2000).

215. Mayr,M. *et al.* Increased risk of atherosclerosis is confined to CagA-positive Helicobacter pylori strains: prospective results from the Bruneck study. *Stroke* **34**, 610-615 (2003).

216. Danesh,J., Collins,R. & Peto,R. Chronic infections and coronary heart disease: is there a link? *Lancet* **350**, 430-436 (1997).

217. Lougheed,M., Zhang,H.F. & Steinbrecher,U.P. Oxidized low density lipoprotein is resistant to cathepsins and accumulates within macrophages. *J. Biol. Chem.* **266**, 14519-14525 (1991).

218. Boekholdt,S.M. *et al.* IL-8 plasma concentrations and the risk of future coronary artery disease in apparently healthy men and women: the EPIC-Norfolk prospective population study. *Arterioscler. Thromb. Vasc. Biol.* **24**, 1503-1508 (2004).

219. Boekholdt,S.M. *et al.* IL-8 plasma concentrations and the risk of future coronary artery disease in apparently healthy men and women: the EPIC-Norfolk prospective population study. *Arterioscler. Thromb. Vasc. Biol.* **24**, 1503-1508 (2004).

220. Moreau,M. *et al.* Interleukin-8 mediates downregulation of tissue inhibitor of metalloproteinase-1 expression in cholesterol-loaded human macrophages: relevance to stability of atherosclerotic plaque. *Circulation* **99**, 420-426 (1999).

221. Naderer,O., Suttle,B.A., Arumugham,T., Min,S.S. & Jones,L.S. Society of Critical Care Medicine 35th Critical Care Congress San Francisco, California, USA January 7-11, 2006. 33(12) Abstract Supplement:A174. *Critical Care Medicine* (2006).

222. Naderer,O.J. *et al.* Safety and pharmacokinetics GR270773, a novel antisepsis compound, in septic patients. Critical Care Medicine. 32(12) Supplement:A174, December 2004. *Critical Care Medicine* (2004).

223. Parker,L.C. *et al.* A phosphatidylserine species inhibits a range of TLR- but not IL-1beta-induced inflammatory responses by disruption of membrane microdomains. *J. Immunol.* **181**, 5606-5617 (2008).

224. Zeng,Y., Tao,N., Chung,K.N., Heuser,J.E. & Lublin,D.M. Endocytosis of oxidized low density lipoprotein through scavenger receptor CD36 utilizes a lipid raft pathway that does not require caveolin-1. *J. Biol. Chem.* **278**, 45931-45936 (2003).

225. Itabe,H. *et al.* Lysosomal accumulation of oxidized phosphatidylcholine-apolipoprotein B complex in macrophages: intracellular fate of oxidized low density lipoprotein. *Biochim. Biophys. Acta* **1487**, 233-245 (2000).

226. Vergeer,M. *et al.* Carotid atherosclerosis progression in familial hypercholesterolemia patients: a pooled analysis of the ASAP, ENHANCE, RADIANCE 1, and CAPTIVATE studies. *Circ. Cardiovasc. Imaging* **3**, 398-404 (2010).

227. Taylor,A.J. *et al.* ARBITER: Arterial Biology for the Investigation of the Treatment Effects of Reducing Cholesterol: a randomized trial comparing the effects of atorvastatin and pravastatin on carotid intima medial thickness. *Circulation* **106**, 2055-2060 (2002).

228. Hoogwerf,B.J. *et al.* Effects of aggressive cholesterol lowering and low-dose anticoagulation on clinical and angiographic outcomes in patients with diabetes: the Post Coronary Artery Bypass Graft Trial. *Diabetes* **48**, 1289-1294 (1999).

229. Nissen,S.E. Effect of intensive lipid lowering on progression of coronary atherosclerosis: evidence for an early benefit from the Reversal of Atherosclerosis with Aggressive Lipid Lowering (REVERSAL) trial. *Am. J. Cardiol.* **96**, 61F-68F (2005).

230. Cannon,C.P. *et al.* Intensive versus moderate lipid lowering with statins after acute coronary syndromes. *N. Engl. J. Med.* **350**, 1495-1504 (2004).

231. Albert,M.A., Danielson,E., Rifai,N. & Ridker,P.M. Effect of statin therapy on C-reactive protein levels: the pravastatin inflammation/CRP evaluation (PRINCE): a randomized trial and cohort study. *JAMA* **286**, 64-70 (2001).

232. Rosenson,R.S., Tangney,C.C. & Casey,L.C. Inhibition of proinflammatory cytokine production by pravastatin. *Lancet* **353**, 983-984 (1999).

233. Naderer,O., Suttle,B.A., Arumugham,T., Min,S.S. & Jones,L.S. Society of Critical Care Medicine 35th Critical Care Congress San Francisco, California, USA January 7-11, 2006. 33(12) Abstract Supplement:A174. *Critical Care Medicine* (2006).

234. Naderer,O.J. *et al.* Safety and pharmacokinetics GR270773, a novel antisepsis compound, in septic patients. Critical Care Medicine. 32(12) Supplement:A174, December 2004. *Critical Care Medicine* (2004).

235. Hajishengallis,G. *et al.* Differential interactions of fimbriae and lipopolysaccharide from Porphyromonas gingivalis with the Toll-like receptor 2-centred pattern recognition apparatus. *Cell Microbiol.* **8**, 1557-1570 (2006).

236. Wang,M. & Hajishengallis,G. Lipid raft-dependent uptake, signaling, and intracellular fate of Porphyromonas gingivalis in mouse macrophages. *Cell Microbiol.* (2008).

Appendices

Recipes

ECV Medium: Medium 199 + Glutamax from GIBCO. **MM-6 Medium:** RPMI 1640 medium (10% FCS, 10ml non-essential amino acids and OPI media supplement) **Running buffer:** BIO-RAD. X1 solution: 25Mm Tris, 192mM glycine and 0.1% (w/v) SDS, pH8.3. **10x PBS:** NaCl, 50.0g. KCl, 1.25g. Na_2HPO_4, 7.2g. KH_2PO_4, 1.25g. dH_2O, make up to. 500ml. **PBS/ 0.02%BSA/ 0.02% NaH_3/ 0.02%:** X1 PBS, 100ml. BSA, 0.02g. NaH_3, 0.02g. **PBS/ 0.02%BSA/ 0.02% NaH_3/ 0.02% Saponin:** X1 PBS, 100ml**.** BSA, 0.02g**.** NaH_3, 0.02g**.** Saponin, 0.02g. **PFA:** Paraformaldehyde, 8.0g**.** dH_2O, 100ml**.** 2X PBS, 100ml. **X2 SDS-PAGE Reducing Sample Buffer:** STOCK, 40ml Final Volume. 0.5M Tris (pH 6.8), 20.0ml. 10% SDS, 6.0ml. Glycerol, 5.0g. 14.3 M B-mercaptoethanol, 4.0ml. Bromophenol Blue, 5.0mg. **X2 SDS-PAGE Non-reducing Sample Buffer:** STOCK, 40ml Final Volume. 0.5M Tris (pH 6.8), 20.0ml. 10% SDS, 16.0ml. Glycerol, 5.0g. Bromophenol Blue, 5.0mg. **Resolving gel 10%:** dH_2O, 4.02ml. 1.5 M Tris-HCl (pH 8.8), 2.5ml. 10% (w/v) SDS, 100.0µl. Acrylamide/Bis, 3.33ml. 10% APS, 50.0µl. TEMED, 5.0µl. **Resolving gel 12%:** dH_2O, 3.5ml. 1.5 M Tris-HCl (pH 8.8), 2.5ml. 10% (w/v) SDS, 100.0µl. Acrylamide/Bis, 4.0ml. 10% APS, 50.0µl. TEMED, 5.0µl. **4% Stacking gel:** dH_2O, 3.05ml. 1.5 M Tris-HCl (pH 8.8), 1.25ml. 10% (w/v) SDS, 50.0µl. Acrylamide/Bis, 0.65ml. 10% APS, 50.0µl. TEMED, 10.0µl. **Running buffer:** Tris, 3.03g. Glycine, 14.4g. SDS, 1.0g. Volume, 1L. **X2 Transfer Buffer:** 20mM Tris-acetate, 4.88g. 0.1% SDS, 20ml. 20% isopropanol, 400ml. dH_2O, 580ml. pH to 8.3, Acetic acid. **Fixing solution (for 1000ml):** Acetic acid, 200ml. Absolute ethanol, 800ml. dH_2O, 1000ml. **Commasie blue (for 200ml):** Methanol, 100ml. Acetic acid, 20ml. dH_2O, 80ml. Commasie blue, 0.6g. **De-stain (for 1000ml):** Ethanol OR IMS, 100ml. Acetic acid, 100ml. dH_2O, 800ml. **Fixing (1000ml):** Ethanol, 400ml. Acetic acid, 100ml. dH_2O, 500ml. **Incubation solution:** Ethanol, 75ml. Sodium acetate, 10.26g. Glutaraldehyde, 1.3ml. Sodium thiosulpate $5H_2O$, 0.5g. Make up to 250ml with dH_2O. **Silver solution:** Silver nitrate, 0.25g. Formaldehyde, 50µl. Make up to 250ml with dH_2O. **Developing solution:** Sodium carbonate, 6.25g. Formaldehyde, 25µl. Make up 250ml with dH_2O. **Stop solution:** EDTA Na_2 $2H_2O$, 3.65g. Make up 250ml with dH_2O. **Collagen:** 10% used (1ml in 9ml X1 PBS). BD Biosciences (rat tail tendon). **Luria broth (1000ml):** Bactopeptone, 10g. Yeast extract, 5g. Sodium chloride 10g. Make up to 1000ml dH_2O. **Lysis buffer (300ml):** Urea, 1.44g. NaCl, 1.7g, Tris-HCL, 17ml. NaH_2PO_4, 1.8g. Imidazole, 2g. (pH8). **Binding buffer (500ml):** NaH_2PO_4, 1.2g. NaCl, 14.6g. (pH8). **Elution buffer (500ml):** NaH_2PO_4, 1.2g. NaCl, 14.6g. Imidazole, 17g. (pH6). **STET buffer:** Sucrose. Triton. EDTA. Tris-HCL. dH_2O. (pH8). **Cleaving buffer:** 50mM Tris-HCL. 150Mm NaCl. 1mM EDTA. 1mM DTT. 0.01% Triton. **ELFO loading buffer (200ml):** Glycerol, 100ml. 50X ELFO, 20ml. dH_2O, 80ml. Bromophenol. **50X ELFO:** (2M Tris, 50mM EDTA). Tris, 242g. EDTA (0.5M), 100ml. pH 7.7 with acetic acid. Make up to 1000ml with dH_2O. **Agarose gel:** Agarose, 1g. ELFO, 100ml.